STABLE ISOTOPE ANALYSIS AND U-Th DATING OF LATE GLACIAL AND HOLOCENE LACUSTRINE SEDIMENTS FROM CENTRAL TURKEY

Jonathan R. Dean

Thesis submitted to The University of Nottingham

for the degree of Doctor of Philosophy

July 2014

School of Geography,

in collaboration with

the National Environment Research Council

Isotope Geosciences Laboratory

Abstract

Water is a politically sensitive resource in the Near East and water stress is increasing. It is therefore vital that there is a strong understanding of past hydrological variability, so that the drivers of change can be better understood, and so that the links between the palaeoclimate and archaeological records in this key region in the development of human civilisation can be investigated. To be of most use, this requires high resolution records and a good understanding of palaeoseasonality.

A sediment sequence spanning ~14,000 years has been retrieved from Nar Gölü, a lake in central Turkey. This thesis presents isotope data from carbonates, diatoms and bulk organic matter, in particular focussing on oxygen isotope ($\delta^{18}O$) analysis of carbonates (which detailed monitoring of the modern lake system shows to be a strong proxy for water balance) and comparing $\delta^{18}O_{carbonate}$ and $\delta^{18}O_{diatom}$ data in order to examine palaeoseasonality. Improved techniques for the interpretation of carbonate isotope records of mixed mineralogies and the mass balance correction of diatom samples contaminated with minerogenic material are also proposed.

Due to the high resolution $\delta^{18}O_{carbonate}$ data, it was possible to show that the rapidity of the Younger Dryas to Holocene transition at Nar Gölü was similar to that seen in North Atlantic records and that centennial scale arid events in the Holocene seem to occur at the time of cold periods in the North Atlantic. Taken together, this suggests a strong teleconnection between the two regions. However, the longer duration of the aridity peaks ~9,300 and ~8,200 years BP at Nar Gölü, compared with the more discrete cooling events at this time in the North Atlantic, suggest that there are additional controls on Near East hydroclimate. There is a multi-millennial scale trend of increasing $\delta^{18}O_{carbonate}$ values from the early to late Holocene. This 'Mid Holocene Transition' has previously been identified in the Near East, however here it is demonstrated that water balance and not a shift in the seasonality of precipitation was the primary cause. Finally, for the first time, the stability of Near East climate in the early Holocene is robustly

demonstrated, suggesting that this could have been a key enabler of the development of agriculture at this time.

Abbreviations

DIC	Dissolved inorganic carbon
EDS	Energy dispersive x-ray spectroscopy
ITCZ	Inter-tropical convergence zone
MC-ICP-MS	Multi-collector inductively coupled plasma mass spectrometer
NAO	North Atlantic Oscillation
PBO	Pre Boreal Oscillation
SEM	Scanning electron microscopy
SPT	Sodium polytungstate
TDIC	Total dissolved inorganic carbon
U-Th	Uranium-thorium
XRD	X-ray diffraction
XRF	X-ray florescence
Years BP	Years before present, i.e. 1950
$\delta^{18}O_{carbonate}$	Ratio of ^{18}O:^{16}O in carbonate
$\delta^{13}C_{carbonate}$	Ratio of ^{13}C:^{12}C in carbonate
$\delta^{18}O_{diatom}$	Ratio of ^{18}O:^{16}O in diatom silica
$\delta^{13}C_{organic}$	Ratio of ^{13}C:^{12}C in bulk organic matter
C/N	Carbon to nitrogen ratio, in weight %
σ	Standard deviation
$\bar{x}$	Mean

Author's publications and presentations

Publications

Dean, J.R., Jones, M.D., Leng, M.J., Sloane, H.J., Roberts, C.N., Woodbridge, J., Swann, G.E.A., Metcalfe, S.E., Eastwood, W.J., Yiğitbaşıoğlu, H., 2013. Palaeo-seasonality of the last two millennia reconstructed from the oxygen isotope composition of carbonates and diatom silica from Nar Gölü, central Turkey. *Quaternary Science Reviews* 66, 35-44.

Dean, J.R., 2012. Book review: The Encyclopedia of Paleoclimatology. *Journal of Paleolimnology* 47, 715-716.

Conference presentations

Dean, J.R., Jones, M.D., Leng, M.J., Roberts, C.N., Metcalfe, S.E., Noble, S.R., 2013. Investigating the nature of climate shifts during the late glacial and early Holocene in the Near East, using a new sub-centennial resolution lake isotope record from Nar Gölü, central Turkey. *AGU, poster*.

Roberts, C.N., Jones, M.D., Eastwood, W.J., Woodbridge, J., Allcock, S., **Dean, J.R.**, 2013. Climate change and the Plague of Justinian. *PAGES Open Science Meeting, poster*.

Dean, J.R., Jones, M.D., Leng, M.J., Roberts, C.N., Metcalfe, S.E., 2012. A new record of late glacial and Holocene climatic change from oxygen isotope analysis of lake sediments from central Turkey. *Quaternary Research Association postgraduate symposium, oral*.

Dean, J.R., Jones, M.D., Leng, M.J., Sloane, H.J., Roberts, C.N., Woodbridge, J., Swann, G.E.A., Metcalfe, S.E., Eastwood, W.J., Yiğitbaşıoğlu, H., 2012. Palaeo-seasonality of the last two millennia reconstructed from the oxygen isotope composition of carbonates and diatom silica from Nar Gölü, central Turkey. *International Paleolimnology Symposium, oral*. Highly commended.

Roberts, C.N., Allcock, S., Woodbridge, J., Jones, M.D., **Dean, J.R.**, Eastwood, W.J., Leng, M.J., Yiğitbaşıoğlu, H., Arnold, F., 2012. 'A tale of two lakes': comparing laminated records for the last 17 ka BP from Cappadocia, Turkey. *International Paleolimnology Symposium, oral*.

Dean, J.R., Jones, M.D., Leng, M.J., Sloane, H.J., Swann, G.E.A., Metcalfe, S.E., Roberts, C.N., Woodbridge, J., Eastwood, W.J., Yiğitbaşıoğlu, H., 2012. Palaeo-seasonality from the difference between the oxygen isotope composition of diatom silica and carbonate from a lake in central Turkey. *Isotopes in Biogenic Silica meeting, oral*.

Dean, J.R., Jones, M.D., Leng, M.J., Roberts, C.N., Metcalfe, S.E., 2012. Assessing the relationship between climate change and societal shifts in the Near East. *Royal Geographical Society postgraduate conference, oral*.

Roberts, C.N., Allcock, S., Woodbridge, J., Jones, M.D., **Dean, J.R.**, Eastwood, W.J., Leng, M.J., Yiğitbaşıoğlu, H., Arnold, F., Sabatier, P., 2012. 'A tale of two lakes': comparing varved records for the last 15 ka BP from Cappadocia, Turkey. *PAGES Varves Working Group, oral.*

Dean, J.R., Jones, M.D., Leng, M.J., Roberts, C.N., Metcalfe, S.E., 2011. A new, high resolution carbonate isotope record of late glacial and Holocene climatic change from the varved sediments of Nar Gölü, central Turkey. *International Limnogeological Congress, poster*.

Dean, J.R., Jones, M.D., Leng, M.J., Sloane, H.J., Roberts, C.N., Woodbridge, J., Metcalfe, S.E., 2011. $\delta^{18}O$ analysis of multiple hosts from the varved sediments of Nar Gölü, central Turkey. *International Union for Quaternary Research Congress, poster*.

Acknowledgments

Firstly, my supervisors Matt Jones and Sarah Metcalfe deserve huge thanks for all their help and support over the past three years, as well as during undergrad. Mel Leng and Steve Noble at NIGL also provided invaluable assistance during lab work and the write up. The work at Nar Gölü was led by Neil Roberts (University of Plymouth), to whom funding was awarded by the National Geographic Society and the British Institute at Ankara. Neil, Samantha Allcock and Warren Eastwood are thanked for fruitful and productive discussions, help with sampling and supplying of data.

Much of the data discussed here would not have been collected without the assistance of other researchers who have contributed to the field work at Nar Gölü over the past decade: Hakan Yiğitbaşıoğlu (who drove us expertly back to Ankara through a blizzard in February 2012), Ersin Ateş, Jessie Woodbridge, Gwyn Jones, Ryan Jones, Fabien Arnaud, Emmanuel Malet, Ceran Şekeryapan, Çetin Şenkul, Murat Türkeş, Mustafa Karabiyikoğlu, Ann England, Damase Mouralis and Jane Reed. This Ph.D. itself was funded by a NERC studentship and isotope analyses and U-Th dating by 4 NIGFSC grants to Matt Jones.

I am also indebted to Hilary Sloane, Andrea Snelling, Ewan Woodley, Chris Kendrick, Carol Arrowsmith, Jonathan Lewis and Neil Boulton who provided training and ran some of the isotope samples discussed here. Thanks also to Graham Morris, Teresa Needham and Dave Clift at Nottingham for supporting my lab work.

On a more personal note, the postgraduate community, especially Gillman, Jorge, Georgie, Jake, Mr. Small Craft, Hez, Lizzie, Northern Jen and Joanna, have provided welcome distractions; I will greatly miss the gossiping, fancy dress house crawls and general banter! The winemakers of Châteauneuf-du-Pape also provided assistance. Finally, massive thanks to my family for their support.

Table of Contents

Chapter 3 | Stable isotope analysis of lacustrine sediments

Chapter 4 | Uranium-thorium dating of lacustrine sediments

Chapter 5 | Site description and previous work at Nar Gölü

Chapter 6 | Methodology

Chapter 7 | Results and interpretation of contemporary waters and sediments

Chapter 8 | Results and interpretation of palaeo stable isotope records

Chapter 9 | Chronology

Chapter 10 | Discussion

Chapter 11 | Conclusions

List of Figures

List of Tables

Chapter 1 | Introduction

1.1 Importance of understanding past hydrological variability in the Near East

Water in the Near East* is a politically sensitive resource (e.g. Issar and Adar, 2010) and water stress in the region is projected to increase during the 21st century (Cruz et al., 2007). Rain-fed agriculture is already impossible across most of the region and the Fertile Crescent, the area of land that can be irrigated by the Jordan, Tigris and Euphrates rivers and one of the first parts of the world in which plants and animals were domesticated (e.g. Bellwood, 2005, Brown et al., 2009), is projected to disappear this century (Kitoh et al., 2008). Turkey has seen increased drought in recent decades (Türkeş, 2003, Sonmez et al., 2005, Toros, 2012) and this trend is likely to continue in the coming decades (Arnell, 2004), with one regional climate model suggesting a 5-6°C increase in mean annual temperatures and a 40% fall in precipitation in central Turkey by the end of this century compared to the late 20th century (Demir et al., 2010). Therefore, an improved understanding of hydrological variability over long timescales is required, in order to put the magnitude of recent climate shifts into context and to identify the drivers of climate in the region. This is vital to assist in the sustainable management of water resources into the future. Moreover, the Near East is the key region in the development of human civilisation, where agriculture and city-based civilisations first developed (e.g. Bourke, 2008, Zohary et al., 2012). It has been proposed that changes in water availability influenced the rise and fall of civilisations in the region (e.g. Issar and Zohar, 2007, Rosen, 2007). In particular, a series of major, decadal- to centennial-scale drought events have recently been identified from ~7,000-3,000 years BP (Bar-Matthews and Ayalon, 2011). Some occur at the same time as major transitions in the archaeological record, such as the end of the Early Bronze Age ~4,100 years BP (Weiss, 1993, Rosen, 2007), suggesting that environmental stress or opportunity could have operated as a pacemaker for societal change (Roberts et al., 2011a).

* The term Near East as used in this thesis refers to the region encompassing modern day Turkey, Israel, Palestine, Syria, Lebanon, Jordan, Iraq and Iran.

1.2 Gaps in knowledge of Near East palaeoclimatology

There remain three main gaps in our knowledge of Near East palaeoclimatology (discussed in more detail in chapter 2):

- There is a requirement for improved chronological precision and high resolution climate records in the late glacial, especially through the Younger Dryas* to Holocene transition (Robinson et al., 2006), so that comparisons with other regional and global climate records can be made, and so the drivers of Near East climate can be better understood.
- Although several oxygen isotope ($\delta^{18}O$) records from lake carbonates from the region have been published in the last decade and regional patterns identified (Roberts et al., 2008), the interpretation of the records is debated. While most records are interpreted as responding to changes in water balance (Jones and Roberts, 2008), the influence of other factors need to be considered more thoroughly. In particular, Stevens et al. (2006) have suggested that changes in the seasonality of precipitation may have been important. Given the marked seasonality of Near East climate (Türkeş, 2003), its important implications for human societies (Rosen, 2007) and the fact that shifts in seasonality are anticipated globally in a warming world (Meehl et al., 2007), this factor needs to be investigated further.
- Other than the recently produced record from the Soreq Cave in Israel for the mid Holocene (Bar-Matthews and Ayalon, 2011), there are no records of a sufficiently high resolution to be able to investigate decadal to centennial scale climate events thoroughly. Understanding rapid, high magnitude climate shifts in the past is increasingly important given the concern than human forcing of climate may increase the probability of such events occurring in the future (Alley et al., 2003), potentially leading to catastrophic economic and ecological turmoil (Adger et al., 2007).

* While the term Younger Dryas was originally a term used to refer to a cold period identified in European pollen records (~12,900-11,700 years BP), the term is now widely applied to describe the last cold period at the end of the last glacial seen in records from around the world. So in this thesis, the terms Younger Dryas (and Bølling-Allerød) are used in reference to Near East records.

1.3 Justification for site choice and methods

To produce a new palaeoclimate record and attempt to address these gaps in our knowledge, Nar Gölü, a maar lake in central Turkey (Figure 1.1), was chosen as the study site. This was because previous work on a shorter, 1,720 year sequence (e.g. Jones et al., 2006, England et al., 2008, Woodbridge and Roberts, 2011) showed its potential for the production of well-dated, high resolution records due to its varved sediments. Nar Gölü is close to Eski Acıgöl, from where a late glacial-Holocene record has already been produced (Roberts et al., 2001). Duplicate records from the same area are necessary to check that proxies are in fact recording regional climate and not responding to lake-specific changes (Fritz, 2008) and sediments with a higher deposition rate than Eski Acıgöl's were required to allow for high resolution analysis. Additionally, these lakes are in an important region for archaeologists, close to the important Neolithic sites of Çatalhöyük and Asikli Höyük (Figure 1.1), and it is important to have climate records from close to archaeological sites when investigating the links between climate and societal change (Jones, 2013).

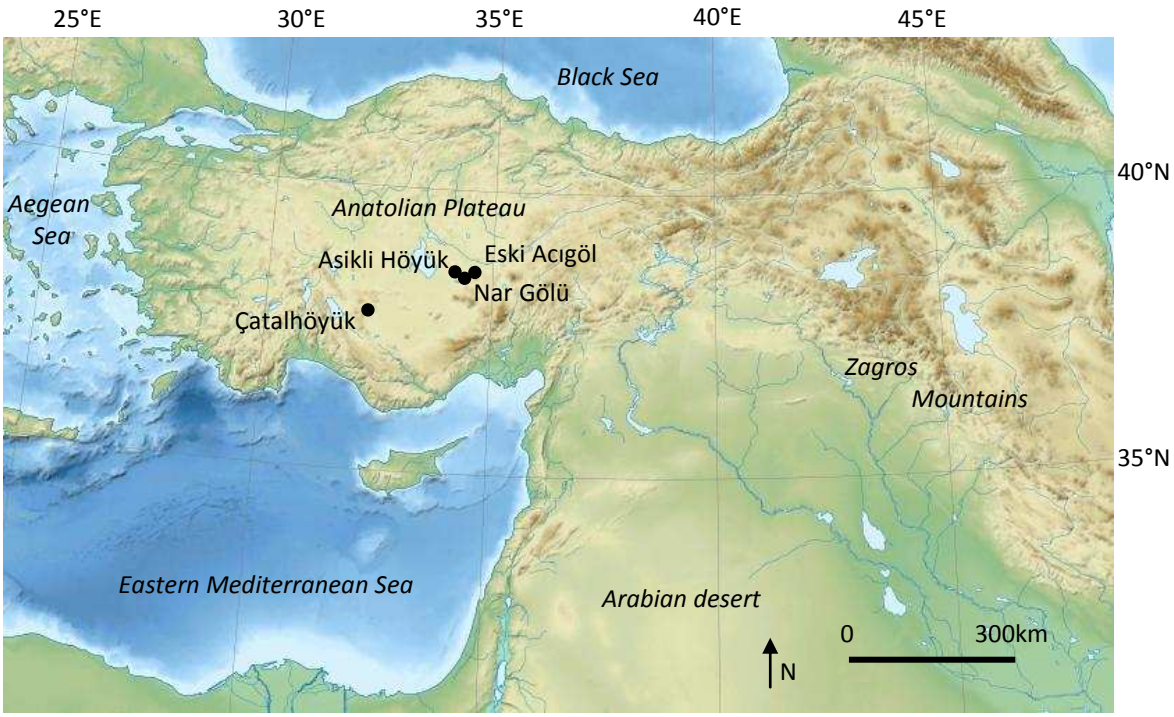

Figure 1.1 *Key topographical features of the Near East and location of Nar Gölü, Eski Acıgöl and selected archaeological sites (map from http://commons.wikimedia.org/wiki/File:Near_East_topographic_map-blank.svg).*

The long history of human activity in the Near East means it is difficult to discriminate between climatic and non-climatic influences on proxy records such as pollen and diatom species (Roberts et al., 2010), but Jones et al. (2005) had already shown that the $\delta^{18}O_{carbonate}$ record from Nar Gölü is a good proxy for regional water balance. Climate has an influence on the stable isotope composition of lake waters and this is recorded in, for example, carbonates and diatoms that precipitate and grow in the lake waters (chapter 3). Therefore, because the main intention of this thesis is to produce a robust palaeoclimate reconstruction, $\delta^{18}O_{carbonate}$ analysis of the new sequence is undertaken. $\delta^{18}O_{diatom}$ data are also produced and compared to $\delta^{18}O_{carbonate}$ data in order to reconstruct palaeoseasonality (Leng et al., 2001).

Unlike the shorter core sequence taken from Nar Gölü in 2001/2 (Jones et al., 2006), not all of the longer core sequence taken in 2010 is varved. The chronologies of most non-varved lake cores are provided by radiocarbon dating. However, Jones (2004) has already shown that due to an old carbon source in Nar Gölü, this is not possible. Therefore, an additional dating method is required and it was decided to use uranium-thorium (henceforth U-Th) dating. U-Th dating of lake sediments is predicated on the assumption that uranium is incorporated into carbonates but thorium is not because it is less soluble, and since uranium decays into thorium at a known rate, the time since deposition can be calculated (Edwards et al., 2003). However, this can be complicated by the presence of detrital and hydrogenous thorium (Haase-Schramm et al., 2004, Torfstein et al., 2013) and/or the loss of uranium due to open system behaviour (Lao and Benson, 1988), which increase the calculated age away from the real age (chapter 4).

1.4 Aims and objectives

The aim of this thesis is to address the gaps in the literature outlined in section 1.2, specifically to produce a high resolution record through the Younger Dryas to Holocene transition so that the rapidity of the shift in the Near East can be compared to other records, to establish what is driving the general trend towards higher oxygen isotope values in Near East lake carbonates through the Holocene (Roberts et

al., 2008) (in particular the influence seasonality might have on the records) and to produce a high resolution record of changes in water balance through the Holocene so that decadal and centennial scale climate shifts can be investigated. This should allow for a better understanding of the drivers of Near East climate in the past and any possible links with societal change.

These aims are addressed, using the methods outlined in section 1.3, through a number of objectives:

- The analysis of contemporary waters and sediments to better understand the Nar Gölü isotope system and better interpret the palaeo record, including the establishment of the likely times of year of carbonate precipitation and diatom growth and the investigation of the transference of the $\delta^{18}O$ signal from the waters to the core sediments.
- The use of $\delta^{18}O_{carbonate}$ data (supported by $\delta^{13}C_{carbonate}$, $\delta^{18}O_{diatom}$, $\delta^{13}C_{organic}$, lithology and carbonate mineralogy data) to produce a reconstruction of changes in water balance through the Holocene and late glacial.
- Exploration of whether comparing $\delta^{18}O$ from diatoms and carbonates can provide insights into seasonality.
- The use of uranium-thorium dating to provide a chronology for the core.
- Comparison of $\delta^{18}O$ record from Nar Gölü to other palaeoclimate records from the Near East and beyond.

1.5 Thesis outline

Chapters 2, 3 and 4 outline the present state of knowledge of Near East palaeoclimatology, the use of stable isotope analysis to produce palaeoclimate reconstructions and U-Th dating to provide chronologies. Chapter 5 introduces the site and chapter 6 discusses the methods used and the methodological developments achieved as part of this thesis. Chapter 7 uses data from contemporary waters and sediments to attempt to better understand the Nar Gölü system. Chapter 8 presents the major results of this thesis: down-core oxygen and carbon isotope data. Chapter 9 shows the U-Th results thus far produced, and the

best estimate of chronology at the time of writing is used in chapter 10 to compare the records to others from the region and beyond, and to the archaeological record where appropriate, to consider the drivers of Near East climate and any potential links between societal and climate change. The implications of this thesis for the stable isotope community and Near East palaeoclimatology are discussed in chapter 11.

Chapter 2 | Climate of the Near East

The current understanding of palaeoclimatology in the Near East needs to be considered, to contextualise and explore in more detail the gaps in knowledge outlined in section 1.2. First, however, the contemporary regional climate needs to be understood, to provide a benchmark against which past climates can be compared and to appreciate what the key drivers of climate are in the present.

2.1 Contemporary climate

2.1.1 Climate dynamics

Precipitation is highest in the coastal and mountainous areas of the region (Figure 2.1). Areas near to the Mediterranean coast, such as Jerusalem, have cool, wet winters and hot, dry summers, whereas in continental areas, such as the Anatolian plateau and the Zagros Mountains (Figure 1.1), precipitation patterns are more characteristic of continental climates, with wet springs as well as winters (Figure 2.2). In Turkey, because of the influence of mountain ranges, the Anatolian plateau and the Black and Aegean Seas, only the southern coast has a truly Mediterranean climate, with precipitation peaking in continental areas in the spring (Türkeş, 1996, 1998). Most precipitation falling on the Near East is ultimately from Atlantic sources, although there is some cyclogenesis in the Mediterranean creating the Genoa and Cyprus low pressure systems (Harding et al., 2009, Türkeş et al., 2009). In winter, the Inter-Tropical Convergence Zone (ITCZ) moves southwards (Ziv et al., 2006) and hence storms can track from the North Atlantic through the Mediterranean, whereas in the summer the ITCZ moves north, which leads to high pressure systems blocking westerly depressions. Central Turkey, and the Near East as a whole, experiences drier winters during more positive North Atlantic Oscillation (NAO) years and vice versa (Cullen and deMenocal, 2000, Tan and Unal, 2003, Türkeş and Erlat, 2003, 2005, Gil et al., 2006, Harding et al., 2009). The North Sea-Caspian Pattern Index is also considered to have an important influence on winter climate (Kutiel and

Benaroch, 2002, Jones et al., 2006). A relationship has been demonstrated between summer Turkish climate and the Indian monsoon, with enhanced monsoon rainfall linked with dry summers (Jones et al., 2006).

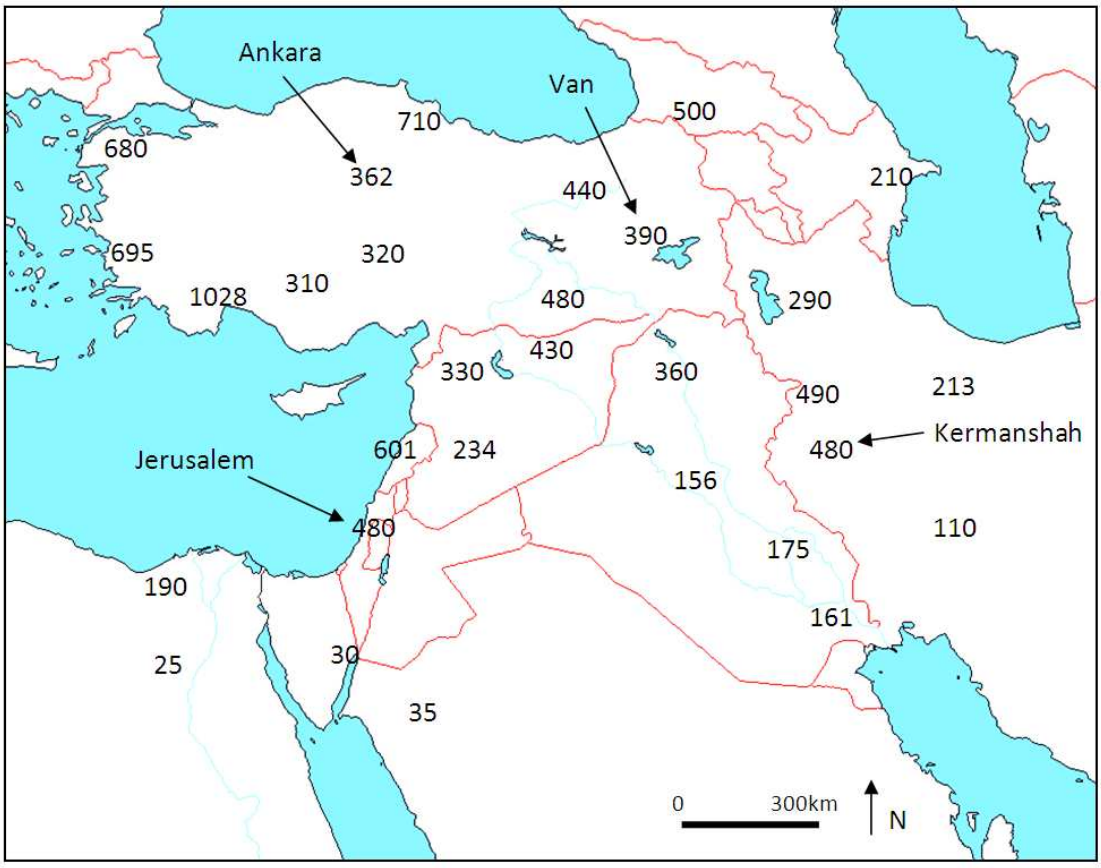

Figure 2.1 *Distribution of annual precipitation values (in mm) across the Near East (data from WMO, 2011). More details for selected sites given on Figure 2.2.*

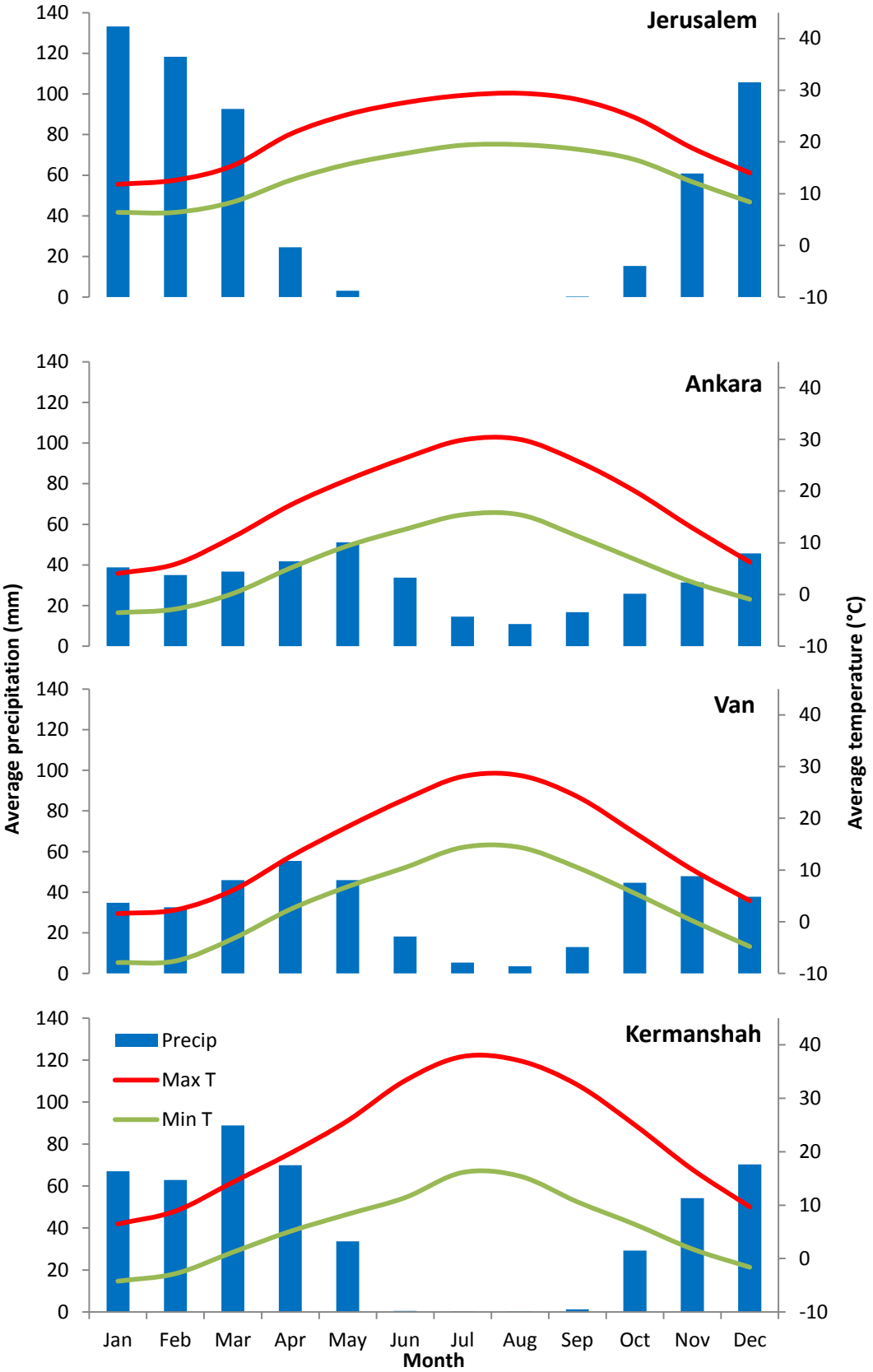

Figure 2.2 *Different precipitation and temperature patterns are seen across the region (data from WMO, 2011), particularly influenced by differences in continentality. Locations of these sites are shown on Figure 2.1.*

2.1.2 Recent trends and predictions for the future

As the Mediterranean is in the transition zone between tropical and mid latitude processes, any shifts in global circulation patterns will have significant effects on the climate of the region (Giorgi, 2006, Giorgi and Lionello, 2008, Dormoy et al., 2009). In the Near East as a whole, average temperatures rose by 1.5°C-4°C during the 20th century (Alpert et al., 2008). Annual and winter precipitation have decreased over most of Turkey since early 1970s (Türkeş, 2003, Toros, 2012). By 2100, it is projected that Near East mean precipitation will have fallen by 25% and mean temperature increased by 4.5°C compared to 1961-1990 (Suppan et al., 2008). Specifically for Turkey, the Hadley Centre RCM (based on A2 scenario) forecasts a 5-6°C increase in mean temperature for interior Turkey by 2071-2100 compared to 1961-1990 and a 40% reduction in precipitation (Demir et al., 2010), putting it in the water stressed category (Arnell, 2004). The decrease in precipitation is likely because of a projected poleward shift of the North Atlantic storm track leading to a weakening of the Mediterranean winter storm track (Evans, 2009). These projections of increased aridity make it even more important to consider how and why climate changed in the past, particularly the conditions during more arid intervals than now.

2.2 Palaeoclimatology

This section is split into three that review the current state-of-knowledge of the three gaps in our knowledge of Near East palaeoclimatology identified in section 1.2. (All dates in this thesis, whether they be calibrated radiocarbon, U-Th, varve counts or ice layer counts, are given in years BP (i.e. years before 1950), in order to aid comparison between records.)

2.2.1 Late glacial: form and timings

Based on previous studies, the general form of the late glacial in the Near East is fairly well understood. At the time of the so called Mystery Interval, ~17,500-14,700 years BP, seen as a cooling in North Atlantic records and possibly initiated by

Heinrich Event 1 (Hemming, 2004, Denton et al., 2006, Barker et al., 2009), there seems to have been a cooling and drying of the Near East, based on geochemical and isotope evidence from the Black Sea (Kwiecien et al., 2009), pollen from the northern Aegean (Kotthoff et al., 2011), geochemical proxies from the Nile Delta (Castaneda et al., 2010), isotopes from Soreq Cave in Israel (Bar-Matthews et al., 1999) and sedimentary evidence from the Dead Sea (Stein et al., 2010) (the locations of key Near East palaeoclimate archives are shown on Figure 2.3). This was followed by increased temperatures and wetter conditions in the region in the Bølling-Allerød ~14,700-12,900 years BP, based on a pollen record from the Aegean (Kotthoff et al., 2008a, Dormoy et al., 2009), geochemical proxies from the Nile Delta (Castaneda et al., 2010), the Black Sea (Bahr et al., 2008) and the Red Sea (Arz et al., 2003, Essallami et al., 2007), pollen evidence from the Balkans (Aufgebauer et al., 2012), isotope records from Lake Van (Lemcke and Stürm, 1997), Eski Acıgöl (Roberts et al., 2001), Soreq Cave (Bar-Matthews et al., 1997) and Iran (Stevens et al., 2012) and ostracod, pollen and diatom evidence from Greece (Frogley et al., 2001, Lawson et al., 2004, Wilson et al., 2008, Jones et al., 2013),

The Younger Dryas, ~12,900-11,700 years BP, was the last cold period of the last glacial and is often linked with meltwater outbursts and a slowdown in North Atlantic circulation (Broecker et al., 1989, Tarasov and Peltier, 2005, Teller, 2012), but is also seen by some as the response to a large comet or meteorite impact event that has been dated to the start of the Younger Dryas (e.g. Firestone et al., 2007, LeCompte et al., 2012). In the Near East, the period was cooler and drier than the Bølling-Allerød and early Holocene, as seen in geochemical records from the Nile Delta (Castaneda et al., 2010), the Red Sea (Arz et al., 2003) and the Black Sea (Bahr et al., 2008), pollen records from the Balkans (Bordon et al., 2009, Aufgebauer et al., 2012) and the Aegean (Dormoy et al., 2009, Kotthoff et al., 2011), diatom evidence from Greece (Jones et al., 2013) and isotope records from Lake Van (Lemcke and Stürm, 1997, Wick et al., 2003), Iran (Stevens et al., 2001, Stevens et al., 2012), Soreq Cave (Bar-Matthews et al., 1997) and Eski Acıgöl (Roberts et al., 2001, Jones et al., 2007).

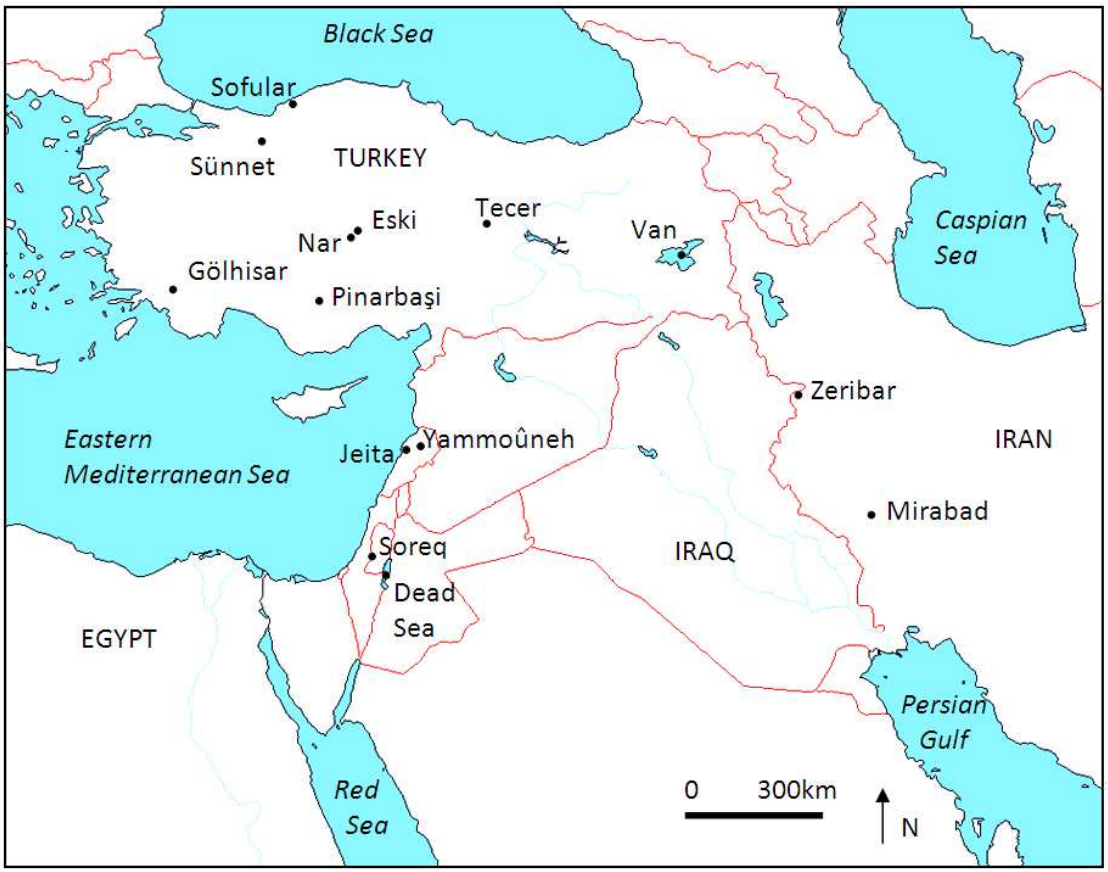

Figure 2.3 *Locations of major palaeoclimate archives in the Near East that will be referred to in this thesis.*

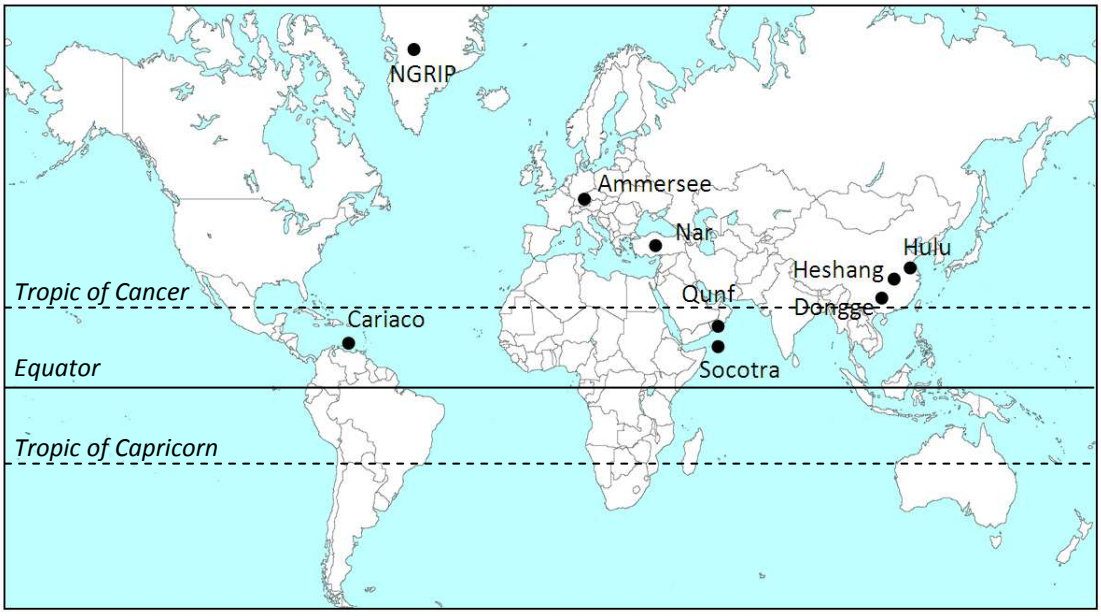

Figure 2.4 *Locations of major palaeoclimate archives from around the world that will be referred to in this thesis.*

In terms of the connection between changes in the North Atlantic and Near East hydroclimate, many authors show that a cooling of the North Atlantic changes the path of, and reduces the frequency of, winter storms that travel from the Atlantic through the Mediterranean and provide the Near East with much of its precipitation. Thus, when the North Atlantic cools, as in the Younger Dryas, the Near East becomes drier (Cullen and deMenocal, 2000, Türkeş and Erlat, 2005, Harding et al., 2009, Rowe et al., 2012).

However, there is some debate in the literature about the form of the shifts in the late glacial in the Near East, namely with the Dead Sea record being interpreted the opposite way to all other records from the region as showing the Younger Dryas was wetter than the Bølling-Allerød and early Holocene (Stein et al., 2010). Kolodny et al. (2005) and Stein et al. (2010) argue that $\delta^{18}O_{carbonate}$ values in the Soreq Cave record in the Younger Dryas were high not because of negative water balance (as argued by Bar-Matthews et al., 1997) but because of increased $\delta^{18}O$ of the Eastern Mediterranean and hence of Near East precipitation. As well as that debate, another that needs to be addressed is the issue of the rapidity of the Younger Dryas to Holocene transition in the region compared to in the rest of the world. Records from Ammersee in Germany (von Grafenstein et al., 1999), Cariaco off Venezuela (Hughen et al., 1996) and NGRIP, the latest Greenland ice core (Rasmussen et al., 2006, Vinther et al., 2006, Steffensen et al., 2008), see Figure 2.4 for locations, show the transition occurring in less than a century, whereas records further away from the North Atlantic, such as Dongge Cave in China (Dykoski et al., 2005), Socotra in Yemen (Shakun et al., 2007), the Nile Delta (Castaneda et al., 2010) and the Red Sea (Arz et al., 2003), see a much longer transition taking many centuries. However, in the Near East, poor chronologies have hampered comparison to these records. In Eski Acıgöl a large transition believed to be the Younger Dryas to Holocene is dated to ~12,000 years BP, the transition in Lake Van is dated to 10,500 years BP and the Soreq Cave chronology is also not secure at this time. Additionally, a lack of high resolution records has made investigation of the rapidity of the transition difficult (Figure 2.5).

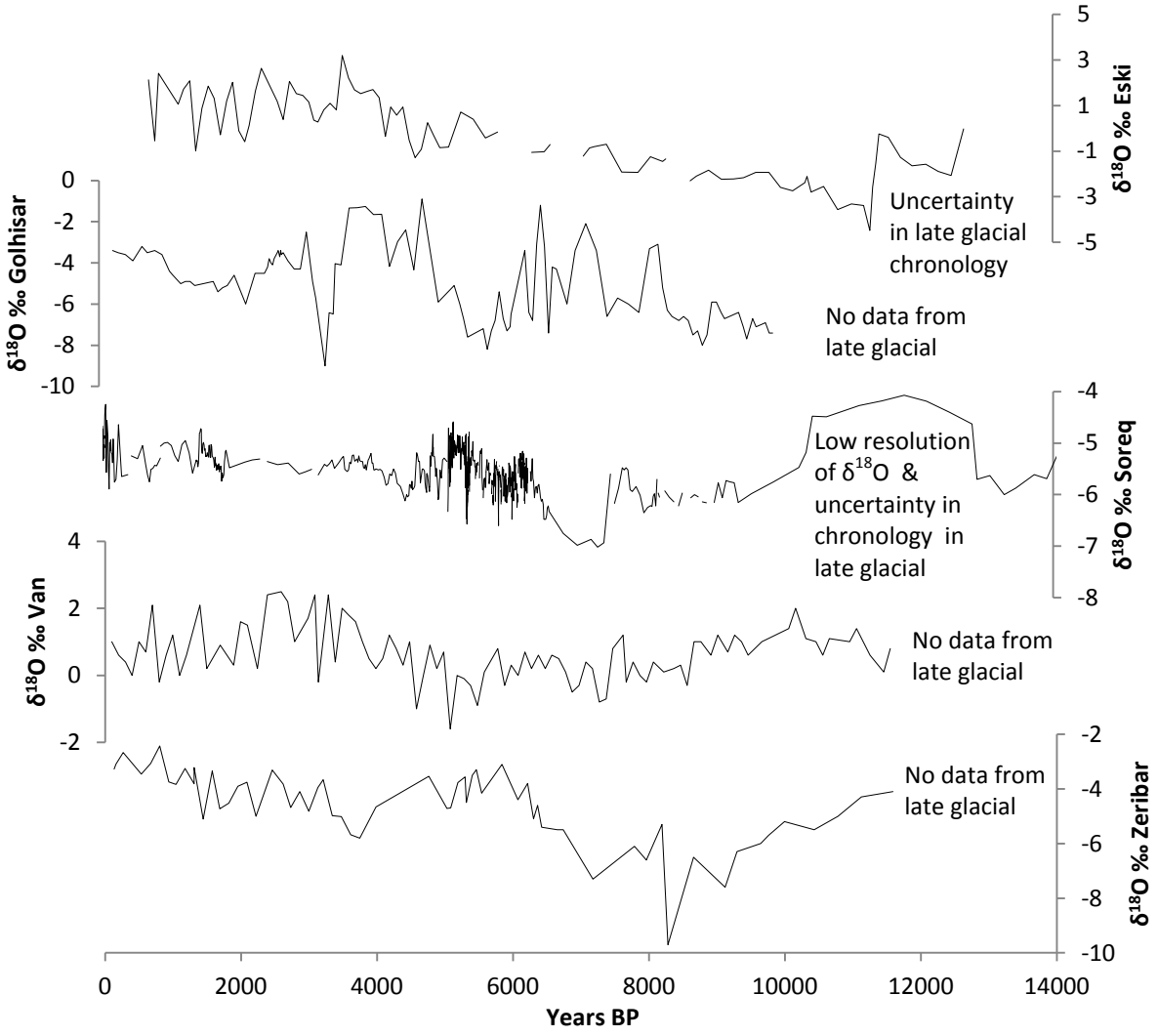

Figure 2.5 *Selected isotope records from the Near East: Eski Acıgöl (Roberts et al., 2001), Gölhisar Gölü (Eastwood et al., 2007), Soreq Cave (Bar-Matthews et al., 1997, Orland et al., 2009, Bar-Matthews and Ayalon, 2011), Lake Van (Wick et al., 2003) and Lake Zeribar (Stevens et al., 2001) (see Figure 2.3 for locations).*

2.2.2 The Holocene: general long terms trends

The second gap in our knowledge is understanding what caused the millennial scale shift to more positive $\delta^{18}O_{carbonate}$ values in Near East lake records in the mid Holocene. (Following the recommendations of Walker et al. (2012), when talking about 'early', 'mid' and 'late' Holocene, the early-mid Holocene boundary is defined at 8,200 years BP and the mid-late Holocene boundary at 4,200 years BP.) Unlike in

North Atlantic region records, where the last major climate shift was the Younger Dryas to Holocene transition, in records from the Near East, Africa and Asia there was a large shift in hydroclimate in the mid Holocene. Many studies have divided the Holocene in the Near East into a wet early Holocene, a transition phase in the mid Holocene and a late Holocene that was more arid than the early Holocene. This is seen in lake isotope records from Turkey including Eski Acıgöl (Roberts et al., 2001, Jones et al., 2007), Gölhisar Gölü (Eastwood et al., 2007), Lake Sünnet (Ocakoglu et al., 2013) and Lake Van (Lemcke and Stürm, 1997) and isotope records from speleothems from Sofular Cave in Turkey (Gokturk et al., 2011), Jeita Cave in Lebanon (Verheyden et al., 2008) and Soreq Cave in Israel (Ayalon et al., 1999, Bar-Matthews et al., 1997, 2003) (Figure 2.5). Many other studies from Israel also suggest a wet early Holocene and dry late Holocene (Neev and Emery, 1995, Goodfriend, 1999, Frumkin et al., 1999, Frumkin et al., 2000, Gvirtzman and Wieder, 2001, McLaren et al., 2004) as do marine records with the S1 sapropel layer in the Eastern Mediterranean Sea, seen to be caused by increased Nile discharge from increased precipitation (Fontugne et al., 1994), dated to ~10,800-6,100 years BP (Ariztegui et al., 2000, Calvert and Fontugne, 2001, De Lange et al., 2008, Rohling et al., 2009), and the isotope record from Lake Yammoûneh in Lebanon (Develle et al., 2010). The development of agriculture in the early Holocene in the Near East has been linked to these more positive water balance conditions (Gupta, 2004, Bellwood, 2005, Willcox et al., 2009).

Near East lake isotope records are interpreted as showing maximum wetness ~7,900 years BP with a shift to drier conditions (known as the Mid Holocene Transition) starting ~7,000 years BP and aridity peaking ~3,000-2,000 years BP (Roberts et al., 2008, 2011a, Finné et al., 2011). When the Near East lake records are combined, they suggest a Holocene precipitation change of <7% (Roberts et al., 2011a), although site specific reconstructions at Soreq Cave and Eski Acıgöl (Table 2.1) suggest larger shifts (Bar-Matthews et al., 1997, Jones et al., 2007). The end of the African Humid Period, a time when much of North Africa was apparently wetter than now, occurred in the mid Holocene, seen as an abrupt rise in wind-blown sediments to the Mauritanian coast 5,500 years BP (deMenocal et al., 2000) or as a more gradual decrease in the

flow of the Nile 8,000-4,000 years BP (Blanchet et al., 2013). The decrease in precipitation turned the 'Green Sahara' into the desert seen today and had a major impact on human settlements (Kuper and Kropelin, 2006). Decreased intensity of monsoon rains at Qunf in Oman (Fleitmann et al., 2003, 2007) and Dongge in China (Dykoski et al., 2005) are also seen at this time. This increased aridity from the Near East to Africa to Asia has been linked to a decline in summer insolation (e.g. deMenocal et al., 2000, Fleitmann et al., 2007) and a southward shift in the ITCZ, and specifically in the Near East to a decline in winter rains (Tzedakis, 2007, Brayshaw et al., 2011a, Roberts et al., 2011b).

Table 2.1 *Precipitation values calculated for Eski Acıgöl (Jones et al., 2007) and Soreq Cave (Bar-Matthews et al., 1997).*

Period	**Estimated precipitation (mm)**		**% difference from late Holocene**	
	Eski Acıgöl	**Soreq Cave**	**Eski Acıgöl**	**Soreq Cave**
Modern	320 ±40	515±65	–	–
Early Holocene	390 ±60	812 ±137	+22%	+58%
Younger Dryas	240 ±60		–25%	
Bølling-Allerød	450 ±50		+41%	

However, while the increases in $\delta^{18}O_{carbonate}$ in Near East lake records, and from the Soreq Cave, are generally interpreted as indicating a shift to drier conditions (Jones and Roberts, 2008) and thus showing the transition from a wet early Holocene to a dry late Holocene (Roberts et al., 2008, 2011a), there are debates in the literature. At first glance, Near East pollen records seem to contradict the isotope records, with a delay of several thousand years between the beginning of the Holocene and increases in arboreal pollen. At Eski Acıgöl, for example, while non-arboreal pollen (e.g. *Pistacia*) did rapidly increase, *Quercus* (oak) did not reach a maximum until ~5,300 years BP (Woldring and Bottema, 2003). At Lakes Van, Mirabad and Zeribar,

the early Holocene pollen record was dominated by steppic indicators such as *Gramineae* and *Pistacia*, with *Quercus* gradually increasing to a maximum ~6,700 years BP (van Zeist and Bottema, 1977). Van Zeist and Bottema (1991) and Roberts and Wright (1993) suggested that low arboreal pollen seen in the early Holocene Near East compared to earlier advances in Europe (Berglund et al., 1996) and Syria (Yasuda et al., 2000) meant the climate was dry. However, as discussed, most lake isotope records from the Near East have been interpreted otherwise. Roberts et al. (2011a) and Roberts (in press) suggest four main explanations for the divergence between isotope and pollen records. Firstly, the pollen record may not accurately reflect the actual vegetation of the area at the time; there may be an underrepresentation of key vegetation types such as insect-pollinated *Rosaceae* (Woldring and Cappers, 2001). Secondly, slow dispersal rates could have meant that trees were simply unable to respond rapidly to changing climate and so they spread slowly from refugia back to parts of the Near East (Hillman, 1996, Van Zeist and Bottema, 1991). Although the Sofular Cave record suggests limited lag between climate and vegetation at the onsets of the Bølling-Allerød and the Holocene with a rapid decrease in $\delta^{13}C$ suggesting fast revegetation by C3 plants (Fleitmann et al., 2009, Gokturk et al., 2011), this may have been because of the presence of refugia in the mountains near to this site (Leroy and Arpe, 2007). Thirdly, high wildfire intensity until 9,000 years BP (Wick et al., 2003, Turner et al., 2010, Vanniere et al., 2011) would have made it difficult for trees to establish (Roberts, 2002).

Fourthly, the seasonality of precipitation may have been important. Alkenone-derived sea surface temperatures (Emeis et al., 2000, Triantaphyllou et al., 2009), speleothem fluid inclusions (McGarry et al., 2004) and glacial evidence from Anatolia (Sarıkaya et al., 2009, Zreda et al., 2011) suggest early Holocene temperatures were several degrees cooler than now. However, the prominence of *Pistacia* in the pollen record suggests winters were milder than today, with temperatures not falling below freezing (Rossignol-Strick, 1999). Therefore, the inferred drops in annual temperature must have been concentrated in the summer. There may also have been a shift in the seasonality of precipitation. An increase in winter-dominated precipitation, especially in the form of large storm events, is inferred from the large

amount of detrital material in the Soreq Cave record at this time (Ayalon et al., 1999). The lack of *Quercus brantii*, today associated with spring-season precipitation, suggests a seasonality shift to winter precipitation and drier springs and summers (Djamali et al., 2010). Summer drought conditions are also suggested by pollen records from the Aegean (summer precipitation estimated at just 60-80 mm (Peyron et al., 2011)) and fire history reconstructions (Wick et al., 2003, Turner et al., 2010, Vanniere et al., 2010, Vanniere et al., 2011). Modelling suggests an increase in winter precipitation during the early Holocene possibly caused by a southward shift in the North Atlantic storm track due to insolation changes (Brayshaw et al., 2010), but no increase in summer precipitation (Dormoy et al., 2009, Brayshaw et al., 2011a). Therefore, even though the early Holocene was 'wetter' than the late Holocene (i.e. more positive water balance), as indicated by the isotope records, summer drought would have meant soil moisture was not high enough to allow for the spread of forests (Tzedakis, 2007).

While the importance of changes in precipitation seasonality in the Near East during the Holocene are well recognised, Stevens et al. (2001, 2006) take this one step further and argue that seasonality was the key driver of $\delta^{18}O_{carbonate}$ records from Lake Zeribar and Lake Mirabad and that the increase in $\delta^{18}O_{carbonate}$ in the mid Holocene was mainly due to a shift from winter- to spring-dominated precipitation. They use pollen records (van Zeist and Bottema, 1977, Bottema, 1986), as well as ostracod and diatom records (Griffiths et al., 2001, Wasylikowa et al., 2006), to suggest that the early Holocene was in fact drier than the late Holocene, rather than a wetter early Holocene with an increased summer drought. This clearly puts their interpretation at odds with those of other Near East records. Stevens et al. (2006) suggest that the discrepancy could be explained by storm tracks flowing over Turkey that then went north over the Caspian Sea instead of over Iran. However, it is considered doubtful that the climate changed from wet to dry in Turkey and dry to wet in western Iran, since the pollen and stable isotope records are so similar (Jones and Roberts, 2008). The interpretation of the $\delta^{18}O_{carbonate}$ records by Stevens et al. (2001, 2006) is complicated. For example, Stevens et al. (2001) had interpreted a $\delta^{18}O_{carbonate}$ peak at 5,400 years BP at Lake Zeribar as showing a peak in spring rainfall

as the continental climate was re-established after the mid-Holocene transition. However, Stevens et al. (2006) argued that Sr/Ca values and pollen data suggest that the $\delta^{18}O_{carbonate}$ record at this time should not actually be interpreted as responding to changes in seasonality but rather as responding to changes in water balance and thus indicating a drought.

Another source of contention is the interpretation of the Dead Sea record. As discussed in section 2.2.1, the Younger Dryas is seen as wetter than the early Holocene (Stein et al., 2010). Additionally, based on pollen data, the early Holocene is seen to be drier than the mid and late Holocene, specifically with the period 6,300-3,500 years BP seen as receiving more than 650 mm of precipitation per year and the period 9,700-6,500 years BP less than 350 mm/year (Litt et al., 2012). Again, this runs contrary to most of the interpretations of Near East records outlined above, including the Soreq Cave record from Israel. Again, Frumkin et al. (2000), Kolodny et al. (2005), Enzel et al. (2008), Stein (2010) and Litt et al. (2012) argue that the Soreq Cave $\delta^{18}O_{carbonate}$ record should be seen as a proxy for changes in the $\delta^{18}O$ of source waters.

2.2.3 The Holocene: centennial scale climate changes

It is now well established that the Holocene, as well as seeing the multi-millennial scale trends discussed in section 2.2.2, saw abrupt centennial scale shifts (Mayewski et al., 2004, Wanner et al., 2008). In the early Holocene, three key cooling events, the Pre Boreal Oscillation (PBO), the 9.3 ka event and the 8.2 ka event, ~11,300 years BP, ~9,300 years BP and ~8,200 years BP respectively, have been linked to slowdowns of North Atlantic thermohaline circulation due to glacial outburst floods (Barber et al., 1999, Fisher et al., 2002, Clarke et al., 2004, Alley and Agustsdottir, 2005, Ellison et al., 2006, Hillaire-Marcel et al., 2007, Thomas et al., 2007, Fleitmann et al., 2008, Yu et al., 2010, Hoogakker et al., 2011, Hoffman et al., 2012). In records from the North Atlantic region, these events are seen to last 100-200 years. They are expressed in many other parts of the Northern Hemisphere as cool/dry events, for example at the time of the PBO in Yemen (Shakun et al., 2007) and Tuscany (Magny

et al., 2007), at the time of the 9.3 ka event in isotope records from Dongge Cave in China (Dykoski et al., 2005) and Qunf Cave in Oman (Fleitmann et al., 2003, Fleitmann et al., 2007) and at the time of the 8.2 ka event at Lake Van (Landmann and Kempe, 2005), Sofular Cave (Gokturk et al., 2011), in the Balkans (Bordon et al., 2009, Aufgebauer et al., 2012), Greece (Pross et al., 2009), Soreq Cave (Bar-Matthews et al., 2003, Almogi-Labin et al., 2009), Eski Acıgöl where wildfire intensity increased (Turner et al., 2008) and in the Eastern Mediterranean where Sapropel S1 was interrupted (Kotthoff et al., 2008b). While the 8.2 ka event is a short and well defined event in most records from the North Atlantic region (Daley et al., 2011), in other parts of the Northern Hemisphere climate anomalies at this time last longer and are less well defined (Rohling and Palike, 2005).

The major issue with Near East isotope records (for example Eski Acıgöl, Lake Van and Soreq Cave) for the early Holocene is that they are not at a high resolution and well-dated enough to properly investigate these centennial scale climate anomalies, meaning it is unclear in particular whether the PBO and the 9.3 ka event have so far not been seen in Near East records because there were no climate changes in the region at these times, or simply because the records thus far produced are too low resolution to pick up the changes.

However, for the mid and late Holocene in the Near East there are more records of a high enough resolution to investigate centennial scale climate changes. Three key centennial scale drought periods have been identified in Near East lake isotope records, from ~5,300-5,000, ~4,300-3,900 and ~3,100-2,800 years BP (Roberts et al., 2011a). These are of particular interest as they coincide with the ends of the Late Chalcolithic, Early Bronze Age and Late Bronze Age respectively. ~5,200 years BP, aridity can be seen in records from Lake Van (Lemcke and Stürm, 1997), the Gulf of Oman (Cullen et al., 2000), Syria (Fiorentino et al., 2008), SE Arabia (Parker et al., 2006), Lake Tecer (Kuzucuoglu et al., 2011) and east Africa (Thompson et al., 2006). Higher resolution analysis of the Soreq Cave isotope record has suggested that rather than there being one dry period, there were three separate wet-dry fluctuations each lasting 150-250 years (Bar-Matthews and Ayalon, 2011). In the

archaeological records at this time, although there is evidence that the late Uruk period society in Mesopotamia 'collapsed' (Weiss, 2003), in other areas civilisation continued to flourish (Kuper and Kropelin, 2006). A wet phase has been identified at the time of the Early Bronze Age II to Early Bronze Age III transition at Soreq Cave ~4,800-4,700 years BP (Bar-Matthews and Ayalon, 2011), followed by another ~4,500-4,300 years BP (Bar-Matthews and Ayalon, 2011) also seen at Lake Tecer (Kuzucuoglu et al., 2011) and in Syria (Fiorentino et al., 2008, Roberts et al., 2011a).

~4,200 years BP, there was period of increased aridity and climate variability (Roberts et al., 2011a), seen in records from the Gulf of Oman (Cullen et al., 2000), the Indus delta (Staubwasser et al., 2003), the Red Sea (Arz et al., 2006), NW Turkey (Ulgen et al., 2012), the Nile Delta (Bernhardt et al., 2012), Eski Acıgöl (Roberts et al., 2001), Gölhisar Gölü (Eastwood et al., 2007), Lake Tecer (Kuzucuoglu et al., 2011) and the Dead Sea (Migowski et al., 2006, Stein et al., 2010, Litt et al., 2012). At Soreq Cave, the period consisted of three dry events from 4,300-4,150, 4,050-4,000 and 3,900-3,850 years BP, with a ~20-30% reduction in precipitation (Bar-Matthews and Ayalon, 2011), again highlighting the importance of high resolution analysis in really disentangling the form of these centennial scale events. The increased aridity ~4,200 years BP could help explain a sharp decline in population, or a change in population distribution and socioeconomic activity, seen in the archaeological record at this time (Dalfes et al., 1997, Cullen et al., 2000, deMenocal, 2001, Algaze and Pournelle, 2003, Kuzucuoglu and Marro, 2007). The dry period is hypothesised to have been a major cause of the 'collapse' of the Akkadian civilisation ~4,110 years BP in Mesopotamia (Weiss, 1993), with a volcanic ash layer providing a direct temporal link between the 'collapse' and an increase in aridity inferred from Mesopotamian dust blown into the Gulf of Oman (Cullen et al., 2000). Increased aridity at this time has also been linked with the decline of the Old Kingdom of Egypt (Stanley et al., 2003) and the Harappan civilisation in the Indus valley (Possehl, 1997, Staubwasser et al., 2003).

Following a generally humid period 3,900-3,500 years BP (Roberts et al., 2011a), there was a significant drought centred on ~3,100 years BP seen at Eski Acıgöl (Roberts et al., 2001), the Sea of Galilee (Langgut et al., 2013), Lake Zeribar (Stevens

et al., 2001), the Eastern Mediterranean Sea (Emeis et al., 2000, Schilman et al., 2001), Jeita Cave (Verheyden et al., 2008), the Dead Sea (Migowski et al., 2006, Stein et al., 2010, Litt et al., 2012) and Lake Tecer (Kuzucuoglu et al., 2011). As with the aridity increases ~5,200 and 4,200 years BP, high resolution analysis suggests the drought ~3,100 years BP actually comprised several drought episodes interspersed within decades of wetter climate (Kuzucuoglu, 2009). The Hittite civilisation declined at the end of the Bronze Age, with their capital Hattusa destroyed ~3,180 years BP (Weiss, 1982). Hittite texts referred to drought at this time (Akurgal, 2001) and there were also crop failures in Syria (Kaniewski et al., 2010).

2.3 Summary

The Near East is in the transition zone between Atlantic- and monsoon-influenced climate systems and the connections between Near East hydroclimate and North Atlantic climate, the Indian Monsoon and the North Sea-Caspian Pattern Index have been identified in contemporary climate. While over the last couple of decades many palaeoclimate records have been produced for the Near East, there are still debates and unanswered questions, namely the form, timing and rapidity of the Younger Dryas to Holocene transition, the general form of the Holocene (specifically whether isotope records should be interpreted as showing a Mid Holocene Transition from wet to dry conditions or whether they should be interpreted in terms of a change in the seasonality of precipitation) and the identification of centennial scale climate changes in the Holocene. Addressing these gaps in the literature, through the production of high resolution and well-dated records and work to better constrain the drivers of $\delta^{18}O_{carbonate}$ in Near East lake isotope records, will help in the investigation of the drivers of Near East climate and the link between the climate and archaeological records.

Chapter 3 | Stable isotope analysis of lacustrine sediments

As discussed in section 1.3, stable isotope analysis of lake sediments (especially $\delta^{18}O_{carbonate}$) was selected as the best way of addressing the knowledge gaps discussed in section 1.2 and chapter 2. Here, the use of stable isotope analysis in the lacustrine environment is reviewed.

3.1 Using lake sediments as archives of environmental change

Lakes can have a variety of origins, from volcanic, to tectonic, to glacial. Over time, lakes become infilled with sediment and these sediments can be useful records of environmental change (Lowe and Walker, 1997). Lake sediments are formed of allochthonous (not formed in the lake) and autochthonous (formed within-lake) organic and inorganic material. If there is a seasonality in the precipitation of sediment fractions, for example carbonate precipitated in the summer and darker organic material throughout the rest of the year, and if the conditions are right (usually stratification of lake waters and anoxic conditions at the bottom to limit turbidity and biological activity), annually laminated/varved sediments can form and be preserved (O'Sullivan, 1983, Ojala et al., 2012). Varved sediments are particularly useful for palaeoenvironmental work as they allow a robust chronology to be derived and for the investigation of annual to sub annual changes in lake conditions.

Lake sediments are composed of a number of components. There are a number of types of carbonate that can form in lakes, the most common being calcite and aragonite, which are chemically the same ($CaCO_3$) but have different crystal structures, and dolomite ($CaMg(CO_3)_2$). While calcite and aragonite are often endogenic, precipitating directly from lake waters (e.g. Romero-Viana et al., 2008, Sondi and Juracic, 2010, Viehberg et al., 2012), the formation of dolomite is more variable, with many studies suggesting a diagenetic origin (Kelts and McKenzie, 1982, Mazzullo, 2000, Vasconcelos et al., 2005). Shifts from precipitation of calcite to aragonite are often linked to evaporatively-driven increases in the Mg/Ca ratio

(Muller et al., 1972, Kelts and Hsu, 1978, Ito, 2001), and dolomite is almost exclusively found in lakes with high Mg/Ca ratios (Last, 1990). Precipitation of endogenic carbonate may be initiated by algal blooms, which draw down CO_2, thereby raising the pH of the lake water and leading to carbonate supersaturation (Siegenthaler and Eicher, 1986, Bronmark and Hansson, 2005, Deocampo, 2010). Biogenic carbonates (the calcareous skeletons and shells of organisms) and detrital carbonate material washed in from the catchment can also be found in lake sediments. Non-carbonate components include diatom silica, organic matter from plants and detrital silicates washed into the lake from the catchment. The isotopic composition of these different components of lake sediments change as variables such as temperature, the isotopic composition of lake waters and catchment vegetation change, and looking at this variability over time can allow for the reconstruction of environment and climate.

3.2 Stable isotope analysis theory

An isotope of an element differs from another by having a different number of neutrons. For example, oxygen has three naturally occurring isotopes: ^{16}O with 8 protons and 8 neutrons, ^{17}O with 8 protons and 9 neutrons and ^{18}O with 8 protons and 10 neutrons. Different isotopes have slightly different physical and chemical properties, and this means the relative proportion of the different isotopes can change in a process known as fractionation.

It was first suggested by Briscoe and Robinson (1925) that physical chemical processes could cause isotopic fractionation of elements. There are two types of processes that can cause fractionation: equilibrium and kinetic effects. In equilibrium fractionation, the forward and backward reaction rates of an isotope are identical: there is no net reaction (Hoefs, 2009). For example, during condensation, the isotopic composition of the liquid and gas phases will change, but the isotopic composition of the liquid and gas phases as a whole will be constant, with fractionation dependent entirely upon temperature. In kinetic fractionations, forward and backward reaction rates are not identical: they are incomplete and

potentially unidirectional processes (Hoefs, 2009). Evaporation is generally a kinetic process, with lighter isotopes preferentially evaporated because their bonds are more easily broken, and air flow removing the evaporated water vapour from the system. Most biological processes are kinetic, with organisms preferentially utilising lighter isotopes because it requires less energy to break their bonds.

Isotope ratios are measured on mass spectrometers. The substance from which isotope data are required is converted to gas (carbonates for example are reacted with acid to produce CO_2), which is then ionised and accelerated through a magnetic field that deflects ions according to their ratio of charge to mass. Light ions are deflected more strongly than heavier ones of the same charge. Multiple collectors are used to collect ions of different masses at the same time (for example for CO_2 masses 44, 45 and 46), and measurements are made by passing the ions through resistors and measuring the intensity of the electrical current produced. The isotopic composition of a sample is measured relative to the isotopic composition of a reference gas in a mass spectrometer. In order for data produced in different laboratories to be compared, references gases are produced relative to an international standard. Carbonate and organic isotope data are given relative to the isotopic composition of Vienna Pee Dee Belemnite (VPDB) and water and diatom silica relative to Vienna Standard Mean Ocean Water (VSMOW). Relative differences in isotopic ratios can be determined far more precisely than absolute isotopic ratios so the delta (δ) notation is used:

$$\delta = \frac{(\text{Rsample} - \text{Rstandard})}{\text{Rstandard}} \text{ x } 1000 \qquad 3.1$$

where R is the ratio of the heavy isotope to light isotope, reported in per mil (‰). A positive δ means the ratio of the heavy to light isotope is higher than in the standard.

3.3 Controls on $\delta^{18}O$ of lake waters

The oxygen isotope composition of lake waters depends on two key factors: the isotopic composition of the input (precipitation) and any modifications to this within

the lake (Leng and Marshall, 2004). The oxygen isotopic composition of precipitation ($\delta^{18}O_{precipitation}$) is a function of a number of factors. The initial influence is $\delta^{18}O$ of the moisture source, as well as sea surface temperature, the relative humidity of the atmosphere and wind regime when the initial water mass evaporates (Darling et al., 2006). Once evaporated, other factors become important, including temperature.

As temperature decreases, $\delta^{18}O_{precipitation}$ becomes lower for two reasons. Firstly, heavier isotopes are preferentially condensed, so the colder it gets the more isotopically depleted the precipitation will be. Secondly, the isotope fractionation factor is temperature dependent. These two factors combined mean that, generally, $\delta^{18}O_{precipitation}/T$ is roughly equal to +0.2-0.7‰°C^{-1} (Dansgaard, 1964), averaging +0.6‰°C^{-1} in mid to high latitudes (Rozanski et al., 1992) (Figure 3.1).

As distance from the moisture source increases, $\delta^{18}O_{precipitation}$ becomes more depleted, because heavier isotopologues ($^{2}H^{1}H^{16}O$ and $H_2{}^{18}O$) are preferentially rained-out. The lowering of temperature with increased altitude additionally leads to progressive isotopic depletion. The type of precipitation is also important. While the isotopic composition of rainfall near the ground surface is close to isotopic equilibrium with near-ground water vapour because raindrops continuously re-equilibrate with the surrounding moisture after leaving the cloud, snow and hail do not and instead reflect equilibrium conditions in the cloud so are more isotopically depleted (Darling et al., 2006). Finally, the amount of precipitation can be important (Dansgaard, 1964). Usually heavier isotopologues are rained-out first but in intense storms even lighter isotopologues will quickly be rained-out, so $\delta^{18}O_{precipitation}$ will be lower than would otherwise be expected.

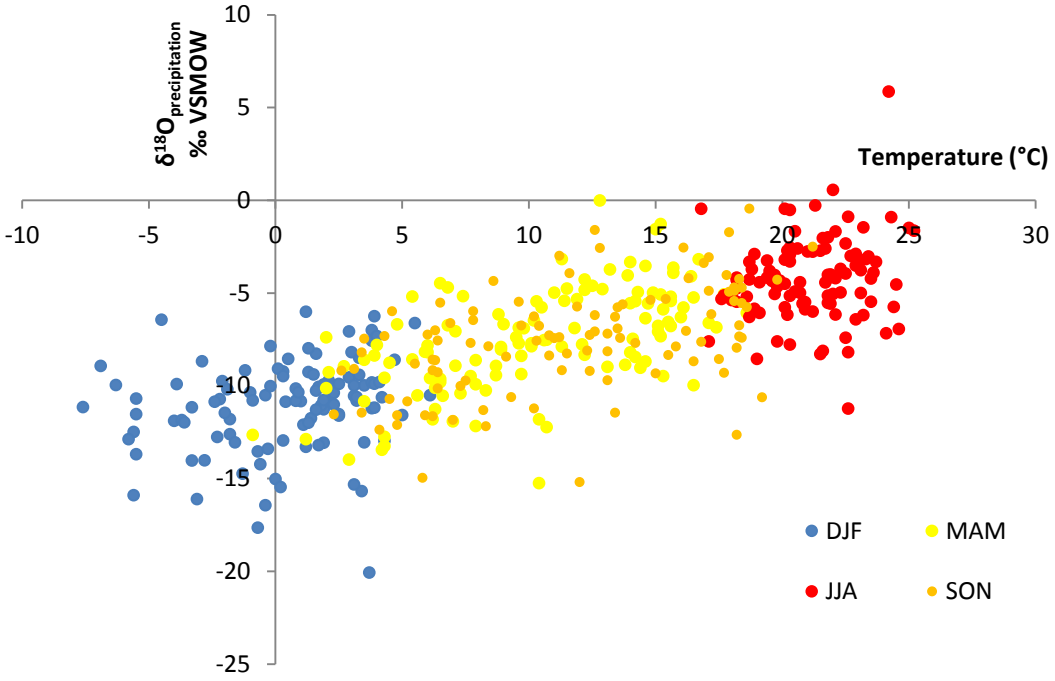

Figure 3.1 *Data from Ankara GNIP station 1964-2009 (IAEA/WMO, 2013) showing the strong relationship between* $\delta^{18}O_{precipitation}$ *and temperature* ($r^2 = 0.55$)*, with* $\delta^{18}O_{precipitation}$ *values for June, July and August (JJA) ~5‰ higher than December, January and February (DJF) values and an overall* $\delta^{18}O_{precipitation}/T$ *relationship of +0.32‰°C*$^{-1}$*.*

The average isotopic composition of precipitation varies globally. Craig (1961) surveyed the isotopic composition of precipitation worldwide and suggested a best fit line, termed the Global Meteoric Water Line (GMWL):

$$\delta D = 8 \times \delta^{18}O + 10 \qquad 3.2$$

Deviations from the GMWL are found in many regions, leading to Local Meteoric Water Lines (LMWL; Figure 3.2).

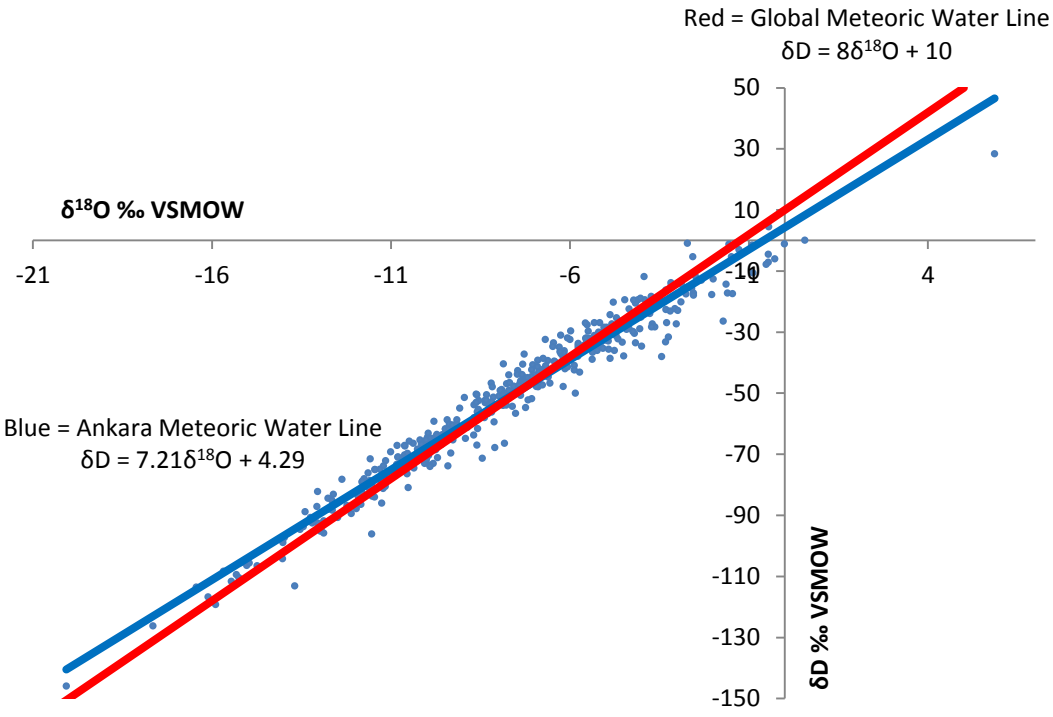

Figure 3.2 *Data from Ankara GNIP station 1964-2009 showing the difference between the Ankara Meteoric Water Line and the Global Meteoric Water Line (IAEA/WMO, 2013).*

The isotopic composition of precipitation that has made its way into a lake may be further modified as the result of within-lake processes, such as evaporation, which are influenced by lake size and the degree of hydrological closure (Table 3.1). Since $\delta^{18}O_{precipitation}$ is variable on short time scales (Darling, 2004), in very small lakes, with short residence times, $\delta^{18}O_{lakewater}$ will not be averaged out sufficiently to reflect mean annual precipitation and seasonal influences will be important (Leng and Marshall, 2004). However, in larger, well-mixed lakes, $\delta^{18}O_{lakewater}$ should be less sensitive to seasonal variations. In hydrologically open lakes, where there is substantial inflow and outflow, $\delta^{18}O_{lakewater}$ tends to plot near the LMWL and values are often assumed to reflect $\delta^{18}O_{precipitation}$ (Leng et al., 2006). In closed lakes, where there is limited inflow and outflow, $\delta^{18}O_{lakewater}$ will plot off the GMWL/LMWL on a local evaporation line. Therefore, $\delta^{18}O_{lakewater}$ in closed lakes is more related to the balance between the isotopic composition of inputs and outputs than to

$\delta^{18}O_{precipitation}$ (Leng et al., 2006). The degree to which $\delta^{18}O_{lakewater}$ is enriched depends on the precipitation:evaporation ratio and the residence time of the lake.

Table 3.1 *The predominant controls of $\delta^{18}O_{lakewater}$ depend on the size of the lake and its degree of hydrological closure (modified from Leng and Marshall, 2004).*

	Very small lake	**Small/medium open lake**	**Small/medium closed lake**	**Large lake**
Residence time	<1 year	>1 year	Decades	Centuries
Main forcing	Seasonality, temperature, $\delta^{18}O_{precipitation}$	Temperature, $\delta^{18}O_{precipitation}$	Precipitation-evaporation ratio	Precipitation-evaporation ratio

3.4 Controls on $\delta^{18}O$ of lake carbonates

If carbonate is precipitated in equilibrium with lake waters, $\delta^{18}O_{carbonate}$ is dependent entirely upon temperature (with a fractionation factor of ~–0.24‰°C^{-1}) and $\delta^{18}O_{lakewater}$. However, disequilibrium effects (known as vital effects in biogenic materials), where carbonates do not precipitate in equilibrium with the lake water, can alter $\delta^{18}O_{carbonate}$ values. For example, almost all freshwater ostracods exert a small vital effect, increasing $\delta^{18}O$ in comparison to equilibrium precipitates (Holmes and Chivas, 2002). Also, where mineral precipitation rates are especially high, kinetic fractionation may mean that $\delta^{18}O_{carbonate}$ values are 2-3‰ below that expected for equilibrium fractionation (Fronval et al., 1995). Another problem that may be encountered is in-wash of old carbonates from the catchment (Leng et al., 2010).

Issues also arise when attempting to produce isotope records from lake cores that contain different types of carbonate because they have different mineral-water fractionation factors, meaning changes in mineralogy can distort the $\delta^{18}O$ signal and make it more difficult to accurately discern climate shifts. As will be discussed in more detail in section 6.3.5, aragonite is ~0.7‰ more positive than calcite formed

under the same conditions and dolomite ~2.7‰ more positive than calcite formed under the same conditions (Hays and Grossman, 1991, Vasconcelos et al., 2005, Kim et al., 2007a). Another issue is that if carbonates form at different times or in different parts of the lake, there will be an additional offset to apply because of differences in temperature and $\delta^{18}O_{lakewater}$ at the times and locations of their formation (e.g. Leng et al., 2013).

3.5 Controls on $\delta^{18}O$ of diatom silica

Diatoms are siliceous algae and their frustules are composed of two layers: a tetrahedrally bonded silica (-Si-O-Si) layer and an outer hydrous (-Si-OH) layer. The former contains oxygen incorporated during silicification, on which oxygen isotope analysis can be carried out (Leng and Swann, 2010). The controls on $\delta^{18}O_{diatom}$ are very similar to those on $\delta^{18}O_{carbonate}$ (Leng and Barker, 2006). The diatom silica-water fractionation factor is ~–0.2‰°C^{-1} (Brandriss et al., 1998, Moschen et al., 2005, Crespin et al., 2010). While Swann et al. (2007, 2008) suggested there could be significant isotope offsets between different (marine) species formed under the same conditions, other studies (Brandriss et al., 1998, Schmidt et al., 2001, Moschen et al., 2005, Schiff et al., 2009) suggest no disequilibrium effect within or between individual diatom taxa. Diatom samples need to be cleaned sufficiently so that minerogenic contamination does not significantly influence $\delta^{18}O_{diatom}$, or mass balance corrections need to be applied to account for the effect of the contamination on $\delta^{18}O_{diatom}$ (e.g. Brewer et al., 2008, Mackay et al., 2011).

3.6 Reconstructing seasonality

Reconstruction of the seasonality of climate, as opposed to annual average conditions or of one season, is increasingly being attempted. Reconstructions of seasonality using isotope analysis of lake sediments have recently been published (e.g. Henderson et al., 2010, Anderson, 2011, Barker et al., 2011, Aguilera et al., 2012, Masi et al., 2013). Orland et al. (2009, 2012) investigated seasonality using oxygen isotope analysis of speleothems from the Soreq Cave, Israel. Pollen has been

used to reconstruct seasonality (e.g. Dormoy et al., 2009, Milner et al., 2012) but because of long history of human occupation in Near East, this proxy often does not provide a clear signal (Peyron et al., 2011).

It was first proposed by Leng et al. (2001) that if carbonates and diatom silica are precipitated at different times of the year, comparing $\delta^{18}O$ from the two hosts could provide information on seasonality. Working on a sediment sequence from hydrologically open Lake Pinarbaşi in Turkey and assuming carbonates were precipitated in the summer and diatoms grew throughout the year but especially in the spring and autumn, they suggested $\delta^{18}O_{carbonate}$ was a proxy for mean summer temperature and $\delta^{18}O_{diatom}$ a proxy for spring snow melt, accounting for the substantial differences between $\delta^{18}O$ trends from the two hosts. Large differences were also seen in the record from Lake Gościąż in Poland (Rozanski et al., 2010), again seemingly because of differences in the time of year of diatom growth and carbonate precipitation. In contrast, a study by Lamb et al. (2005), using the sediments of Lake Tilo in the Ethiopian Rift Valley, found that while $\delta^{18}O_{diatom}$ was more variable (interpreted as being the result of tephra contamination) and did not pick up two arid events seen in the $\delta^{18}O_{carbonate}$ record, the general trends were the same because diatom growth and carbonate precipitation occur at similar times of the year. Therefore, with knowledge of the times of year of diatom growth and carbonate precipitation, and if contamination in diatom isotope samples can be dealt with, comparison of $\delta^{18}O$ from the two hosts can provide insights into seasonality.

3.7 Controls on $\delta^{13}C$ of lake carbonates and organic matter

$\delta^{13}C$ of dissolved inorganic carbon (DIC) in lake waters is controlled by three main factors, with the typical changes in $\delta^{13}C$ through the system summarised on Figure 3.3. Firstly, the isotopic composition of inflowing waters is important. Groundwaters and rivers typically have $\delta^{13}C$ values for calcite between –10 and –15‰. Most of the carbon flowing into lakes comes from plants and soils, and $\delta^{13}C$ will be influenced by plant type since C4 plants have higher $\delta^{13}C$ values than C3 plants (Figure 3.3). Secondly, in closed lakes there is sufficient time for CO_2 exchange between the

atmosphere and the lake water and as ^{12}C is preferentially degassed $\delta^{13}C_{DIC}$ can increase. Atmospheric CO_2 has a $\delta^{13}C$ value of ~–7.8‰ and under isotopic equilibrium $\delta^{13}C_{DIC}$ in a lake will be ~+2‰ (Leng and Marshall, 2004). Thirdly, there is preferential uptake of ^{12}C by aquatic plants during photosynthesis, meaning that as these plants die and take their ^{12}C to the bottom of the lake, $\delta^{13}C_{DIC}$ increases. Conversely, if organic material on the lake bottom is then oxidised, ^{12}C will be released back into the lake carbon pool (Leng and Marshall, 2004). Preferential draw down of ^{12}C by sulphate-reducing bacteria (Kelts, 1988, Komor, 1994, Fenchel et al., 1998) and methanogens (e.g. Aloisi et al., 2000) in the sediment can decrease $\delta^{13}C_{DIC}$, although methanogenesis can often result in very positive $\delta^{13}C_{DIC}$ values if the CH_4 produced escapes into the lake water (Talbot and Kelts, 1986, Gu et al., 2004, Leng et al., 2013).

During the precipitation of carbonate from lake waters, there is a only a small and predictable fractionation effect, meaning $\delta^{13}C_{carbonate}$ is ~1‰ more positive than $\delta^{13}C_{DIC}$ (at 16°C) (Leng and Marshall, 2004). Consequently, $\delta^{13}C_{carbonate}$ can provide insights into past changes in $\delta^{13}C_{DIC}$. $\delta^{13}C_{carbonate}$ is also influenced by changes in carbonate mineralogy. Less is known about the effect on carbon isotopes than on oxygen isotopes, but it has been estimated that aragonite $\delta^{13}C$ values are ~1.8‰ more positive than equivalent calcite values (Rubinson and Clayton, 1969, Grossman, 1984). An important use of $\delta^{13}C_{carbonate}$ data is to support the interpretation of $\delta^{18}O_{carbonate}$ data. If $\delta^{13}C_{carbonate}$ and $\delta^{18}O_{carbonate}$ co-vary (r>0.7), then a lake is seen to be hydrologically closed (Talbot, 1990), although it is now recognised that the relationship is more complex than this, with covariation only apparent in lakes that have attained hydrological closure over extended time frames (Li and Ku, 1997).

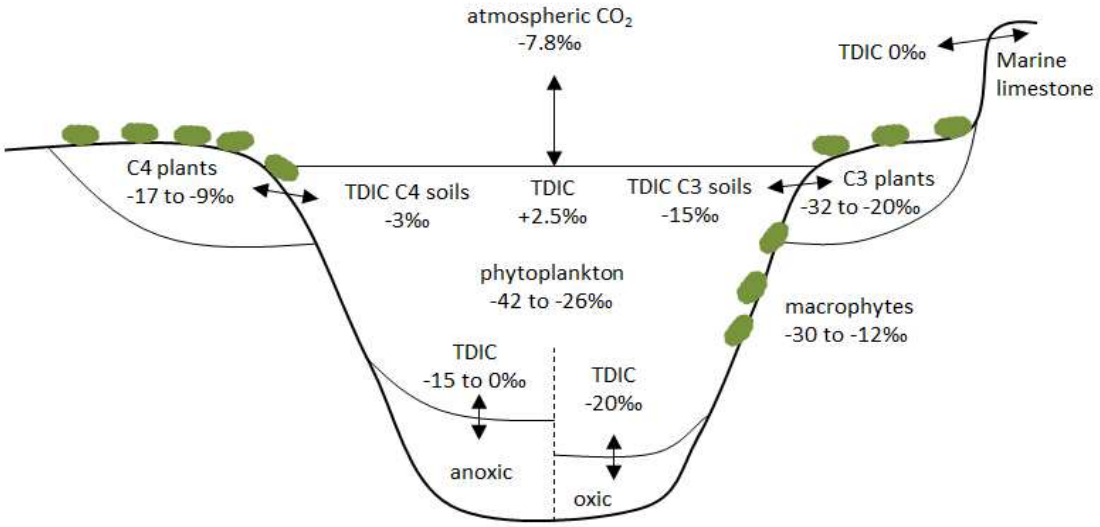

Figure 3.3 *$\delta^{13}C$ values for the major carbon sources in lakes and examples of resulting $\delta^{13}C_{DIC}$. Modified from Leng and Marshall (2004).*

$\delta^{13}C$ is also measured on lacustrine organic matter. It is dependent on DIC, as discussed above, from which aquatic plants fix their carbon, and on differences in $\delta^{13}C$ between types of organic matter (Meyers and Teranes, 2001, Leng and Marshall, 2004). $\delta^{13}C_{organic}$ data are interpreted in conjunction with C/N ratios (Figure 3.4). C/N values of <10-12 are typical of lacustrine algae, 10-20 of submergent and floating aquatic macrophytes and >20 of emergent macrophytes and terrestrial plants. C3 plants typically fractionate CO_2 (~–7.8‰) into $\delta^{13}C$ values of ~–27‰ and C4 plants into values of ~–13‰ (Meyers and Teranes, 2001). When most of the carbon is from terrestrial sources, $\delta^{13}C_{organic}$ will mainly reflect changes in the type of vegetation, with an increase suggesting increases in C4 plant growth and hence increased aridity. When most of the carbon is from aquatic sources, $\delta^{13}C_{organic}$ can be used as a reliable palaeoproductivity proxy. Even small changes in the type of vegetation can make interpretation of bulk $\delta^{13}C_{organic}$ in terms of palaeoproductivity problematic, so $\delta^{13}C$ is being increasingly carried out on specific biomarkers and on diatoms (Street-Perrott et al., 2004, Barker et al., 2013, Leng and Henderson, 2013).

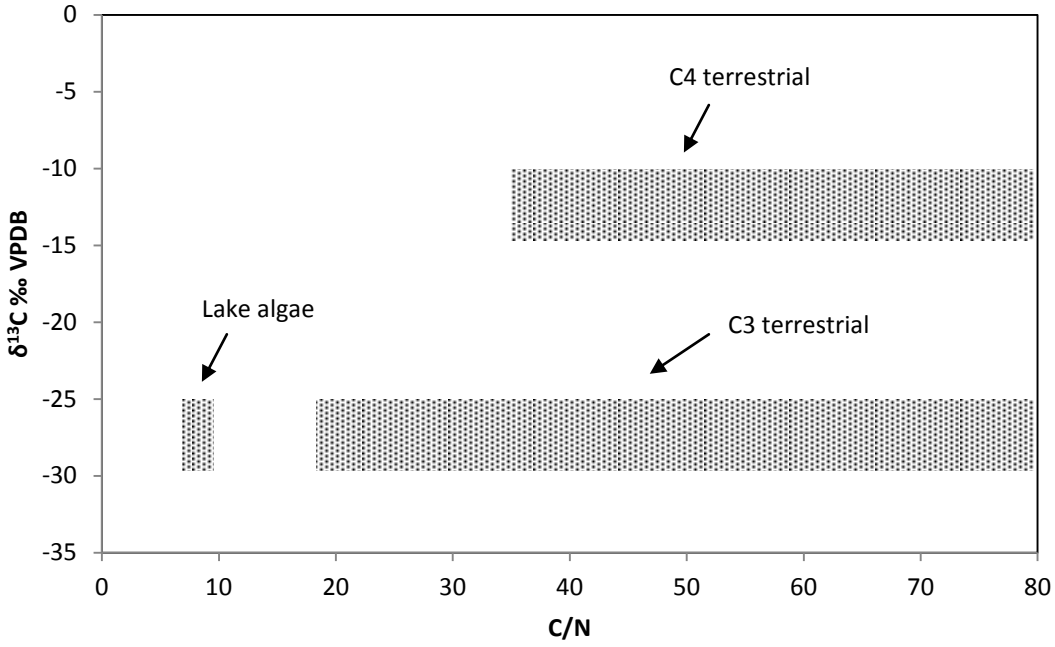

Figure 3.4 *Typical $\delta^{13}C$ and C/N ratios of terrestrial and lake-derived organic matter. $\delta^{13}C$ of terrestrial C3 plants and lake algae can be very similar, but the two sources can be distinguished using C/N ratios (Meyers and Teranes, 2001).*

3.8 Summary

Isotope analysis of lake sediments can be used to reconstruct past climate changes, but careful consideration of the controls of the isotope signal is required. In open lakes, $\delta^{18}O_{carbonate}$ often reflects $\delta^{18}O_{precipitation}$, whereas in closed lakes it is often used as a proxy for changes in water balance. It has been proposed that $\delta^{18}O_{carbonate}$ and $\delta^{18}O_{diatom}$ data can be compared to provide insights into palaeoseasonality. $\delta^{13}C$ from bulk organic matter is difficult to interpret but can be used to investigate changes in the sources of organic matter and productivity. Because isotopic records are dependent on multiple climatic and non-climatic variables that will differ between sites, each lake isotope record must be interpreted within its own isotopic setting: an understanding of the modern system is vital if sediment core records are to be properly interpreted (chapter 7).

Chapter 4 | Uranium-thorium dating of lacustrine sediments

U-Th dating was selected as the best potential method to produce age-estimates for the Nar Gölü sequence, to supplement the varve chronology, because radiocarbon dating had been shown to be difficult (Jones, 2004) and there is carbonate present that could be analysed. In this chapter, the application of U-Th dating to lacustrine sediments and the potential issues that may be encountered are discussed.

4.1 Principles of U-Th dating

U-Th dating is a radiometric technique used on carbonates from sediments spanning the time period from hundreds to over 500,000 years (Walker, 2005). It does not measure the accumulation of stable isotopes, like U-Pb dating, but rather calculates age by measuring the extent to which equilibrium has been restored between ^{230}Th and ^{234}U, nuclides that are part of a longer decay series beginning at ^{238}U and ending at ^{206}Pb (Figure 4.1). At a time equal to ~7 half-lives of ^{230}Th, in a closed system, the decay series ^{238}U to ^{234}U to ^{230}Th should reach near secular equilibrium (Bourdon et al., 2003, Zhao et al., 2009), with the activity (number of disintegrations per unit time per unit weight of material (Walker, 2005)) of all nuclides in the decay series equal (i.e. [^{234}U/^{238}U] and [^{230}Th/^{234}U] = 1). Fractionation, which resets this decay sequence and causes disequilibrium, is the premise behind U-Th dating. In the lacustrine environment, because uranium is more soluble than thorium, the former tends to be precipitated with calcium and incorporated into calcite and aragonite crystals as a trace element whereas the latter is very insoluble so tends to be found in lower quantities in lake waters (Edwards et al., 2003). Therefore, in lake sediments there is, theoretically, an initial state of disequilibrium, with [^{230}Th/^{234}U] at zero. As ^{234}U decays, the amount of ^{230}Th in the calcite will increase. Over time, the system will progress towards secular equilibrium, and the predictability of this allows the age since fractionation to be established. The basic ^{230}Th age equation, originally from Broecker (1963), was re-expressed by Haase-Schramm et al. (2004) as:

$$\left[\frac{230_{\mathrm{Th}}}{238_{\mathrm{U}}}\right] = \left(1 - e^{-\lambda_{230}t}\right) + \left(\left[\frac{234_{\mathrm{U}}}{238_{\mathrm{U}}}\right] - 1\right) \mathrm{x} \left(\frac{\lambda_{230})}{(\lambda_{230} - \lambda_{234}}\right) \mathrm{x} \left(1 - e^{-(\lambda_{230} - \lambda_{234})t}\right) \quad 4.1$$

where square brackets symbolise activity ratios, λ = decay constant and t = age. The equation is solved for age iteratively or graphically (Figure 4.2). Initial [^{234}U/^{238}U] disequilibrium, due to the preferential weathering of ^{234}U, also needs to be taken into account, using the equation expressed by Haase-Schramm et al. (2004) as:

$$\left[\frac{234_{\mathrm{U}}}{238_{\mathrm{U}}}\right]_{\mathrm{initial}} = \left[\frac{234_{\mathrm{U}}}{238_{\mathrm{U}}}\right] \mathrm{x}\, e^{\lambda_{234}t} - 1) \quad 4.2$$

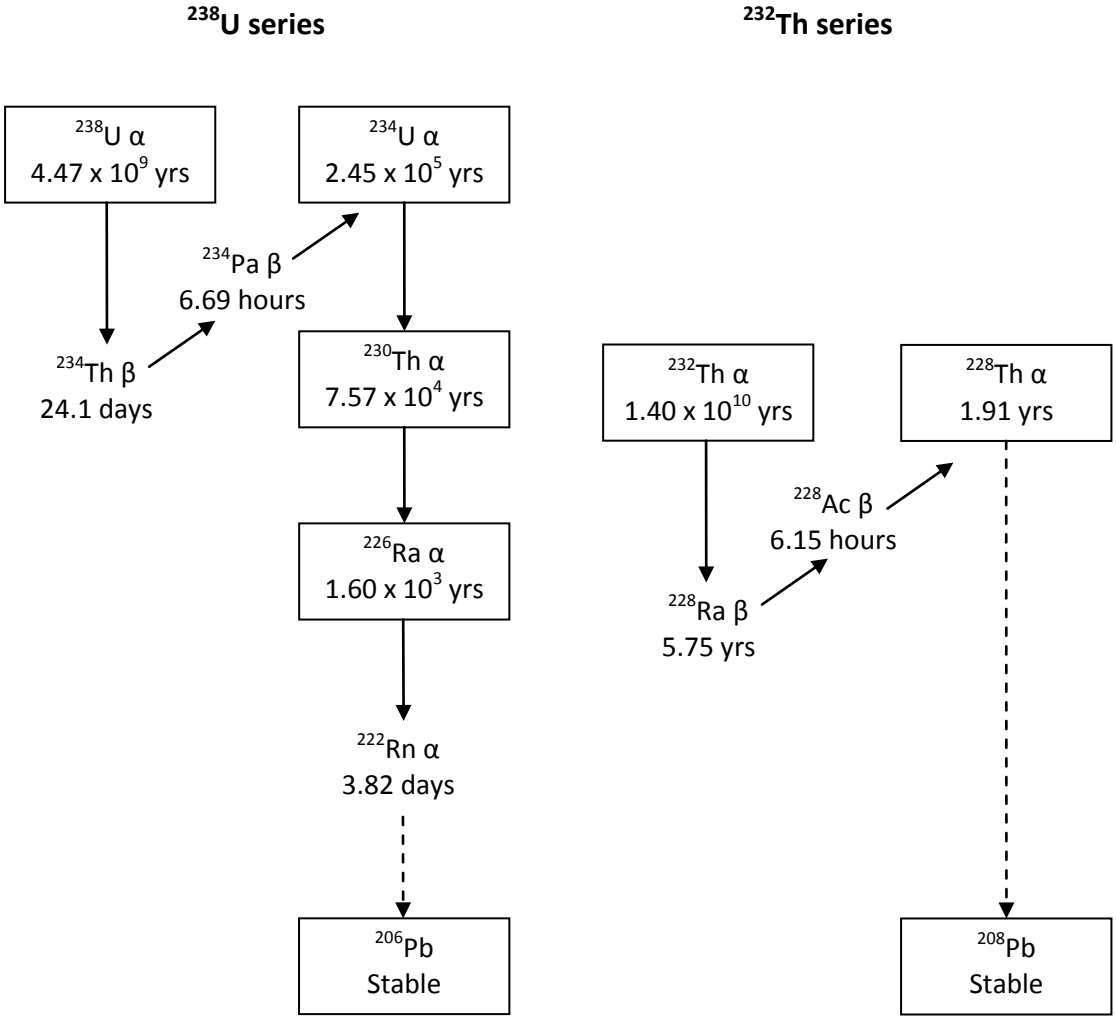

Figure 4.1 *^{238}U and ^{232}Th decay series, with half lives taken from Bourdon et al. (2003) and references therein.* α *signifies alpha decay and* β *beta decay.*

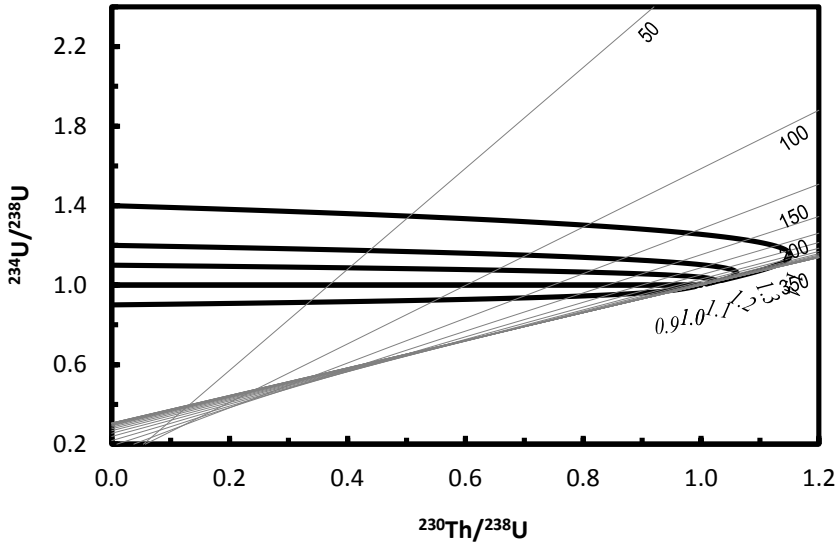

Figure 4.2 *Graph from Isoplot software (Ludwig, 2012) used to calculate U-Th age.*

Eq. 4.1 should only be used when two key assumptions are met: (1) that the system has been closed, i.e. that there has been no addition or removal of nuclides since deposition, and (2) that initial [^{230}Th/^{238}U] = 0 (Walker, 2005).

4.2 Open system behaviour

The first assumption may be violated if calcite or aragonite undergoes recrystallisation (Lao and Benson, 1988) and strategies for checking this assumption has not been violated include verification by an independent dating source and petrographic and geochemical evidence for a lack of alteration (Placzek et al., 2006). The unpredictability of open system behaviour and the resultant uranium loss (which could lead to an increase in U-Th age from actual age) means it is presently not possible to correct for the effect of this.

4.3 When initial [^{230}Th/^{238}U] ≠ 0: detrital contamination and hydrogenous thorium

Ideally for U-Th dating, there would be a complete fractionation of uranium and thorium when sediments are laid down, with only uranium incorporated into carbonates. However, initial thorium can come from detrital material (detrital thorium) or from the water column (hydrogenous thorium), and without correction leads to age-estimates older than the date the sediment was actually deposited.

Firstly, a situation where hydrogenous thorium is negligible is considered. It is difficult to separate the carbonate and detrital components physically or chemically so it has to be corrected for after analysis (Bischoff and Fitzpatrick, 1991). If the amount of detrital material is small, initial ^{230}Th can be corrected for using the [^{230}Th/^{232}Th] ratio (e.g. Fritz et al., 2007). However, usually the total sample dissolution isochron approach (Bischoff and Fitzpatrick, 1991, Luo and Ku, 1991) needs to be used when working with lake sediments (e.g. Rowe et al., 1999, Roberts et al., 2001, Haase-Schramm et al., 2004, Sakaguchi et al., 2009, Shanahan et al., 2013, Torfstein et al., 2013). Here, samples are assumed to be comprised of two components, the carbonate and detrital fractions. By analysing three or more sub samples with varying proportions of the two components from the same level in the core, it is possible to extrapolate to an end-member that only contains ^{230}Th produced from radioactive decay (Edwards et al., 2003).

The presence of hydrogenous thorium, in addition to detrital thorium, complicates the correction, because the isochron approach assumes that initial [^{230}Th/^{232}Th] is the same between sub-samples. If there are variable mixtures of detrital and hydrogenous components with different [^{230}Th/^{232}Th] ratios, there will be different initial [^{230}Th/^{232}Th] values between sub samples. Hydrogenous thorium could be incorporated into carbonates from the water column after attaching to particles that are then incorporated into carbonates or directly from the water into carbonates (Lin et al., 1996). If hydrogenous thorium is absorbed by detrital particles with a constant water-particle partition coefficient and if detrital thorium is constant, then the

hydrogenous thorium to detrital thorium ratio will be the same among sub samples (Lin et al., 1996) (Figure 4.3).

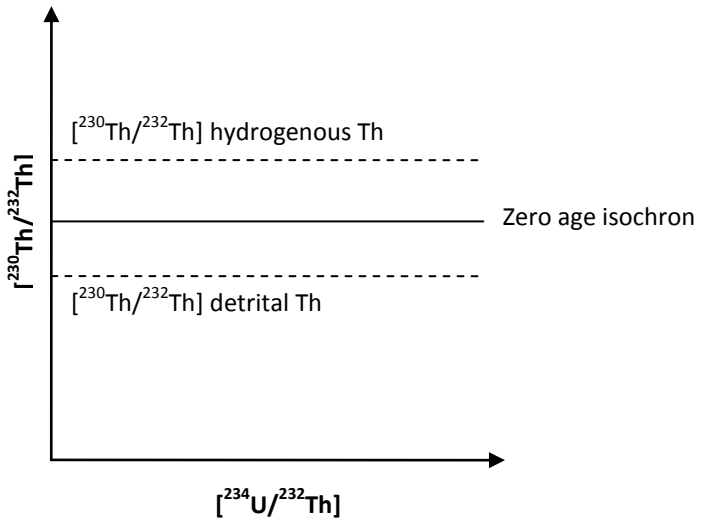

Figure 4.3 *Effect of detrital thorium and hydrogenous thorium absorbed by detrital particles on zero age isochron (modified from Lin et al., 1996).*

If the uptake of hydrogenous thorium is by direct inclusion of dissolved thorium into the carbonate crystal structure in constant proportion to the amount of authigenic uranium, the zero age isochron will have a positive slope (Lin et al., 1996) (Figure 4.4).

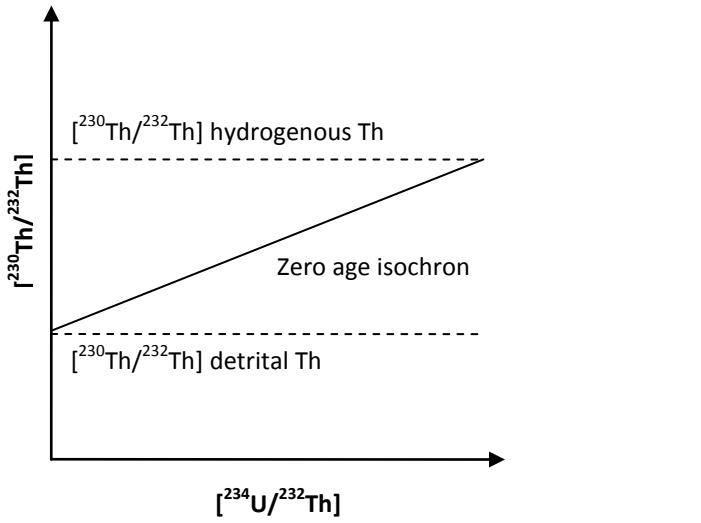

Figure 4.4 *Effect of detrital thorium and hydrogenous thorium directly included into carbonates on zero age isochrons (modified from Lin et al., 1996).*

Where there is hydrogenous thorium from both detrital-absorption and direct incorporation, the situation is more complicated, with different mixing slopes between hydrogenous and detrital thorium. If there is a significant amount of direct incorporation of hydrogenous thorium into carbonates and/or if [^{232}Th/^{234}U] of the carbonate phase is significantly greater than zero, there will be a positive slope on the zero age isochron (Figure 4.5).

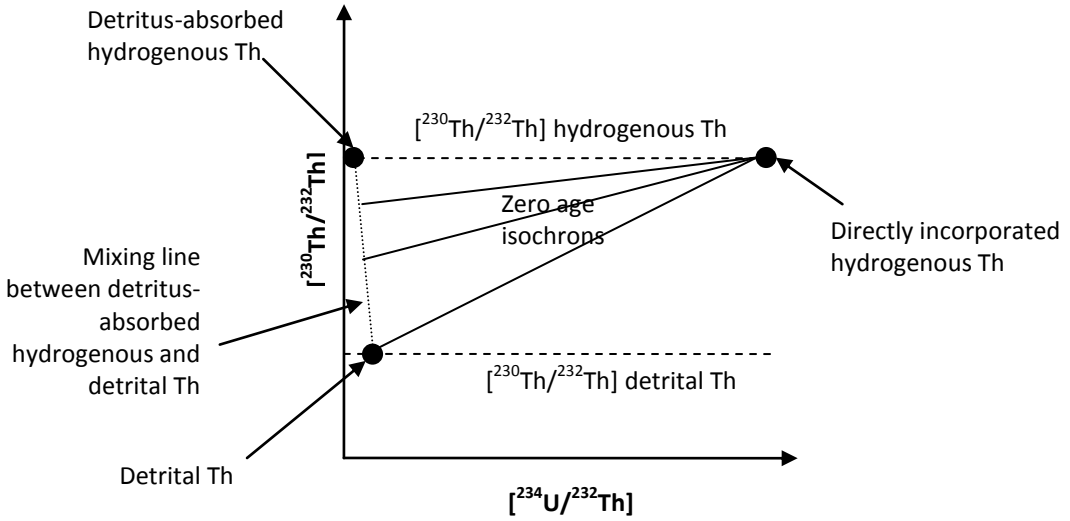

Figure 4.5 *Effect of detrital thorium and hydrogenous thorium both directly included into carbonates and absorbed onto detrital particles on zero age isochrons, with zero age isochrons varying at one end along a mixing line between hydrogenous and detrital thorium and pivoted at the other end at the value of directly incorporated hydrogenous thorium (modified from Lin et al., 1996).*

Haase-Schramm et al. (2004) and Torfstein et al. (2009, 2013) have established the state-of-the-art for dealing with hydrogenous thorium, based on their work on the Dead Sea sediments. Modern aragonite found precipitating on driftwood was analysed and after the isochron correction the ages were still 340 years too old. Therefore, all other isochron ages were adjusted by simply subtracting 340 years, assuming the offset was constant through time. This offset is fairly small, because

there was not much difference in [^{230}Th/^{232}Th] between the detrital and hydrogenous thorium components.

4.4 Developments in mass spectrometric methods

In the 1980s, thermal ionisation mass spectrometry (Edwards et al., 1987, Ludwig et al., 1992, Stirling et al., 1995) replaced alpha counting as the way to measure uranium and thorium activity ratios, allowing ratios greater than 10^5 to be measured (Goldstein and Stirling, 2003). More recently, multi-collector inductively coupled plasma mass spectrometers (MC-ICP-MS) (Halliday et al., 1995, Hellstrom, 2003, McCulloch and Mortimer, 2008, Shen et al., 2012) have increased the speed and sensitivity of measurements. The advantages of ICP-MS include the efficient ionisation of most elements and effectively a constant mass discrimination of the plasma source that can be precisely corrected for and is considered to be independent of the chemical properties of the element (Goldstein and Stirling, 2003).

4.5 Summary

In lakes, because uranium is more soluble than thorium, the former is more readily incorporated into carbonates, hence causing fractionation and disequilibrium in the uranium decay series. U-Th dating is based on the calculation of the extent to which equilibrium has been restored between ^{230}Th and ^{234}U. Potential issues include open system behaviour and the presence of detrital and hydrogenous sources of thorium, meaning that U-Th dating of lake sediments is in general more difficult and less accurate than U-Th dating of speleothems.

Chapter 5 | Site description and previous work at Nar Gölü

This chapter provides an introduction to the site and gives details of the previous work undertaken.

5.1 Overview

Nar Gölü is a small (~0.7 km^2) but relatively deep (>20 m) lake in the Cappadocia region of central Turkey (Figures 5.1 and 5.2). It is a maar lake (Gevrek and Kazanci, 2000), formed by water infilling of a crater produced by an explosion resulting from groundwater-magma interaction (Cohen, 2003). As described in Woodbridge and Roberts (2011), the lake is weakly alkaline and oligosaline to mesosaline, with sodium and chloride the major ions. The lake is thought to be monomictic.

Figure 5.1 *Location of Nar Gölü (38°20'24.43"N, 34°27'23.69"E, 1363 m.a.s.l.) in central Turkey, with Niğde (37°58'N, 34°41'E, 1300 m.a.s.l.; site of the nearest meteorological station) and Ankara (39°52'N, 32°52'E, 940 m.a.s.l.; site of the nearest GNIP station) also shown.*

Nar Gölü lies within the Göllüdağ volcanic complex, with the crater itself dated to around 1.6-1.3 million years BP (Gevrek and Kazanci, 2000). The east and west sides

of the crater are comprised mainly of basalt, with the southern side dominated by ignimbrite (visible as lighter deposits on the far side of the lake on Figure 5.2A) (Gevrek and Kazanci, 2000). The volcanic geology means there is plenty of silica available for diatom growth and the pH of ~8 means both carbonates and diatoms are preserved in sediments. The lack of carbonate in the catchment removes the potential for problems associated with detrital carbonate contamination (Leng et al., 2010).

Figure 5.2 *A: Nar Gölü in July 2010, looking south at ignimbrite outcrops, taken during the main coring period during the hottest July on record. B: In February 2012, the lake surface was partly frozen and snow >50 cm deep blanketed the catchment.*

The small surface area compared to depth and the anoxic conditions at the bottom of the lake lead, presently, to the preservation of varved sediments (section 3.1). At the southern end of the lake there is an alluvial fan (but with no stream activity observed during any of the field seasons) as well as hot springs assumed to be heated by geothermal processes. Two cold springs have also been found in the southern wall of the crater, which are seasonal. There is no surface outflow, but

there is probably a significant amount of groundwater throughflow. Jones et al. (2005) estimated that only 24-33% of the water entering the lake comes from direct precipitation or surface runoff. Evaporation is estimated to account for 43-58% of the water leaving the lake, with the rest from groundwater outflow (Jones et al., 2005). There is little vegetation on the north, east and western slopes apart from deciduous oak (*Quercus cerris*). Pine trees have been planted on the alluvial fan. *Phragmites* and other emergent macrophytes grow around the lake, apart from around the hot springs (England et al., 2008).

5.2 Regional climate

The climate of the region is continental Mediterranean (Kutiel and Turkes, 2005) with annual precipitation at Niğde, 45 km from Nar Gölü, averaging 339 mm between 1935 and 2010. July, August and September are very dry, receiving only 6% of the total precipitation, while April and May are the wettest months, accounting for 27% of the total (Figure 5.3). The hottest months are July and August, when temperatures average +23°C, while from December to February temperatures average +0.7°C. Measured evaporation at Niğde between 1935 and 1970 was 1547.6 mm per year (Meteoroloji-Bulteni, 1974).

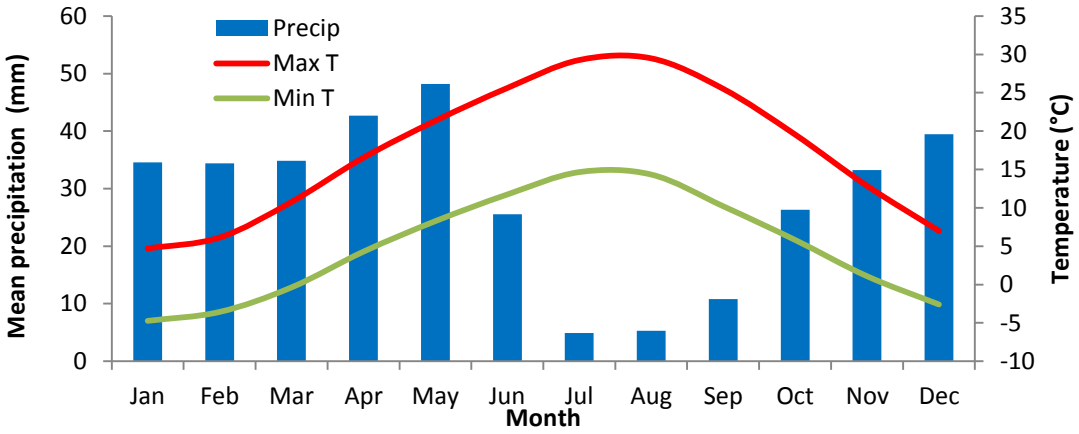

Figure 5.3 *Climate of Niğde showing monthly minimum and maximum temperatures and precipitation totals averaged from 1935-2010. The location of Niğde relative to Nar Gölü is shown on Figure 5.1. Data collected by the Turkish Meteorological Service and supplied by Murat Türkeş.*

5.3 Previous work at Nar Gölü

5.3.1 Coring and monitoring work

Following pilot coring in 1999, sediment cores taken in 2001/2, using Glew (Glew et al., 2001), Mackereth (Mackereth, 1958) and Livingstone (Livingstone, 1955) corers, produced a 3.76 m sequence (NAR01/02 sequence) used for stable isotope, pollen, microcharcoal and diatom analysis (Jones et al., 2005, Jones et al., 2006, England et al., 2008, Turner et al., 2008, Woodbridge and Roberts, 2010). A further core was taken in 2006 using a Glew corer and used for diatom analysis. The 2001/2 and 2006 cores are laminated throughout and ^{210}Pb and ^{137}Cs dating on the top 50 cm of the NAR01/02 sequence and the analysis of modern sediment from traps indicates the couplets are annual (Jones et al., 2005). Analysis of sediment traps and thin sections suggested organic material (which includes diatom silica) is deposited throughout the year and is darker in colour than carbonate material, which is deposited in the late spring/early summer sometimes following the spring algal blooms (Woodbridge and Roberts, 2010). The varve cycle is sometimes interrupted by grey clastic layers: allochthonous material originating from catchment erosion. The varves meant counting could be used to date the cores. A maximum counting uncertainty of 2.5% was calculated, although true dating precision is likely to be much more reliable (Jones et al., 2005). There is no evidence of benthic life in any of the cores. The lake has a residence time of 8-11 years (Jones, 2004), meaning any inter-annual signal in δ^{18}O will be smoothed. Additionally, as detailed in section 6.1.1, water samples were taken, geochemical measurements made and sediments traps deployed, in order to understand the modern limnology of the lake.

5.3.2 Stable isotope analysis of the NAR01/02 sequence

The varved sediments of the NAR01/02 cores meant accurate proxy data-climate calibrations could be derived. Jones et al. (2005) compared the oxygen isotope record for 80 years to instrumental records of temperature, precipitation, wind speed, relative humidity and calculated values of evaporation, and found significant

relationships between the $\delta^{18}O$ record and summer temperatures and evaporation, which suggested these were the main controls on the isotope hydrology of the lake. However, modelling showed that although the dominant controls on $\delta^{18}O$ seem to be summer temperatures and evaporation, these two factors cannot explain the magnitude of the change seen in the $\delta^{18}O$ records. For example, a large shift to more positive $\delta^{18}O$ values in the 1960s (–10 years BP) is associated with a reduction in summer temperatures and an increase in relative humidity, however additional factors, such as the amount of precipitation, would be required to amplify the observed $\delta^{18}O$ change. The Nar Gölü $\delta^{18}O_{carbonate}$ record was therefore taken as a proxy for regional water balance (Jones et al., 2006). $\delta^{18}O$ and $\delta^{13}C$ analyses were carried out on the carbonates from each of the top 900 varves, and then on the following 825 varves at 5 year intervals. Increased aridity was inferred 1,650-1,450 years BP and 550-0 years BP and increased wetness 1,390-1,200 years BP and 950-600 years BP (Figure 5.4). Increased $\delta^{18}O$ values occur at the same time as shifts in carbonate mineralogy from calcite to aragonite, which supports the interpretation of shifts to a more evaporative system (Kelts and Hsu, 1978, Jones et al., 2005). As outlined in section 2.1.1, Jones et al. (2006) demonstrated links between Turkish climate and the NAO index in winter and the Indian monsoon in the summer.

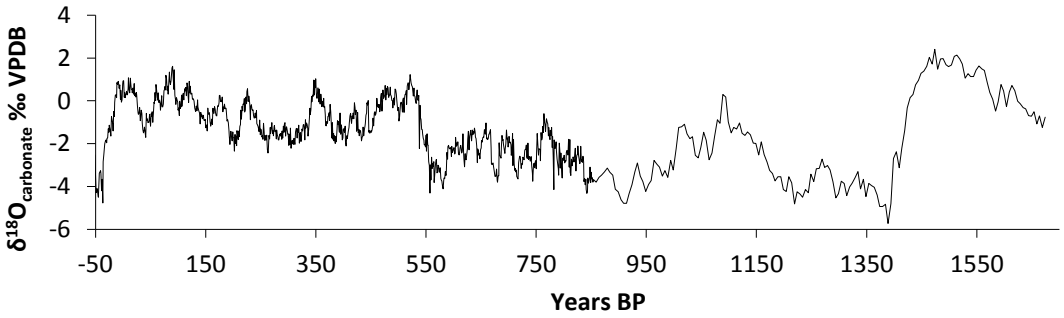

Figure 5.4 *$\delta^{18}O$ of the NAR01/02 record, as published in Jones et al. (2006).*

5.3.3 Diatom species work on the NAR01/02 sequence

Diatom-inferred conductivity showed a good correspondence with the $\delta^{18}O$ record (Jones et al., 2006) for most of the record, when the freshwater bloom species were

left out of calculations (Figure 5.5) (Woodbridge and Roberts, 2011). From the Little Ice Age onwards, the two records became decoupled, with increased bloom events possibly related to human disturbance in the catchment. The majority of diatom species were found to be represented in both the modern and palaeo environments, suggesting dissolution is not a significant issue (Woodbridge and Roberts, 2010). Freshwater species *Nitzschia paleacea*, *Synedra acus* and *Stephanodiscus parvus* were identified as bloom species (Woodbridge and Roberts, 2010, 2011). Based on sediment trap data and thin section analysis, *N. paleacea* and *S. parvus* probably bloom immediately prior to carbonate formation, while *S. acus* blooms in the autumn or early spring (Woodbridge et al., 2010). In contrast, *Cyclotella meneghiniana* dominates biovolume calculations before 1,150 years BP (Woodbridge and Roberts, 2011). An endemic diatom genus (species *Clipeoparvus anatolicus*) has been identified in Nar Gölü (Woodbridge et al., 2010).

5.3.4 Pollen and charcoal work on the NAR01/02 sequence

England et al. (2008) suggested the landscape around Nar Gölü has been 'open' for the past 2,000 years. Most pollen deposited in Nar Gölü is probably regional, rather than local, in origin, since there are relatively high levels of pine pollen over the last 2,000 years, yet pine trees do not naturally grow in Cappadocia (England et al., 2008). From 1,650-1,170 years BP, a strong cultural imprint is indicated by cereal pollen such as rye, wheat and barley. Charcoal influx was low. From 1,170-1,000 years BP, there was an increase in tree pollen and a decrease in anthropogenic indictors, which corresponds with a period of major societal change in the Byzantine world (Figure 5.5), followed by a decrease in tree pollen and an increase in cereal pollen indicting a return to anthropogenic domination of the landscape 1,000-120 years BP. From 120 years BP to present there were sustained decreases in grass pollen, probably reflecting the destruction of steppe grasslands for cereal production with the intensification of agriculture. Changes in the pollen record do not coincide with changes in the isotope record.

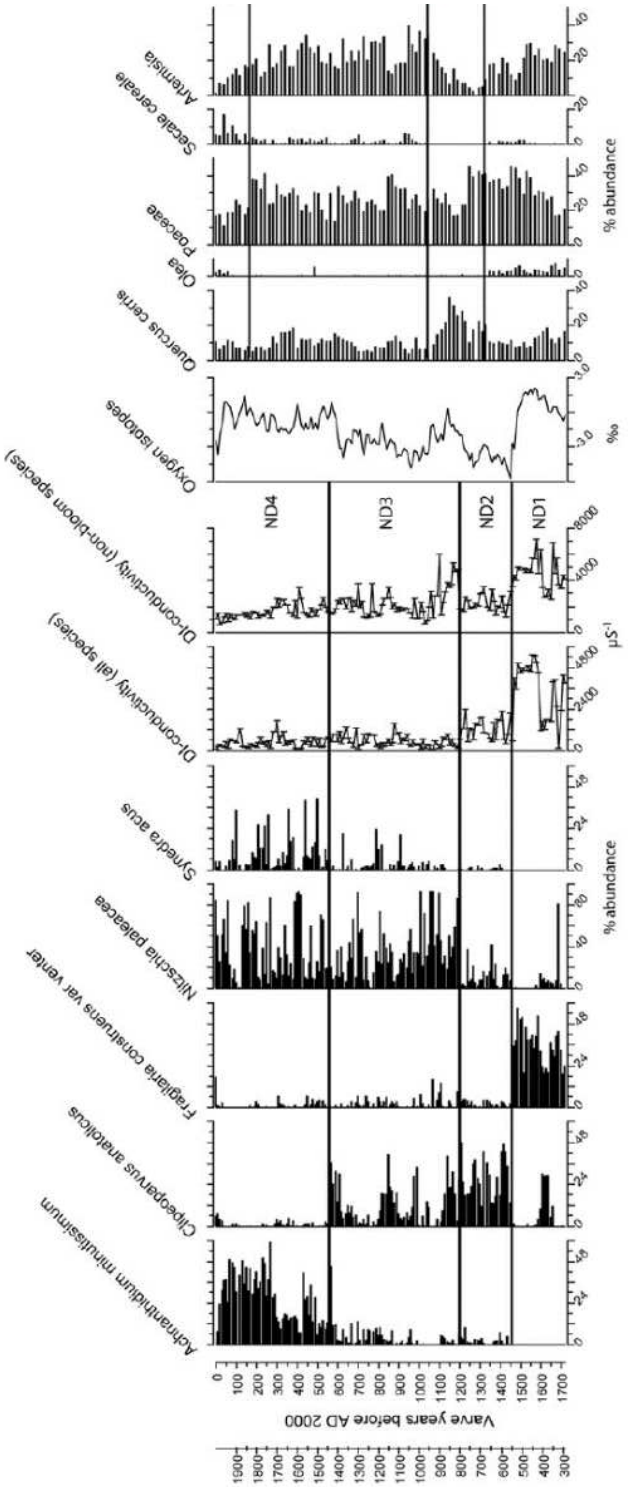

Figure 5.5 *Selected diatom species and DI-inferred conductivity from the NAR01/02 record, compared to* $\delta^{18}O_{carbonate}$ *and pollen records (Jones et al., 2006, England et al., 2008, Woodbridge and Roberts, 2011).*

5.4 Summary

Nar Gölü is a closed lake, with waters evaporatively enriched in ^{18}O. Carbonates and diatoms are both preserved in its sediments. The climate of the area is very seasonal, in terms of temperature and precipitation. Previous work has suggested $\delta^{18}O_{carbonate}$ from Nar Gölü sediments is a good proxy for regional water balance and that, over the past 1,720 years at least, varves have formed.

Chapter 6 | Methodology

In an attempt to address the aims outlined in section 1.5, a number of methods were used. Firstly, field work was carried out to retrieve longer cores than those previously analysed from Nar Gölü and to collect more water samples so that inter- and intra-annual changes in the oxygen isotope composition of Nar Gölü could be investigated, in order to better interpret the palaeo record. Secondly, since Jones et al. (2005) had already shown that $\delta^{18}O_{carbonate}$ from Nar Gölü sediments is a good proxy for regional water balance, $\delta^{18}O_{carbonate}$ analysis was carried out at a high resolution through the record. $\delta^{13}C_{carbonate}$ and $\delta^{13}C_{organic}$ data were produced to support the interpretation of $\delta^{18}O_{carbonate}$. Thirdly, following the proposal of Leng et al. (2001) that comparing $\delta^{18}O$ from diatoms and carbonates can provide insights into seasonality if the two hosts form at different times of the year, and because of the marked seasonality of Near East climate (sections 2.1.1, 5.2), $\delta^{18}O_{diatom}$ analysis was carried out through the record. Fourthly, since Jones (2004) had shown that radiocarbon dating was not possible at Nar Gölü, U-Th dating was combined with varve counting in an attempt to provide a chronology. The methods used, and the methodological development achieved as part of this thesis, are detailed in this chapter.

All stable isotope analyses were carried out at NIGL under the direction of Prof. Melanie Leng. The preparation of all samples, other than some of the diatom isotope samples, was carried out by the author. The majority of the carbonate isotope analyses were carried out by the author. Water, organic and diatom isotope analyses were carried out by NIGL staff. U-Th dating was undertaken at NIGL under the supervision of Dr. Stephen Noble.

6.1 Field work

6.1.1 Water and sediment trap sampling

Unlike proxies such as pollen and diatoms, it is not possible to apply modern analogue or transfer function techniques to stable isotope records because of their dependence on multiple climatic and non-climatic variables (Tian et al., 2011). Therefore, it is essential to understand the isotope hydrology of each individual site and the first stage of this is monitoring of the modern lake system. Consequently, on each visit to the lake by members of the Nar Gölü project team (including those led by the author in September 2011 and February 2012), samples for stable isotope analysis were taken, to monitor changes in the isotopic composition of the lake through time and to investigate the relationship between this and changes in lake level, as measured using a weighted tape and/or a Garmin® Fish Finder. Lake waters were also sampled for pH, conductivity and temperature, measured on a Myron® meter, to monitor changes in the general lake state through time. When weather permitted, depth profiles were taken from the deepest part of the lake through the water column using a Van Dorn bottle or a Glew corer to investigate the stratification of the lake. Lake surface samples were taken at 0.5 m depth to remove any direct effects of exchange with the atmosphere. Where it was not possible to go out on the lake (for example in February 2012 due to blizzards and ice cover), samples had to be taken from the lake edge. Lake edge samples were also taken by members of the local community between March and June 2012. Spring waters were sampled as these are seen to be representative of precipitation isotope values (Jones et al., 2005). Water samples were brought back to the UK in sealed plastic bottles that had been washed three times in the sample and completely filled to prevent isotopic exchange with any air bubbles. Snow samples were taken in February 2012 by packing fresh snow into a sample bag, which was sealed airtight until the snow had melted and then transferred into sample bottles. Where possible, the samples were refrigerated until analysis could be undertaken.

Simple sediment traps (Jones, 2004) have been deployed to monitor the timing of sedimentation processes in the lake and to investigate how the isotope signal is transferred from the water to carbonate and diatoms deposited in the sediments. Traps were secured onto a rope with a float on the surface and an anchor on the bottom, with traps at a variety of depths.

6.1.2 Coring

The author participated in the main coring season in July 2010 that retrieved the 21.5 m NAR10 core sequence that formed the basis of this thesis. While the deepest part of the lake had already been identified using a Garmin® Fish Finder before the NAR01/02 cores were taken, a seismic survey of the lake was carried out to produce a more detailed bathymetric map (Figure 6.1) and from this a location in the deepest part of the lake with the least disturbed sediments, furthest away from the alluvial fan, was chosen for the coring site (Figure 6.2).

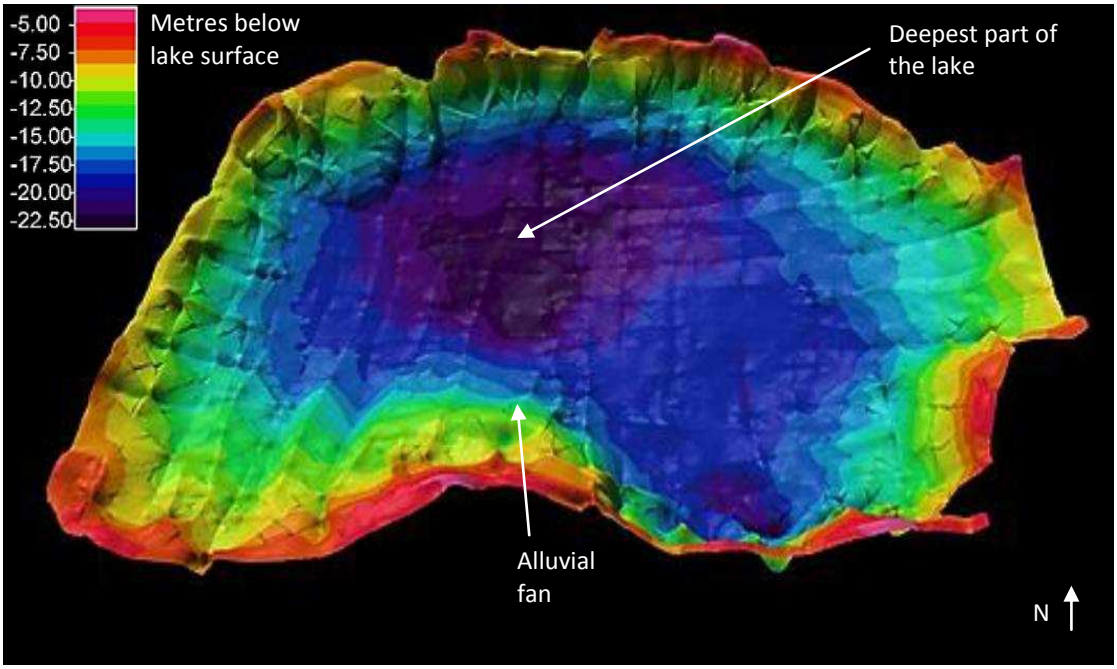

Figure 6.1 *1m gridded lake bathymetry data showing lake depth variability in Nar Gölü in July 2010, with dark blue indicating the deeper waters where the cores were taken from. Map taken from Smith (2010).*

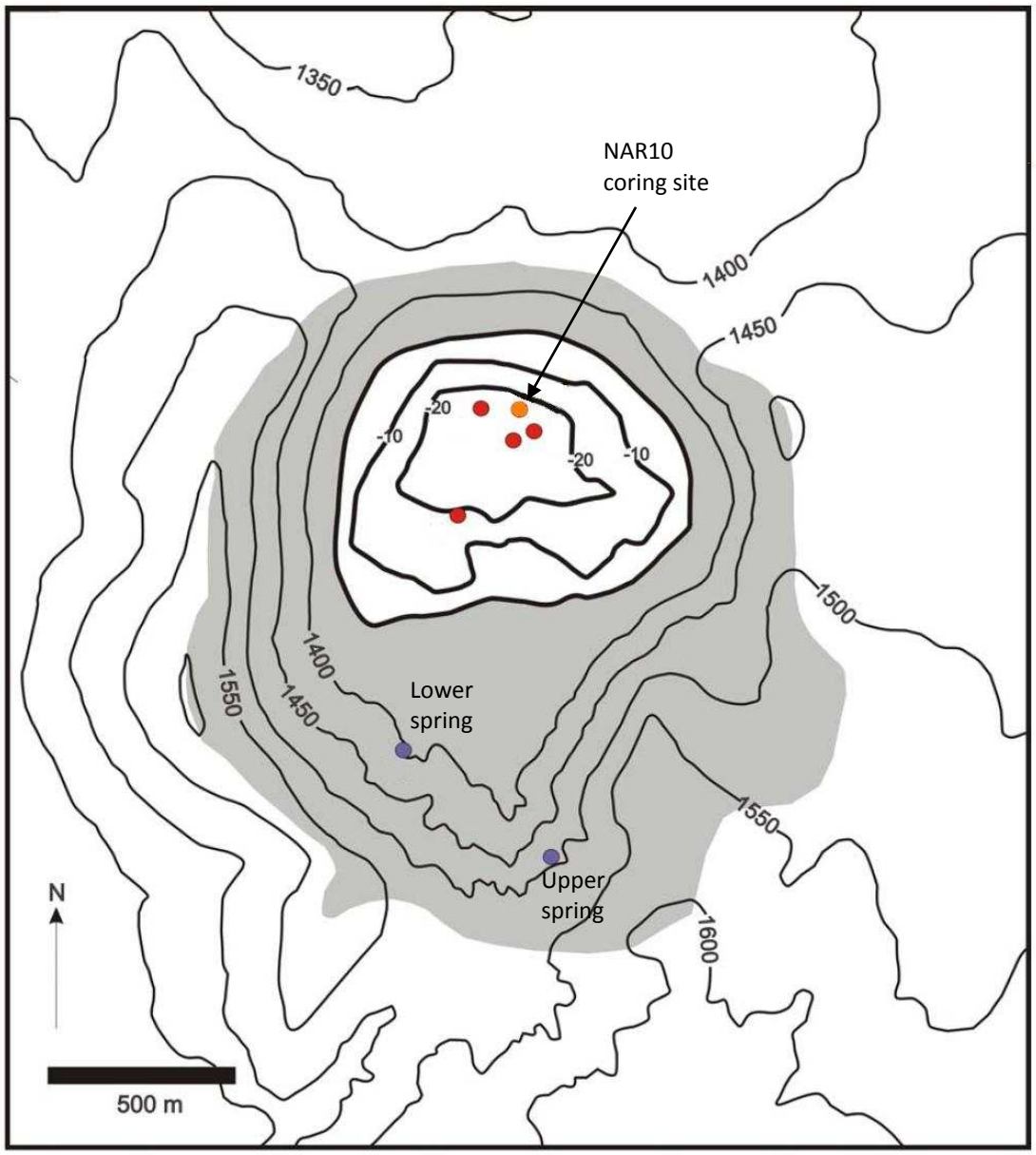

Figure 6.2 *Nar Gölü catchment (shaded grey) showing locations of NAR01/02 coring (red circles), NAR10 coring (orange circle; the three drives were just 2 metres apart) and of the two catchment cold springs (blue circles). Map modified from Jones (2004).*

Since Nar Gölü was more than 20 m deep in 2010 and the aim was to retrieve many more metres of sediment than had been retrieved by Livingstone and Mackereth corers in 2001/2, a UWITEC hammer-piston coring system was used, operated by the

CNRS EDYTEM team based at Chambéry in France. The coring took place from a floating aluminium platform (Figure 6.3) with core drives being 2 or 3 m long and 6.3 or 9 cm in diameter. Three parallel drives were made in an attempt to retrieve as continuous a sequence as possible. In total, 55 m of sediment was returned to the UK with the tubes packed either end with Oasis to keep sediments in place. Since monitoring data were available for over a decade, a Glew core was also taken so that sediments from the last decade could be compared to lake water isotope data and depth measurements in order to better understand the drivers of the isotope records and hence better interpret the palaeo record.

Figure 6.3 *UWITEC coring system on Nar Gölü in July 2010.*

6.2 Analysis of waters

6.2.1 Stable isotope analysis of waters

Water samples were analysed at NIGL for isotopes using an equilibration method for oxygen (Epstein and Mayeda, 1953) and a zinc-reduction method for hydrogen

(Coleman et al., 1982, Heaton and Chenery, 1990) on a VG SIRA mass spectrometer. Isotopic ratios were defined in relation to the Vienna Standard Mean Ocean Water (VSMOW) international standard, and analytical reproducibility was 0.05‰ for $\delta^{18}O$ and 2‰ for δD. Total dissolved inorganic carbon (TDIC) was precipitated from lakewater samples using barium chloride and washed three times in distilled water and $\delta^{13}C$ measured in the same way as for sediment core carbonates, as discussed in section 6.3.4.

6.2.2 Water chemistry

Water samples were also brought back to be analysed for major ions, in order to investigate whether the lake waters were chemically stratified and to look at changes in the Mg/Ca ratio (which is of particular importance when working with carbonates). Chloride, nitrate, phosphate, sulphate, sodium, potassium, magnesium and calcium concentrations were measured on samples as soon as possible after returning from the field on a Metrohm ion chromatogram in the School of Geography, University of Nottingham. This produced data in mg/L. So that unit concentrations of all ions are chemically equivalent they were converted to milliequivalents per litre (meq/L) (Table 6.1).

Table 6.1 *Conversion factors from mg/L to meq (Hem, 1970).*

Ion	**Conversion factor**
Ca^{+2}	x 0.04990
Cl^{-}	x 0.02821
Mg^{+2}	x 0.08226
NO_3^{-}	x 0.01613
PO_4^{-3}	x 0.03159
K^{+}	x 0.02557
Na^{+}	x 0.04350
SO_4^{-2}	x 0.02082

6.3 Analysis of sediments: stable isotope analysis of carbonates

6.3.1 Initial laboratory work

In September 2010, the cores were cut in half lengthways, cleaned, described and photographed. Some sediments were laminated, some were not. The cores from the three drives were matched by looking for similarities in the lithology (as illustrated by Figure 6.4), with the cores with the best preserved sediments chosen to make up a master sequence (Figure 6.5). One half was sampled for isotopes and other proxies and the other half kept as an archive.

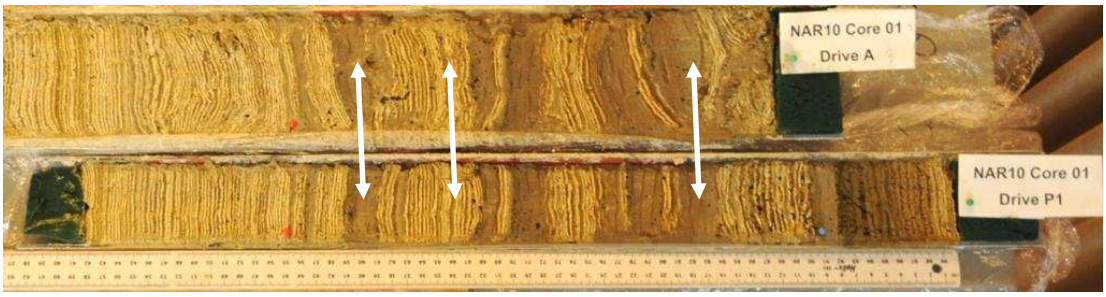

Figure 6.4 *Glew core P1 matched to core 01A by lining up turbidites and varve patterns.*

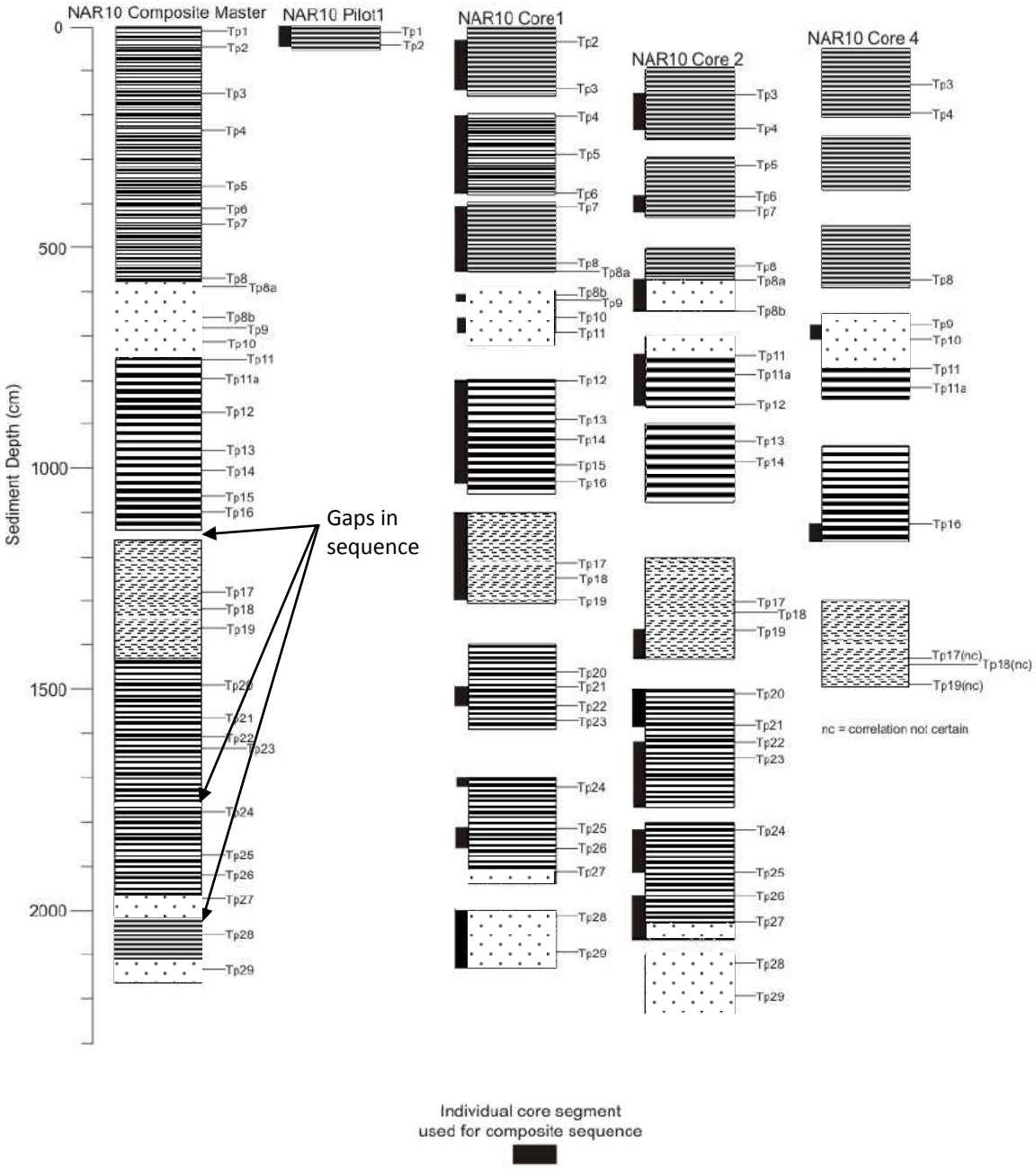

Figure 6.5 *NAR10 master sequence and the individual core sections. The sequences were matched at tie-points (Tp) and the least disturbed core sections chosen to make up the master sequence. Diagram modified from Allcock (2013).*

6.3.2 Sample selection

$\delta^{18}O_{carbonate}$ was selected as the main proxy to be used in this thesis because as discussed in section 1.3 it had already been shown to be a good proxy for regional water balance. In order to address the gaps in the literature identified in section 1.2, in particular the investigation of the Younger Dryas to Holocene transition and decadal and centennial scale changes in the Holocene, high resolution sampling was required. Previously, the highest resolution lake isotope record from the Near East was from Eski Acıgöl (Roberts et al., 2001) where there was a mean sampling interval for the last 9,000 years of 85 years. In laminated sections of the NAR10 cores, samples were taken every 20 varve years. In the unlaminated sections, samples were taken every 4 cm, as this was the average spacing that 20 varves took up in nearby sections.

6.3.3 Carbonate mineralogy

The aim of using stable isotope analysis of carbonates to extend the reconstruction of water balance changes cannot be achieved without first investigating the mineralogy of the carbonates being analysed (i.e. calcite, aragonite, dolomite, ankerite, siderite, etc.), because under the same conditions (i.e. $\delta^{18}O_{lakewater}$ and temperature) different types of carbonate will acquire different $\delta^{18}O$ and $\delta^{13}C$ values due to different mineral-water fractionation factors (Tarutani et al., 1969, Land, 1980) (section 3.4). Mineralogy was investigated by X-ray diffraction (XRD) in the Faculty of Engineering, University of Nottingham. In an XRD, x-rays are fired at the sediment at an angle, and by measuring how they diffract as they pass through the sediment and matching this pattern to a database of recorded patterns, the mineral being analysed can be identified. Samples were disaggregated in 5% sodium hypochlorite in 500 ml beakers for 24 hours to remove organic matter and then sieved at 75 µm to remove any shells, ostracods, etc., in order to be confident that the XRD data (and isotope data to be produced later) were just for authigenic carbonate. The beakers were then filled with distilled water, the carbonate left to settle for 24 hours and the water poured off (repeated three times) to displace the

sodium hypochlorite solution. After drying at 40°C, the carbonate was homogenised in an agate pestle and mortar. Where sufficient material was available, cavity mounts were prepared, whereas smaller samples were smeared onto a glass mount (Hardy and Tucker, 1988). The scanning range used was 5-65° 2θ and the scan rate was 2° 2θ per minute with a step size of 0.05. The TRACES program by Diffraction Technology was used to identify which minerals were present. Not all samples run for carbonate isotopes could be analysed for XRD due to the high costs of using the equipment. Where two or more minerals were present, the proportions of each were (semi)quantitatively determined by calculating the area under the peaks (which were assumed to be regular triangles) and the percentage of aragonite compared to calcite was estimated from experimentally calibrated conversion curves (Hardy and Tucker, 1988).

As discussed in section 6.3.5, accurate determinations of the proportions of calcite to aragonite are not required because it is not necessary to correct for differences in their mineral-water fractionation factors in Nar Gölü data. However, the XRD picked up dolomite in some samples, so further testing using a PANalytical X'Pert Pro diffractometer at the British Geological Survey, Keyworth (scanning from 4.5-85° 2θ at 2.76° 2θ per minute) was carried out because of the requirement for accurate quantitative determinations of the proportion of this mineral, which was achieved by Rietveld analysis, using PANalytical HighScore Plus software. Scanning Electron Microscopy (SEM) was also used to provide images of the carbonate crystals to help investigate how they formed and an Energy Dispersive x-ray Spectroscopy (EDS) probe to provide elemental information to aid in mineral identification.

6.3.4 Stable isotope analysis of carbonates

~10 mg of those samples containing 100% calcite and/or aragonite, prepared as outlined in section 6.3.3, were weighed into a glass vial and placed in a reaction vessel with anhydrous phosphoric acid, which was then pumped to create a vacuum (Figure 6.6A). The carbonate was reacted with the phosphoric acid:

$$3CaCO_3 + 2H_3PO_4 \rightarrow Ca_3(PO_4)_2 + 3CO_2 + 3H_2O \quad 6.1$$

and left for a minimum of 16 hours at 25°C (McCrea, 1950, Craig, 1957). The liberated CO_2 was pumped through a cold trap to remove the remaining water. The CO_2 was frozen in collection vessels using liquid nitrogen, while other gases were pumped away. Stable isotope measurements were made on a dual inlet (VG Optima) mass spectrometer (Figure 6.6B), where the collected CO_2 was compared to a standard. The 44 (assumed to comprise $^{12}C^{16}O_2$), 45 ($^{13}C^{16}O_2$) and 46 ($^{12}C^{16}O^{18}O$) mass fractions were measured and $\delta^{13}C$ and $\delta^{18}O$ calculated relative to the Vienna Pee Dee Belemnite (VPDB) international standard. As can be seen from Eq. 6.1, all of the carbon from the $CaCO_3$ remains in the gas measured by the mass spectrometer but only two thirds of the oxygen does. Therefore, a correction needs to be applied to the $\delta^{18}O$ data to account for the acid-gas fractionation (Sharp, 2007). The acid-gas fractionation factor used here was 1.01025 for both calcite and aragonite (Sharma and Clayton, 1965). It is acknowledged that, particularly for aragonite, other acid-gas fractionation factors are available (Kim et al., 2007b), however 1.01025 is used for all data from calcite and aragonite produced at NIGL. Repeat measurements were made on 33 samples giving an analytical reproducibility of 0.09‰ for $\delta^{18}O$ and 0.04‰ for $\delta^{13}C$ (1σ).

Dolomite, however, does not fully react at 25°C for 16 hours and, as discussed in sections 6.3.5 and 8.2.2, substantially different mineral-water fractionation factors and different modes of formation mean $\delta^{18}O$ data from dolomite will not be easily comparable to calcite or aragonite data. Al-Aasam et al. (1990) previously showed how carbonates with mixed mineralogies could be reacted selectively to overcome some of these issues. Experimental work at NIGL (Sloane, 2004) showed how samples containing <20% dolomite (i.e. >80% calcite or aragonite) could be reacted at 16°C for 1 hour to release enough CO_2 from the calcite and aragonite parts without a fractionation factor, but limit the amount of CO_2 liberated from dolomite (Figure 6.7), meaning $\delta^{18}O$ data comparable to those from 100% calcite/aragonite can be produced, albeit with analytical reproducibility slightly increased to 0.2‰ (although for the samples analysed from the Nar Gölü cores, the analytical

reproducibility was lower at 0.08‰ for $\delta^{18}O$ and 0.13‰ for $\delta^{13}C$, 1σ, n=6). There are no published acid-gas fractionation factors for a calcite or aragonite reaction at 16°C so the correction was adjusted so gas $\delta^{18}O$ values at 16°C were converted to those expected at 25°C before the Sharma and Clayton (1965) acid-gas fractionation factor was used to convert to solid values. Samples containing 20-80% dolomite were not run for isotopes, since too much dolomite would be liberated for them to be run at 16°C for 1 hour (error exponentially increases to unacceptable levels) and dolomite levels were not high enough for them to be treated as dolomites and reacted at 100°C. Samples containing >80% dolomite (as determined by the PANalytical X'Pert Pro diffractometer) were reacted at 100°C for 16 hours to ensure a complete reaction before running for isotopes, with the acid-gas fractionation factor of 1.00913 used (Rosenbaum and Sheppard, 1986). A breakdown of the number of samples reacted in the three different ways and the number of samples that could not be run for isotopes is shown in Table 6.2.

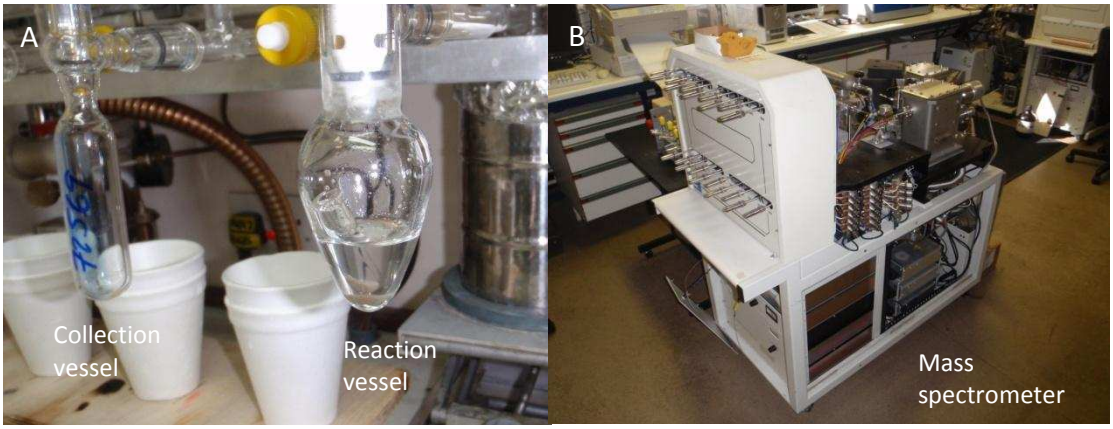

Figure 6.6 *A: Offline CO_2 extraction at NIGL. Ground carbonate samples are placed in vial with phosphoric acid, a vacuum is created and the reaction vessel is sealed. Once at the desired reaction temperature (25°C for 100% calcite/aragonite), the vessel is shaken so that carbonate powder comes into contact with and reacts with the acid. The vessels are then put onto the extraction line and CO_2 pumped into collection vessel. The sealed collection vessels are then attached to the mass spectrometer (B), unsealed, and the CO_2 released for isotope analysis.*

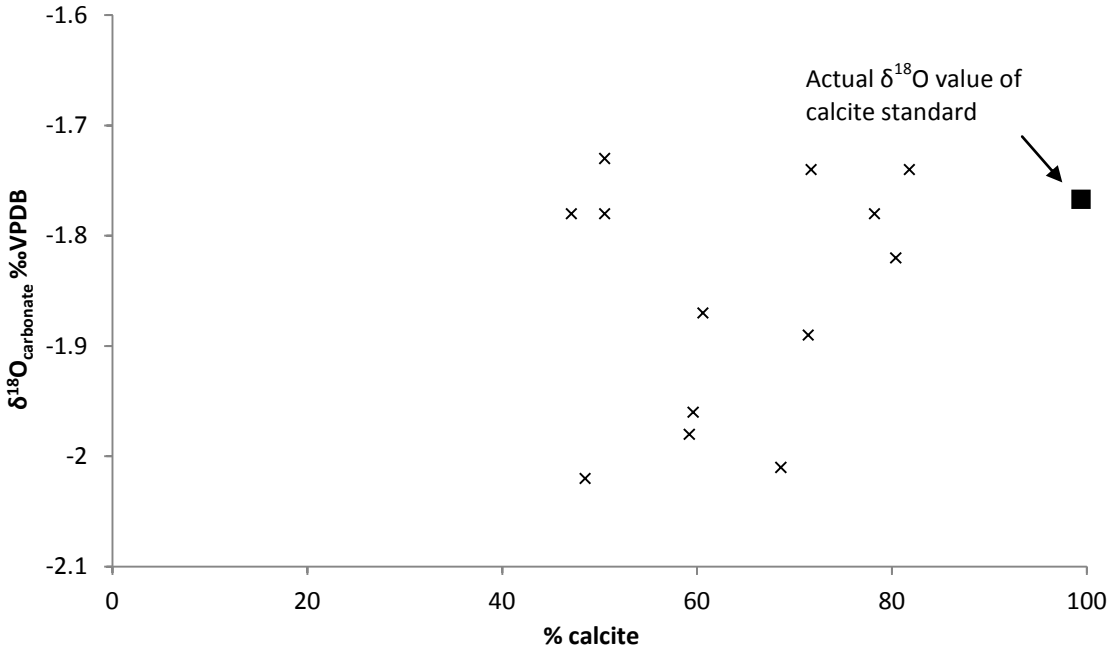

Figure 6.7 *$\delta^{18}O$ of samples reacted at 16°C for 1 hour containing mixtures of dolomite and calcite standards, showing how the offset from the actual $\delta^{18}O$ value of calcite increases as the proportion of dolomite in the sample increases (Sloane, 2004).*

Table 6.2 *Breakdown of the number of carbonate samples analysed from the NAR10 core sequence by the three different reaction methods.*

Reaction details	Mineralogy	n
25°C 16 hours	100% calcite/aragonite	337
16°C 1 hour	>80% calcite/aragonite, <20% dolomite	131
100°C 16 hours	> 80% dolomite	5
Not run	20-80% dolomite	29

6.3.5 Mineral-water fractionation factors

Calcite, aragonite and dolomite formed under the same conditions will have different $\delta^{18}O$ values due to differing mineral-water fractionation factors. Aragonite is typically seen to be more positive than calcite formed under the same conditions (Tarutani et al., 1969, Grossman and Ku, 1986, Kim et al., 2007a) and dolomite is more positive

than aragonite and calcite formed under the same conditions (Vasconcelos et al., 2005). To quantify the offsets, palaeotemperature equations for the different minerals are presented here; the offsets differ very slightly from those stated in the literature because different acid-gas fractionation factors are used in different studies. Here, the Sharma and Clayton (1965) acid-gas fractionation factor is used and the calcite and aragonite equations are corrected for this (H. Wierzbowski, pers. comm.). The calcite palaeotemperature equation of O'Neil et al. (1969) was expressed by Hays and Grossman (1991) as:

$$T = 15.7 - 4.36 \times (\delta^{18}O_{calcite} - \delta^{18}O_{lakewater}) + 0.12 \times (\delta^{18}O_{calcite} - \delta^{18}O_{lakewater})^2 \quad 6.2$$

where $\delta^{18}O_{calcite}$ is expressed against VPDB, $\delta^{18}O_{lakewater}$ against VSMOW and T in °C. Another calcite palaeotemperature equation was derived by Kim and O'Neil (1997):

$$T = \frac{18000}{1000LN\left(\frac{1000+\delta^{18}O_{calcite}}{1000+\delta^{18}O_{lakewater}}\right)+32.17} - 273.15 \quad 6.3$$

where $\delta^{18}O_{calcite}$ and $\delta^{18}O_{lakewater}$ are expressed against VSMOW and T in °C. VSMOW can be converted to VPDB using the Coplen et al. (1983) equation:

$$\delta^{18}O_{VPDB} = 0.97002 \times \delta^{18}O_{VSMOW} - 29.98 \quad 6.4$$

Eqs. 6.2 and 6.3 are used in this thesis because they are derived from experiments on inorganic carbonates, rather than on biogenic carbonates (e.g. Epstein and Mayeda, 1953, Anderson and Arthur, 1983, Erez and Luz, 1983). Values produced by these equations differ slightly so data from both are presented to provide a comparison. The aragonite palaeotemperature equation of Kim et al. (2007a) is used instead of, for example, Grossman and Ku's (1986), because the former study was on inorganically precipitated aragonite:

$$T = \frac{17880}{1000LN\left(\frac{1000+\delta^{18}O_{aragonite}}{1000+\delta^{18}lakewater}\right)+30.77} - 273.15 \quad 6.5$$

where $\delta^{18}O_{aragonite}$ and $\delta^{18}O_{lakewater}$ are expressed against VSMOW and T in °C.

Vasconcelos et al. (2005) produced a palaeotemperature equation for bacterially mediated dolomite precipitation at +25-45°C:

$$T = \sqrt{\frac{2785000}{1000LN\left(\frac{1000+\delta^{18}O_{dolomite}}{1000+\delta^{18}O_{lakewater}}\right)+0.24}} - 273.15 \qquad 6.6$$

where $\delta^{18}O_{dolomite}$ and $\delta^{18}O_{lakewater}$ are expressed against VSMOW and T in °C.

Using a fixed $\delta^{18}O_{lakewater}$ and varying temperatures, these equations are plotted on Figure 6.8. At 20°C, aragonite $\delta^{18}O$ is 0.7‰ more positive than calcite $\delta^{18}O$ precipitated under the same conditions when calculated using Eq. 6.2 or 0.9‰ more positive when calculated using Eq. 6.3. Dolomite $\delta^{18}O$ is 2.7‰ more positive than calcite precipitated under the same conditions calculated using Eq. 6.2 or 2.8‰ more positive using Eq. 6.3.

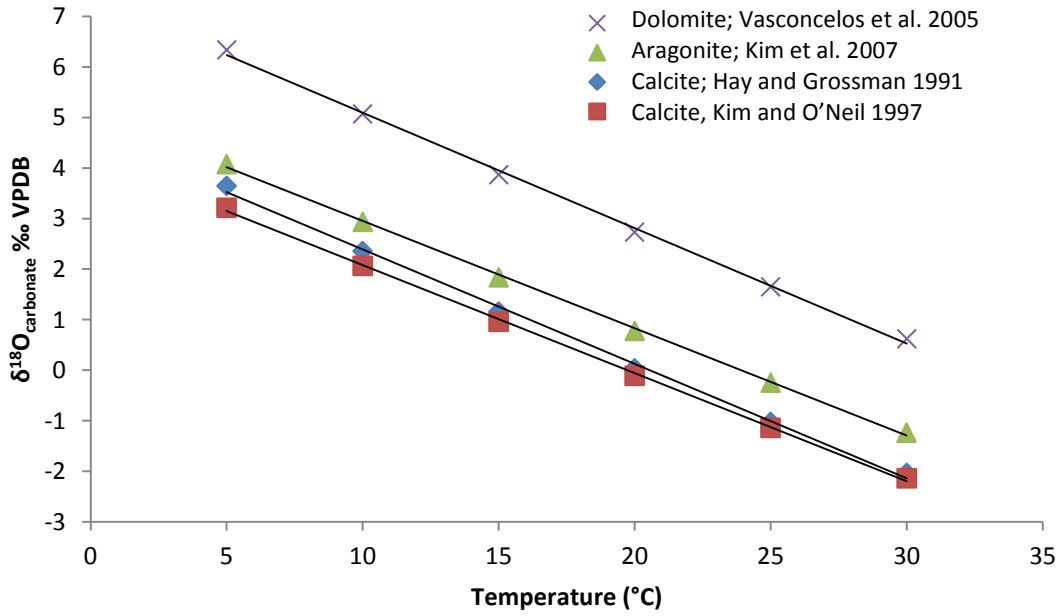

Figure 6.8 *Comparison of different equilibrium calculated $\delta^{18}O_{carbonate}$ values for different temperatures for calcite, aragonite and dolomite. Here, a constant $\delta^{18}O_{lakewater}$ value of –1‰ was used, although the offsets are independent of $\delta^{18}O_{lakewater}$.*

The offset between aragonite and calcite (0.7-0.9‰) is smaller than the large shifts seen in the Nar Gölü record (section 8.1.3), and indeed probably even smaller than this because of the presence of high-magnesium calcite in Nar Gölü (Jones et al., 2005). At six levels of the NAR10 sequence, three individual calcite crystals were analysed by EDS and the average Ca:Mg ratio was 18.2 mol%, which based on the definition of Gierlowski-Kordesch (2010) means Nar Gölü calcite is high-magnesium. The offset in $\delta^{18}O$ between aragonite and high-magnesium calcite formed under the same conditions is even less than 0.7-0.9‰ (Tarutani et al., 1969, Jimenez-Lopez et al., 2004). Consequently, $\delta^{18}O$ values are not corrected for changes in mineralogy between calcite and aragonite. This is consistent with the previously published carbonate isotope record from Nar Gölü (Jones et al., 2006). However, dolomite is ~2.7‰ more positive than calcite formed under the same conditions, so this did need to be corrected for:

$$\delta^{18}O_{\text{dolomite-corrected}} = \delta^{18}O_{\text{dolomite-raw}} - \left(\left[\frac{\%_{\text{dolomite}}}{100}\right] \text{x } 2.7\right) \qquad 6.7$$

6.4 Analysis of sediments: stable isotope analysis of diatom silica

6.4.1 Sample selection

It was not possible to analyse samples for $\delta^{18}O_{diatom}$ at the same resolution as those analysed for $\delta^{18}O_{carbonate}$ because the preparation and analysis is much more time-intensive and costly. Regardless, the reason for producing $\delta^{18}O_{diatom}$ data was to investigate whether comparison with $\delta^{18}O_{carbonate}$ data could offer insights into seasonality and help address the gap in our knowledge of the general form of the Holocene, so high resolution data were not required. Samples from the NAR01/02 cores were already sampled and analysed for $\delta^{18}O_{diatom}$ at a 10 year resolution (Dean et al., 2013). From the NAR10 cores, after the production of the $\delta^{18}O_{carbonate}$ data, it was apparent that the general millennial scale trends could have been picked up at a resolution 8 times lower, so this resolution was selected as the base for the $\delta^{18}O_{diatom}$ analysis (Figure 6.9). However, samples from what is assumed to be the late glacial

period (1957-2169 cm depth) were taken at a resolution only twice as low since it is assumed sampling for $\delta^{18}O_{carbonate}$ was at a lower temporal resolution here because of lower deposition rates. Also, samples were taken at only a x2 lower resolution from 1507.2-1547.7 cm depth and at the same resolution as $\delta^{18}O_{carbonate}$ from 831.7-1077.7 cm depth because these periods see large scale fluctuations in the $\delta^{18}O_{carbonate}$ record and it was deemed interesting to produce two high resolution isotope records for these periods.

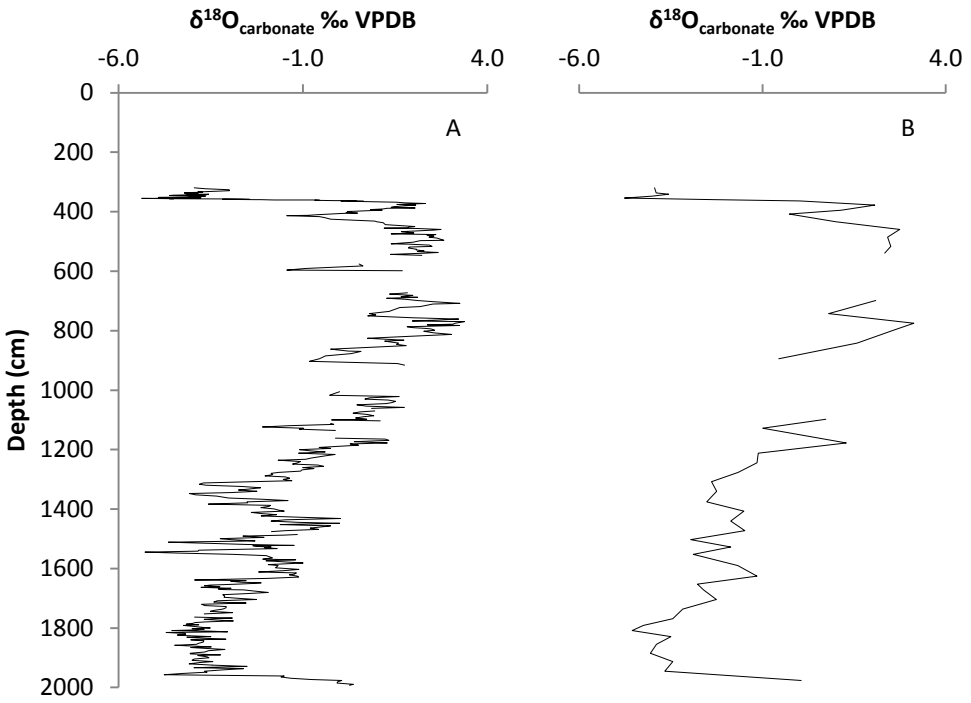

Figure 6.9 *Comparison of $\delta^{18}O_{carbonate}$ data at full resolution (A) and 8 times lower (B).*

6.4.2 Cleaning of samples for diatom isotope analysis

It is important that samples for $\delta^{18}O_{diatom}$ analysis are as free as possible of contamination as the method liberates oxygen from other components of the sediment as well as diatoms. The cleaning process used in this study was similar to that of Morley et al. (2004), although modified by the addition of a nitric acid stage (Tyler et al., 2007) because of the high organic content of some of the Nar Gölü samples.

Firstly, samples were left in beakers for 24 hours in 10% hydrochloric acid to remove carbonates. The samples were then transferred to centrifuge tubes and washed three times with distilled water, before 63% nitric acid was added for 24 hours to remove organics. After washing, 30% hydrogen peroxide was added to complete the removal of organic material, with tubes heated to 75°C in a water bath for ~48 hours or until reaction had ended, and again washed. Additional stages were required to remove minerogenic material, which cannot be dissolved by these chemical stages. This tends to settle out faster than diatom frustules, so it was sometimes possible to pipette the latter off into fresh centrifuge tubes, leaving contaminants behind. Samples were then sieved at 10 µm, which meant that small diatom frustules, including the endemic species *Clipeoparvus anatolicus* (Woodbridge et al., 2010), were lost from the sample, but EDS showed that unsieved samples were on average 43% more contaminated than sieved samples because of the presence of clay-sized minerogenic material. Finally, sodium polytungstate (SPT) was used on the samples prepared by the author (not on NAR01/02 samples not prepared by the author); diatom frustules should float in a specific gravity of ~2.3 whereas silt-sized minerogenic material will remain at the bottom of the tube. This stage can be problematic as SPT needs to be removed from the samples otherwise it will itself become a contaminant. Here it was flushed from samples by filtering them with distilled water at 0.45 µm.

6.4.3 Stable isotope analysis of diatom silica

As described by Leng and Sloane (2008), cleaned samples were dehydrated by outgassing at room temperature, following which BrF_5 was used at low temperature to remove the hydrous outer layer of diatom silica (Labeyrie and Juillet, 1982) which readily exchanges with any water it comes into contact with. The samples were then reacted with BrF_5 at a higher temperature (450°C) to separate silicon and oxygen. The oxygen was converted into CO_2 by exposure to graphite (Clayton and Mayeda, 1963), which was separated from other gases using cold traps. $^{18}O/^{16}O$ was measured on a Thermo Finnigan MAT 253 and values reported against VSMOW. This

method has been verified through an inter-laboratory comparision exercise (Chapligin et al., 2011).

6.4.4 Mass balance correction of diatom isotope data

The process described in 6.4.2 can sometimes yield samples of a sufficient purity that contamination is not an issue. However, even when SPT is used, diatom samples can remain contaminated, especially when minerogenic material is attached to diatoms by electrostatic charges or trapped within diatoms (Figure 6.10) and where there is not a significant density contrast between diatoms and the contaminants (Brewer et al., 2008). Even the samples from NAR06 and NAR10 on which SPT was used contained an average of 10% non-diatom silicate material. Contamination in samples from Lake Baikal, initially analysed by Morley et al. (2005) and reanalysed by Mackay et al. (2011), averaged 29.2% despite the use of SPT. In sediments like these, mass balancing has to be used to account for the effect of contamination on $\delta^{18}O_{diatom}$. Morley et al. (2005) and Mackay et al. (2008) estimated percentage contamination using light microscopy on randomly selected areas. However, point counting gives a surface area, not volume, and only a semi-quantitative assessment of contamination. Lamb et al. (2007) and Brewer et al. (2008) used X-ray Florescence Spectroscopy (XRF), Chapligin et al. (2012) used Inductively Coupled Plasma Optical Emission Spectroscopy and Swann and Patwardhan (2011) used Fourier Transform Infrared Spectroscopy to provide more accurate contamination estimates. The abundance of elements such as aluminium is typically used to reflect the level of contamination (Brewer et al., 2008).

For Dean et al. (2013), the samples from the NAR01/02 core sequence were analysed by EDS, because an XRF was not available at the time. X-rays are fired at the sample which excites electrons and the number and energy of x-rays emitted is measured and can be used to quantify the elements present in the sample. Prepared samples were viewed at 100x magnification under SEM (so a large area could be analysed), and EDS was used to detect O, Na, Mg, Al, Si, P, S, K, Ca, T, Mn and Fe. Since most clay-sized minerogenic material should have been removed by sieving at 10 µm and

carbonates and organics by chemical processes, most of the contamination in 'clean' samples was assumed to be from minerogenic material presumably washed in from the catchment and similar in size, shape and specific gravity to the diatoms. To test the accuracy of the EDS in measuring contamination, a series of samples with known mineralogy were analysed. The aluminium content of 8 samples from Lake Baikal, previously analysed for $\delta^{18}O_{diatom}$ and XRF (Mackay et al., 2011), and 10 samples with known mixtures of mica, montmorillonite, kaolinite and chlorite, were compared to aluminium measured on the EDS. This showed a similar underestimation of contamination to that found by Chapligin et al. (2012), so measured contamination values were divided by 0.64 to compensate. However, this correction led to a slight overestimation of error, with some samples reporting over 100% contamination, which is obviously impossible, so an additional correction was applied to reduce the contamination range from 0 to 100% (Dean et al., 2013).

The amount of contamination in samples as a percentage of overall content was calculated by Brewer et al. (2008):

$$\%_{\text{contamination}} = \left(\frac{\text{sample}_{\text{Al}}}{\text{contamination}_{\text{Al}}}\right) \text{x } 100 \qquad 6.8$$

where sample_{Al} is the measured aluminium concentration in each sample analysed for $\delta^{18}O_{diatom}$ and $\text{contamination}_{Al}$ is the average percentage of aluminium in Nar Gölü silt samples (in Dean et al., 2013: 8.6% ±0.5, n=7) that were prepared and run in the same way as $\delta^{18}O_{diatom}$ samples. A mass balance correction, also used by Mackay et al. (2011) for Lake Baikal samples, was used to account for the impact of contamination on the $\delta^{18}O$ values:

$$\delta^{18}\text{O}_{\text{corrected-diatom}} = \frac{(\delta^{18}\text{O}_{\text{diatom}} - \delta^{18}\text{O}_{\text{contamination}} \text{ x } [\frac{\%_{\text{contamination}}}{100})}{\frac{\%_{\text{diatom}}}{100}} \qquad 6.9$$

where $\delta^{18}O_{diatom}$ is the original isotope value of the 'cleaned' diatom sample, $\%_{contamination}$ and $\%_{diatom}$ are estimated by EDS and $\delta^{18}O_{contamination}$ is the isotope value

of contamination. The latter can be estimated in a number of ways. Measuring the contamination directly is difficult, as much of the minerogenic material is removed during processing of the diatom samples, such that the end member contaminant left in the diatom samples is the minerogenic material that has been through the chemical and physical separation processes. Therefore, in Dean et al. (2013), a modified version of the linear regression method of Chapligin et al. (2012) was used, which gives an estimated end member contamination $\delta^{18}O$ value for Nar Gölü sediments of 16.5‰ (Figure 6.11).

Figure 6.10 *SEM image of Campylodiscus clypeus highlighting the difficulties of producing a contaminant-free diatom sample when minerogenic matter attaches to diatoms.*

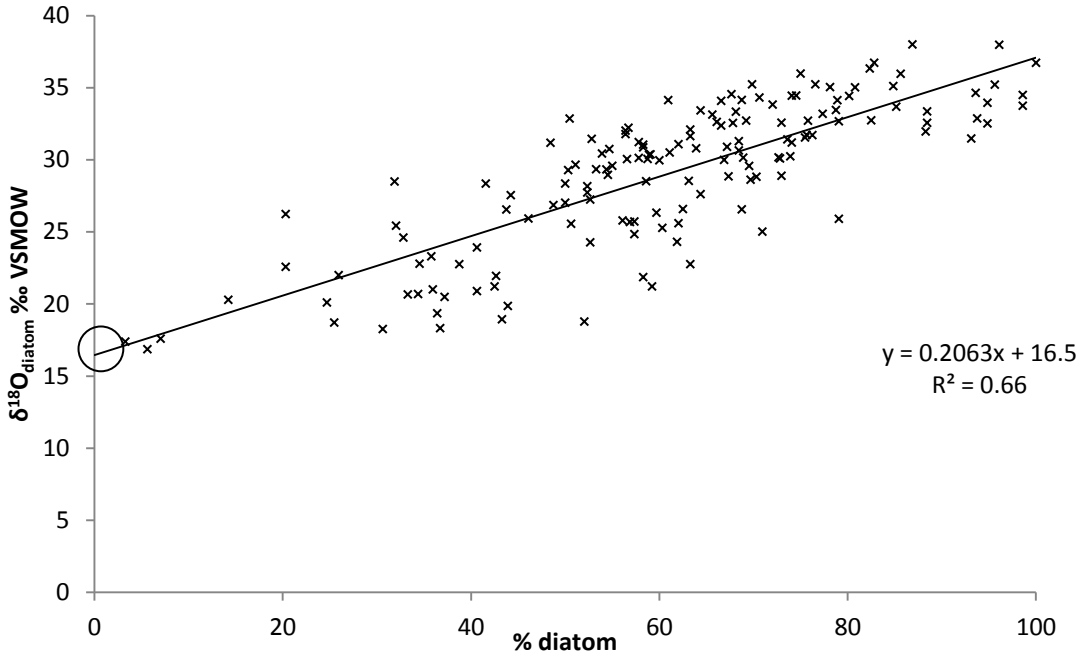

Figure 6.11 *$\delta^{18}O_{diatom}$ plotted against $\%_{diatom}$; the intercept value at 0% diatom (i.e. 100% contamination) can be used in Eq. 6.9 to represent the $\delta^{18}O_{contamination}$.*

Samples for diatom isotope analysis were also carried out on samples from the NAR10 core (this time all prepared by the author and with the addition of an SPT stage), and the mass balance correction was carried out with a few modifications. Since the analysis of the NAR01/02 diatom isotope samples and the use of EDS to assess their contamination, the School of Geography had purchased an XRF (a Panalytical εpsilon 3 XL). An issue with the work of Dean et al. (2013) was the large uncertainties associated with the assessment of contamination using EDS. Therefore, the more accurate and precise (analytical reproducibility of 0.03% (1σ) compared to 0.5% on EDS) XRF was used on all NAR10 samples and also, so that data were directly comparable, on NAR01/02 samples with sufficient material remaining. The XRF works on the same principles as the EDS and it was set up to quantify the proportions of Na, Mg, Al, Si, P, S, K, Ca, T, Mn and Fe using the Panalytical Omnion program, although the XRF calculated oxide % rather than elemental %. To establish whether the mass balance modelling of Dean et al. (2013) is still valid with the more reliable contamination assessments, data for samples measured by both the EDS and XRF are

compared. Firstly, Al% values from the EDS were converted to Al_2O_3 values to allow for comparison:

$$Al_2O_3 \text{ wt\%} = Al \text{ wt\%} \times 1.8895 \qquad 6.10$$

Figure 6.12A shows that the EDS significantly underestimates Al_2O_3 wt% compared to the more reliable XRF, highlighting the necessity for the correction used in Chapligin et al. (2012) and Dean et al. (2013). Indeed when this correction is applied, contamination values from the EDS and XRF are more in line with each other (Figure 6.12B), although a significant difference is the underestimation of contamination by the EDS at low Al_2O_3 levels. In addition to the use of XRF to assess contamination, another difference in the mass balance correction approach used in this thesis compared to that used in Dean et al. (2013) is that instead of using Figure 6.11 to calculate the $\delta^{18}O$ of contamination, 9 turbidites from along the core were prepared and run in the same way as the diatom isotope samples, giving a mean value of 16.0‰ (±1.0‰ (1σ)) which was very close to the value of 16.5‰ from the intercept on Figure 6.11. Errors from individual components of the mass balancing are outlined in Table 6.3 and were combined to calculate the overall error associated with the correction. The error associated with the variability in $\delta^{18}O_{contamination}$ is increased here compared to that in Dean et al. (2013), but overall error is reduced because of the more accurate XRF (samples that were mass balance corrected for Dean et al. (2013) averaged ±2.7‰ error whereas when those same samples were re-analysed by XRF and the new mass balance correction applied as outlined above, errors averaged ±1.9‰).

Table 6.3 *Sources of error associated with new mass balance correction of $\delta^{18}O_{diatom}$ data.*

Source of error	**Magnitude of error**
Diatom isotope measurement analytical reproducibility (1σ)	0.3‰
Al_2O_3 measurement analytical reproducibility (1σ)	0.03%
Variance in Al_2O_3 composition of turbidites (from $\bar{x}$ of 14.56%) (1σ)	1.6%
Variance in $\delta^{18}O$ value of turbidites from $\bar{x}$ of 16.0‰ (1σ)	1.0‰

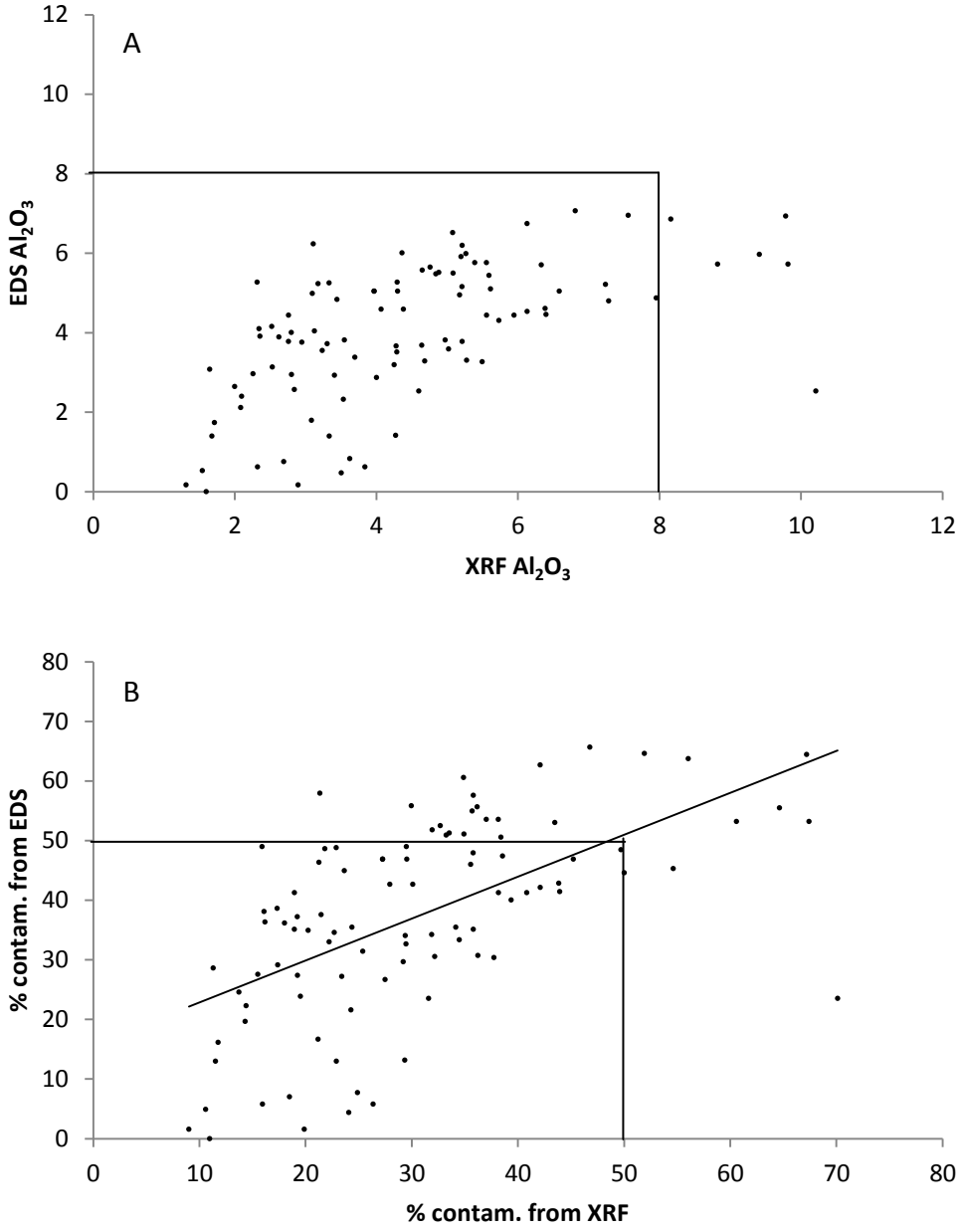

Figure 6.12 *Comparison of data produced by EDS and XRF, A: Al_2O_3 values and B: contamination values after correction applied to EDS data.*

The breakdown of the diatom samples that could and could not be run for isotopes, because they were too contaminated or because the preparation was not successful, is shown in Table 6.4. In Dean et al. (2013) 129 samples were included in the analysis, but fewer from the NAR01/02 sequence are included here in the re-analysis because some samples had insufficient material left for XRF. No samples from the NAR10 core

were seen to have >60% minerogenic contamination, however some of the samples were rejected before XRF because they had large undissolvable lumps of concreted carbonate that could not be separated from diatom silica, and this was another end member that would have been difficult to correct for. Additionally, some samples had insufficient material for isotope analysis. More samples to those selected using the sampling strategy in 6.4.1 were prepared from the late Holocene section in an attempt to produce a more continuous isotope record, however again these samples yielded insufficient material and/or were contaminated with concreted carbonate.

Table 6.4 *Breakdown of the samples prepared for diatom isotope analysis and the numbers that had to be rejected due to contamination.*

Sample	**Action**	**n**
NAR01/02 samples >60% contamination or insufficient material remaining to XRF	Reject	57
NAR01/02 samples <60% contamination after XRF	Accept	95
NAR10 samples >60% contamination after XRF	Reject	0
NAR10 samples <60% contamination	Accept	90
NAR10 silt end member samples	Accept	7
NAR10 samples with insufficient material and/or too contaminated with concreted carbonate	Not run for isotopes	33
NAR10 samples lost because of tube explosion in centrifuge	Not run for isotopes	2

Diatom isotope data are presented fully in section 8.1.3, however here data from the NAR01/02 cores are shown to demonstrate the implications of changing the method of mass balance correction from that in Dean et al. (2013) to the new method outlined above. Figure 6.13 shows the original mass balance corrected data from the NAR01/02 cores published in Dean et al. (2013) compared to re-calculated values using the modifications to the mass balance approach described above. Although the actual values are slightly different, the general trends are very similar, with periods of low $\delta^{18}O$ (+20 to +25‰) ~1,450, 1,250 and 120 years BP, although the period of

fairly low values ~1,000 years BP is not seen using the new mass balance method. The overall similarities mean the general interpretations of Dean et al. (2013) are still valid.

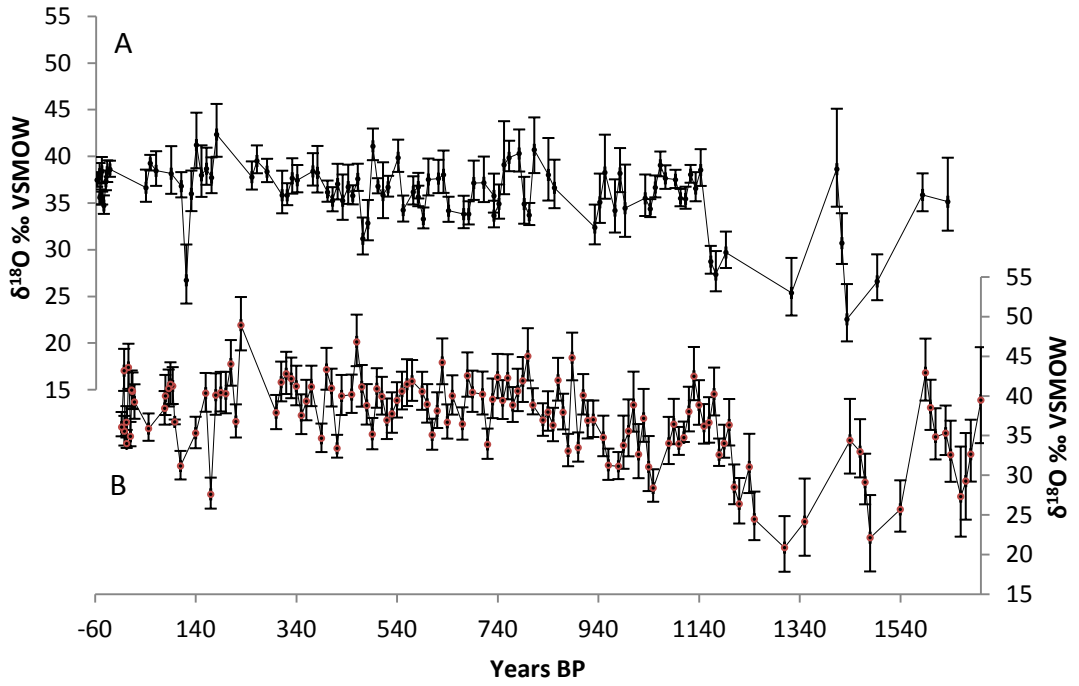

Figure 6.13 *The difference between NAR01/02 diatom isotope trends in this thesis (A) and published in Dean et al. (2013) (B). Not all samples originally run and mass balance corrected could be included in A because many did not have sufficient material left to allow for XRF analysis. However, the general trends are very similar.*

Despite the improvement in the accuracy and precision of estimating the amount of aluminium in diatom samples, it is still likely that $\%_{contamination}$ is overestimated because some minerogenic material will be removed by the first fluorination stage before $\delta^{18}O$ is measured (Swann and Leng, 2009) and diatom frustules can incorporate aluminium, so Al% in the samples does not just reflect minerogenic contamination (Beck et al., 2002, Koning et al., 2007, Swann, 2010, Ren et al., 2013). To investigate the latter effect, SEM was used to identify individual clean diatoms (i.e. with no detrital material visible at all, example shown in Figure 6.14) and the

Al_2O_3 wt% of the individual diatoms was measured by EDS, averaging 1.0% ±0.4 (1σ) across 16 samples. This suggests that there are significant amounts of diatom-bound aluminium. A correction was applied to account for this. 14.56% Al_2O_3 still represents 100% contamination but 1‰ Al_2O_3 now represents 0% contamination, because it is suggested here that diatom-bound aluminium would lead to 1‰ Al_2O_3 in pure diatom samples. A sample containing 100% diatoms and 0% contamination would have 1% removed from the Al_2O_3 measurements, a sample containing 50% diatoms and 50% contamination 0.5% removed from the Al_2O_3 measurement, and so on, and the mass balance correction re-applied. The validity of this correction could be questioned due to the uncertainty in the actual amount of diatom-bound aluminium and whether this varies between samples, but while this correction reduces the values of the data, it has no effect on the trends (Figure 6.15).

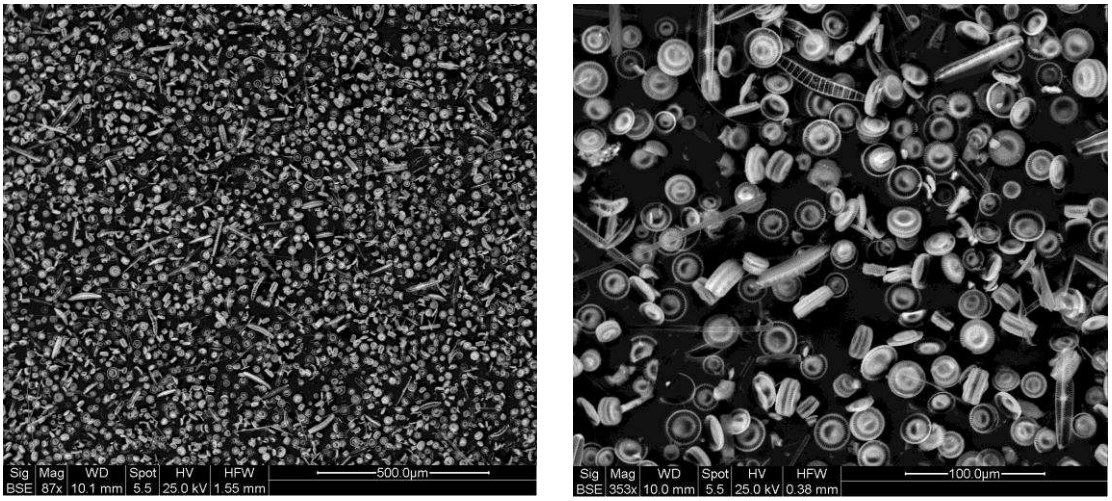

Figure 6.14 *Sample from 1507.2 cm viewed under SEM, shown by XRF to contain 0.38% Al_2O_3 but with no detrital material visible, taken to suggest diatom-bound aluminium could account for a significant proportion of the Al_2O_3 in diatom samples.*

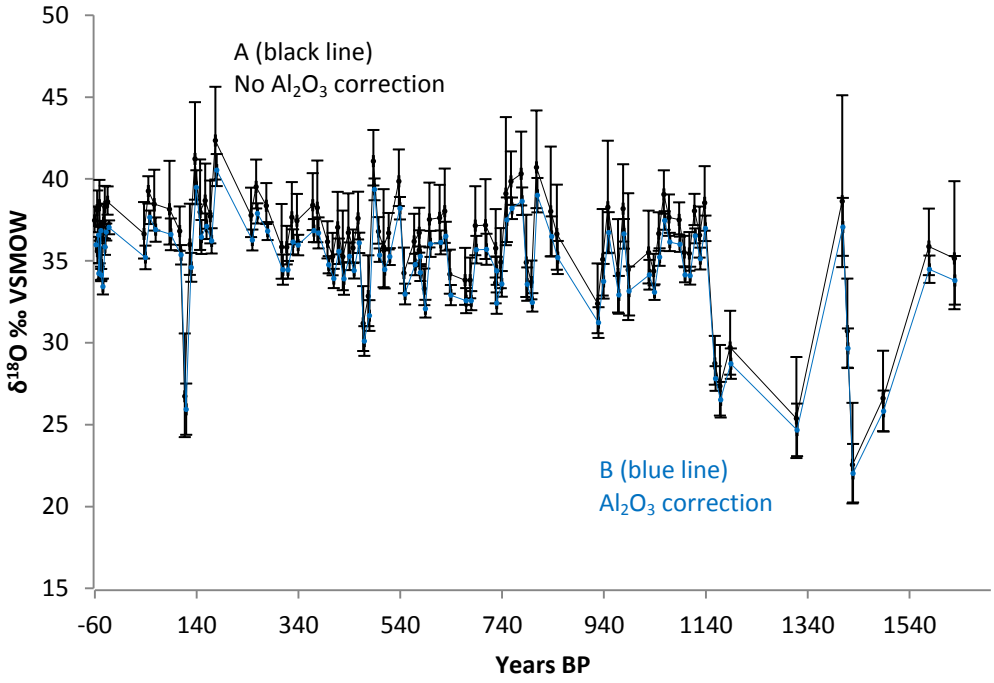

Figure 6.15 The effect of reducing Al_2O_3 values to correct for the influence of diatom-bound aluminium on the NAR01/02 diatom isotope record. A: without a reduction in measured Al_2O_3 values. B: with a reduction in Al_2O_3 values. Although $\delta^{18}O$ values are lower in B because contamination is calculated to be lower and therefore less of a correction is made (average $\delta^{18}O_{corrected}$ values of +36.0‰ in A and +34.7‰ in B), the trends very similar.

6.4.5 Diatom palaeotemperature equation

Where estimations of $\delta^{18}O_{lakewater}$ need to be made, the equation of Crespin et al. (2010) is used:

$$T = 245.3 - 6.25 \times (\delta^{18}O_{diatom} - \delta^{18}O_{lakewater}) \quad 6.11$$

where $\delta^{18}O_{lakewater}$ and $\delta^{18}O_{diatom}$ are expressed on the VSMOW scale and T in °C.

6.5 Palaeorecord: analysis of organics

6.5.1 Carbon isotope and C/N on bulk organics

Although carbon isotopes and changes in the productivity of the lake through time were not the major focus of this thesis, it was decided to undertake some analyses at a low resolution to provide another proxy record that could help with the interpretation of the carbonate isotope record. Samples were disaggregated in hydrochloric acid for 24 hours in 500 ml beakers to remove carbonates. The beakers were then filled with distilled water, the organic material left to settle for 24 hours and poured off (repeated twice more) to displace the hydrochloric acid. Dried samples were homogenised in an agate pestle and mortar. Samples containing 1-2 mg of material were weighed into tin cups and analysed for C/N and $\delta^{13}C$ in a Carlo Erba NA1500 and a VG Optima mass spectrometer. Samples were carried into a furnace by helium gas and fully combusted, with excess oxygen and water removed by passage through hot copper and magnesium perchlorate. The remaining N_2 and CO_2 were passed through a thermal conductivity detector to calculate the C/N ratio by calibration to the laboratory standard. The CO_2 was then frozen at –170°C and N_2 and helium removed, after which the CO_2 entered the mass spectrometer and $\delta^{13}C$ values were calculated relative to VPDB. Analytical reproducibility was 0.1‰. C/N values are given in wt%.

6.5.2 Oxygen isotope analysis of cellulose

An attempt was also made to isolate aquatic cellulose from the Nar Gölü sediments. Cellulose is hypothesised to record $\delta^{18}O_{lakewater}$ without a temperature effect (Edwards and McAndrews, 1989, Wolfe et al., 2005) so it can be combined with $\delta^{18}O$ values of diatom silica and/or carbonates to calculate lake water temperatures (e.g. Rozanski et al., 2010). The cleaning method used followed that of Wolfe et al. (2001, 2007). Firstly, samples were added to 125 ml glass screw top jars (rather than centrifuge tubes because of the toxicity of the chemicals used) and 10% hydrochloric acid was added and left for 24 hours to remove carbonates. Samples were then

frozen and freeze dried. 100 ml 2:1 toluene:ethanol mix was added, the lid screwed firmly on and stirred and left for 48 hours to remove lipids, resins and tannin. This was decanted after 48 hours, 100 ml of acetone added, decanted after 24 hours and left to air dry. Sodium chlorite, acidified to pH 4-5 with concentrated acetic acid, was then added to samples and left for 10 hours, after which the solution was decanted and refilled and left for another 10 hours, to remove lignin. 17 g sodium hydroxide was then mixed with 100 ml distilled water and added to samples for 15 minutes to remove xylan, mannan and other polysaccharides. 35 g sodium hydrosulphite, 52 g ammonium citrate and 14 g hydroxylamine hydrochloride were added to 1 L distilled water, and then 75 ml of this added to samples which were left in a water bath at 60°C for 2 hours and at room temperature for 24 hours, to remove oxyhydroxides. Between each of these stages, the chemical solutions were decanted off and the sample washed with distilled water three times. Finally, samples were transferred to centrifuge tubes and SPT of 1.9-2.0 specific gravity was added, to separate the cellulose from minerogenic matter. Finally, the SPT was flushed from samples by filtering them with distilled water at 0.45 µm. However, the samples were still contaminated (mainly with diatoms) and there was very little, if any, cellulose (Figure 6.16). Other researchers following this method have had similar issues (J. Tyler, pers. comm.). While another method (Wissel et al., 2008) could have been followed, since it seems that limited cellulose material was available and the method is time-consuming and requires the use of expensive and dangerous chemicals, it was decided to not proceed with cellulose oxygen isotope analysis.

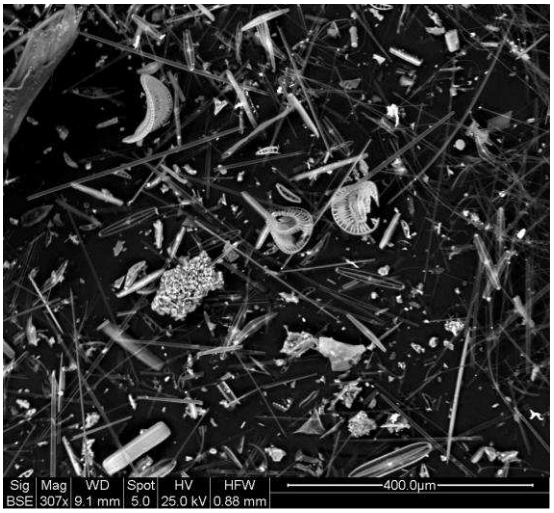

Figure 6.16 *Sample prepared using the Wolfe et al. (2001, 2007) method, with significant contamination and limited organic material.*

6.6 U-Th dating

Some of the NAR10 core sequence has varves (chapter 9), so counts were made of these sections independently by two people and recounted until agreement (to within 5 varve years) was reached (Allcock, 2013). However, there were sections that were not varved and U-Th dating (chapter 4) was used in an attempt to provide an absolute chronology for the core (as discussed in section 1.3, radiocarbon dating was not possible).

6.6.1 Laboratory methods and data handling

Samples were weighed into savillex beakers. 16M HNO_3 was added, which dissolved the carbonate fraction, and then the contents of the beaker was poured into centrifuge tubes and centrifuged. The carbonate fraction was pipetted off back into the beaker and spiked with ^{236}U-^{229}Th tracer solutions, and the samples left overnight at 110°C. The silicate fraction was left in another beaker in 16M HNO_3 at 100°C for 12 hours, then 16M HNO_3 and 30% H_2O_2 were used to oxidise organics, followed by 29M HF and 16M HNO_3 to remove the silicon. Finally, 12M $HClO_4$ and 16M HNO_3 were added and the beakers connected to an Evapoclean Telfon distillation elbow, which with heating allowed the acids to be distilled across the elbow leaving the sample dry. $HClO_4$ was used to ensure a complete dissolution of the silicate fraction, as used in other studies (Luo and Ku, 1991, Lin et al., 1996, Blard et al., 2011). Samples from the silicate fraction were then rehydrated in HNO_3 and added back to the carbonate fraction.

1M HCl and FeCl were added to the recombined mix and Fe was co-precipitated with uranium and thorium by adding ammonia solution to create $FeOH_2$, which contains the uranium and thorium. Samples were then centrifuged and the supernatant discarded. 16M HNO_3 and H_2O_2 were added to the precipitate to aid oxidation of organics. The solution was then added, with HNO_3, to anion-exchange columns filled with resin which trapped the uranium and thorium. The latter was released and

collected by washing 8M HCl through the resin (uranium remained trapped), and afterwards uranium was released from the resin and collected below by washing with 0.2M HCl. The process was repeated for thorium in a final clean-up stage and both fractions were then left in 16M HNO_3 and 30% H_2O_2 a final time before drying down.

Samples were analysed on a Thermo Neptune Plus MC-ICP-MS. Samples were dissolved in 0.2M HCL and 0.05M HF, sampled using an auto-sampler which was thoroughly washed in acid between runs and carried through the MC-ICP-MS using high purity Ar and trace N_2 gas. For uranium measurements, ^{233}U, ^{235}U, ^{236}U and ^{238}U beams were measured on Faraday detectors, while the ^{234}U beams were measured on more sensitive secondary electron multiplier detectors. 100 measurements were made for uranium isotopes and 75 for thorium isotopes.

Corrections needed to be made to the measured isotope values. Firstly, instrumental mass fractionation (preferential early vaporisation of lighter isotopes by the ICP) was corrected for by comparison to a standard, spiked with a ^{233}U-^{236}U tracer solution. Secondly, some values were derived from Faraday detectors and some (where beams were smaller and a more sensitive detector was required) from the secondary electron multiplier detector and equivalent values were derived from measurements of the un-spiked CRM 112a standard. Data were also corrected for on-peak zeros measured on pure acid solutions, for hydride interferences and for down-mass ion scattering due to ion collisions in the MC-ICP-MS flight tube. Final data reduction to uranium and thorium activity ratios and ages was done on a NIGL-developed Excel spreadsheet using the Isoplot 3.0 (Ludwig, 2012).

6.6.2 Correcting for detrital and hydrogenous thorium

To correct for detrital thorium, the isochron approach was used. Isochron ages are calculated in a [$^{232}Th/^{238}U$] vs. [$^{234}U/^{238}U$] vs. [$^{230}Th/^{238}U$] plot (Ludwig and Titterington, 1994, Ludwig, 2012) (Figure 6.17). In the Isoplot program, they are visualised in 2D in Osmond-type diagrams, where the correction for initial

[^{230}Th/^{238}U] ratio is derived from the y-intercept of a [^{232}Th/^{238}U] vs. [^{230}Th/^{238}U] plot and the correction for initial [^{234}U/^{238}U] values is derived from the y-intercept on a [^{232}Th/^{238}U] vs. [^{234}U/^{238}U] plot (Osmond et al., 1970). Corrected [^{230}Th/^{238}U] and [^{234}U/^{238}U] can then be inserted into Eq. 4.1, assuming the assumptions of a closed system and that all initial ^{232}Th and ^{230}Th are from detritus and [^{234}U/^{238}U] and [^{230}Th/^{232}Th] of detritus is the same in all samples.

An attempt was made to establish if hydrogenous thorium was an issue in the Nar Gölü sediments by running core sediments from the top, varved part of the sequence that were of a known age, as was done with the Dead Sea sediments (Haase-Schramm et al., 2004, Torfstein et al., 2009, 2013) (section 4.3). Once the isochron approach has been used to correct for detrital thorium, any offset from zero age (sediment trap material) or varve age (core sediments) would be due to the presence of hydrogenous thorium. If this offset of U-Th isochron age from actual age can be assumed to be constant through the rest of the record, then this offset can simply be subtracted from the U-Th isochron age.

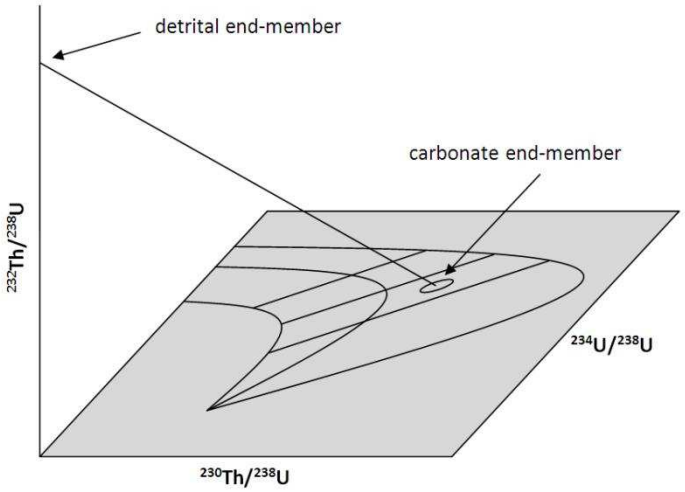

Figure 6.17 *Hypothetical 3D isochron plot (modified from Ludwig and Titterington, 1994).*

6.7 Summary

The main focus of this thesis is $\delta^{18}O_{carbonate}$ because it has already been shown to be a good proxy for regional water balance in Nar Gölü (Jones et al., 2005) and can therefore be used to investigate the aims of this thesis (section 1.4). $\delta^{13}C_{carbonate}$, $\delta^{18}O_{diatom}$, $\delta^{13}C_{organic}$, C/N, lithology and carbonate mineralogy data were also produced, as summarised in Figure 6.18, to assist in its interpretation. A chronology was provided by varve counting and U-Th dating. Methodological issues had to be overcome, namely how to deal with dolomite in carbonate isotope samples, mass balance correction of diatom isotope samples contaminated with minerogenic material and U-Th dating of dirty carbonates.

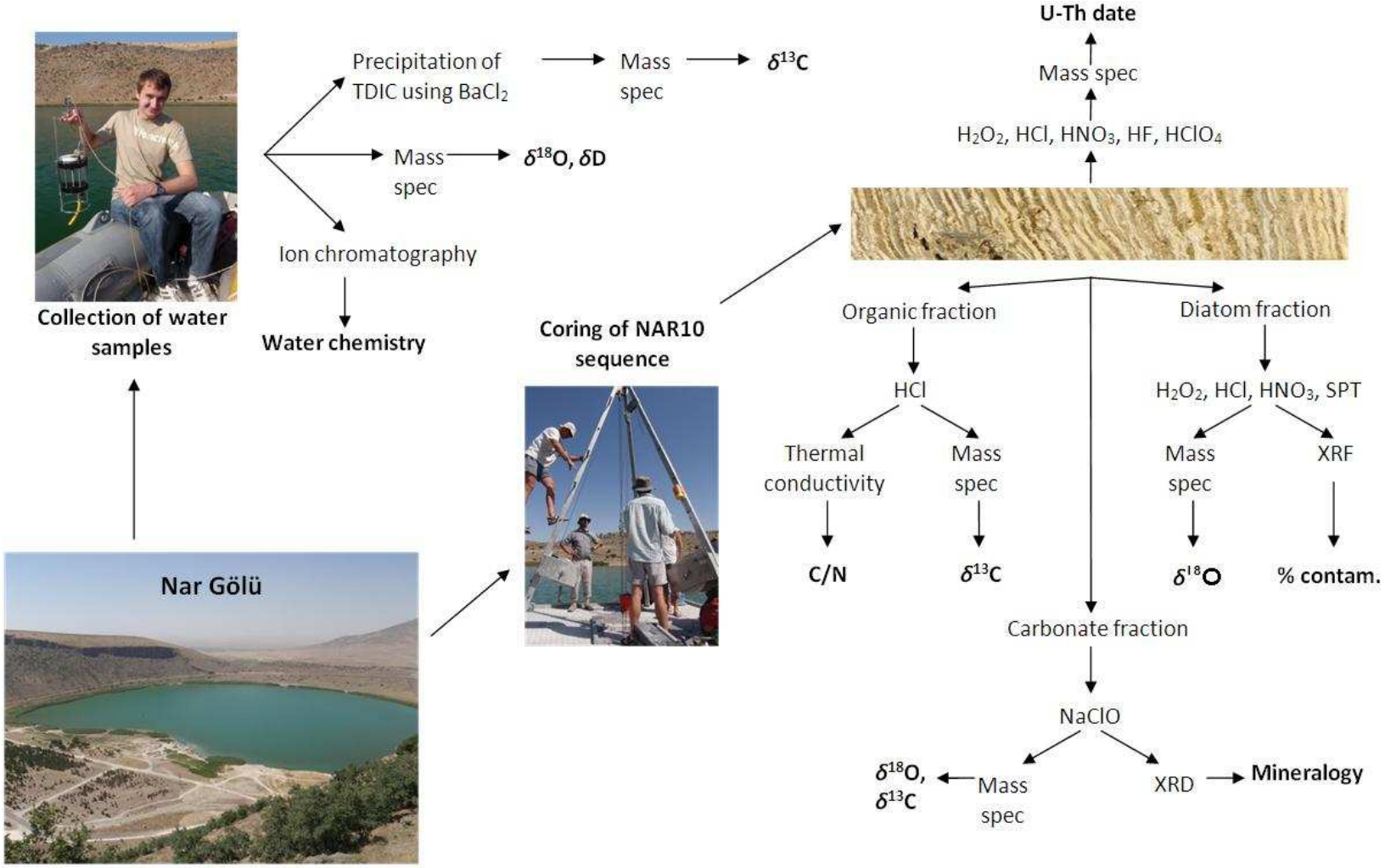

Figure 6.18 *Summary of methods used in this thesis.*

Chapter 7 | Results and interpretation of contemporary waters and sediments

Since the work outlined in chapter 5 was carried out, monitoring of the lake has continued and with the taking of the NAR10 cores (section 6.1.2) it has been possible to compare $\delta^{18}O_{lakewater}$, sediment trap $\delta^{18}O_{carbonate}$ and core $\delta^{18}O_{carbonate}$, to investigate the transference of the isotope signal through the system, with the objective of being able to better interpret the palaeo record in chapters 8 and 10. In particular, two issues are addressed:

- Inter-annual variability in $\delta^{18}O_{lakewater}$ and $\delta^{18}O_{carbonate}$ from sediment cores and sediment traps: making comparisons with lake depth and other data to investigate the drivers of oxygen isotopes in the Nar Gölü system, building on the work of Jones et al. (2005).
- Intra-annual variability in $\delta^{18}O_{lakewater}$ and the timing of carbonate precipitation and diatom growth: attempting to understand whether there are differences in the time of year carbonate precipitates and diatoms grow in Nar Gölü and if so whether lake conditions are significantly different at these times, and whether comparing $\delta^{18}O$ from the two hosts may provide insights into seasonality. This builds on the work of Jones et al. (2005), Woodbridge and Roberts (2010) and Dean et al. (2013).

7.1 Inter-annual variability

7.1.1 Oxygen isotopes

As discussed later in section 7.2, water samples have been taken from the lake at different times of the year. However, this section aims to understand inter-annual variability, so values from around the same time of year in multiple years were required. Most field work has been carried out at Nar Gölü in July, so data from this month are presented here. Sometimes it was possible to take samples from the middle of the lake, but sometimes only edge samples could be taken. Although

samples from the centre may be considered more representative of overall lake conditions, as edge samples from shallow water may be more affected by evaporation, in years where both centre and edge samples were taken the difference is only ±0.3‰ (1σ, n=4), which is small considering the size of the inter-annual isotopic shifts seen in the record. Therefore, edge samples in 2000 and 2005 have been combined with centre samples from the other years in order to provide a more complete record.

Jones et al. (2005) had shown through calibration with the meteorological record and modelling that the major driver of $\delta^{18}O_{carbonate}$ at Nar Gölü is water balance, which is what would be expected from a closed lake with a long residence time (Leng and Marshall, 2004). However, these conclusions were based on a water isotope record of limited temporal resolution. Here, more data are presented which support the assertion that water balance is the key driver of $\delta^{18}O_{carbonate}$ at Nar Gölü. Firstly, it is possible to show that the effect of factors other than water balance on $\delta^{18}O_{carbonate}$ in Nar Gölü over the last decade has been limited. As discussed in section 3.4, $\delta^{18}O_{carbonate}$ is dependent upon temperature and $\delta^{18}O_{lakewater}$ at the time of carbonate precipitation (Leng and Marshall, 2004). The importance of the former can be ruled out, since the fractionation factor is –0.24‰°C^{-1} and Figure 7.1 shows that temperatures have actually risen over the past decade, which means if this was the main driver of $\delta^{18}O_{carbonate}$, $\delta^{18}O_{carbonate}$ values would have fallen. $\delta^{18}O_{lakewater}$ can therefore be seen to be the main influence on $\delta^{18}O_{carbonate}$.

The main influences on $\delta^{18}O_{lakewater}$ can be split into two factors. Firstly, $\delta^{18}O_{precipitation}$ will be considered. Spring waters at Nar Gölü are assumed to reflect local precipitation as they fall on the Ankara meteoric water line (Figure 7.2). There has not been a substantial increase in $\delta^{18}O$ of spring waters over the decade (from –10.54‰ in August 2001 to –10.57‰ in April 2013), which suggests changes in $\delta^{18}O_{precipitation}$ have not been large enough to drive the increase in $\delta^{18}O_{lakewater}$ observed over the past decade (Figure 7.1). Therefore, the second main influence on $\delta^{18}O_{lakewater}$, modification within-lake, seems the likely explanation, with $\delta^{18}O$ recording changes in water balance.

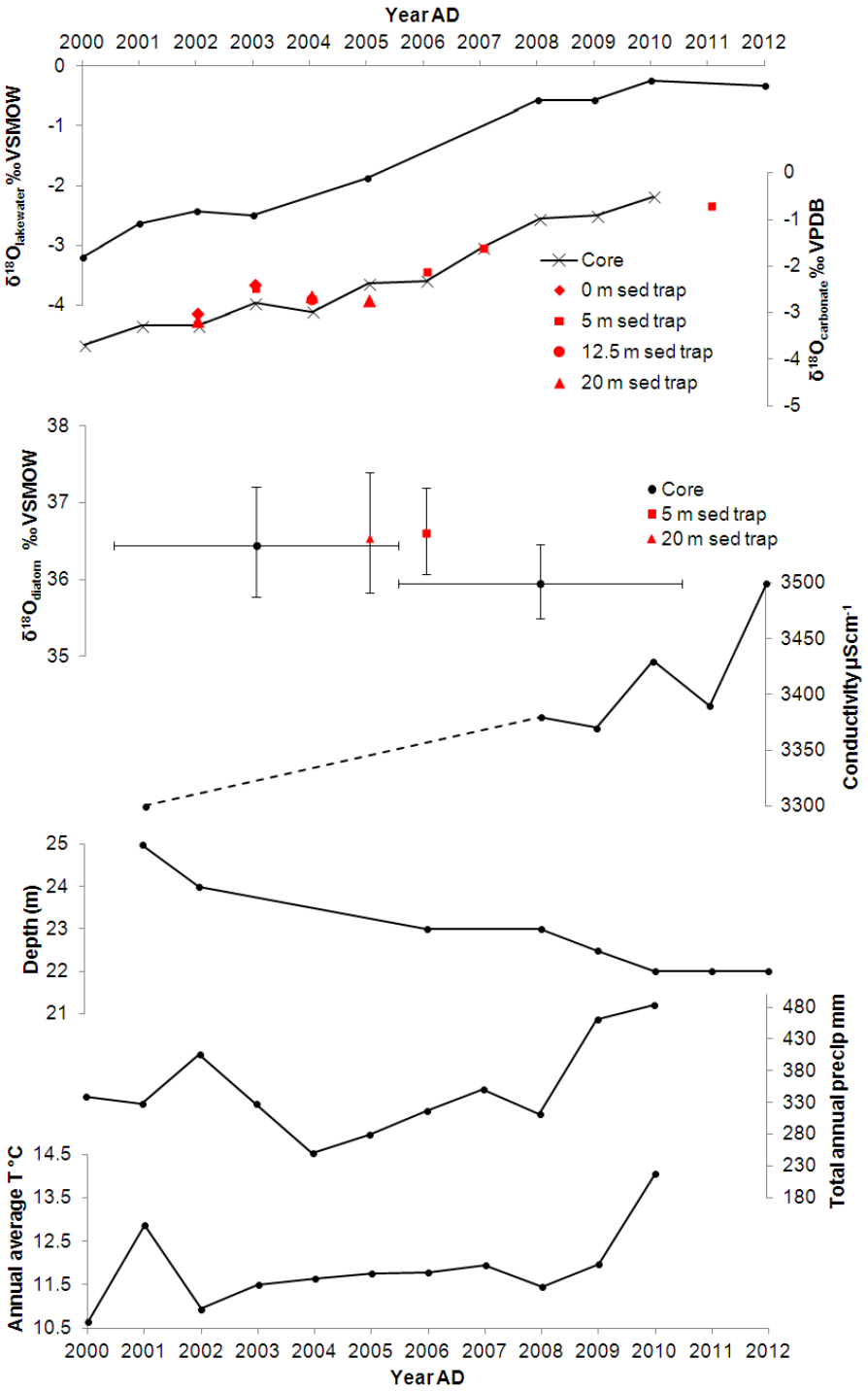

Figure 7.1 *$\delta^{18}O_{lakewater}$ (from July surface samples), $\delta^{18}O_{carbonate}$ from core and sediment traps, $\delta^{18}O_{diatom}$ from core and sediment traps (x-axis error bars show the years the core samples represent and y-axis error bars the uncertainties associated with isotope measurements and mass balance correction) and conductivity (from July surface water samples), plotted with changes in maximum lake depth and meteorological data from Niğde showing rises in temperature and precipitation in the 2000s (data collected by the Turkish Meteorological Service).*

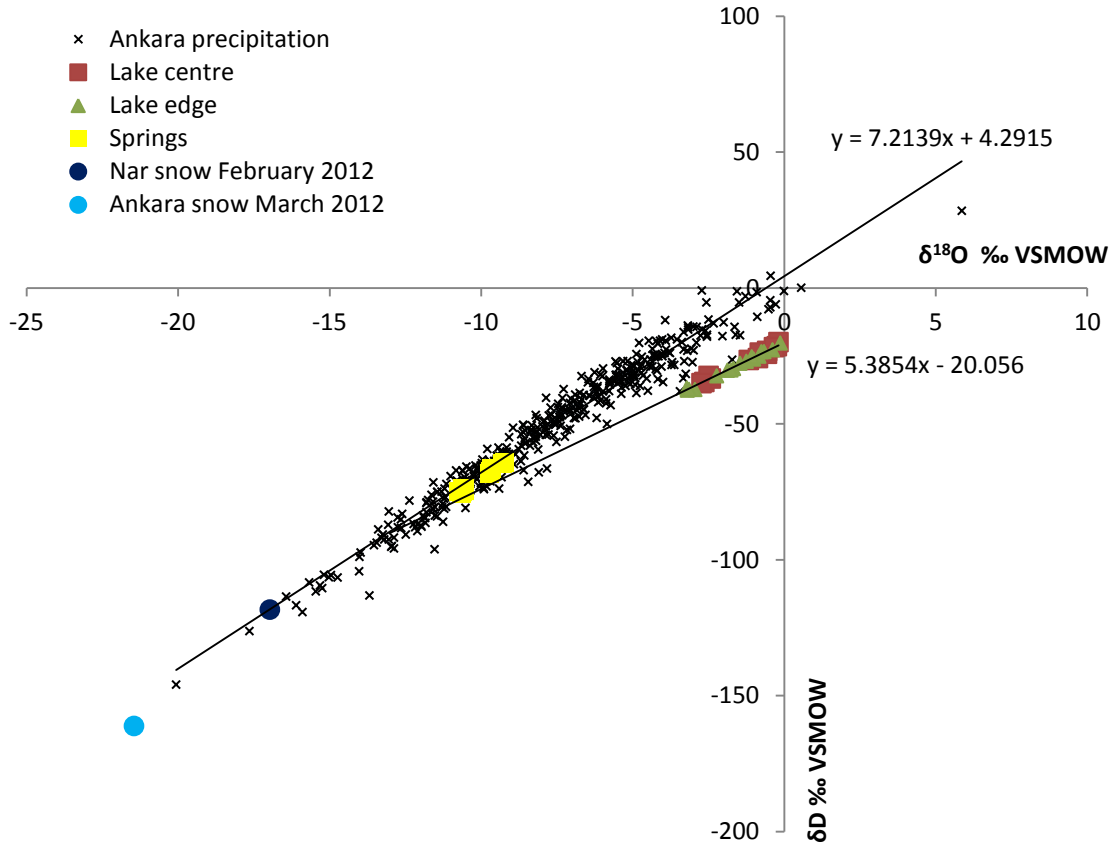

Figure 7.2 *δD-δ^{18}O plot with data from the Ankara GNIP station 1964-2009 (IAEA/WMO, 2013) defining the LMWL. Lake waters plot off the LMWL suggesting evaporative enrichment.*

There are a number of factors that support the interpretation of water balance being the main driver of δ^{18}O in the Nar Gölü system. Firstly, Figure 7.2 shows the hot and cold spring water δ^{18}O values plot on the local meteoric water line, suggesting they represent a weighted average of precipitation, whereas the lakewater δ^{18}O values plot off the line, suggesting evaporative enrichment within-lake. Secondly, $\delta^{18}O_{lakewater}$ and $\delta^{18}O_{carbonate}$ trends seem to follow changes in the depth of the lake. July $\delta^{18}O_{lakewater}$ values have become more positive over the last decade (from –3.20‰ in 2000 to a peak of –0.24‰ in 2010 and –0.34‰ in 2012 (Figure 7.1), suggesting that evaporation is currently exceeding precipitation and groundwater inflow. $\delta^{18}O_{carbonate}$ values increased from –3.7‰ in 2000 to –0.5‰ in 2010 and there is a very strong, positive and significant relationship between $\delta^{18}O_{lakewater}$ and

$\delta^{18}O_{carbonate}$ (r = +0.99, n=8, p<0.005). As $\delta^{18}O_{carbonate}$ and $\delta^{18}O_{lakewater}$ values have fairly consistently increased over the last decade, the maximum depth of the lake has fallen from ~25 m to ~22 m (Figure 7.1). Nar Gölü has a residence time of 8-11 years (Jones, 2004), which means the response of the lake to changes in climate will be delayed and smoothed, so $\delta^{18}O$ data from the last decade should be viewed in the context of what was going on in the years before. Figure 7.1 shows that since the mid-1990s precipitation has actually increased slightly (average 352 mm 2001-2010 compared to 339 mm 1935-2011), however DJF precipitation has decreased (average 91 mm 2001-2010 compared to a mean of 108 mm from 1935-2011). Annual temperatures have risen since 1992 to an average of +12.0°C 2001-2010 compared to +11.1°C 1935-2010, and JJA temperatures average +22.8°C 2001-2010 compared to 21.4°C 1935-2010. Of the 10 hottest months on record as measured by average temperature, 8 were in the 2000s. Higher temperatures will have meant more evaporation and the shift of precipitation away from DJF to other months when temperatures are higher will likely have meant less of this precipitation made its way into the lake due to evaporation on route, and these factors can explain the observed fall in lake levels.

Thirdly, water chemistry data also suggest the lake is closed and experiences significant evaporation. Conductivity has increased over the past decade, which supports the argument that water balance has become more negative (Figure 7.1). The trend in conductivity is less clear than the increase in $\delta^{18}O$, although there has been a gradual upwards trend from 3300 μScm^{-1} in July 2001 to 3370 μScm^{-1} in July 2009 to 3433 μScm^{-1} in July 2010 and 3500 μScm^{-1} in July 2011. Table 7.1 shows an increase in the concentration of some major ions from 1999, 2010 and 2012, although the gap in water chemistry data between these times means it is difficult to investigate trends reliably. The increase in the Mg/Ca ratio, caused by concentration of magnesium due to evaporation and loss of calcium due to precipitation of calcium carbonate (Kelts and Talbot, 1990), is of particular significance as it seems to have had an influence on the mineralogy of the carbonates precipitated in the lake. There was a shift from calcite precipitation 1987-2010 to aragonite precipitation in 2011 and 2012, seen in sediment traps, surface precipitates (Figure 7.3) and sediment

cores. This sort of mineralogical shift is seen to be caused by an increase in the Mg/Ca ratio of the lake (Muller et al., 1972, Kelts and Hsu, 1978, Ito, 2001), which favours the precipitation of aragonite over the calcite, because the presence of Mg^{2+} ions decreases calcite precipitation rates while having no effect on aragonite formation (Berner, 1975, De Choudens-Sanchez and Gonzalez, 2009).

Table 7.1 *Major ion concentrations in Nar Gölü surface waters.*

	Concentration meq/L						
	SO_4^{-2}	**Cl^-**	**Na^+**	**K^+**	**Mg^{2+}**	**Ca^{+2}**	**Mg/Ca**
August 1999	3.2	27.4	16.5	3.7	8.5	3.0	2.9
July 2010	3.8	22.7	16.2	3.6	15.4	1.0	16.2
July 2012	4.1	23.9	16.9	3.8	16.5	1.2	13.3

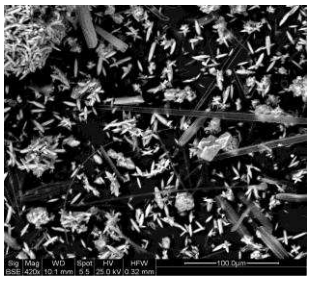

A

B

Figure 7.3 *A: sediment trap material from 2011 showing 'rice' shaped aragonite crystals as well as diatoms. B: 'white-out' around the edges of Nar Gölü lake in July 2012 and inset an SEM image identifying this as aragonite.*

$\delta^{18}O_{diatom}$ is seen to have similar drivers to $\delta^{18}O_{carbonate}$ (Leng and Barker, 2006, Leng and Swann, 2010), so following the logic outlined above $\delta^{18}O_{diatom}$ should also be a proxy for water balance. However, single varves do not yield sufficient diatom silica for $\delta^{18}O_{diatom}$ analysis (5 year bulk samples had to be used) and there are errors associated with the mass balance correction. Consequently, there are only two $\delta^{18}O_{diatom}$ samples for the period covered by the monitoring data and there is no difference between the two values outside of error (Figure 7.1). This prevents a comparison with lake depth and highlights the difficulties of $\delta^{18}O_{diatom}$ interpretation compared with $\delta^{18}O_{carbonate}$ interpretation in Nar Gölü (Dean et al. 2013). However, the similarity of sediment trap values to sediment core values does suggest diagenetic/dissolution/maturation effects (e.g. Moschen et al., 2006) are not significantly altering the isotope signal between diatom growth and deposition. Woodbridge and Roberts (2010) also showed that the vast majority of diatom species are present in both the modern and palaeo records.

7.1.2 Carbon isotopes

There is less of a clear increase in $\delta^{13}C_{carbonate}$ values from the core sediments (Figure 7.4), although values do increase from +12.4‰ in 2000 to +14.4‰ in 2010. July $\delta^{13}C_{TDIC}$ values increased from +10.8‰ in 2000 to +12.1‰ in 2012, although values fell to a minimum of +9.8‰ in 2010. While $\delta^{13}C_{TDIC}$ values 1-2‰ lower than $\delta^{13}C_{carbonate}$ core values are expected (Leng and Marshall, 2004), the lack of a relationship between the two variables is difficult to explain.

Hot spring waters have similar $\delta^{18}O$ values to waters in the cold springs, which as discussed are seen to represent precipitation, and these values are enriched by evaporation once the waters make their way into the lake (Figure 7.5). However, the hot spring waters have $\delta^{13}C$ values significantly higher than the cold springs (mean +4.1‰ compared to –11.6‰ respectively). It is difficult to account for such positive $\delta^{13}C$ values in the hot springs. Preferential degassing is considered an unlikely explanation, as this would lead to enrichment in $\delta^{18}O$ as well. The mean value of the hot springs 2000-2013 is –10.30‰, similar to the mean of the cold springs of

–10.62‰. One hypothesis is that the hot springs are composed of meteoric waters that have fallen to depth and interacted with so far unidentified carbonate rocks with high $\delta^{13}C$ values. $\delta^{13}C_{TDIC}$ values in the lake waters are even higher than in the hot springs, with a mean of +10.5‰ 1997-2012. As discussed in section 3.7, three main factors influence TDIC in lake waters: isotopic composition of inflowing waters, exchange with the atmosphere and changes due to organic processes and diagenesis. Such high $\delta^{13}C_{TDIC}$ values in the lake waters are probably due to a combination of the originally high $\delta^{13}C_{TDIC}$ coming into the lake from the hot springs, and then further modification due to exchange with the atmosphere with preferential degassing of ^{12}C, preferential uptake of ^{12}C by aquatic plants and the locking away of ^{12}C in the anoxic sediments, and potentially methanogenesis where CH_4 is preferentially produced using ^{12}C leaving the remaining TDIC pool with more positive $\delta^{13}C$ values (Talbot and Kelts, 1986, Gu et al., 2004, Leng et al., 2013). A more detailed discussion of the carbon isotope system at Nar Gölü is beyond the scope of this thesis, as it would not significantly contribute to the aims outlined in section 1.4.

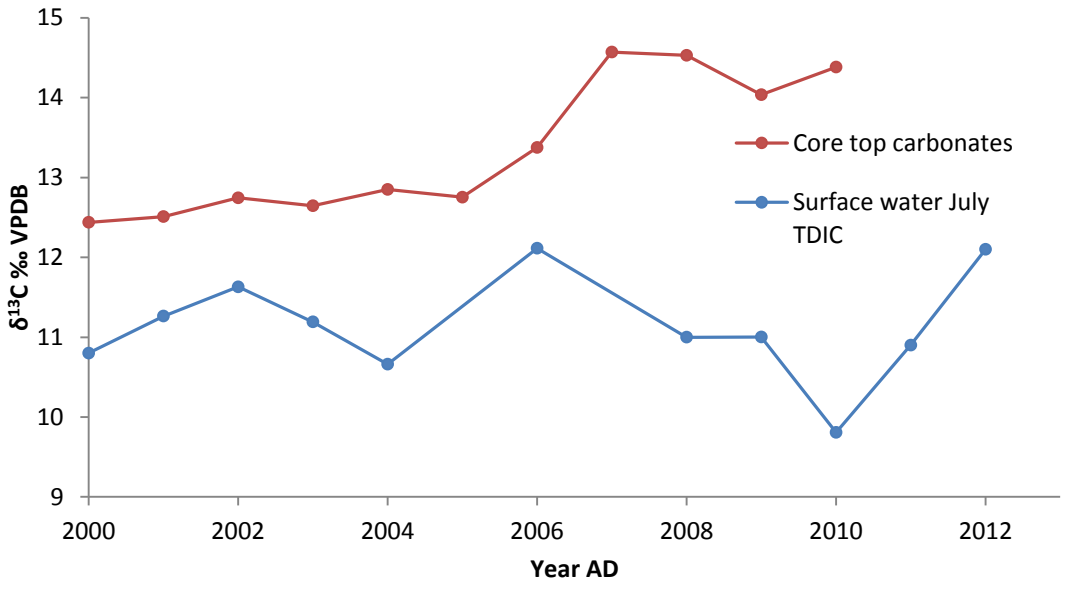

Figure 7.4 *$\delta^{13}C_{TDIC}$ from July waters and $\delta^{13}C_{carbonate}$ from core sediments.*

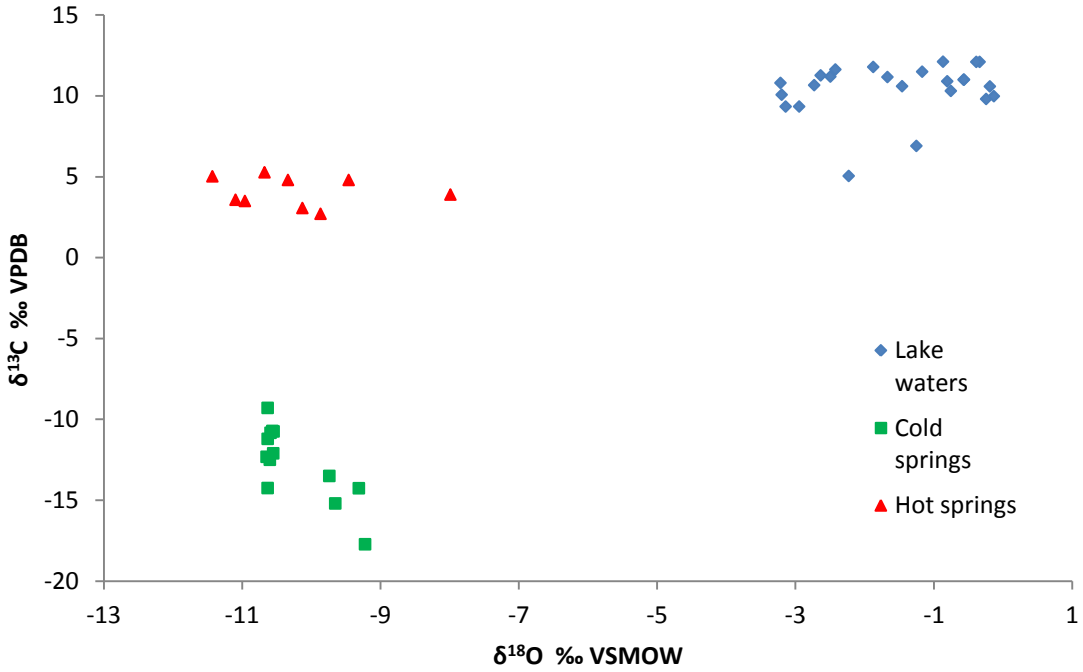

Figure 7.5 *$\delta^{13}C$-$\delta^{18}O$ plot showing the similarity of hot and cold spring $\delta^{18}O$ values but significant enrichment in $\delta^{13}C$ in the hot springs, and even higher $\delta^{13}C$ and $\delta^{18}O$ values in the lake compared to in the springs.*

7.2 Intra-annual variability

7.2.1 Isotopic variability

Figure 7.6 shows the variability in oxygen and carbon isotopes and water chemistry from edge samples taken between June 2011 and July 2012. $\delta^{18}O$ values reach a peak of –0.13‰ in mid-September 2011 before falling to –1.76‰ in mid-March 2012 and then increasing to –0.39‰ in mid-July 2012. Conductivity values also reach a peak in mid-September 2011 at 3539 μScm^{-1}, before declining to 2190 μScm^{-1} in late February 2012 and rising again to 3522 μScm^{-1} by July 2012. $\delta^{13}C_{TDIC}$ values were higher in June 2011 (+10.9‰) than September 2011 (+10.6‰), although as with the $\delta^{18}O$ values there is a decline to lower values in early 2012 (+6.9‰ in late February) before an increase to +12.1‰ by July 2012. Magnesium concentrations decline from a peak of 15.6 meq/L in June 2011 to a minimum of 3.2 meq/L in late February 2012 and then rising again to 16.5 meq/L by July 2012, whereas calcium concentrations

show the opposite trend, shifting from 1.4 meq/L in June 2011 to 4.0 meq/L in late February 2012 to 1.2 meq/L in July 2012.

There are three explanations for the lowering of $\delta^{18}O_{lakewater}$ and salinity in the winter and its increase in the summer. Firstly, the water in the lake as a whole could become more isotopically depleted in the autumn, winter and spring due to precipitation entering the lake, which is fresh and isotopically depleted relative to the lake water (average $\delta^{18}O$ of cold springs, assumed represent precipitation, was –10.62‰ 2000-2013). Although not quantified, lake levels were visibly higher in February 2012 than they had been in September 2011 suggesting this factor might be important. It is not surprising that $\delta^{18}O_{lakewater}$ is lowest in mid March, since Figure 7.7 shows this is around the time the snow from the catchment was melting and would have entered the lake and Figure 5.3 shows precipitation is greatest in the spring. Secondly, stratification of lake waters in the summer leads to more positive $\delta^{18}O$ values in surface waters. Figure 7.8 shows that in the summer the waters of Nar Gölü are thermally, chemically and isotopically stratified, with warmer and isotopically more positive waters in the epilimnion, followed by a shift at ~7 m to colder and isotopically more depleted values (although conductivity trends are ambiguous). Comparisons of the depth profiles from April, June, July and September (although note these profiles are from different years) show that the thermo- and iso-clines become more enhanced as the year progresses, with a 1.00‰ difference between surface and bottom water $\delta^{18}O$ values in September 2011 compared to a 0.75‰ difference in July 2010, 0.24‰ in June 2011 and 0.23‰ in April 2013. It was not possible to take samples through the water column during the February visit of 2012 due to adverse weather conditions, but tiny tag temperature loggers suggest that, at least thermally, the lake is mixed from late November to early March (Eastwood et al., unpublished data). The third explanation for differences in $\delta^{18}O$ between seasons is snowmelt (which is very isotopically depleted: a snow sample taken from the catchment in February 2012 had a value of –16.98‰) forming a freshwater lid due to the density contrast with underlying saline waters. This is observed in Greenland and Canada (McGowan et al., 2003, Willemse et al., 2004, McGowan et al., 2008, Pieters and Lawrence, 2009). In Dean et al. (2013) it was

suggested that this might have occurred in Nar Gölü in the past, in order to explain how $\delta^{18}O_{lakewater}$ values calculated from $\delta^{18}O_{diatom}$ in parts of the core were so low. $\delta^{18}O_{lakewater}$ values for March 2012, when Figure 7.7 shows the snow was melting, are not as low as would be expected if a freshwater lid had formed. However, this is not to say a freshwater lid may not have occurred in the past if there was more snowfall, as will be discussed in section 10.4. Therefore, in the present, intra-annual variability in $\delta^{18}O$ of surface waters seems to be driven by both summer stratification and changes in the isotopic composition of the lake as a whole resulting from seasonal precipitation:evaporation variability.

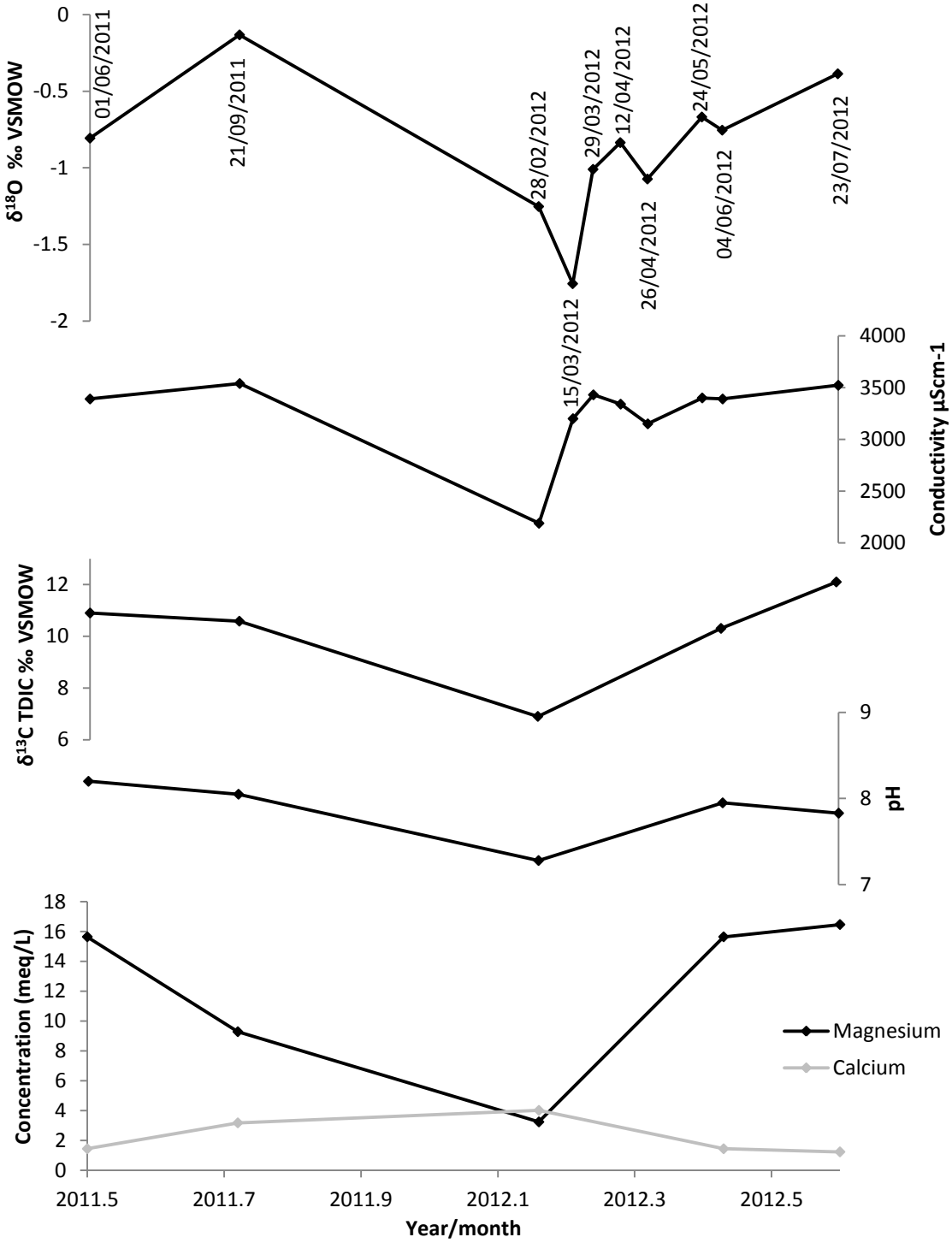

Figure 7.6 *Isotope and chemistry data from June 2011 to July 2012 from lake edge samples taken during field visits and by members of the local community.*

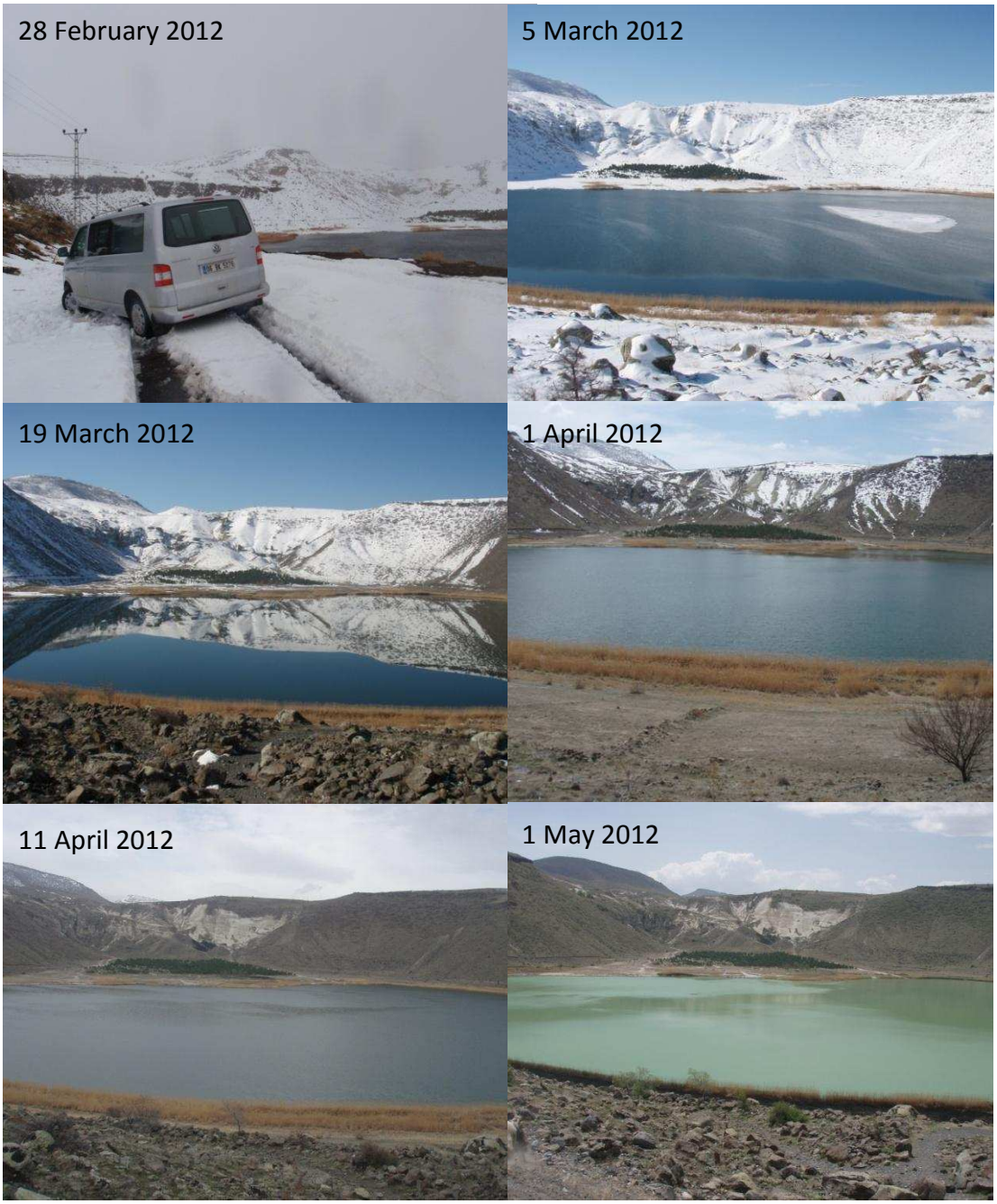

Figure 7.7 *Nar Gölü through the spring of 2012, showing snow starting to melt and ice disappearing from lake by 19 March, snow completely melted from the catchment by 11 April and a 'greening' of the lake on 1 May.*

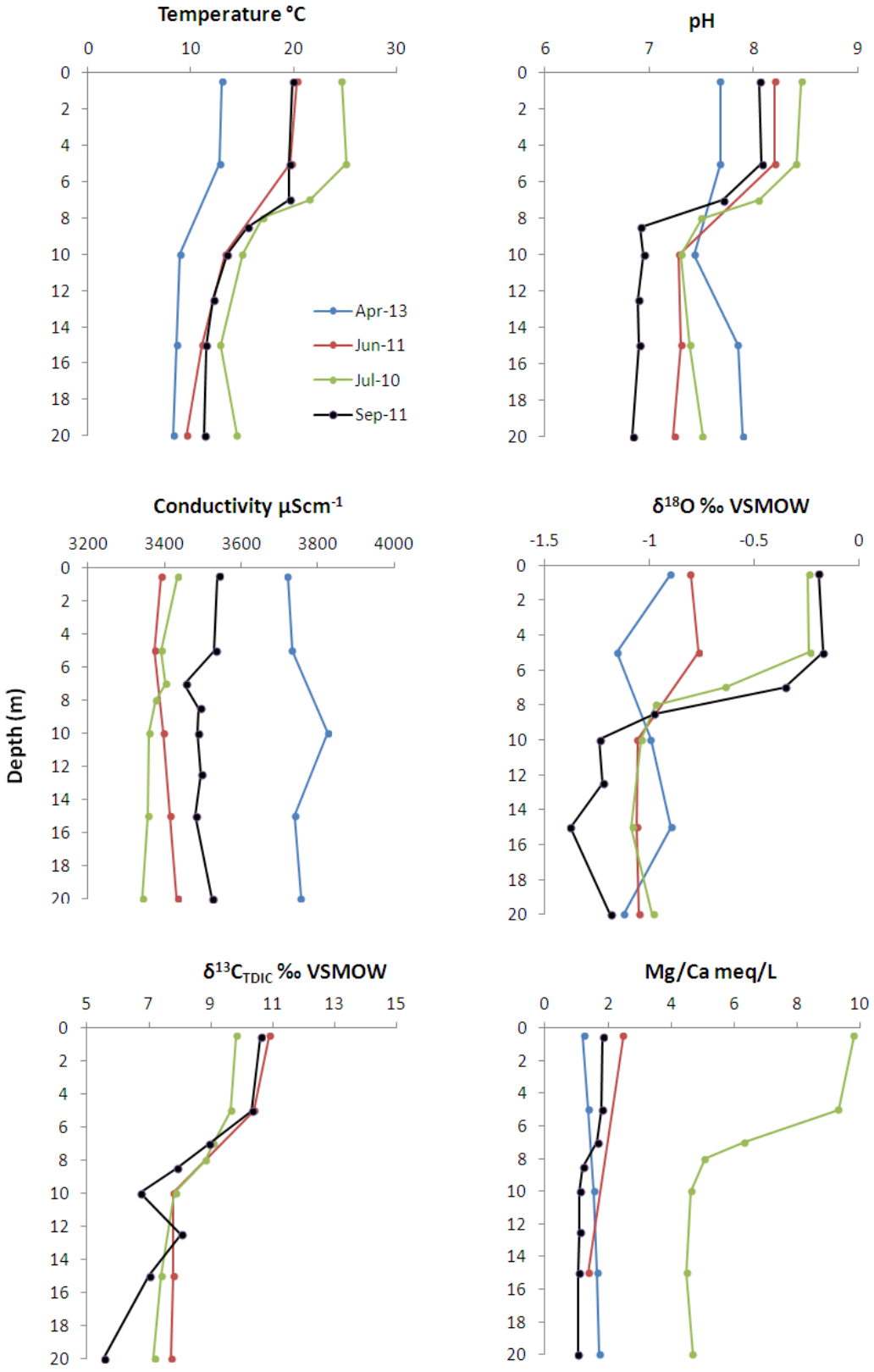

Figure 7.8 *Depth profiles showing changes in temperature, isotopic composition and chemistry with depth and how this varies between different times of the year.*

7.2.2 Timing of carbonate precipitation

In Dean et al. (2013) it was suggested that diatom growth was weighted towards the spring and carbonate precipitation to May-June. Here this can be investigated further. Carbonate precipitation in surface waters is supported by the fact that sediment traps at 5 m depth tend to be covered in carbonate, whereas deeper ones do not. In the summer, calcium values at the surface are lower than at depth, suggesting draw down of calcium carbonate from the surface waters at this time (Reimer et al., 2009). Analysis of the stratigraphy of sediment traps collected in July in the early 2000s shows carbonate deposited on top of organic matter (Jones, 2004). The topmost sediments from Glew cores retrieved in April 2013 were composed of organic material, not carbonates, and calcium concentration was still higher in surface waters than at depth. This all suggests that carbonate precipitation peaks sometime after April but before July. Thin section analysis shows that *Nitzschia paleacea* bloom layers directly precede carbonate layers on average 1 year in 5 (Woodbridge and Roberts, 2010), suggesting carbonate precipitation may in some years be initiated by the diatom blooms drawing down CO_2 and raising pH which can lead to carbonate supersaturation (Siegenthaler and Eicher, 1986, Bronmark and Hansson, 2005, Deocampo, 2010). In other years, non-diatom algae may initiate the carbonate precipitation. Carbonate may precipitate through a large proportion of the year, and Jones (2004) showed variance in $\delta^{18}O_{carbonate}$ with depth in the sediment trap suggesting this was the case, but $\delta^{18}O_{carbonate}$ measured in the palaeo record from a whole-year varve will be weighted towards the time of maximum precipitation, which as discussed from observations appears to be between May and July. Modelling using Eqs. 6.2 and 6.3 can be used to better investigate the timing of carbonate precipitation, but before the equations are used it needs to be shown that carbonate is precipitating in isotopic equilibrium with lake water and that there are no dissolution/diagenetic effects.

At Nar Gölü, whole lake white-outs have been described by local villagers and in July 2012, aragonite was seen precipitating around the edges of the lake in a ‘white-out’ event (Figure 7.3), as has been documented in many other lakes (e.g. Romero-Viana

et al., 2008, Sondi and Juracic, 2010, Viehberg et al., 2012). The $\delta^{18}O_{carbonate}$ value of the precipitate (–1.3‰) is below that expected based on the trend over the last decade to more positive values (Figure 7.1), which suggests this precipitate is not typical of the $\delta^{18}O_{carbonate}$ values derived from the analysis of a whole carbonate varve from core sediments or sediment trap samples which would be representative of the whole year (although core and trap sediments are not yet available for 2012). Average temperature at the mean time of carbonate precipitation is likely to be lower than the temperature of +25.6°C recorded when the aragonite was precipitating, which would result in a higher $\delta^{18}O_{carbonate}$ from samples containing carbonate from the whole year. However, because the temperature, $\delta^{18}O_{carbonate}$ and $\delta^{18}O_{lakewater}$ (–0.39‰) are all known, it is possible to use Eq. 6.5 to show that the surface precipitate formed in equilibrium within error (actual value –1.3‰; equilibrium predicted value –1.8‰, ±0.1‰ analytical reproducibility, ±0.9‰ error from the equation (Kim et al., 2007a)).

Investigation of the possible influences of dissolution and diagenesis on the isotope signal is also required. SEM images of calcite and aragonite from the core (e.g. calcite in Figure 7.9) have the characteristics of primary precipitates with no features such as rounding or etching of calcite crystals suggesting diagenetic alteration (as seen in e.g. Kelts and Hsu, 1978, Talbot and Kelts, 1986, Katz and Nishri, 2013). Also, the fact that there are only limited differences in $\delta^{18}O_{carbonate}$ between sediment traps at different depths and between sediment traps and core sediments suggests the $\delta^{18}O$ signal is preserved (Figure 7.1).

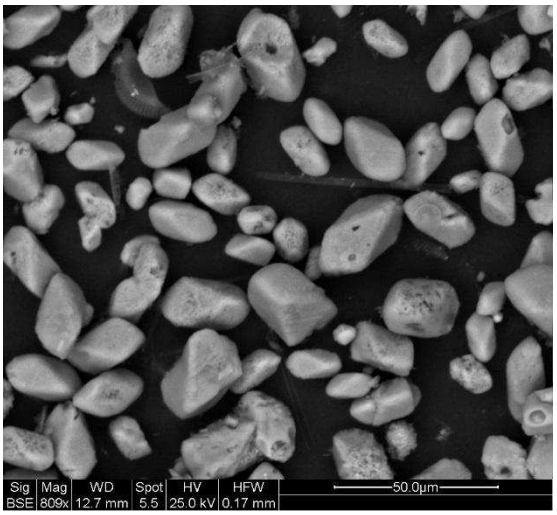

Figure 7.9 *Rhombic calcite crystals from the early Holocene, showing minimal etching or rounding which would be indicative of dissolution or formation through diagenetic processes.*

Therefore, since it seems carbonate forms in equilibrium (at least in July 2012) and the influence of dissolution and diagenesis on the isotope record is minimal, it is possible to run Eqs. 6.2 and 6.3 using various $\delta^{18}O_{lakewater}$ and temperature values and compare calculated equilibrium values to measured core $\delta^{18}O_{carbonate}$ values through the monitoring period, in an attempt to better determine the time of year to which carbonate precipitation is weighted. Based on the observations and analysis of sediment outlined above, it was assumed that most carbonate precipitated after diatom growth, probably sometime between May and June, and in surface waters. Therefore, likely surface water temperature and $\delta^{18}O$ values for these times are used. Temperatures clearly vary from year to year, but data loggers suggest temperatures change from ~+12.5°C in the beginning of May to ~17.5°C in mid-June and ~22.5°C by mid-July (Eastwood et al., unpublished data). In 2012, $\delta^{18}O_{lakewater}$ values were 0.7‰ lower in May compared to July, while in 2009 $\delta^{18}O_{lakewater}$ was 0.6‰ lower. Consequently, in this modelling exercise, temperatures ranging from +12.5°C to +22.5°C and $\delta^{18}O_{lakewater}$ values from measured July values and back at 0.2‰ intervals to those likely in the beginning of May (0.8‰ lower) were used. All varves 2001-2010 were composed of calcite and both Eqs. 6.2 and 6.3 were used and values compared (Figures 7.10 and 7.11). Using both equations, predicted

$\delta^{18}O_{carbonate}$ values hit measured $\delta^{18}O_{carbonate}$ values at temperatures of ~+15-17.5°C. At +17.5°C, in most years, $\delta^{18}O_{lakewater}$ values found in July are required to predict $\delta^{18}O_{carbonate}$ accurately, but actual temperatures in July are likely several degrees higher than this. At +15°C, particularly using Eq. 6.2, $\delta^{18}O_{lakewater}$ values predicted for early May are required in most years to accurately predict actual $\delta^{18}O_{carbonate}$, but at this time temperatures are likely to have been lower than that. However, at ~+16°C and a $\delta^{18}O_{lakewater}$ value –0.4‰ lower than July, the actual $\delta^{18}O_{carbonate}$ values are hit by the predictions. These $\delta^{18}O_{lakewater}$ values and temperatures are representative of conditions around early to mid-June. Although there are considerable uncertainties associated with the equations, this estimation is in line with the observations outlined above. Therefore, it is assumed carbonate precipitation in Nar Gölü, at least over the last decade, has been weighted towards early to mid June.

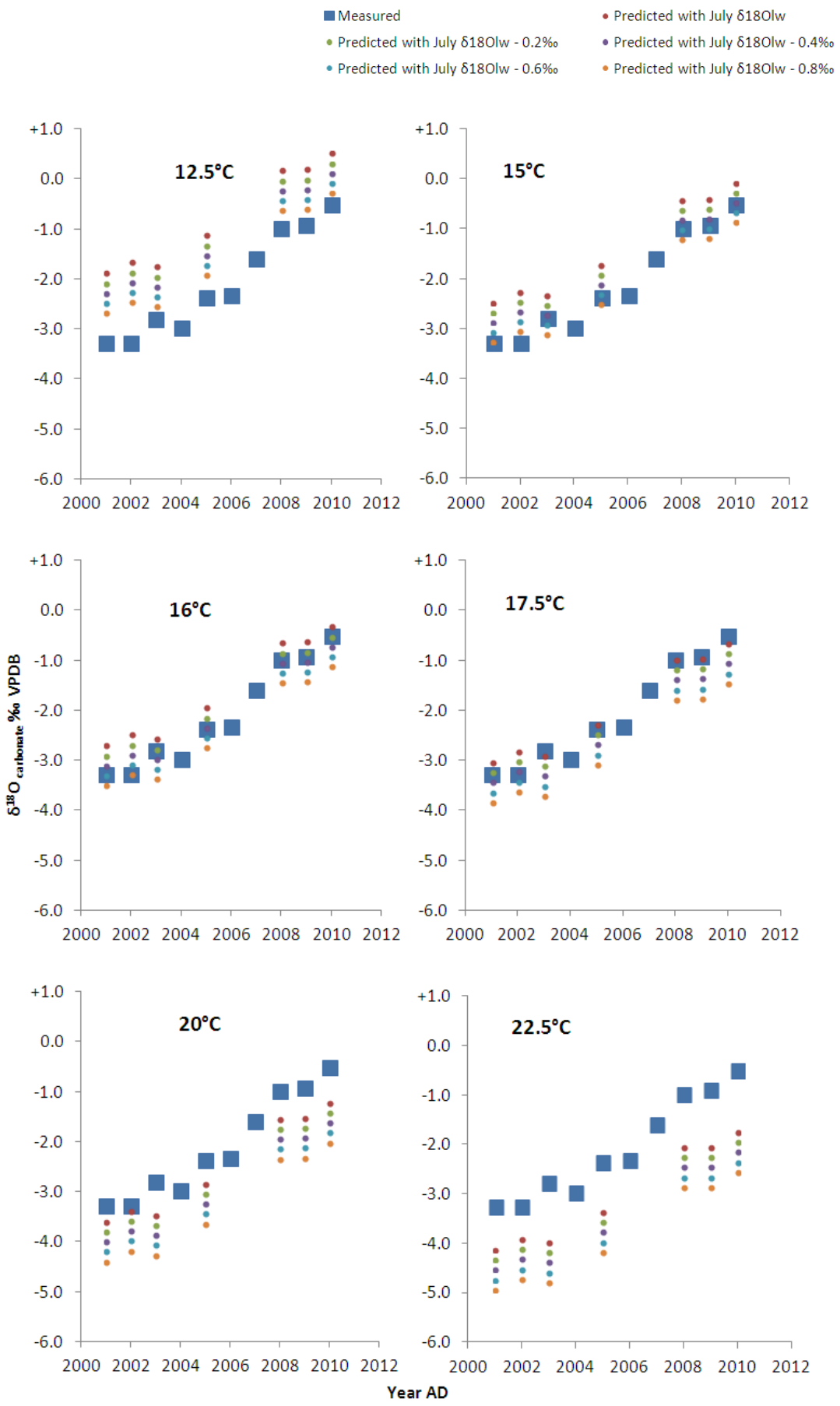

Figure 7.10 *Predicted $\delta^{18}O_{calcite}$ values (Eq. 6.2) compared to measured $\delta^{18}O_{calcite}$.*

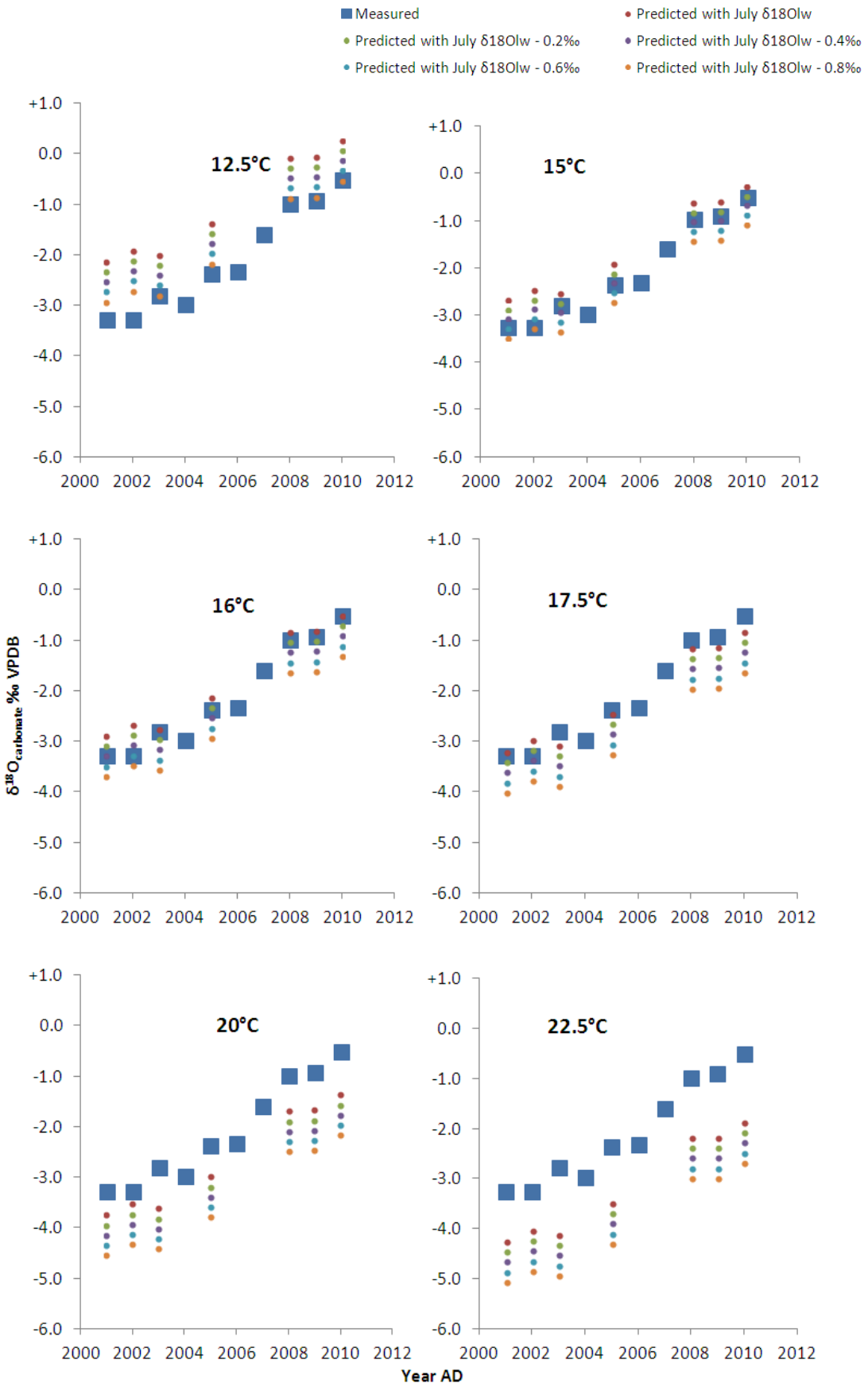

Figure 7.11 *Predicted $\delta^{18}O_{calcite}$ values (Eq. 6.3) compared to measured $\delta^{18}O_{calcite}$.*

7.2.3 Timing of diatom growth

As discussed, the majority of diatom growth seems to occur before carbonate precipitation, based on examination of sediment trap stratigraphy and thin sections (Jones et al., 2005, Woodbridge and Roberts, 2010). If diatom growth occurred just before carbonate precipitation, then there will not be much variation in lake conditions between then and the time of year to which carbonate precipitation is weighted. In an attempt to better constrain the time of year of growth, the same modelling exercise as carried out for carbonate isotopes in Figures 7.10 and 7.11 was carried out using Eq. 6.11 (Figure 7.12). The only way to make predicted $\delta^{18}O_{diatom}$ values even come close to hitting most of the corrected $\delta^{18}O_{diatom}$ values is to use temperatures <10°C and $\delta^{18}O_{lakewater}$ values from late July or September (July $\delta^{18}O_{lakewater}$ +0.2‰) which is clearly impossible. However, as outlined in section 6.4.5, it is suspected that some of the Al_2O_3 in diatom samples is due to diatom-bound aluminium and not detrital contamination. While an attempt was made to correct for this (section 6.4.4), it is possible that 1% Al_2O_3 was an underestimation of the amount of diatom-bound aluminium in pure diatom samples and the mass balance correction is still over-correcting. Consequently, the raw $\delta^{18}O_{diatom}$ values may be closer to the true value than the corrected value. The sample from 2006-2010 has the lowest Al_2O_3 value (1.5‰) of the samples plotted on Figure 7.12 and when viewed under SEM did not appear to have much, if any, detrital contamination, suggesting it is the least contaminated. Therefore, its raw measured $\delta^{18}O_{diatom}$ value is used here. Predicted $\delta^{18}O_{diatom}$ values hit this value at a temperature of +15°C and a $\delta^{18}O_{lakewater}$ value 1.0‰ lower than July, which could represent conditions in the lake in early May; or a temperature of 17.5°C and a $\delta^{18}O_{lakewater}$ value 0.8‰ lower than July, representative of conditions in late May to early June; or a temperature of 22.5°C and a $\delta^{18}O_{lakewater}$ value 0.2‰ higher than July, representative of conditions in September. The first two would support the observations outlined above that suggest growth is weighted towards the spring. The last of these shows that growth in the autumn is also possible. Therefore, while it is still not possible to reliably conclude which time of the year diatom growth is weighted to, by combining

observations and modelling the best guess would be in the spring up to several months before carbonate precipitation.

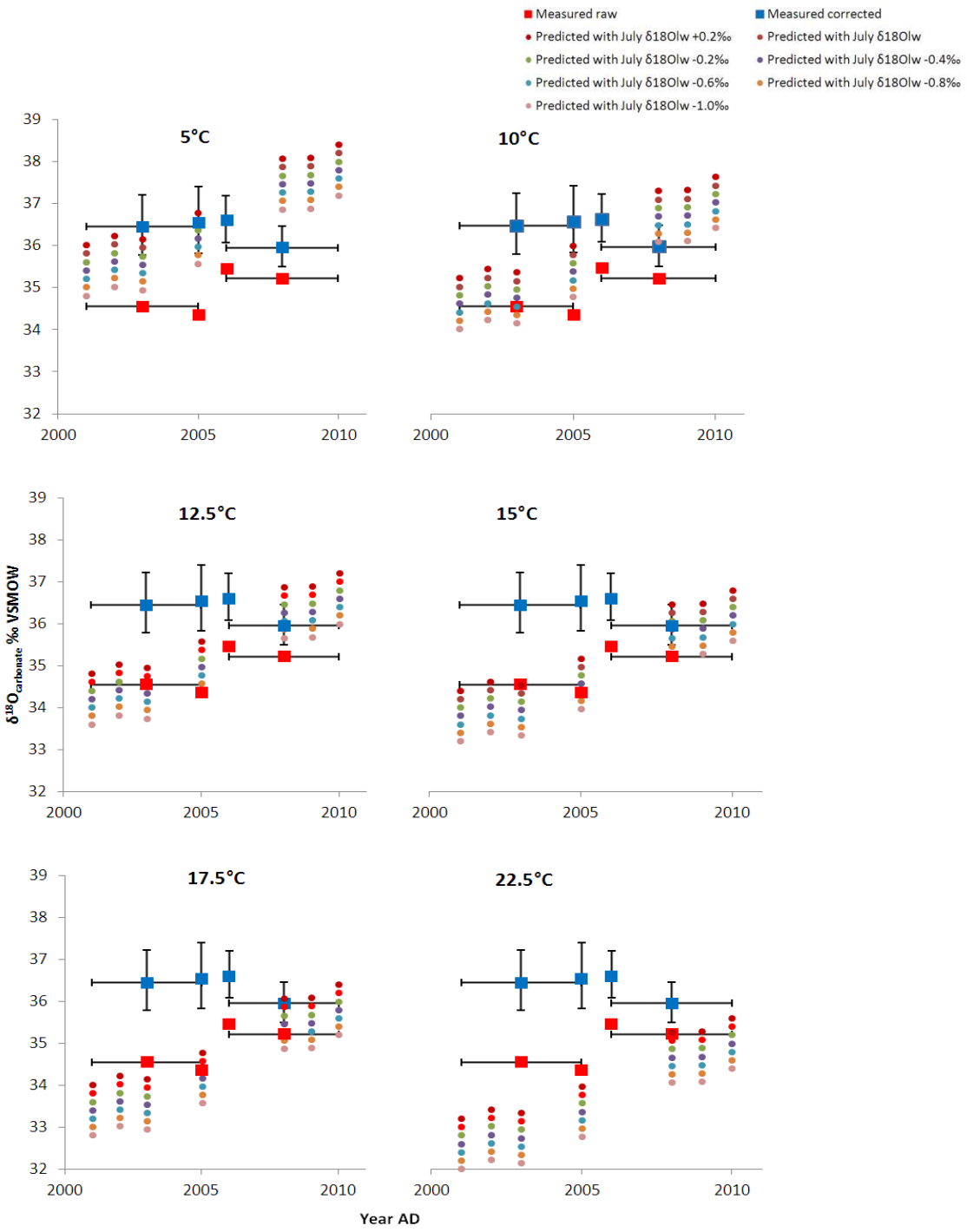

Figure 7.12 *Predicted $\delta^{18}O_{diatom}$ values from Eq. 6.11 compared to measured $\delta^{18}O_{diatom}$ (mass balance corrected and raw).*

7.3 Summary

New data presented here support the work of Jones et al. (2005), who suggested that water balance is the major driver of $\delta^{18}O_{lakewater}$ and $\delta^{18}O_{carbonate}$ in Nar Gölü. $\delta^{18}O_{diatom}$ has the same drivers as $\delta^{18}O_{carbonate}$ (Leng and Barker, 2006), however not enough data are available from the last decade to investigate this specifically for Nar Gölü. Intra-annual variability in $\delta^{18}O$ of surface waters, from which carbonate precipitates and some diatom species grow, appears to be driven by changes in the overall isotopic composition of the lake due to autumn, winter and especially spring precipitation, and stratification of waters in the summer. It is tentatively assumed that carbonate precipitation, at least over the last decade, has been weighted toward June. It is harder to determine the time of year to which diatom growth is weighted, but here it is estimated that it is weighted to the spring up to several months earlier than carbonate precipitation. This means that their $\delta^{18}O$ should be recording water balance at different times of the year, and it has been shown that there is substantial intra-annual variability in $\delta^{18}O$ in Nar Gölü. Hence, comparison of the two records could provide insights into seasonality. Now that a better understanding of the contemporary Nar Gölü system has been developed, it will be possible to better interpret the palaeo record.

Chapter 8 | Results and interpretation of palaeo stable isotope records

This chapter presents the data from the NAR10 core sequence and preliminary interpretations are made.

8.1 Results

8.1.1 Lithology

There are three main types of lithology found in the NAR10 core sequence (Figure 8.1). 68% of the sequence has mm-thick laminations: alternating carbonate and organic layers (0-598, 1161-1755, 1762-1965 and 2053-2133 cm) sometimes interrupted by grey turbidite layers. 18% of the sequence has larger cm-thick laminations (754-1139 cm). 12% is non-laminated, sometimes consisting of hard, concreted layers (598-754, 1965-2023, 2037-2053 and 2133-2169 cm). As discussed in sections 5.3.1 and 9.2, the mm-thick laminations are annual laminations (varves), whereas the bands are not believed to be annual as they are thicker and are not simply alternating carbonate and organic layers.

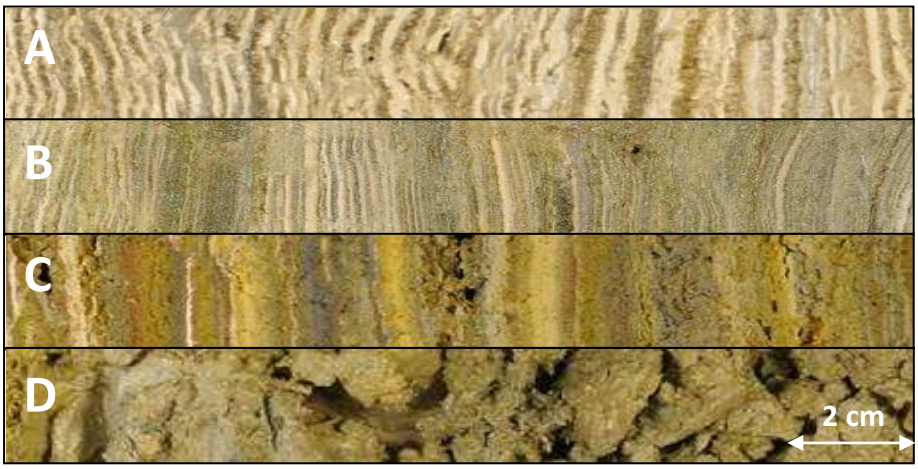

Figure 8.1 *Photographs of cores after opening showing different lithologies found in the sequence. A and B show the mm-thick laminations. C shows the cm-thick bands and D the hard, concreted non-laminated sediments.*

It is estimated, based on drive depths recorded during coring, that 43 cm is missing from the sequence in three places, totalling 2% of the record (1139-1161, 1755-1762 and 2023-2037 cm). Despite taking three parallel cores, there was not a good enough overlap in these places (Figure 6.5).

8.1.2 Core overlap

Rather than producing new data from the most recent 1,720 years of the record, data from the NAR01/02 sequence were used. The NAR01/02 and NAR10 sequences were matched by eye (using the NAR01/02 photo archive) at tie-points where terbidites or distinctive varve patterns allowed correlation (as detailed in Allcock, 2013), however to confirm that the cores were overlapped in the right place and that the different core sequences were representative of each other, $\delta^{18}O_{carbonate}$ data were produced from the NAR10 record and compared to the NAR01/02 data (Jones et al., 2006). There is a very strong match for the period of overlap 1,300-1,500 years BP (Figure 8.2). The $\delta^{18}O_{carbonate}$ values from the matched points are very similar, suggesting the $\delta^{18}O_{carbonate}$ values from the two core sequences are analogous. Any offset in ages is small and within the expected counting error (Jones, 2004).

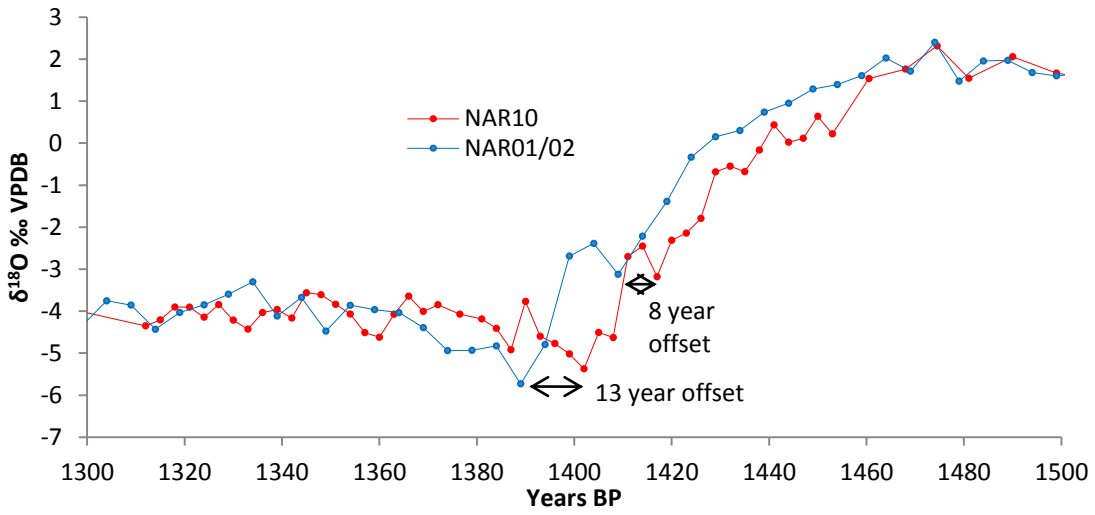

Figure 8.2 *$\delta^{18}O_{carbonate}$ data from NAR10 and NAR01/02 cores through a major transition showing a 8-13 year offset based on wiggle matching of the isotope records.*

8.1.3 Isotope data through the whole sequence

Figure 8.3 shows all isotope data ($\delta^{18}O$ and $\delta^{13}C$ from carbonates, $\delta^{18}O$ from diatoms, $\delta^{13}C$ from bulk organics, plus C/N on bulk organics; summary statistics given in Table 8.1) plotted against depth, along with carbonate mineralogy and lithology data. Carbonate mineralogy data are not given quantitatively because, as outlined in section 6.3.3, the XRD and the process of manually calculating the area under peaks is not that accurate, so in calcite/aragonite zones >50% calcite is defined as calcite and >50% aragonite is defined as aragonite, although most samples were actually one or the other and not mixtures of the two. Where dolomite is present, samples are shown as containing <20% dolomite (those samples that were reacted for isotope analysis at 16°C as outlined in section 6.3.4) and those containing >20% dolomite (those samples that could not be run for carbonate isotopes). In the sections where dolomite is present, more often than not the other form of carbonate is aragonite, although some calcite is present at times in small quantities. While these samples contain dolomite, the $\delta^{18}O$ data produced from these samples using the 16°C reaction will be just from the aragonite/calcite fractions. Not every sample run for isotopes could be analysed by XRD because of financial constraints, but from the data that were available, and combined with looking at changes in the colour of carbonate varves in the core (aragonite is noticeably lighter than calcite), robust estimates are believed to have been made.

The data have been zoned, largely based on major changes in the $\delta^{18}O_{carbonate}$ trends since these data are the highest resolution of all the isotope records, to allow discussion of the results. The trends in $\delta^{18}O_{carbonate}$, $\delta^{13}C_{carbonate}$, $\delta^{13}C_{organic}$ and $\delta^{18}O_{diatom}$ are broadly similar through the record (Figure 8.3). Starting from the bottom of the core and working up to the present day, $\delta^{18}O$ and $\delta^{13}C$ values from carbonates decrease from means of –1.5‰ and +13.9‰ respectively in zone 1 to –2.8‰ and +13.4‰ in zone 2, before increasing once more to –0.7‰ and +15.6‰ in zone 3. These changes are matched by a shift from non-laminated aragonite-rich sediments throughout most of zone 1 to laminated and more calcite-rich sediments

in zone 2 and back to non-laminated and aragonite- and dolomite-rich sediments in zone 3. $\delta^{18}O_{diatom}$ values change less between zones 1 and 2.

$\delta^{18}O$ and $\delta^{13}C$ from carbonates then decrease to means of –3.5‰ and +13.0‰ in zone 4. This is the least variable of all the 11 zones with standard deviation values of 0.6 and 0.4 for $\delta^{18}O_{carbonate}$ and $\delta^{13}C_{carbonate}$ respectively (Table 8.1). Zone 5 $\delta^{18}O_{carbonate}$ values are much more variable and on average higher, with aragonite in parts of the record where $\delta^{18}O_{carbonate}$ values are higher and calcite where $\delta^{18}O_{carbonate}$ is lower. $\delta^{13}C_{organic}$ also increases slightly, but average $\delta^{18}O_{diatom}$ does not increase significantly, although a lack of samples from zone 5 is an issue. The shift from a mean $\delta^{18}O_{carbonate}$ value of –2.1‰ in zone 5 to the largest zone mean for the record of +1.5‰ in zone 9 seems to occur in two phases, in zones 6 and 8. Zone 7 has highly variable isotope values but overall there appears to be no increase in $\delta^{18}O_{carbonate}$ from beginning to end. In zone 6, as $\delta^{18}O_{carbonate}$ values are increasing, there is still calcite and varved sediments, and it is at the switch to zone 7 that the varves disappear and there is a shift to first aragonite, then aragonite with <20% dolomite and then aragonite >20% dolomite. In parts of zone 9, where the highest $\delta^{18}O_{carbonate}$ values are seen, there are non-laminated sediments and dolomite. There is an increase in $\delta^{13}C_{carbonate}$ from zone 4 to 9 but it is less clear cut than the increase in $\delta^{18}O_{carbonate}$. $\delta^{13}C_{organic}$ increases while the C/N ratio shows a steady decrease from mean values of 24.4 in zone 4 to 11.0 in zone 9. $\delta^{18}O_{diatom}$ increases from zone 4 and the maximum value is seen in zone 7, not zone 9 like with $\delta^{18}O_{carbonate}$, probably because of the gaps in the record in zone 9 when many samples could not be run (section 6.4.4), and because $\delta^{18}O_{diatom}$ decreases before the end of zone 9, whereas a sharp decrease in $\delta^{18}O_{carbonate,}$ $\delta^{13}C_{carbonate}$ and $\delta^{13}C_{organic}$ occurs slightly later, into zone 10. All isotope records then show an increase into zone 11 and there is an increase in number of C/N peaks.

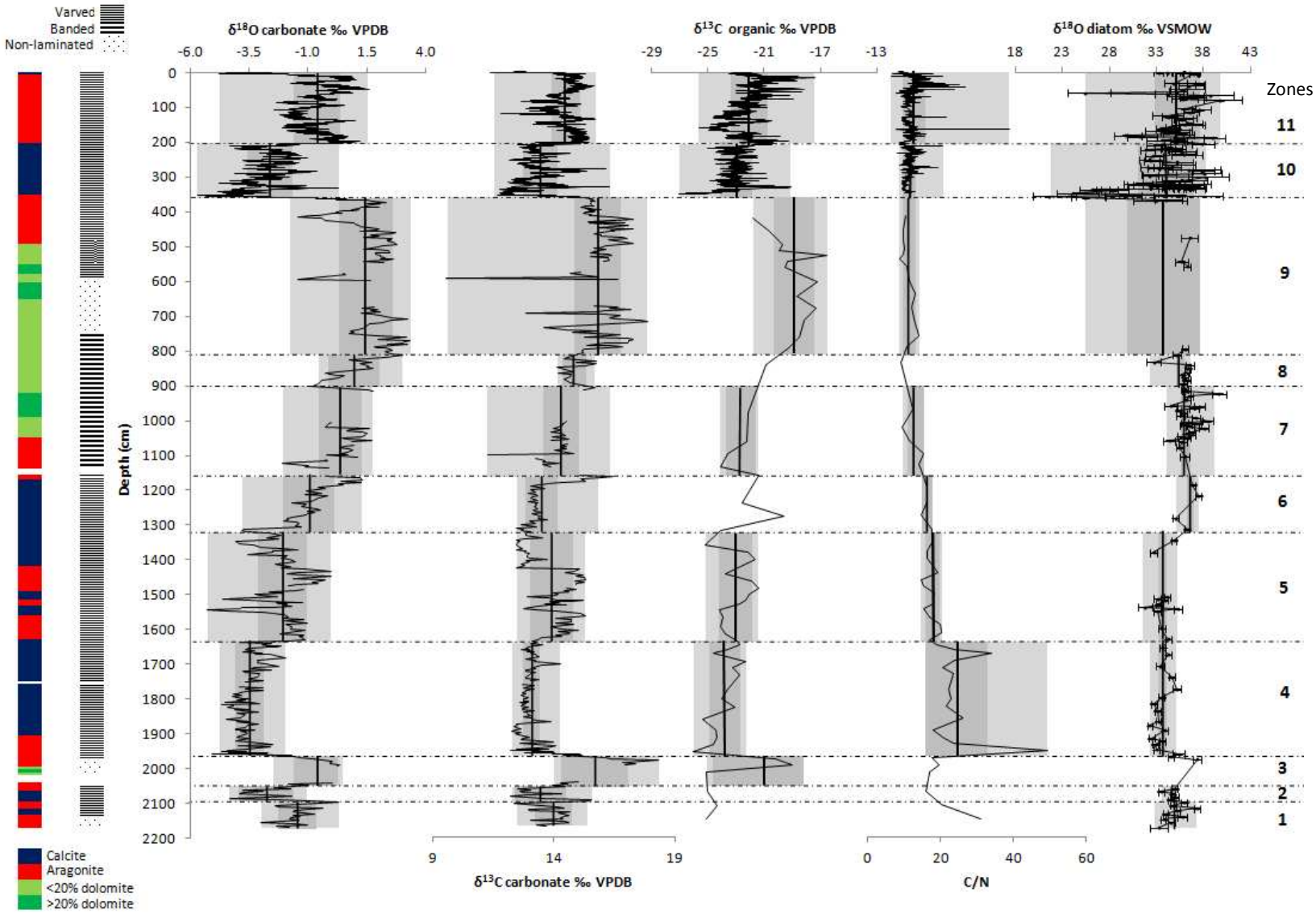

Figure 8.3 *Carbonate mineralogy, lithology and isotope data plotted against depth. Where there are sufficient data, minimum and maximum (light grey boxes), ±1σ (dark grey boxes) and mean (black line) values are shown for each zone. In the dolomite sections, the other main type of carbonate is aragonite.*

Table 8.1 *Summary statistics for the 11 zones defined from the combination of the NAR01/02 and NAR10 sequences (statistics only given for zones with three or more samples).* $\bar{x}$*= mean,* σ = standard deviation.

		Carbonates			**Organics**		**Diatoms**
Zone	**Depth (cm)**	**δ^{18}O ‰ VPDB**	**δ^{13}C ‰ VPDB**	**Co-variance (r)**	**δ^{13}C ‰ VPDB**	**C/N**	**δ^{18}O ‰ VSMOW**
11	0-204	$\bar{x}$ = –0.6 σ = 1.0	$\bar{x}$ = +14.5 σ = 0.7	0.71	$\bar{x}$ = –22.1 σ =1.3	$\bar{x}$ =12.3 σ = 2.8	$\bar{x}$ = +35.6 σ = 2.4
10	204-354	$\bar{x}$ = –2.6 σ = 0.9	$\bar{x}$ = +13.4 σ = 0.7	0.79	$\bar{x}$ = –23.0 σ = 1.1	$\bar{x}$ =11.3 σ = 1.6	$\bar{x}$ = +33.9 σ = 2.9
9	360-807	$\bar{x}$ = +1.5 σ = 1.1	$\bar{x}$ = +15.9 σ = 1.0	0.51	$\bar{x}$ = –19.0 σ = 1.5	$\bar{x}$ =11.0 σ = 1.6	$\bar{x}$ = +35.5 σ = 3.8
8	812-894	$\bar{x}$ = +1.0 σ = 1.1	$\bar{x}$ = +14.8 σ = 0.5	0.42			$\bar{x}$ = 35.6 σ = 0.3
7	902-1165	$\bar{x}$ = +0.4 σ = 0.9	$\bar{x}$ = +14.3 σ = 0.8	0.24	$\bar{x}$ = –22.7 σ = 1.1	$\bar{x}$ = 12.8 σ =2.1	$\bar{x}$ = 36.4 σ = 0.2
6	1169-1316	$\bar{x}$ = –1.0 σ = 1.1	$\bar{x}$ =+13.4 σ = 0.7	0.70		$\bar{x}$ =15.8 σ = 1.0	$\bar{x}$ = +36.1 σ = 0.1
5	1320-1632	$\bar{x}$ = –2.1 σ = 1.0	$\bar{x}$ = +13.8 σ = 0.9	0.59	$\bar{x}$ = –23.1 σ = 1.2	$\bar{x}$ =17.5 σ = 1.7	$\bar{x}$ = +33.6 σ = 0.2
4	1638-1957	$\bar{x}$ = –3.5 σ = 0.6	$\bar{x}$ = +13.0 σ = 0.4	0.63	$\bar{x}$ = –23.8 σ = 1.1	$\bar{x}$ =24.4 σ = 8.0	$\bar{x}$ = +33.6 σ = 0.2
3	1961-2053	$\bar{x}$ = –0.7 σ=0.9	$\bar{x}$ = +15.6 σ = 1.4	0.77	$\bar{x}$ = –21.4 σ = 3.3	$\bar{x}$ =18.1 σ = 1.2	
2	2057-2093	$\bar{x}$ = –2.8 σ = 1.2	$\bar{x}$ = +13.4 σ = 1.1	0.96			$\bar{x}$ = +34.5 σ = 0.03
1	2097-2161	$\bar{x}$ = –1.5 σ = 0.8	$\bar{x}$ = +13.9 σ = 0.8	0.74			$\bar{x}$ = +34.9 σ = 0.4

8.2 Interpretation

8.2.1 Lithology

Varves form in lakes because of seasonal variation in sedimentation. In Nar Gölü, as discussed in section 7.2.2, carbonate precipitation seems to be concentrated in the summer (forming the light varves) and diatom and other algal growth in other times of the year (forming the darker varves). The reason that varves are preserved in Nar Gölü in the present is probably because of its deep waters in relation to its surface area. This limits turbidity and re-suspension of sediment and favours the formation of anoxic bottom waters, limiting bottom-dwelling organisms and resulting bioturbation, although changes in wind speed and temperature as well as simply lake depth may also influence the preservation of varves (O'Sullivan, 1983, Ojala et al., 2000, Zolitschka, 2007, Ojala et al., 2012). In the present day, cores taken from 15 m water depth are still laminated, and if wind speed, temperature, etc. stayed the same then lake levels presumably would have had to have fallen below this level in the past for non-laminated sediments to have formed. So, a shift from varved to non-varved (i.e. banded or non-laminated) could be seen to indicate a shift to lower lake levels. Therefore, varved sediments are taken to indicate when lake levels were highest and non-laminated when they were lowest. The presence of banded sediments in zones 4-6 in the transition from varved to non-laminated sediments is interesting as in the rest of the sequence there are simply changes between varved and non-laminated. Looking at Figure 8.3, it can be seen that the banded sediments appear in a *gradual* transition in the $\delta^{18}O_{carbonate}$ values, in zones 7 and 8, which are intermediate between the low $\delta^{18}O_{carbonate}$ values of zones 4 and 5 and the high $\delta^{18}O_{carbonate}$ values in zone 9. The $\delta^{18}O_{carbonate}$ transition seen e.g. 1989-1957 cm when there was simply a shift from non-laminated to varved is a lot more rapid. Therefore, banded sediment may form when the lake is stuck in a state between stratified every year (leading to varved sediments) and never stratified (leading to non-laminated sediments), and in rapid transitions the shift from stratified every year to never stratified occurs too quickly for this intermediate to occur.

8.2.2 Carbonate mineralogy

As discussed in section 7.1.1, shifts from calcite to aragonite in Nar Gölü are believed to be due to a change in the Mg/Ca ratio of the lake (Muller et al., 1972, Kelts and Hsu, 1978, Ito, 2001), which favours the precipitation of aragonite over calcite (Berner, 1975, De Choudens-Sanchez and Gonzalez, 2009), and therefore carbonate mineralogy changes can be used as proxy for water balance. Figure 8.3 shows there is a link with lithology, for example a transition to aragonite ~1139 cm occurs at the same time as a shift from varved to banded sediments. Towards the bottom of the core, changes from calcite to aragonite coincide with changes from varved to non-laminated sections.

In addition to calcite and aragonite, there is another type of carbonate present in the sequence. XRD peaks were initially interpreted as suggesting the non-calcite/aragonite crystals seen in Figure 8.4 were ankerite because the main peaks were at ~2.9 angstroms (dolomite is usually at 2.889, Fe-dolomite at 2.895 and ankerite at 2.906). However, EDS analysis of these individual crystals showed very little Fe (average 0.07 at%, a Mg/Fe atomic ratio of 218). Since ankerite is seen to contain much more Fe than this, for example one definition giving an Mg/Fe ratio of <4 (Howie and Broadhurst, 1958), the samples were defined as dolomite. The difference in peak locations from those of stoichiometric (ideal) dolomite were likely caused by the high Ca/Mg ratio of the dolomite in these samples, which can shift the main peak location close to that expected of ankerite (Lumsden, 1979). Indeed EDS data show the average Ca:Mg ratio based on analysis of three crystals from six different samples containing dolomite was 2.3, whereas 'ideal' dolomite would have a ratio of 1.

Unlike calcite and aragonite, dolomite has not been observed forming in Nar Gölü in the recent past so its precipitation dynamics have to be inferred by careful consideration of the palaeo record. Dolomite in lake sediments can originate from the detrital inwash of old dolomite (Leng et al., 2010), from primary precipitation or from diagenetic precipitation in sediments. The former mode can be discounted, as

the crater geology is dominated by basalt and ignimbrite (section 5.1). Primary dolomites are rare in lake sediments, however where they do occur they have rhombic crystals (Sabins, 1962). The crystals in Figure 8.4 are not rhombic.

It is possible that dolomite formed authigenically within the sediments, replacing calcite or aragonite during early diagenesis. Studies have demonstrated the importance of microbes in dolomite precipitation, both sulphate-reducing bacteria (e.g. Vasconcelos and McKenzie, 1997) and methanogens (e.g. Kelts and McKenzie, 1982). The processes of sulphate-reduction and methanogenesis create conditions such as increased pH and total alkalinity and decreased calcium and magnesium hydration (Mazzullo, 2000, Armenteros, 2010) that allow kinetic constraints on dolomite formation to be overcome, producing what is termed organic-diagenetic or organogenic dolomite. As well as this passive role, it is possible that bacteria may be actively involved in dolomite precipitation, perhaps acting as a nuclei for precipitation (e.g. Warthmann et al., 2000). Sulphate-reducing conditions tend to leave the DIC pool (from which carbonates form) depleted in ^{13}C (Kelts, 1988, Komor, 1994, Fenchel et al., 1998); while the same can be true of methanogenesis (e.g. Aloisi et al., 2000), if the CH_4 produced escapes from the system the DIC pool will become very enriched in ^{13}C (Talbot and Kelts, 1986, Gu et al., 2004, Leng et al., 2013). Since Nar Gölü carbonates have high $\delta^{13}C$ values (dolomite average in the late Holocene of ~+14.5‰ and TDIC value from surface waters averaging +10.5‰ 1997-2012), methanogenesis is considered the most likely. Methanogenesis requires anoxic conditions, and while dolomite in Nar Gölü is found in non-laminated sections when the lake waters were likely not stratified, Vasconceleos and McKenzie (1997) found dolomite forming in an anoxic 'black sludge layer' above the sediment and below a totally mixed water column, so anoxic conditions could have existed in Nar Gölü sediments even with lower water levels. As well as the high $\delta^{13}C$ values of dolomite, an organogenic origin is favoured by a number of other factors. Firstly, as discussed, the Nar Gölü dolomite is calcium-rich, which is characteristic of early diagenetic dolomites, including those associated with methanogenesis (Vasconcelos and McKenzie, 1997, Armenteros, 2010). Secondly, the crystals do bear some resemblance to dolomite crystals interpreted elsewhere to be associated with

organogenesis; for example Deng et al. (2010) described abundant microstructures and pores, and these can be seen on Figure 8.4.

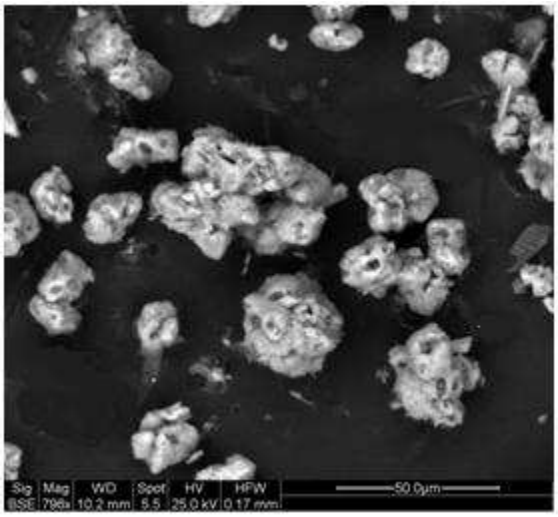

Figure 8.4 *Dolomite crystals viewed under SEM, showing non-rhombic shapes and microstructures, suggesting a diagenetic origin.*

Dolomite formation requires sufficient magnesium (Mazzullo, 2000), so the appearance of dolomite in the sediments suggests magnesium was even more concentrated than at times when aragonite formed. Although there are issues of linking carbonate mineralogy and Mg/Ca ratio (Bristow et al., 2012) and Mg/Ca ratio and aridity (Shapley et al., 2010), the occurrence of dolomite in Nar Gölü sediments is associated with other markers of aridity, as has been suggested elsewhere (Last, 1990, Deocampo, 2010).

As discussed in section 6.3.5, whereas the difference between the mineral-water fractionation factors of calcite (especially the high-magnesium calcite in the Nar Gölü sequence) and aragonite is so small (especially given the size of the isotopic shifts seen in the record) that it does not need to be corrected for, the difference between dolomite and calcite/aragonite formed under the same conditions is a lot greater. Additionally, since it has been argued that the dolomite in Nar Gölü sediments is organogenic, this means it will have formed under different conditions (temperature,

$\delta^{18}O_{lakewater}$) to calcite and aragonite, which are seen as endogenic, forming in surface waters. For this reason, where there was <20% dolomite the 16°C reaction was used and where there was >20% dolomite no $\delta^{18}O_{carbonate}$ data were produced (section 6.3.4). However, 5 samples containing >80% dolomite were run using the 100°C reaction temperature to ensure all dolomite reacted, to establish if any sense could be made of the results. When the values were corrected for mineralogy (Eq. 6.7), the samples at 566 and 571 cm in particular appear lower than the $\delta^{18}O_{aragonite/calcite}$ values nearby in the sequence (Figure 8.5). Since high amounts of dolomite are seen to have formed in the most magnesium-concentrated waters, it is difficult to explain why $\delta^{18}O_{dolomite}$ was not high at this time. This supports the argument that dolomite formed under different conditions from calcite and aragonite, however these differences in temperature and $\delta^{18}O_{lakewater}$ are difficult to correct for, especially as dolomite is not likely to form at a discrete time of the year like calcite and aragonite, but rather over a much longer period of time (Kelts and McKenzie, 1984). So while $\delta^{18}O_{dolomite}$ data cannot be used, carbonate mineralogy change, in itself, is useful for supporting palaeoclimate interpretations.

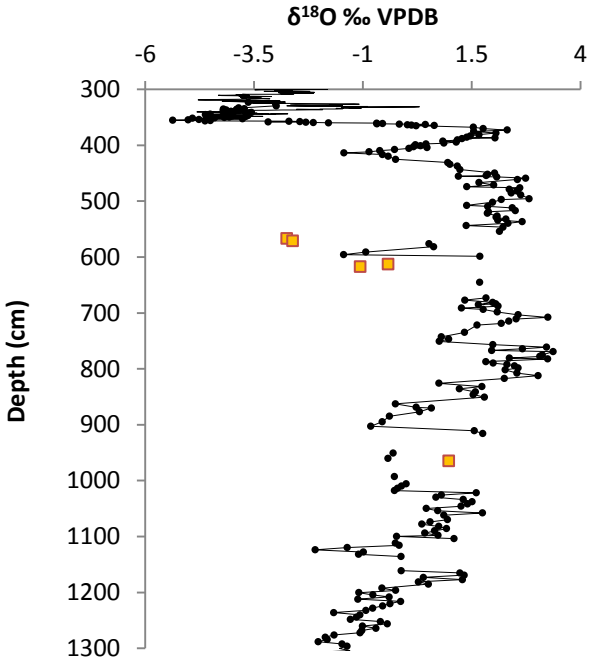

Figure 8.5 *Comparison of $\delta^{18}O$ data from calcite and aragonite (black) to $\delta^{18}O$ from dolomite corrected for mineralogy (orange).*

8.2.3 Carbon isotopes and $\delta^{18}O_{carbonate}$-$\delta^{13}C_{carbonate}$ covariation

While it is beyond the scope of this thesis to discuss in detail the controls on $\delta^{13}C$ trends in Nar Gölü, some understanding of the carbon isotope system is required to aid the interpretation of the $\delta^{18}O$ data. Covariation between $\delta^{13}C_{carbonate}$ and $\delta^{18}O_{carbonate}$ is traditionally used to investigate changes in lake hydrology over time. In a closed lake, while evaporation preferentially removes ^{16}O, increasing $\delta^{18}O_{lakewater}$ as evaporation increases, outgassing of CO_2 also preferentially removes ^{12}C from the system, increasing $\delta^{13}C_{DIC}$ and hence $\delta^{13}C_{carbonate}$ (Li and Ku, 1997). Where there is a strong co-variance between $\delta^{13}C_{carbonate}$ and $\delta^{18}O_{carbonate}$, this indicates that the lake has remained closed and the two records are being controlled by a related mechanism (Talbot, 1990, Leng and Marshall, 2004). For the NAR01/02 and NAR10 records as a whole there is a strong positive covariation (r=0.85) indicating the lake has been closed. However, Table 8.1 shows changes in the r-value between zones, with zones 7, 8 and 9 in particular having lower values. Such values could be interpreted as showing the lake was more hydrologically open at this time. However, a closer examination of Figure 8.3 shows 'flatter' isotope trends in zones 7 and 9 and the small size of zone 8, which would have meant the r-values were reduced compared to other zones where there were larger shifts and more data (Li and Ku, 1997, Leng et al., 2006). This means there need not have been a more open, fresh lake at this time. Indeed, this is supported by the carbonate mineralogy data: in zones 7, 8 and 9 there is dolomite in the sediments, which is interpreted as indicating a lake enriched in magnesium, i.e. not fresh. While $\delta^{18}O$-$\delta^{13}C$ covariation is complex and not a simple record of changes in the hydrology of a lake (Li and Ku, 1997), it does appear that Nar Gölü has been a hydrologically closed lake through the period represented by the NAR10 sequence.

It is suggested, therefore, that the major control on $\delta^{13}C_{carbonate}$ has been changes in the residence time of the lake, linked to changes in water balance. The $\delta^{13}C_{organic}$ record shows similar trends to the $\delta^{13}C_{carbonate}$ record. Both are influenced by $\delta^{13}C_{DIC}$ but $\delta^{13}C_{organic}$ can be strongly influenced by changes in the type of organic matter (Meyers and Teranes, 2001) and $\delta^{13}C_{carbonate}$ by carbonate mineralogy shifts. The

increase in $\delta^{13}C_{organic}$ from zones 4 to 9, if interpreted solely in terms of changes in the source of organic matter, would suggest an increase in the proportion of C4 vegetation in the lake sediments away from C3 vegetation or lake algae. However, C/N values, which are mainly influenced by the source of organic matter (Meyers and Teranes, 2001), indicate actually there was an increase in the proportion of organic matter from lake algae (Figure 8.6). This shift in C/N could be because of a decrease in catchment vegetation (linked to increased human activity and deforestation in the region over the past couple of millennia as seen in the pollen record (England et al., 2008)), increased algal productivity due to increased temperatures in the late compared to the early Holocene (Jones et al., 2007) or a decrease in the inwash of catchment vegetation. This, and the strong similarity between the $\delta^{13}C_{organic}$ and $\delta^{13}C_{carbonate}$ trends, suggests that changes in the source of organic matter are not the key influence on $\delta^{13}C_{organic}$ and that residence time is likely the main control.

Large peaks in C/N can sometimes be due to major inputs of terrestrial organic matter due to intense precipitation events (e.g. Meyers and Teranes, 2001, Panizzo et al., 2008). However, comparison of the C/N data with the Ti ITRAX record (Allcock, 2013), which is seen as a more reliable proxy for inwash events (linked to human disturbance or tectonism) because unlike the C/N ratio it is not affected by other factors such as changes in catchment vegetation composition, shows there is not a strong relationship (Figure 8.7). This suggests the peaks in C/N cannot be used as a proxy for increased inwash.

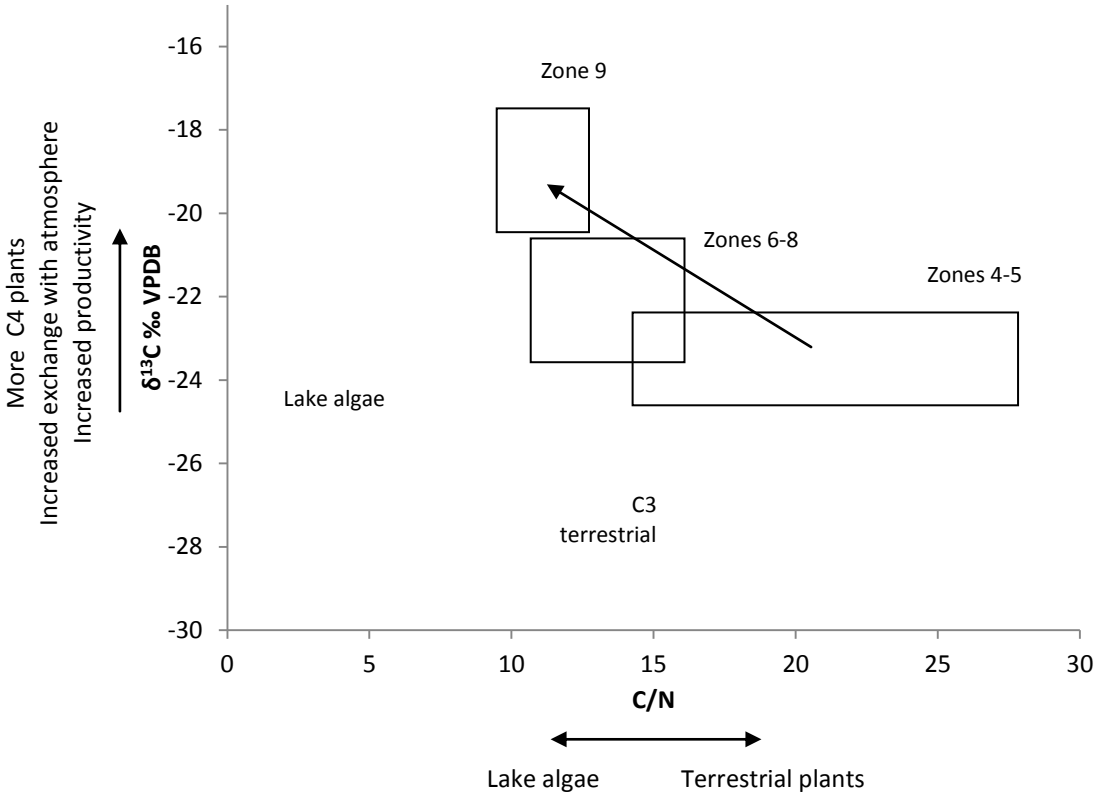

Figure 8.6 *$\delta^{13}C_{organic}$ vs C/N plot with boxes representing ±1σ from mean $\delta^{13}C_{organic}$ and C/N values. The major trend in the record, the increase in $\delta^{13}C_{organic}$ and decrease in C/N from zones 4-5 to zone 9, is shown. Typical values for lake algae and C3 terrestrial plant material (Meyers and Teranes, 2001) are shaded. Typical C/N values for C4 plants are >35 and plot off the scale here.*

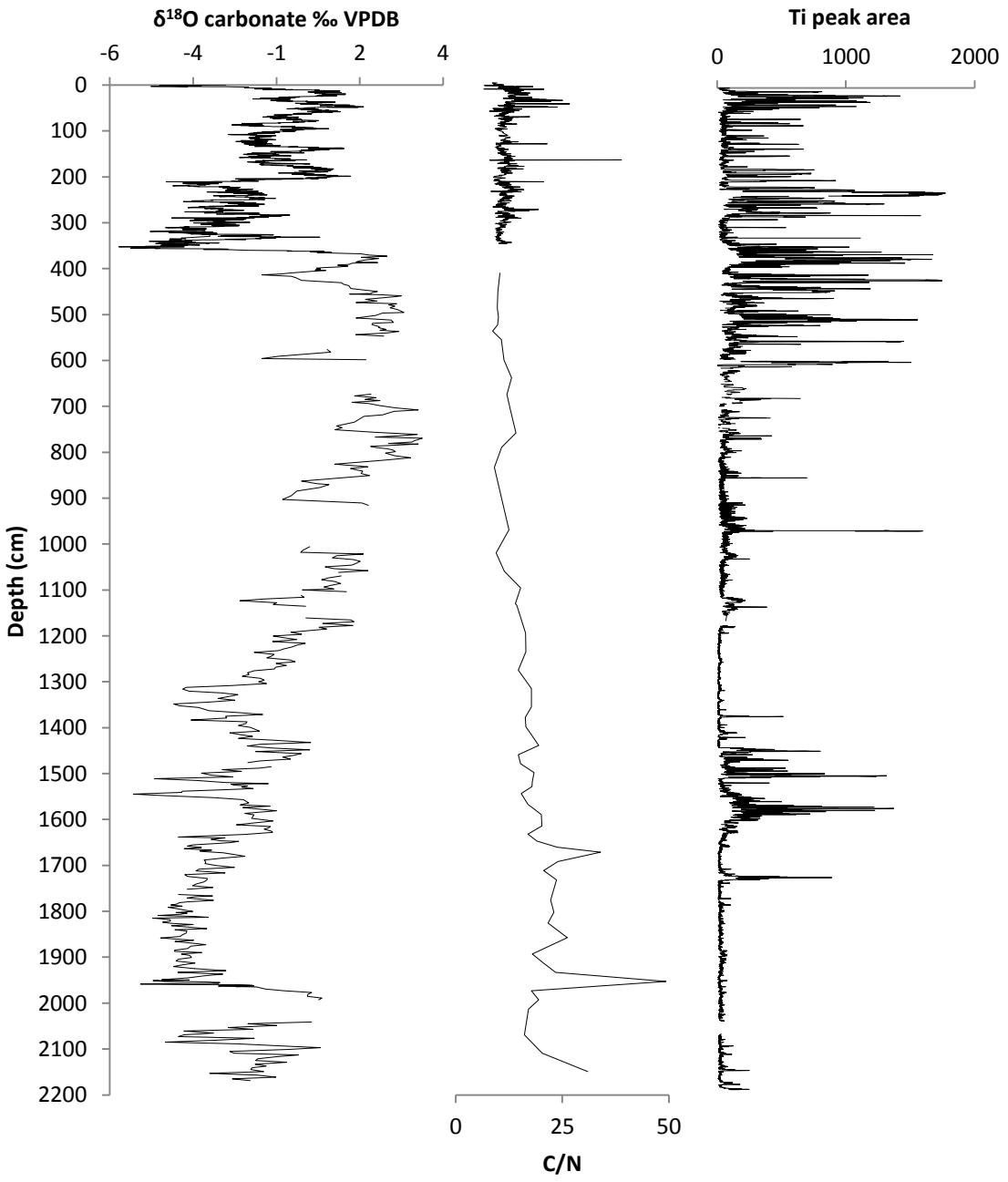

Figure 8.7 *$\delta^{18}O_{carbonate}$, C/N and Ti data from ITRAX (Allcock, 2013). There seems to be little relationship between the peaks in C/N and peaks in Ti, suggesting the former cannot be used as a proxy for inwash events.*

8.2.4 Diatom species and $\delta^{18}O_{diatom}$ data

The interpretation of the $\delta^{18}O_{diatom}$ record is hampered by the lack of samples that could be successfully run, in particular from zones 3 and 9. As discussed in section 6.4.4, part of the reason for this was contamination, however the other reason was that many samples from these zones had insufficient diatom silica. There were still diatoms growing in the lake at this time, but there must have been a preservation issue. Woodbridge and Roberts (2010) showed there is limited dissolution in the present day, with only one species found in sediment trap samples and not in core sediments. However, if pH was higher in the past than the values shown on Figure 7.6, which is not unlikely given that the lake level was probably lower to account for the non-laminated sediments, then there may have been more diatom dissolution, especially if pH values rose above 9 (Iler, 1979, Barker et al., 1994, Leng and Barker, 2006). This adds further support to the assertions that these zones saw the most negative water balance. The preliminary diatom assemblage data also support this (Woodbridge et al., unpublished data). There is an increase in % benthic from zones 5 to 9 (Figure 8.8). Such an increase is often seen as an indicator of a lake level fall because this will initiate a movement of the benthic zone towards the centre of the lake, closer to where cores are generally taken from, meaning more benthic species will be incorporated into the core sediments (e.g. Laird et al., 2011). Additionally, diatom-inferred conductivity values are higher between ~350 and 1,600 cm than at the beginning and end of the record, indicating that the lake waters were the most saline in this period.

Despite the gaps in the diatom isotope record, it appears that overall there is a general similarity between the $\delta^{18}O_{diatom}$ and $\delta^{18}O_{carbonate}$ trends, with higher values in zone 3 than zones 1 and 2, low values in zones 4 and 5 and higher values in zones 7, 8 and 9, then a fall to zone 10 and a rise again into zone 11. This is not surprising given the drivers of both are the same (Leng and Barker, 2006). Changes in $\delta^{18}O_{diatom}$ in this record should not be the result of contamination, since mass balancing has been used to correct for the effect of this, and there is not a strong relationship between % contamination and $\delta^{18}O_{diatom}$, with high levels of contamination found in

samples that have both high and low $\delta^{18}O_{diatom}$ values (Figure 8.8). Moreover, temperature can be excluded as a key driver of $\delta^{18}O_{diatom}$ because of the size of the shifts in the record: it would take an unrealistic temperature change of 62°C, for example, to explain the 12.4‰ shift between 366 and 355.6 cm, assuming a temperature coefficient of ~–0.2‰ (Brandriss et al., 1998, Moschen et al., 2005, Crespin et al., 2010). While species vital effects in diatoms have been shown to be of limited importance in influencing $\delta^{18}O_{diatom}$ (Brandriss et al., 1998, Schmidt et al., 2001, Moschen et al., 2005, Swann et al., 2006, Schiff et al., 2009), changes in the time of year diatoms grow in Nar Gölü could influence $\delta^{18}O_{diatom}$ because of differences in temperature and $\delta^{18}O_{lakewater}$ between seasons. However, the general similarity with the $\delta^{18}O_{carbonate}$ record suggests this may not be the case: the fact that, as with $\delta^{18}O_{carbonate}$, $\delta^{18}O_{diatom}$ values are higher when there is aragonite and/or dolomite in sediments, there are non-laminated sediments, % benthic diatoms is highest and $\delta^{13}C$ is high, suggests the main driver is water balance.

There are some small differences in the $\delta^{18}O_{carbonate}$ and $\delta^{18}O_{diatom}$ trends at certain times. For example, $\delta^{18}O_{diatom}$ values begin to decline before $\delta^{18}O_{carbonate}$ values at the end of zone 9 and unlike in the $\delta^{18}O_{carbonate}$ record there seems to be no significant difference between values in zones 1 and 2 in $\delta^{18}O_{diatom}$. To compare the two records properly, they really need to be viewed on the same scale by conversion to $\delta^{18}O_{lakewater}$ values. However, this requires knowledge of the likely temperature changes over time, and since there is no temperature proxy from the Nar Gölü record, this will be undertaken in chapter 10 once a chronology has been established and independent temperature records can be used.

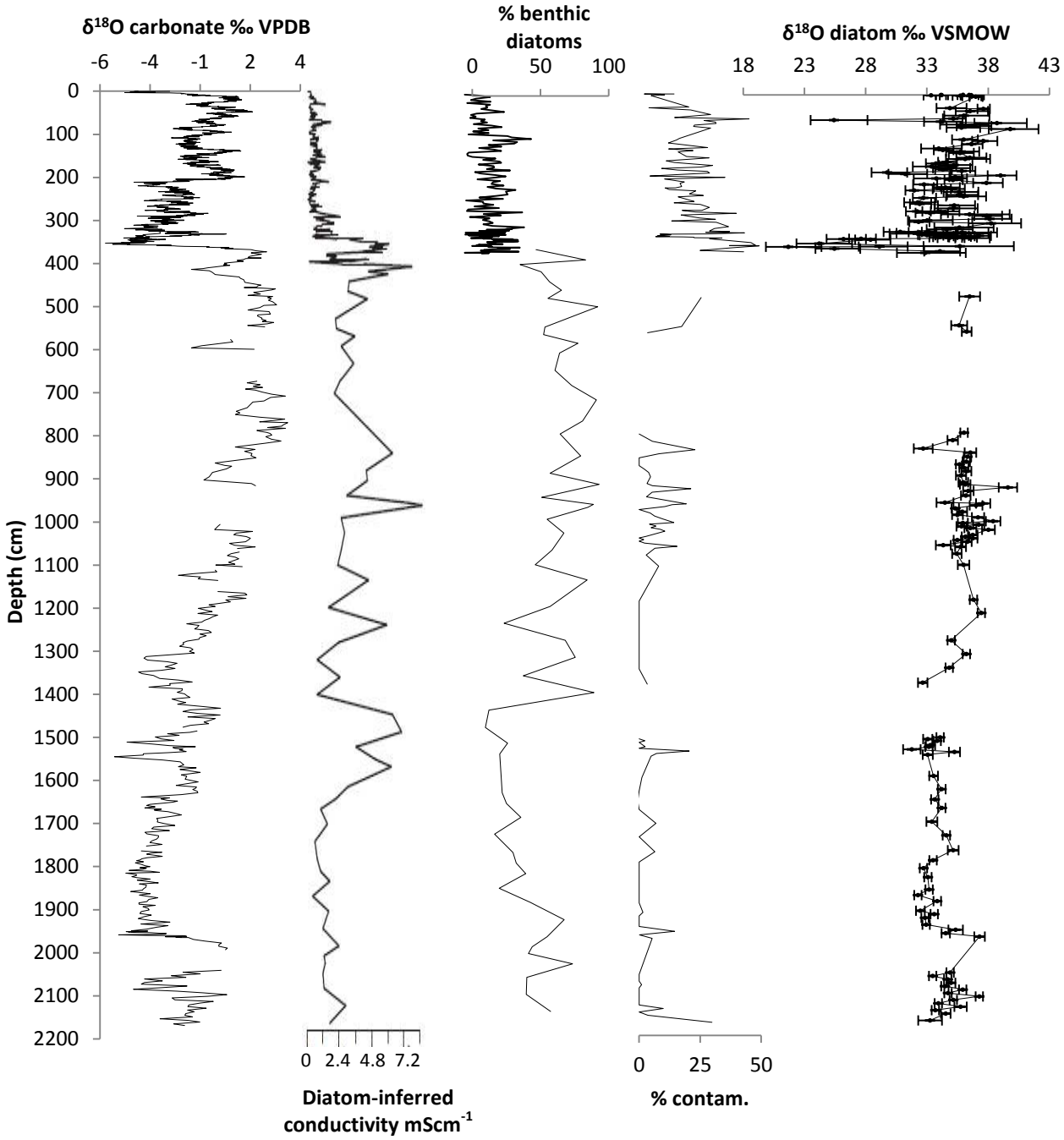

Figure 8.8 *$\delta^{18}O_{carbonate}$ data compared to diatom inferred conductivity and % benthic diatoms (Woodbridge and Roberts, 2011, Woodbridge et al., unpublished data) and $\delta^{18}O_{diatom}$ data, with % contamination of diatom isotope samples shown.*

8.2.5 Comparison of isotope and pollen records

A preliminary pollen record has been produced from the NAR10 sequence (Figure 8.9). While there is an increase in arboreal pollen in zone 4, it is much slower than the decrease in $\delta^{18}O_{carbonate}$, and maximum arboreal pollen (and also specifically *Quercus robur* and *Q. cerris*) values are reached in zone 7 when the other proxies suggest increasingly arid conditions. The possible reasons for the differences between pollen and isotope records in the region are outlined in section 2.2.2. However, *Poaceae* abundance does increase rapidly into zone 4 as $\delta^{18}O_{carbonate}$ decreases, supporting the assertion there was a rapid shift to wetter conditions.

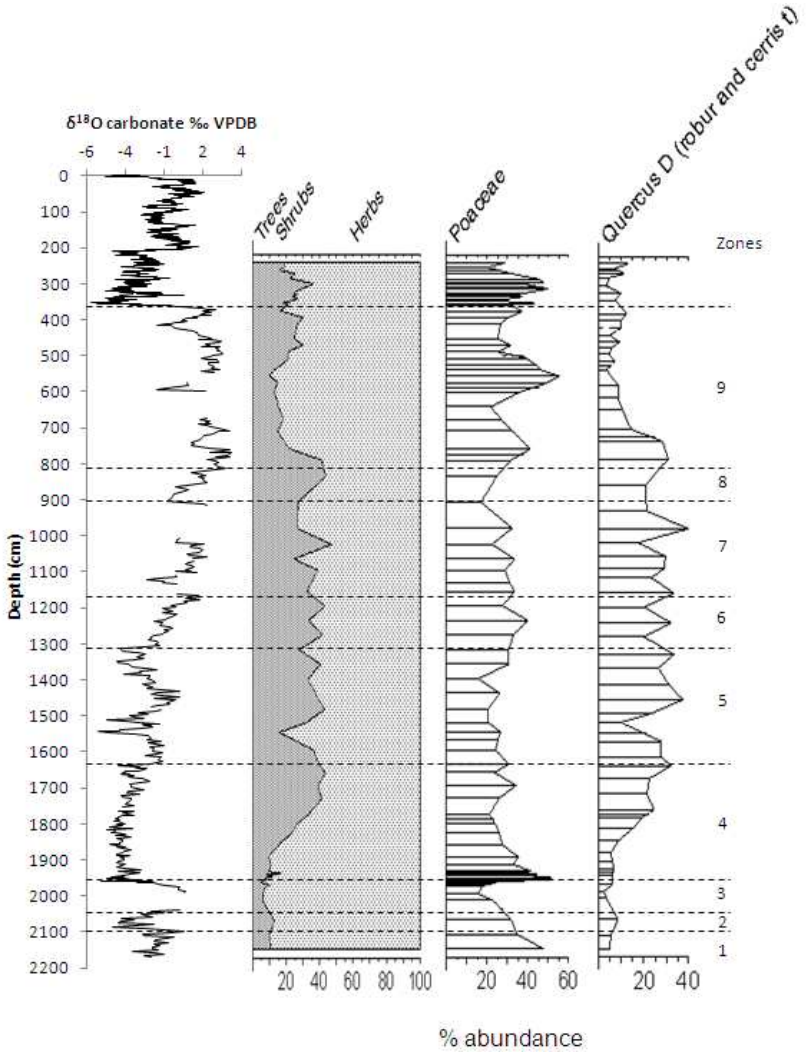

Figure 8.9 *$\delta^{18}O_{carbonate}$ and preliminary pollen data (Eastwood et al., unpublished data).*

8.3 Summary

Lithology (shifts between varved, banded and non-laminated) is believed to change in Nar Gölü particularly in response to variations in lake level, which will influence whether the lake is stratified and hence whether varves can be preserved. Carbonate mineralogy (shifts between calcite, aragonite and dolomite) is seen to respond to changes in the magnesium concentration of the lake, with high levels of magnesium leading to aragonite and/or dolomite precipitation. It is argued that in Nar Gölü, dolomite has an organogenic origin, and therefore $\delta^{18}O_{dolomite}$ values are not easily comparable to those from calcite and aragonite, which are endogenic and form in surface waters. While there is generally a strong relationship between $\delta^{18}O_{carbonate}$, lithology and carbonate mineralogy, there are slight differences in how they each respond. For example, during the transition 1989-1957 cm, while there is a shift from non-laminated to varved at 1965 cm, there is not a shift to calcite until ~1900 cm ~390 varves later. Similarly, varved sediments appear at 598 cm but dolomite only disappears from the sediments ~497 cm. This demonstrates that different proxies respond at different rates. However, the fact $\delta^{18}O_{carbonate}$ is higher when sediments are non-laminated, aragonite/dolomite is present and the benthic:planktonic diatom species ratio is higher and $\delta^{18}O_{carbonate}$ is lower when sediments are varved, calcite is present and the benthic:plankonic diatom species ratio is lower, coupled with the strong covariation of $\delta^{18}O_{carbonate}$ and $\delta^{13}C_{carbonate}$ as well as the work on the recent past in section 7.1.1 and of Jones et al. (2005), all suggests the major driver of $\delta^{18}O_{carbonate}$ in the sequence has been water balance. This will be investigated further, using independent temperature and $\delta^{18}O_{source}$ records, once a chronology is established. However, it appears that, combining the interpretations of the proxies, zone 3 was drier than zones 1 and 2, there was a rapid transition to wetter conditions in zone 4 and a gradual increase in aridity during zones 6-8 to a peak in zone 9, before another rapid transition to wetter conditions in zone 10 and then a gradual increase in aridity to the present day.

Chapter 9 | Chronology

A chronology needs to be established before the record can be compared to other palaeoclimate and archaeological records. This chapter will outline the progress made with U-Th dating so far and, combined with the varve counts made and detailed in Allcock (2013), produce a working chronology for this thesis.

9.1 U-Th dating

First, 4 samples (from 549, 1779, 1978 and 2058 cm depth) were run using the standard U-Th method (Edwards et al., 2003), however the [^{230}Th/^{232}Th] ratio was low, indicating lots of detrital thorium, and there were very large errors (Tables 9.1 and 9.2). Consequently, all subsequent samples were run using the total sample dissolution isochron approach as detailed in section 6.6.2. Samples from 1355 and 1852 cm depth were initially selected to be run but the errors were still unacceptably large. As demonstrated in the Osmond plot for sample 1355 cm (Figure 9.1), there was insufficient variability between the individual sub samples to be able to fit a line through the data with a good degree of certainty.

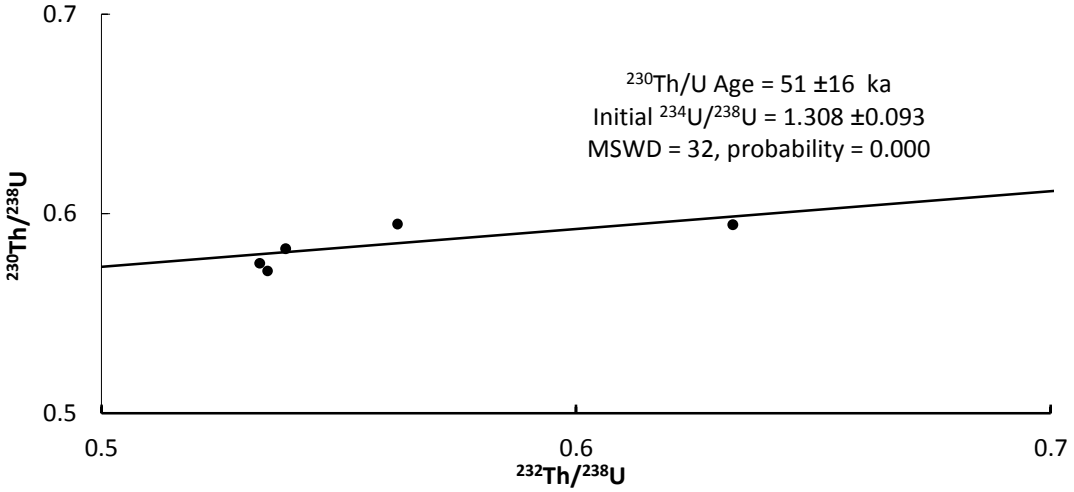

Figure 9.1 *Osmond plot for sample at 1355 cm showing the poor spread between the 5 sub samples, leading to a large error.*

However, of more concern is the fact the dates are far older than expected for the depths in the core, for example 29,900 ±3,600 years BP for the sample at 1852 cm. The $\delta^{18}O_{carbonate}$ record can be matched to the lower resolution but dated record from nearby Eski Acıgöl. Figure 9.2 shows that the trends are very similar, with the transition in Nar Gölü at 1989-1957 cm to very low values and then a quick recovery to slightly higher values seeming to match the form of the transition in Eski Acıgöl dated to ~12,000 years BP: the Younger Dryas to Holocene transition. Through the Holocene in Eski Acıgöl there is a gradual increase to more positive values and there is a very similar trend in the Nar Gölü record. This all points towards the transition ~1989-1957 cm in Nar Gölü being the Younger Dryas to Holocene transition. Additionally, between the top of the Nar Gölü sequence and the middle of this transition, 8,005 varves had been counted, in addition to 563 cm of non-varved sediments. To get a date of 29,900 years BP would require the non-varved section to have a deposition rate of just 0.02 cm/y and this is difficult to imagine in Nar Gölü since the average deposition rate (as discussed in more detail in section 9.2) for the varved sections is estimated to be 0.18 cm/y. If the deposition rate were the same in the non-varved section, this would give a more realistic estimate of 3,128 years, or assuming a lower deposition rate of for example 0.13 cm/y, 4,330 years. Using these deposition rates and added to the 8,005 years seen in the varved sections, it can be estimated that the sequence from the present day to 1963 cm represents between 11,133 and 12,335 years. The only large-scale climate transition seen in Near East records from dry to wet (as a transition to lower $\delta^{18}O_{carbonate}$ in Nar Gölü is seen to represent; section 8.3) in the period 11,000 to 12,500 years BP is the Younger Dryas to Holocene transition (Figure 2.5) (Roberts et al., 2008), which again suggests that the shift 1989-1957 cm in Nar Gölü is just that.

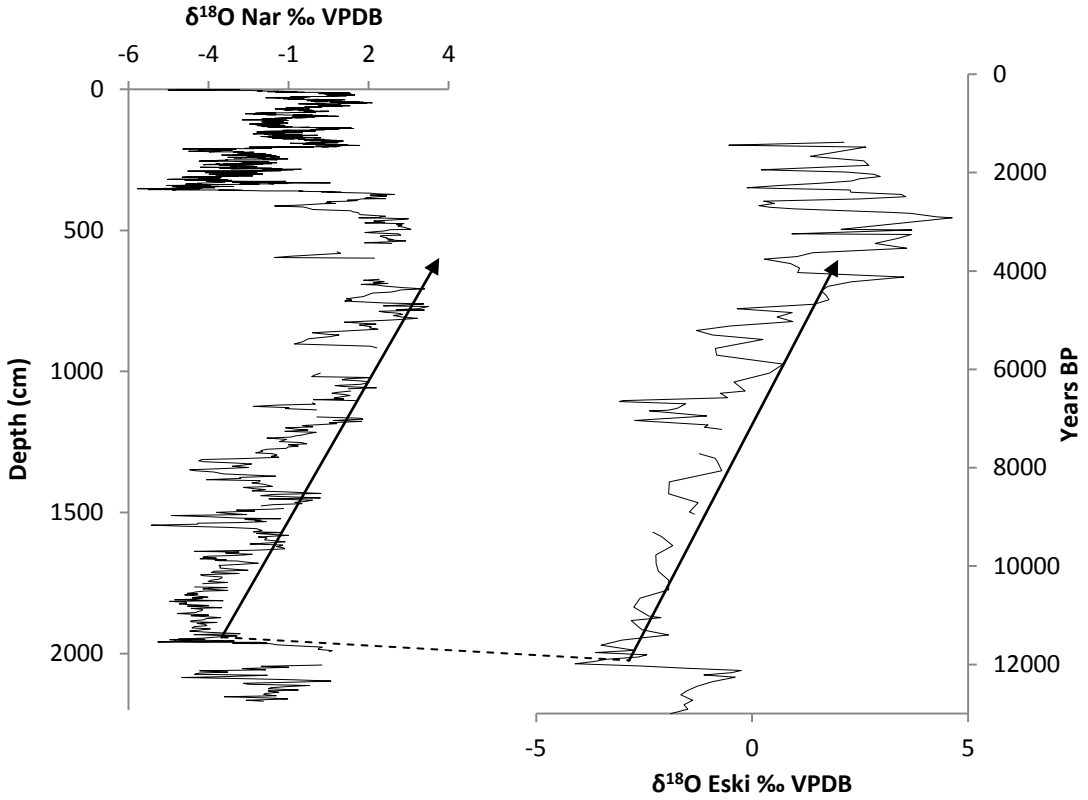

Figure 9.2 *$\delta^{18}O_{carbonate}$ from Nar Gölü plotted against depth and compared to $\delta^{18}O$ from Eski Acıgöl plotted against age (Roberts et al., 2001), showing the similarities between the transition defined as the Younger Dryas to Holocene in Eski Acıgöl and that from 1989 to 1957 cm in Nar Gölü, matched by dotted line. After this there are continuing similarities between the two records record, with a general trend to more positive values the middle section, shown by the arrows.*

Since the dates derived from the first two samples analysed by the isochron approach were deemed to be substantially older than comparison with other records and varve counting suggested, it was thought possible that hydrogenous thorium might be an issue (section 4.3). To investigate this, samples were analysed for U-Th from the top section where the varves provided an independent dating technique, to attempt to establish the offset of U-Th age from the actual age (Haase-Schramm et al., 2004, Torfstein et al., 2009, 2013). Specifically, a carbonate crust from a sediment trap float (standard method) as well as core sediments and sediments dated to 1,000 varve years before present (isochron approach) were run. However, as shown in

Table 9.2, again the errors on these three samples were too large for the dates to be useful, with low uranium and high [$^{230}Th/^{232}Th$] ratios.

Table 9.1 *U-Th elemental data, with uncertainty given at 2 standard error.*

Sample		U ppm	^{232}Th ppm	$^{234}U/^{238}U$	$^{230}Th/^{232}Th$	$^{230}Th/^{238}U$	$\delta^{234}U$
549 cm		0.74	0.71	1.35±14.02	0.87	0.02±1532.76	261.10
1779 cm		0.12	0.06	1.27±6.62	1.76	0.18±57.96	232.34
1978 cm		0.09	0.12	1.36±22.35	1.46	0.43±76.14	229.86
2058 cm		0.10	0.20	1.32±52.51	0.88	0.08±1113.96	138.62
1355 cm	A	0.06	0.10	1.35±31.42	1.08	0.24±214.21	193.49
	B	0.06	0.10	1.36±31.47	1.07	0.23±224.63	198.03
	C	0.06	0.12	1.39±43.09	0.94	0.14±519.14	184.64
	D	0.06	0.10	1.36±31.85	1.08	0.24±211.13	197.92
	E	0.07	0.11	1.36±34.46	1.06	0.24±233.64	191.28
1852 cm	A	0.21	0.33	1.27±31.30	1.17	0.31±150.21	150.61
	B	0.26	0.43	1.29±34.25	1.17	0.34±150.44	156.78
	C	0.24	0.40	1.29±34.74	1.17	0.35±148.57	157.74
	D	0.20	0.32	1.27±33.52	1.17	0.33±151.12	147.09
	E	0.25	0.44	1.30±38.52	1.13	0.34±168.80	151.64
	F	0.26	0.46	1.28±37.46	1.15	0.35±155.49	146.73
Zero age float		0.07	0.07	1.18±16.05	0.91	0.04±715.58	127.66
Zero age core	A	0.13	2.01	0.98±67.17	0.83	0.01±11137.51	53.74
	B	0.98	4.08	1.00±408.31	0.83	0.00±222131.76	0.55
	C	0.61	2.30	0.66±2316.49	0.83	0.14±13875.16	12.28
	D	0.47	1.57	1.33±431.80	0.84	0.08±9745.17	27.78
	E	1.02	4.20	1.00±431.70	0.82	0.12±4850.71	-0.15
1ka core	A	0.70	2.07	1.75±161.32	0.84	0.04±7148.02	136.45
	B	0.38	1.11	1.66±156.26	0.83	0.00±409470.62	123.29
	C	0.41	1.23	1.70±166.86	0.84	0.02±17205.96	123.81
	D	0.40	1.24	1.78±199.06	0.83	-0.04±-10138.77	118.10
	E	0.87	2.75	1.97±221.82	0.84	0.07±6108.87	133.46
1949 cm	A	0.44	0.13	1.30±3.50	2.24	0.15±38.86	279.58
	B	0.47	0.12	1.31±3.12	2.37	0.14±35.73	283.22
	C	0.30	0.13	1.30±5.14	1.81	0.15±55.84	267.14
	D	3.18	1.50	1.31±5.93	1.69	0.15±63.44	270.09
	E	0.33	0.16	1.31±6.17	1.68	0.16±64.33	268.53

Table 9.2 *U-Th dates derived from data in Table 9.1.*

Sample depth/age		**Age (ka)**	**Error (ka)**	**Isochron age (ka)**	**Isochron error (ka)**
549 cm		1.3	20.4	-	-
1779 cm		16.6	10.2	-	-
1978 cm		40.8	36.0	-	-
2058 cm		6.8	77.8	-	-
1355 cm	A	20.7	47.6	51	16
	B	19.7	47.5		
	C	11.6	63.0		
	D	21.2	48.2		
	E	20.7	52.0		
1852 cm	A	30.2	50.1	29.9	3.6
	B	32.7	55.0		
	C	33.5	55.8		
	D	32.1	54.1		
	E	32.7	61.7		
	F	34.7	60.7		
Zero age (float)		3.4	24.5	-	-
Zero age (core top)	A	0.9	103.5	0.9	8.3
	B	0.3	628.4		
	C	26.0	3794.0		
	D	6.4	637.6		
	E	13.7	688.5		
1ka core	A	2.7	198.8	-2.0	53
	B	0.0	200.9		
	C	1.2	210.6		
	D	-	-		
	E	3.9	245.8		
1949 cm	A	13.0	5.3	11.77	0.57
	B	12.6	4.7		
	C	13.3	7.8		
	D	13.5	8.9		
	E	13.8	9.3		

However, one sample, from 1949 cm depth, was the first sample which had acceptable errors and an apparently sensible date. This sample differs from those run previously in that the uranium concentration is higher, there is strong variability between sub samples leading to more of a spread on the isochron diagram (Figure 9.3) and the [^{230}Th/^{232}Th] ratio is higher indicating detrital thorium makes up less of the total thorium than was the case in the other samples. The former point could be related to the fact this sample was composed of aragonite whereas all the other samples were composed of calcite, and some studies have suggested less favourable uptake of uranium into calcite compared to aragonite (Reeder et al., 2001, Ortega et al., 2005). The strong variability in the amount of detritus between sub samples is because this section had large organic and carbonate varves so it was possible to produce sub samples composed of different types of material, in comparison to the sub samples from 1355 and 1852 cm which were more homogenous (Figure 9.4). Within the error of the date, ±570 years, there is only one major transition: the one from 1989-1957 cm that as outlined above, based on varve count estimations and matching with the Eski Acıgöl record, is the Younger Dryas to Holocene.

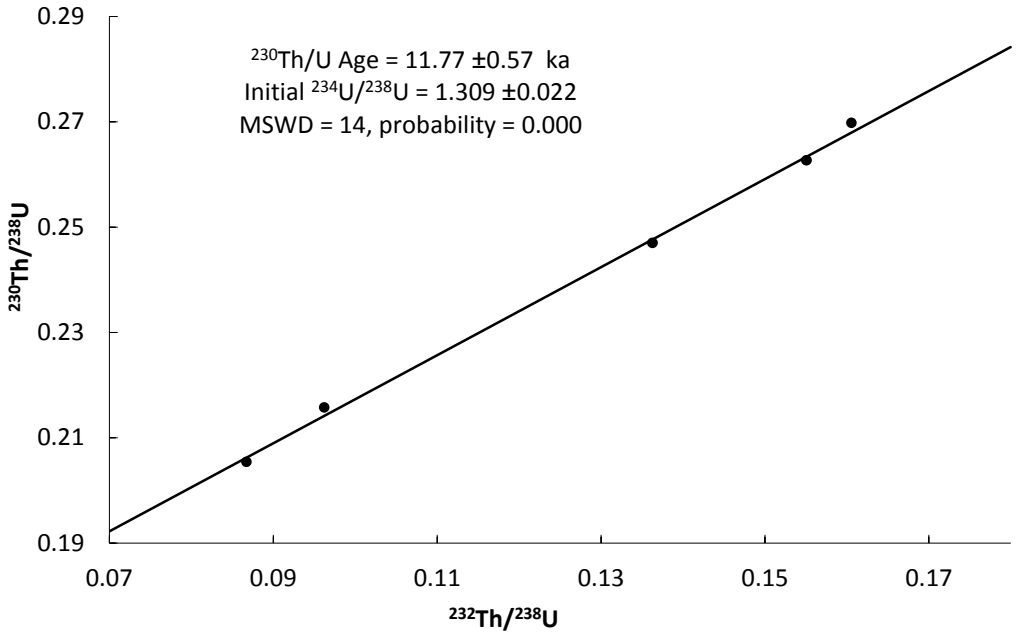

Figure 9.3 *Osmond plot for sample at 1947 cm, with a much better spread between the 5 sub samples leading to much reduced error.*

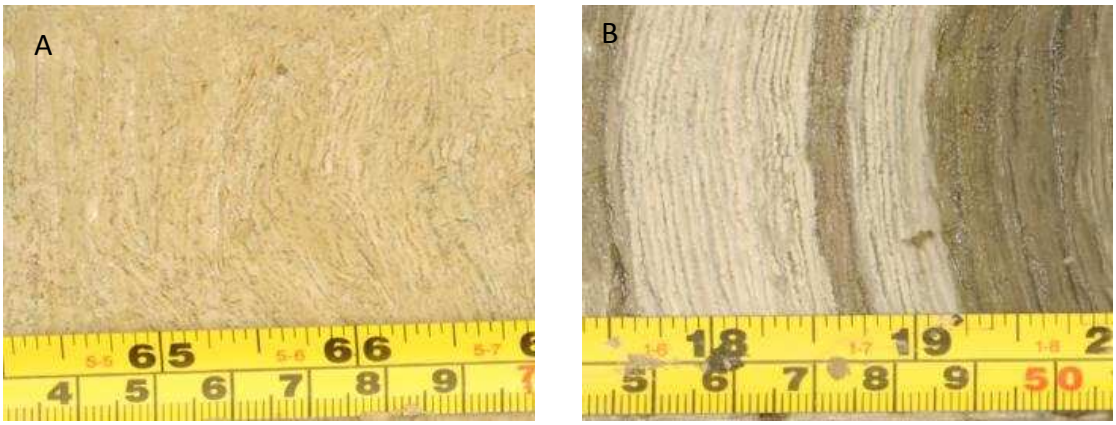

Figure 9.4 *A: core at 1355 cm from where an unsuccessful sample was taken for U-Th, showing homogeneity of sediments, whereas in B from 1949 cm the sediments are more heterogeneous which meant there was greater variability between sub samples and the isochron correction was more robust.*

9.2 Combination of U-Th date with varve counts to produce a working chronology

A summary of how the varve chronology and the U-Th date were combined to provide a chronology for the whole Nar Gölü sequence is shown on Figure 9.5. The record is varved from the present day back 2,626 varves (598 cm), i.e. from –60 to 2,566 years BP (all dates for the new sequence are given in years BP (i.e. before 1950) to aid comparison with other studies). Jones et al. (2005) showed that the laminations were annual (varves) using ^{137}Cs and ^{210}Pb dating. Laminations which have a similar appearance to those in this top section are seen from 1161-1965 cm and 2053-2133 cm, so here it is assumed these are annual as well. From the U-Th date of 11,707 ±570 years BP at 1949 cm, it was therefore possible to count back to 1965 cm (11,870 years BP; or a range of 11,300 to 12,440 years BP using the U-Th date error) and up to 1161 cm (6,488 years BP, range 5,918 to 7,058 years BP), although the varves from 1161-1427 cm are harder to count so the chronology for this period is less certain. Above 1161 cm the sediments have laminations but these do not appear to be annual as they are much thicker than the other laminated sections and they are not simple alterations of carbonate and organic material, and

the section from 598-753 cm is non-laminated. Therefore, the only way to provide a rough chronology for the period 598-1161 cm (2,566 to 6,488 years BP) was to assume a linear deposition rate of 0.14 cm/y (although using the maximum and minimum errors the deposition rate could be between 0.13 and 0.17 cm/y). The age-depth plot (Figure 9.6) shows that the estimated deposition rate for this time is not too dissimilar from the deposition rate for the varved sections where the deposition rate can be reliably calculated, suggesting that the estimated chronology that was applied to this section is sensible.

The dating of the late glacial section is the most difficult, with no U-Th dates and only a floating varve chronology. The records from Eski Acıgöl (Roberts et al., 2001) and Soreq Cave (Bar-Matthews et al., 1997) are interpreted as suggesting that the Younger Dryas in the Near East was dry and was preceded by a wetter Bølling-Allerød, which is taken to suggest that zone 3 in the Nar Gölü record is the Younger Dryas and zones 1 and 2 the Bølling-Allerød. However, as Figure 2.5 shows, these other records are too low resolution to be able to identify subtle changes and they have unreliable chronologies, which means it is not possible to wiggle match the Nar Gölü $\delta^{18}O$ record to these. Another option was to use the NGRIP isotope record and the GICC05 chronology (constructed from the NGRIP, GRIP and DYE-3 ice cores (Rasmussen et al., 2006, Vinther et al., 2006)), because of its high resolution and robust chronology. (Maximum counting error for the late glacial in the GICC05 chronology is ~140-170 years (Rasmussen et al., 2006), and although actual error may be greater due to bias in annual layer identification, and there are differences of a few decades between the GICC05 and GISP2 chronologies in the late glacial, the dating is more robust than any record from the Near East in this period.) A date is assigned to top of the varved section at 2053 cm by wiggle matching with the NGRIP $\delta^{18}O$ record: it appears to be ~12,810 years BP, in the transition from the Bølling-Allerød to the Younger Dryas (Figure 9.7). The varves were counted down from this point to 13,506 years BP. Past this point, a chronology was not estimated because there were no varves to be counted and there was no potential for wiggle matching, meaning the last 9 samples shown on Figure 9.7 are not included on plots against age shown in chapter 10.

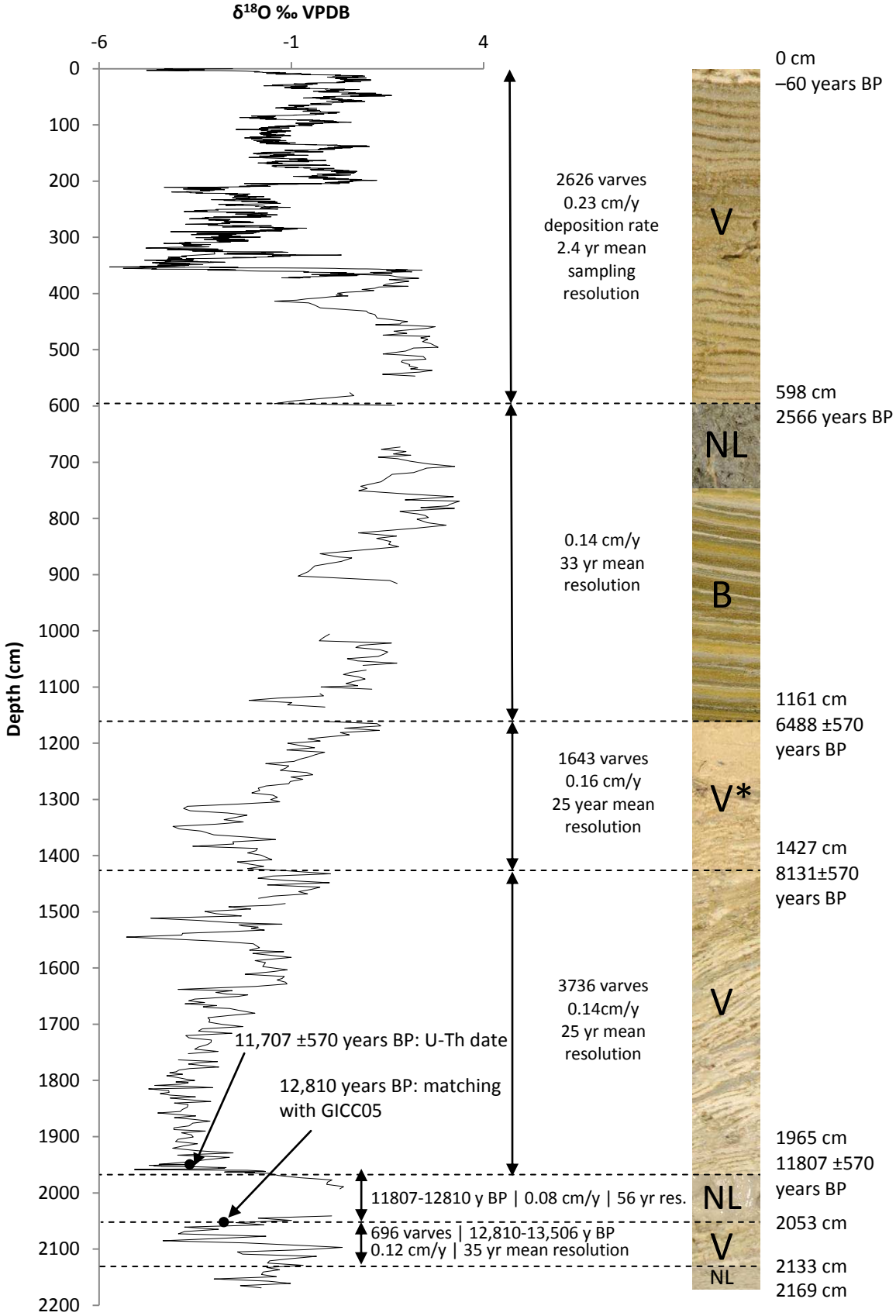

Figure 9.5 *Chronology applied to Nar Gölü core sequence, with dates given in years BP and errors based on U-Th date uncertainty, V = varved, V* = varved but difficult to count, B = banded and NL = non-laminated. 0-598 cm is dated by varve counting and 1161-1965 cm by varve counting from U-Th date at 1949 cm.*

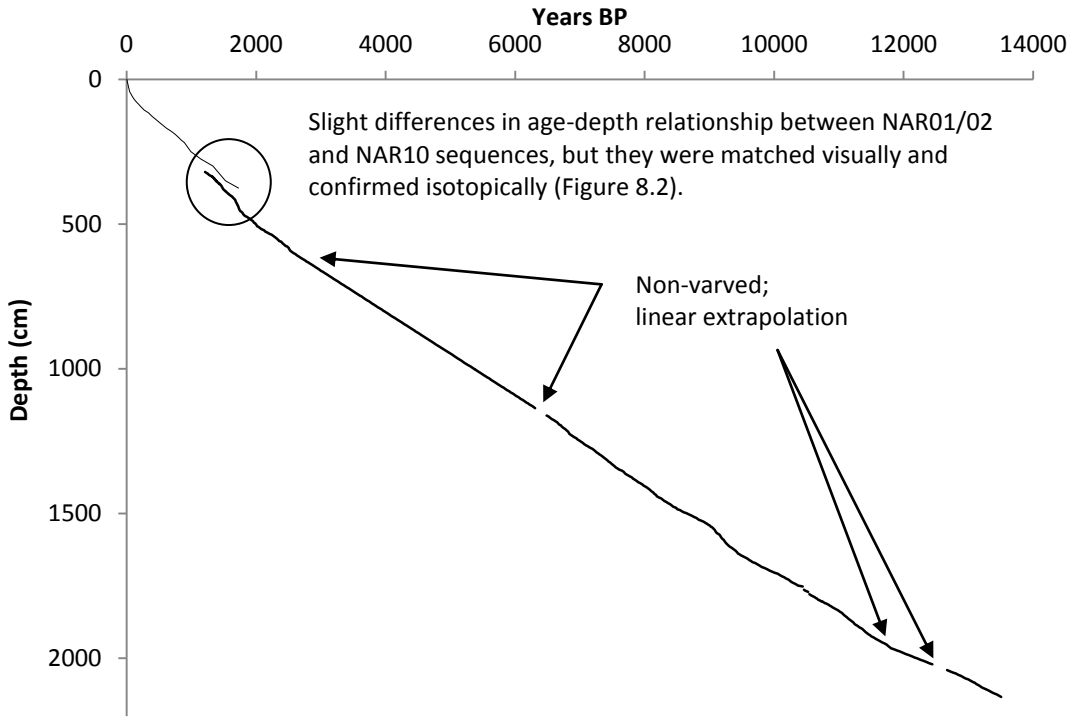

Figure 9.6 *Age-depth plot for the NAR01/02 and NAR10 master sequences. The parts of the sequence that were non-varved and where a linear accumulation rate had to be assumed, between 598-1161 cm and 1965-2053 cm, are highlighted. The steeper the gradient of the line, the greater the amount of sediment per unit time, which is probably linked to a combination of accumulation rate and compaction over time.*

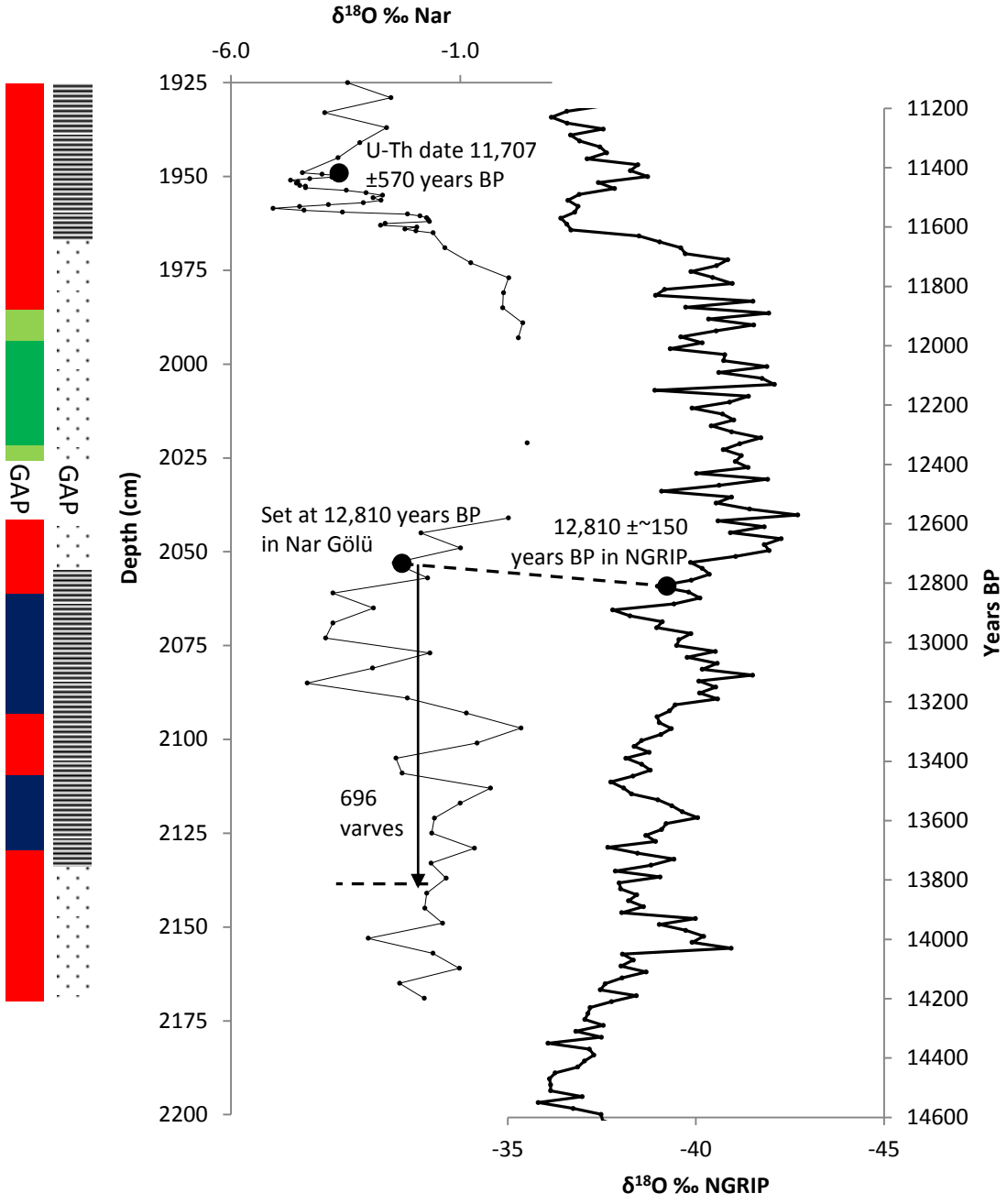

Figure 9.7 *Wiggle matching Nar Gölü record with NGRIP in the late glacial; 2053 cm in Nar Gölü is fixed at 12,810 years BP, during the Bølling-Allerød to Younger Dryas transition in NGRIP, and varve counting is used to extend the Nar Gölü chronology down from this point. There is a gap in the core sequence 2023-2037 cm.*

9.3 Summary

The combination of the one successful U-Th date and the varve counts has yielded a working chronology. Since the sequence is varved from the U-Th date through the early Holocene, the chronology of this part of the Nar Gölü sequence is considered fairly secure, although not as secure as the varved section from the top down to 2,566 years BP. The chronology of the mid to late Holocene section in between these varved sections is even less secure because a linear deposition rate had to be assumed. The chronology of the late glacial section is considered to be the most insecure.

Chapter 10 | Discussion

The provision of a working chronology means it is possible in this chapter to tentatively use temperature and $\delta^{18}O_{source}$ reconstructions from elsewhere to attempt to model water balance changes, and more robustly investigate the drivers of the $\delta^{18}O_{carbonate}$ record. Then, the isotope trends from Nar Gölü can be compared to other records to investigate the controls on Near East hydroclimate and any potential links with the archaeological record. For ease, the location maps from chapter 2 of these other palaeoclimate archives are reproduced here (Figures 10.1 and 10.2).

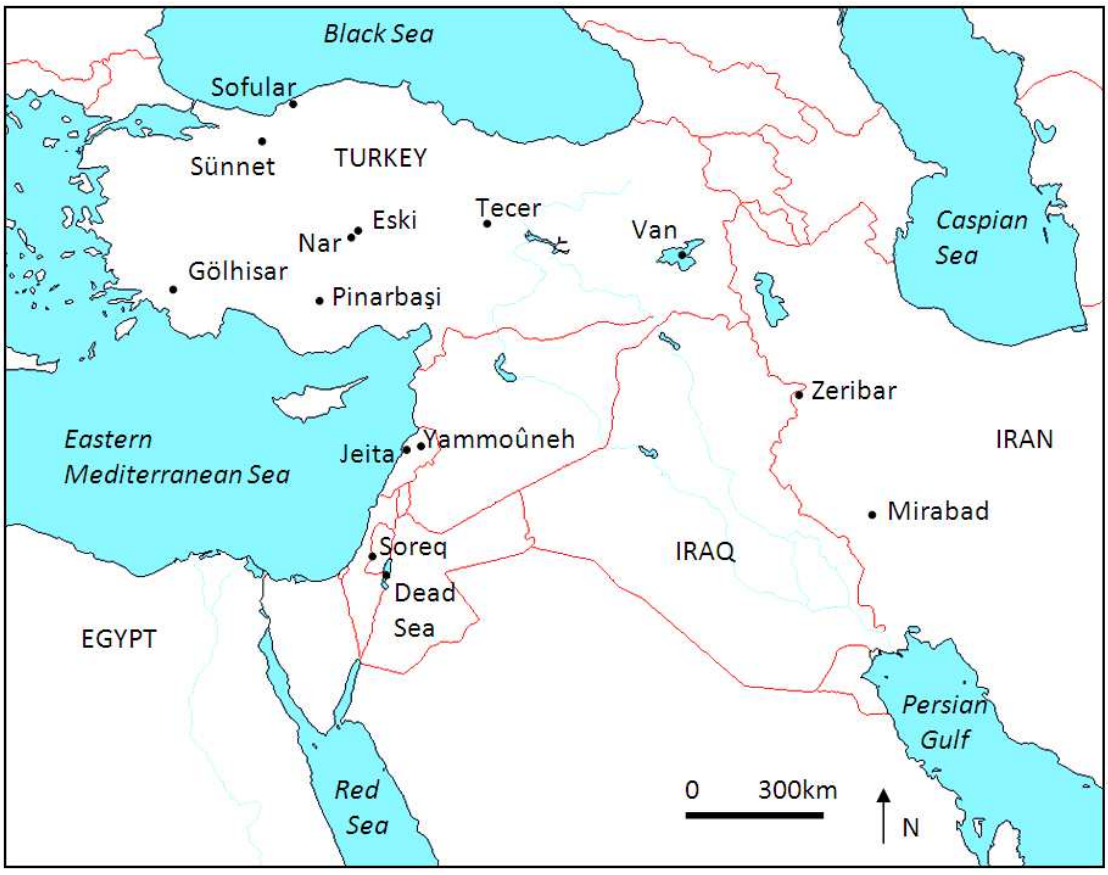

Figure 10.1 *Locations of major palaeoclimate archives in the Near East that will be referred to in this thesis.*

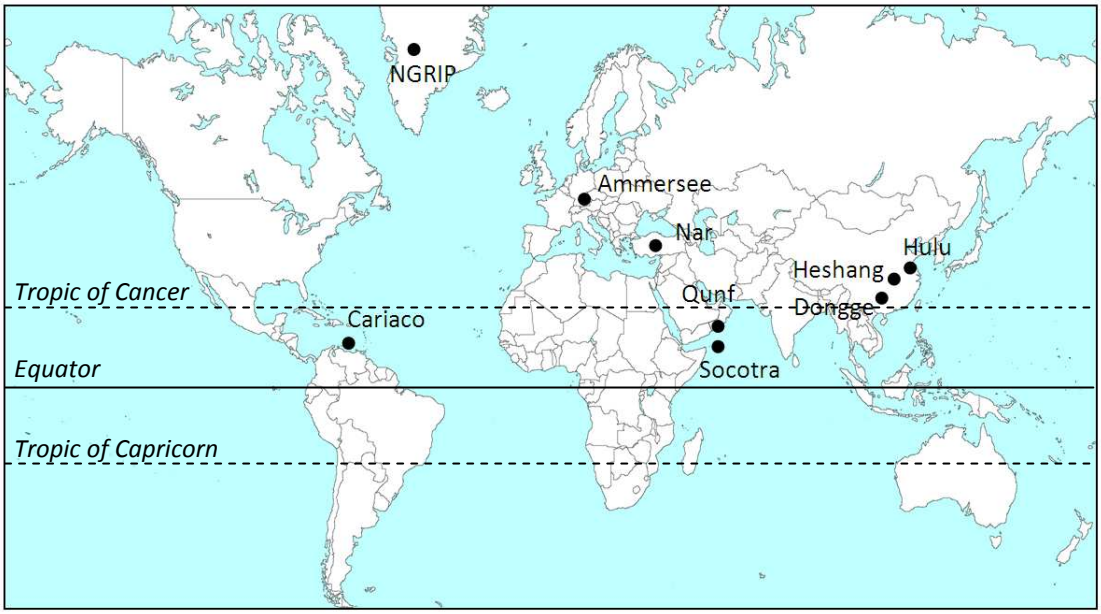

Figure 10.2 *Locations of major palaeoclimate archives from around the world that will be referred to in this thesis.*

10.1 The late glacial

10.1.1 Overview of trends

There appears to be a two stage Bølling-Allerød at Nar Gölü, with higher $\delta^{18}O$ values in zone 1, falling to much lower values in zone 2, suggesting that the time just before the transition into the Younger Dryas was the wettest of the Bølling-Allerød at Nar Gölü (Figure 10.3). The shift from varved to non-laminated sediments and from calcite to aragonite to aragonite/dolomite, which as discussed in chapter 8 is interpreted as indicating a shift to more negative water balance, supports the interpretation of increasing aridity from the Bølling-Allerød to the Younger Dryas. While there are currently no other records at the same resolution as Nar Gölü from the Near East for this time, the Bølling-Allerød is seen to be wetter than the Younger Dryas based on records from the Aegean (Kotthoff et al., 2008a, Dormoy et al., 2009), the Nile Delta (Castaneda et al., 2010), the Black Sea (Bahr et al., 2008), the Red Sea (Arz et al., 2003, Essallami et al., 2007), the Balkans (Aufgebauer et al., 2012), Lake Van (Lemcke and Stürm, 1997), Eski Acıgöl (Roberts et al., 2001), Greece

(Frogley et al., 2001, Lawson et al., 2004, Wilson et al., 2008, Jones et al., 2013), Soreq Cave (Bar-Matthews et al., 1997) and Iran (Stevens et al., 2012). As in the Nar Gölü record, in high resolution temperature records from the North Atlantic region (von Grafenstein et al., 1999, Rasmussen et al., 2006, Vinther et al., 2006, Blaga et al., 2013) a two stage Bølling-Allerød is apparent, with the warmest part just before the transition into the Younger Dryas (Figure 10.4), separated from the cooler earlier period by a peak in coolness called the Gerzensee Oscillation that occurred 300 years before the end of the Bølling-Allerød in NGRIP (Rasmussen et al., 2006, Vinther et al., 2006). An aridity peak occurs 375 varves before what seems to be the end of the Bølling-Allerød in Nar Gölü, and given the chronological uncertainty it is possible these peaks occurred at a similar time.

One of the debates outlined in section 2.2.1 is whether the Younger Dryas in the Near East was drier or wetter than the early Holocene. Most isotope records are interpreted as showing the former, for example those from Lake Zeribar (Snyder et al., 2001, Stevens et al., 2001), Lake Van (Wick et al., 2003), Eski Acıgöl (Roberts et al., 2001) and Soreq Cave (Bar-Matthews et al., 1997), with Jones et al. (2007) suggesting from the Eski Acıgöl record that the Younger Dryas in central Turkey saw 180-300 mm of precipitation per year compared to 330-450 mm per year in the early Holocene (see Figure 10.1 for locations of Near East palaeoclimate archives). However, estimates of the level of the Dead Sea suggest the Younger Dryas was wetter than the early Holocene, based on a salt unit 11,000-10,000 years BP on top of an erosional unconformity (Stein et al., 2010). Kolodny et al. (2005) and Stein et al. (2010) argued that $\delta^{18}O$ values in Soreq Cave in the Younger Dryas were high not because of negative water balance but because of the increased $\delta^{18}O$ of the Eastern Mediterranean Sea and hence of Near East precipitation. Shifts in Nar Gölü from non-laminated to varved and from aragonite/dolomite to calcite (Figure 10.3), a rapid increase in the abundance of *Poaceae* and a decrease in the benthic:planktonic diatom species ratio (Figure 8.8) suggest there was actually a change from dry to wet, at least in central Turkey.

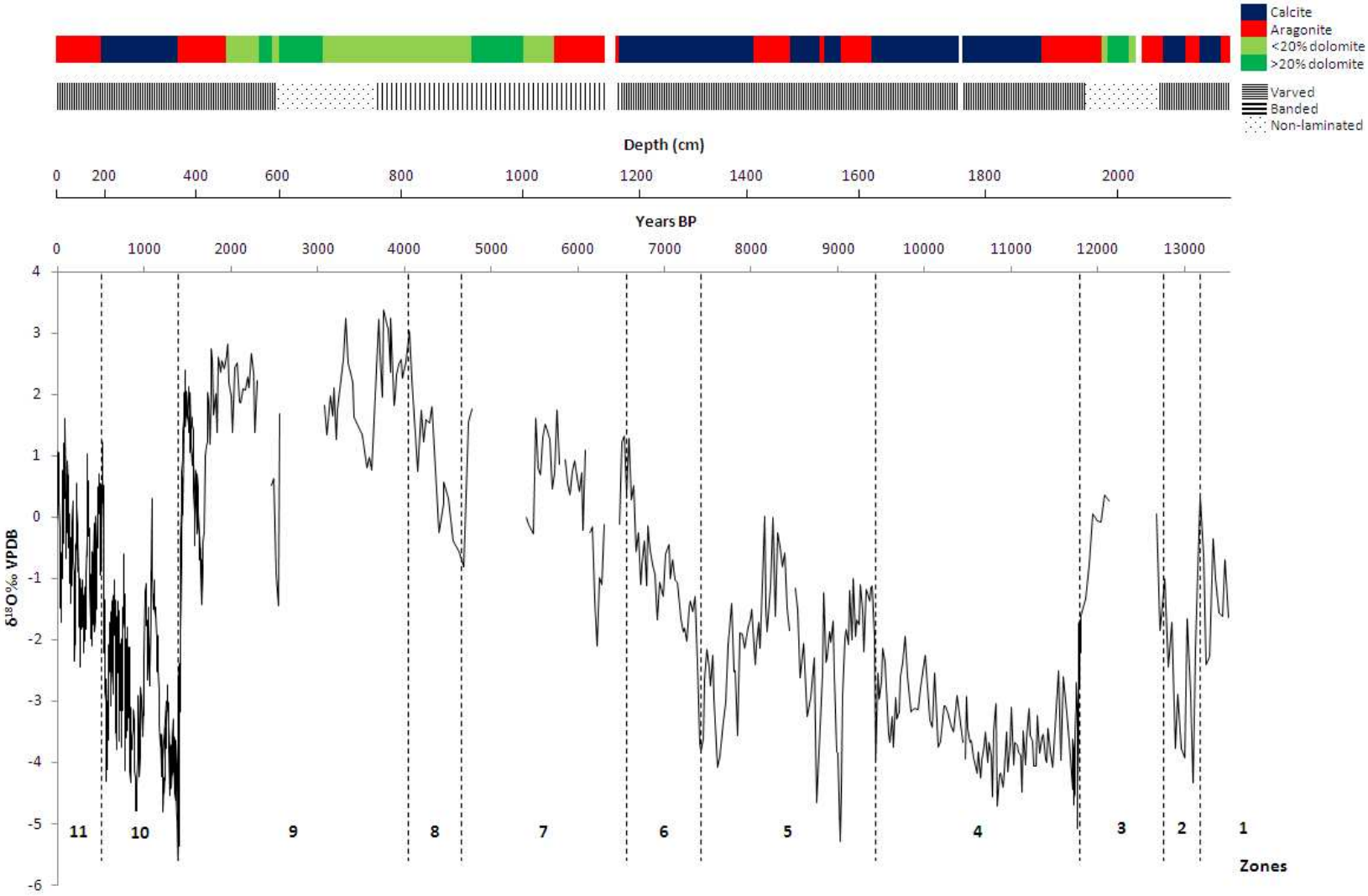

Figure 10.3 *$\delta^{18}O_{carbonate}$ record plotted against time as well as depth, making zones 1 and 2 part of the Bølling-Allerød, 3 the Younger Dryas, 4 and 5 the early Holocene, 6, 7 and 8 the mid Holocene and 9, 10 and 11 the late Holocene, using the Holocene sub-divisions proposed by Walker et al. (2012). The bottom 9 samples in zone 1 are not included, as discussed in section 9.2.*

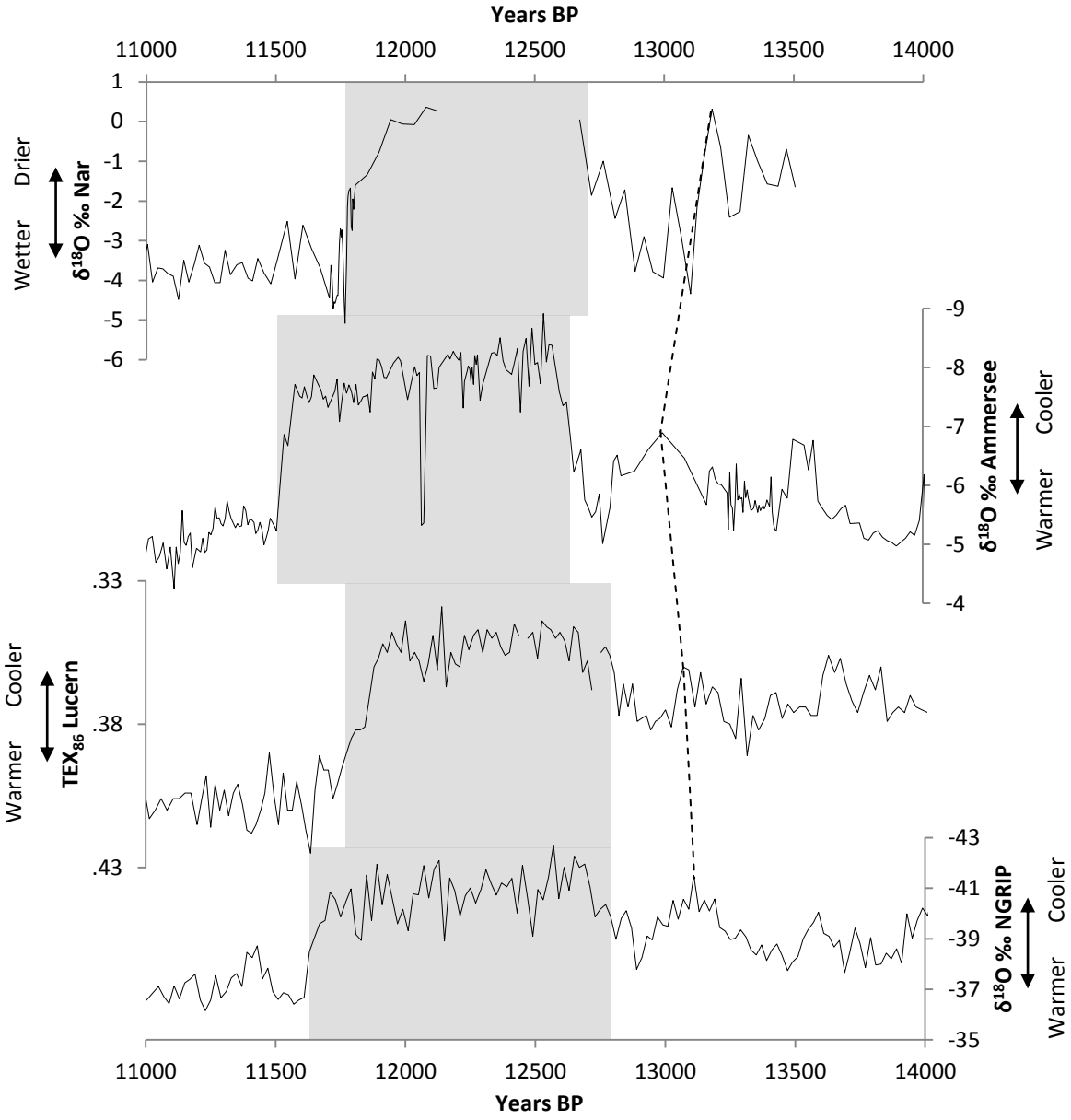

Figure 10.4 *Nar Gölü $\delta^{18}O$ compared to temperature proxy records from the North Atlantic region arranged in order of increasing distance from Nar Gölü: $\delta^{18}O$ from Ammersee in Germany (von Grafenstein et al., 1999), TEX_{86} from Lake Lucern in Switzerland (Blaga et al., 2013) and $\delta^{18}O$ from NGRIP (Rasmussen et al., 2006, Vinther et al., 2006). The Younger Dryas is shaded grey. Shifts at the time of the Gerzensee Oscillation are matched by the dotted line.*

However, before the decrease in $\delta^{18}O_{carbonate}$ can be used to support this, the impact of source effect, temperature, carbonate mineralogy and seasonality on the record

need to be taken into account. The shift from the maximum $\delta^{18}O_{carbonate}$ value of zone 3 in the Younger Dryas (a mean value for this period cannot be used as so many samples from this time could not be run), +0.5‰, to the mean of –3.5‰ for zone 4 in the early Holocene, represents a –4.0‰ shift. Firstly, the potential for temperature to explain this shift needs to be considered. Jones et al. (2007), based on Eastern Mediterranean sea surface temperature reconstructions (Emeis et al., 2000), estimated that the Younger Dryas in central Turkey was 4°C cooler than the early Holocene, which is within the range estimated by Sarıkaya et al. (2009) from glacial evidence from continental Turkey and similar to the estimate of Triantaphyllou et al. (2009) from U_{37}^{k} analysis of cores from the Aegean Sea. The temperature effect on $\delta^{18}O_{carbonate}$ is expressed in two ways: when carbonate precipitates there is a decrease of 0.24‰ for every 1°C rise in temperature and opposing this there is an increase in $\delta^{18}O_{precipitation}$ with increasing temperature (+0.32‰°C^{-1} based on GNIP data from Ankara 1964-2009 (Figure 3.1) (IAEA/WMO, 2013) and assuming this relationship held true in the past). Combined, this means there will be a 0.08‰ increase in $\delta^{18}O_{carbonate}$ for every 1°C temperature rise. This means an increase of 4°C, by itself, into the early Holocene would have led to a rise in $\delta^{18}O_{carbonate}$ of 0.32‰, whereas actually there was a fall of 4‰. Even though there is uncertainty in the temperature values used here, it is clear that temperature could not have forced $\delta^{18}O_{carbonate}$ shifts of the magnitude actually seen. Secondly, the shift from aragonite to calcite could only account for up to ~0.7‰ of the fall in $\delta^{18}O_{carbonate}$ due to changing fractionation factors. Thirdly, the shift in the $\delta^{18}O$ of the Eastern Mediterranean Sea is estimated to have been –1.5 to –3‰ from the Younger Dryas to the Holocene (Kolodny et al., 2005), while the shift to more negative values in the North Atlantic Ocean was likely even smaller than –1.5‰ (Elderfield and Ganssen, 2000). In calculations here, the median value for the Eastern Mediterranean Sea is used (–2.25‰), although with the acknowledgment this may be an overestimation since some of the precipitation will have originated in the North Atlantic.

Therefore, in total, adding the temperature effect (+0.32‰), the carbonate mineralogy effect (–0.7‰) and the $\delta^{18}O_{source}$ effect (–2.25‰) together, 2.6‰ of the

shift to lower values can be explained, leaving 1.4‰ unexplained and potentially due to a shift to more positive water balance.

However, a change in the seasonality of precipitation and the type of precipitation may have had some effect and also need to be considered. A lack of $\delta^{18}O_{diatom}$ data for the Younger Dryas means palaeoseasonality cannot be investigated by comparing these data with $\delta^{18}O_{carbonate}$ at this time, as will be done for the Holocene in section 10.2.2. However, it is fairly likely that since there is some snow in the winter in central Turkey nowadays, if temperatures were ~5°C cooler than now in the Younger Dryas (Emeis et al., 2000) then snow would have made up a greater proportion of the overall precipitation total than in most of the Holocene. Snow $\delta^{18}O$ is significantly lower than rain $\delta^{18}O$ (a fresh snow sample taken in late February 2012 from the Nar Gölü catchment had a $\delta^{18}O$ value of –16.98‰) because it reflects equilibrium conditions in the cloud rather than being in isotopic equilibrium with near-ground water vapour (section 3.3) (Darling et al., 2006, IAEA/WMO, 2013). So, opposing the trends to more negative $\delta^{18}O_{carbonate}$ due to any shift to more positive water balance from zone 3 to 4 would be a move to less snowfall which would have the opposite effect on $\delta^{18}O_{carbonate}$. Were it possible to take this latter effect into account, it could mean that more than –1.4‰ of the $\delta^{18}O_{carbonate}$ shift is unexplained and therefore due to water balance change.

This could help explain why the $\delta^{18}O_{carbonate}$ values in zone 3 in the Younger Dryas are not as high as zone 9 in the late Holocene, despite the fact lithology and carbonate mineralogy suggest lake levels were roughly as low in both zones (Figure 10.3). The mean value of $\delta^{18}O_{carbonate}$ in zone 9 in the late Holocene is +1.0‰ higher than the maximum zone 3 (Younger Dryas) value. The temperature shift of +5°C from the Younger Dryas to late Holocene (Emeis et al., 2000) would have led to a rise in $\delta^{18}O_{carbonate}$ of 0.4‰ (mineral-water fractionation effect and $T/\delta^{18}O_{precipitation}$ effect), the carbonate mineralogy is the same (aragonite and dolomite, but only $\delta^{18}O_{aragonite}$ was measured because of the special reaction outlined in section 6.3.4) and $\delta^{18}O_{source}$ is estimated to have declined by 2.25‰ as discussed above. This means that if these variables alone were influencing $\delta^{18}O_{carbonate}$, values in zone 9 would be 1.85‰

lower, not 1.0‰ higher, than the zone 3. This unexplained 2.85‰ could suggest that zone 9 of the late Holocene had less snowfall than zone 3, which would lead to higher $\delta^{18}O_{carbonate}$. Additionally, the discrepancy could be explained by the fact that lower temperatures in the Younger Dryas compared to the Holocene would have meant less evaporation, so while lake levels would have dropped in the Younger Dryas because of less precipitation (Jones et al., 2007), there would not have been as much evaporative enrichment of $\delta^{18}O_{lakewater}$ as in zone 9.

Therefore, changes in temperature, carbonate mineralogy, $\delta^{18}O_{source}$ and the seasonality/type of precipitation could not have accounted for the magnitude of the $\delta^{18}O_{carbonate}$ shift from the Younger Dryas to the early Holocene, so it was probably mainly due to a shift to more positive water balance. This is supported by other proxy data, especially carbonate mineralogy, lithology and the benthic:planktonic diatom species ratio (Woodbridge et al., unpublished), which all suggest drier conditions in the Younger Dryas, compared to the early Holocene (chapter 8).

10.1.2 Rapidity of transitions

The rapidity of the transition at Nar Gölü from the Bølling-Allerød to the Younger Dryas is difficult to estimate because of the poor chronology (based on wiggle matching with NGRIP) and a gap in the sequence. However, based on the working chronology, it appears that it takes just over 200 years for the transition from the low $\delta^{18}O_{carbonate}$ values of zone 2 to the high values of zone 3 to occur (Figure 10.5). For the Younger Dryas to Holocene transition, the latter part of the transition is varved and has been analysed at a very high resolution. The magnitude of the entire transition is 5.1‰ and takes ~180 years, but over half of the transition (2.9‰) occurs in just 9 varve years (Figure 10.6). After this, there is a shift back to more positive $\delta^{18}O_{carbonate}$ values, in an excursion that lasts 27 years, before more negative $\delta^{18}O_{carbonate}$ values are reached once more. This shows the Younger Dryas to Holocene transition, as recorded in Nar Gölü, was not a simple, linear shift from one state to another.

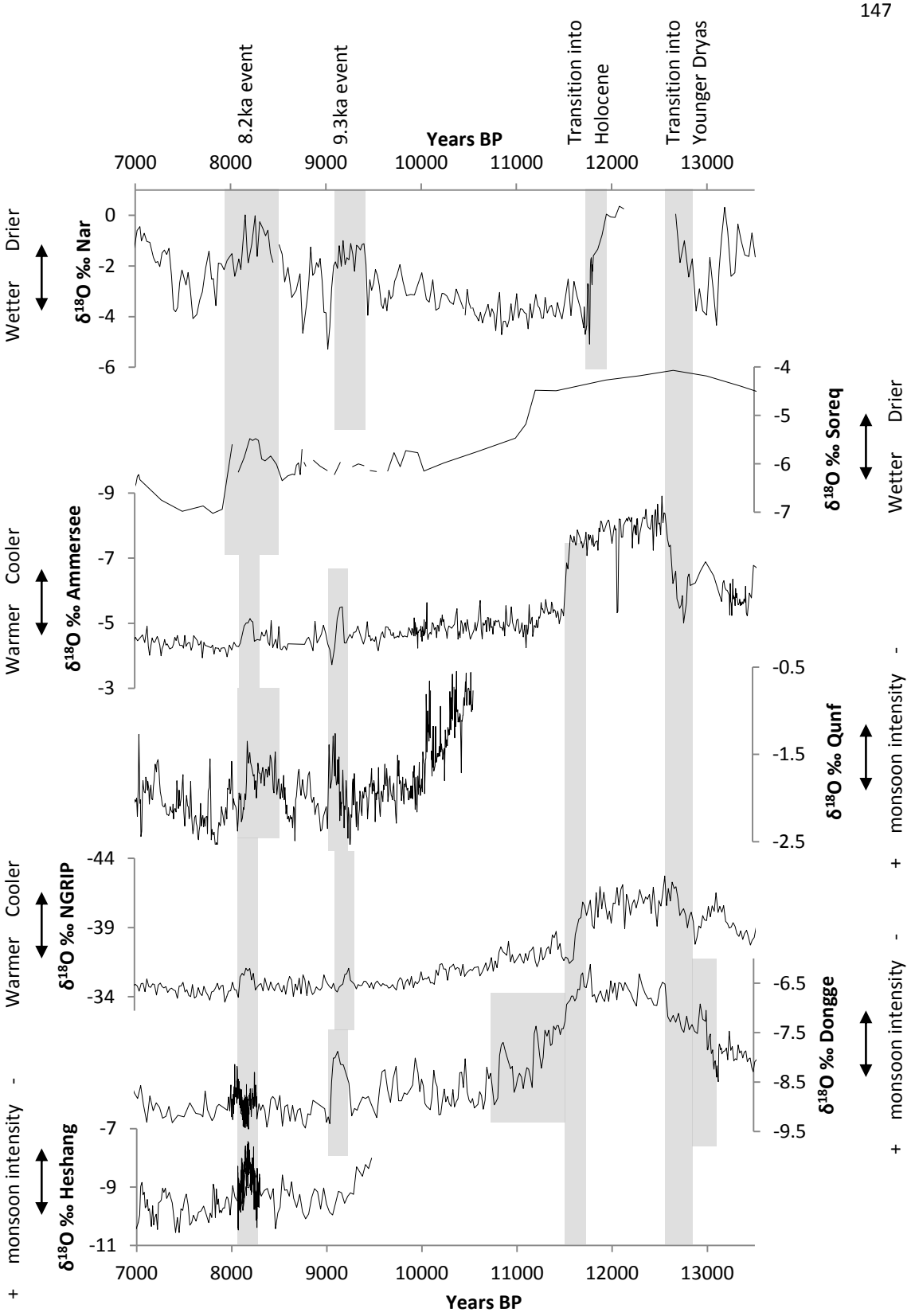

Figure 10.5 *Nar Gölü $\delta^{18}O$ data for the late glacial and early Holocene, compared to records arranged in order of distance from Nar Gölü: Soreq Cave (Bar-Matthews et al., 1997), Ammersee (von Grafenstein et al., 1999), Qunf (Fleitmann et al., 2003, 2007), NGRIP (Vinther et al., 2006, Rasmussen et al., 2006), Dongge (Dykoski et al., 2005) and Heshang (Hu et al., 2008, Liu et al., 2013).*

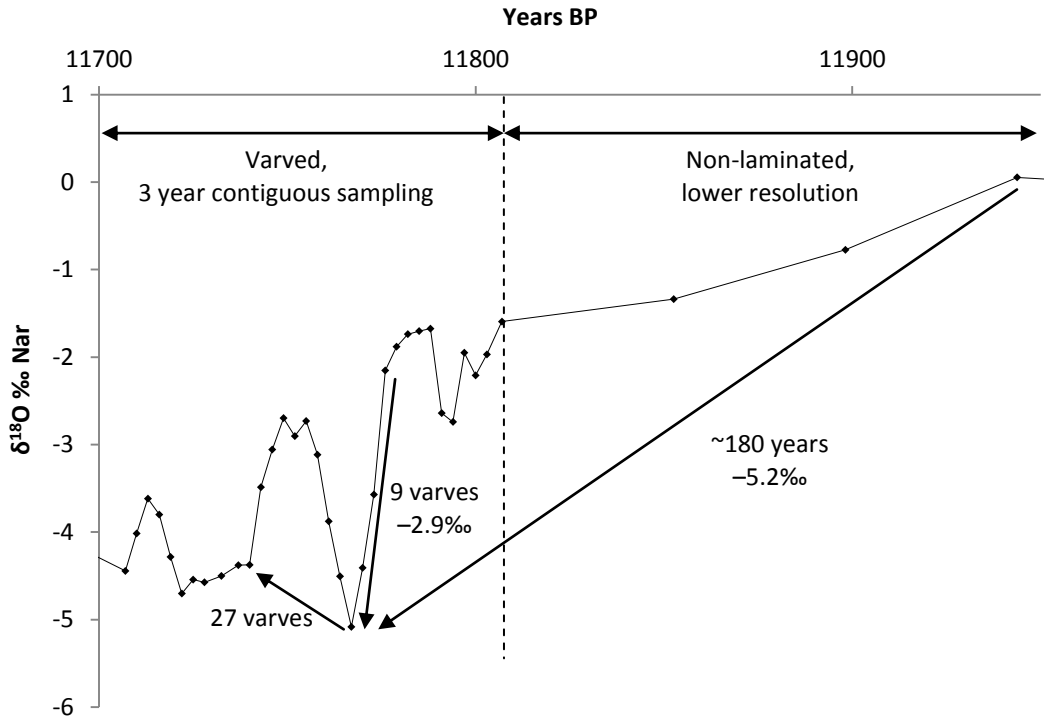

Figure 10.6 *Detail of the $\delta^{18}O_{carbonate}$ record for the Younger Dryas to Holocene transition at Nar Gölü, with the varved section analysed at a very high resolution, demonstrating the rapidity of the latter part of the transition.*

As in records from the North Atlantic region, such as NGRIP (Rasmussen et al., 2006, Steffensen et al., 2008), Ammersee (von Grafenstein et al., 1999), Cariaco (Hughen et al., 1996) and southern France (Genty et al., 2006), the Bølling-Allerød to Younger Dryas transition in Nar Gölü is more gradual than the transition from the Younger Dryas to the Holocene. In these records, the former takes >200 years, whereas the latter takes <100 years in the North Atlantic and slightly longer in Nar Gölü (but still <200 years). In records further away from the North Atlantic that are responding to changes in the intensity of the Asian monsoon, such as the $\delta^{18}O$ speleothem records from Dongge (Dykoski et al., 2005), Hulu (Wang et al., 2001) and Socotra (Shakun et al., 2007) (Figure 10.2), the Bølling-Allerød to Younger Dryas transition is much more gradual, taking many hundreds of years (Figure 10.5). Likewise, the Younger Dryas to Holocene transition in Dongge (Dykoski et al., 2005) and, although the transition is not covered in its entirety, seemingly also in Qunf (Fleitmann et al., 2003, 2007), is more gradual than in Nar Gölü and records from the North Atlantic. Shakun et al.

(2007) suggest this could be because the Asian monsoons are driven by the temperature contrast between the ocean and the continent, so records will be influenced by the Southern Hemisphere as well as changes in North Atlantic circulation, compared to records from Greenland, Europe and the Near East which will mainly have been influenced by the latter.

10.1.3 Summary

The Younger Dryas in Nar Gölü appears to have been significantly drier than the Bølling-Allerød and the early Holocene and at least as dry as zone 9 in the late Holocene, supporting the interpretations of other records from the region including the Soreq Cave isotope record (Bar-Matthews et al., 1997) but contrary to the interpretations of the Dead Sea record (Stein et al., 2010, Litt et al., 2012). While it is not possible to determine whether the transitions were synchronous with those in other parts of the world because of the U-Th dating error (it can only be said that the Younger Dryas to Holocene transition occurred sometime between ~11,200 and 12,300 years BP), rapidity can be considered. The rapid nature of the transitions in Nar Gölü into the Younger Dryas and Holocene, as is seen in records from the North Atlantic region, and in contrast to records from further east in the Northern Hemisphere, suggests a strong teleconnection between changes in the circulation of the North Atlantic, which are considered by many to have been the cause of the Younger Dryas cooling (Broecker et al., 1989, Tarasov and Peltier, 2005, Teller, 2012), and Near East hydroclimate. Since a significant amount of the precipitation that falls in central Turkey has North Atlantic origins (section 2.1.1), a reduction in cyclogenesis during the Younger Dryas is likely to have reduced the frequency of and changed the path of Mediterranean storm tracks and led to less precipitation falling in the Near East, a conclusion reached in previous studies of Near East palaeoclimatology (Bartov et al., 2003, Prasad et al., 2004, Rowe et al., 2012).

10.2 General trends through the Holocene

10.2.1 Comparison to other records

The overall similarity with the Eski Acıgöl record (Figure 10.7), while not surprising given their geographical proximity, is useful in confirming that the isotope records are recording regional palaeoclimate variations and not just responding to lake-specific factors (Fritz, 2008). The overall trends of the Nar Gölü $\delta^{18}O_{carbonate}$ record through the Holocene are similar to those seen in lake isotope records from across the region (Roberts et al., 2008, 2011a), with low values in the early Holocene and a gradual rise in the mid Holocene to a peak ~3,000-2,000 years BP (Figure 10.7). More specifically, the other records suggest maximum wetness ~7,900 years BP and a shift to drier conditions beginning ~7,000 years BP, and although the chronology weakens after zone 6 with the disappearance of the varves, similar trends are seen in the Nar Gölü record (Figure 10.7). There is initially a steep and sustained increase in $\delta^{18}O_{carbonate}$ in zone 6 (beginning at ~7,400 years BP based on the working chronology, or taking into account the U-Th dating error sometime between 6,850 and 7,994 years BP) lasting just over 800 varve years. There is then a period where there was no overall rise (zone 7), before the transition is completed with the rise in zone 8, ending ~4,000 years BP. Although harder to discern because of the low resolution of the records, it could also be inferred from the Eski Acıgöl and Gölhisar Gölü records that the Mid Holocene Transition was not steady but was divided into at least two phases of increasing $\delta^{18}O_{carbonate}$ values (Figure 10.7). There are some differences with other records, for example a large negative anomaly in $\delta^{18}O_{carbonate}$ in Gölhisar Gölü ~3,500 years BP and the increase in $\delta^{18}O_{carbonate}$ beginning only ~6,000 years BP in Lake Van. This is probably due to a combination of variability in climate changes between different parts of the region and differences in hydrology between lakes (for example the large size of Lake Van will probably have made it less responsive to climate change (Roberts et al., 2011a)).

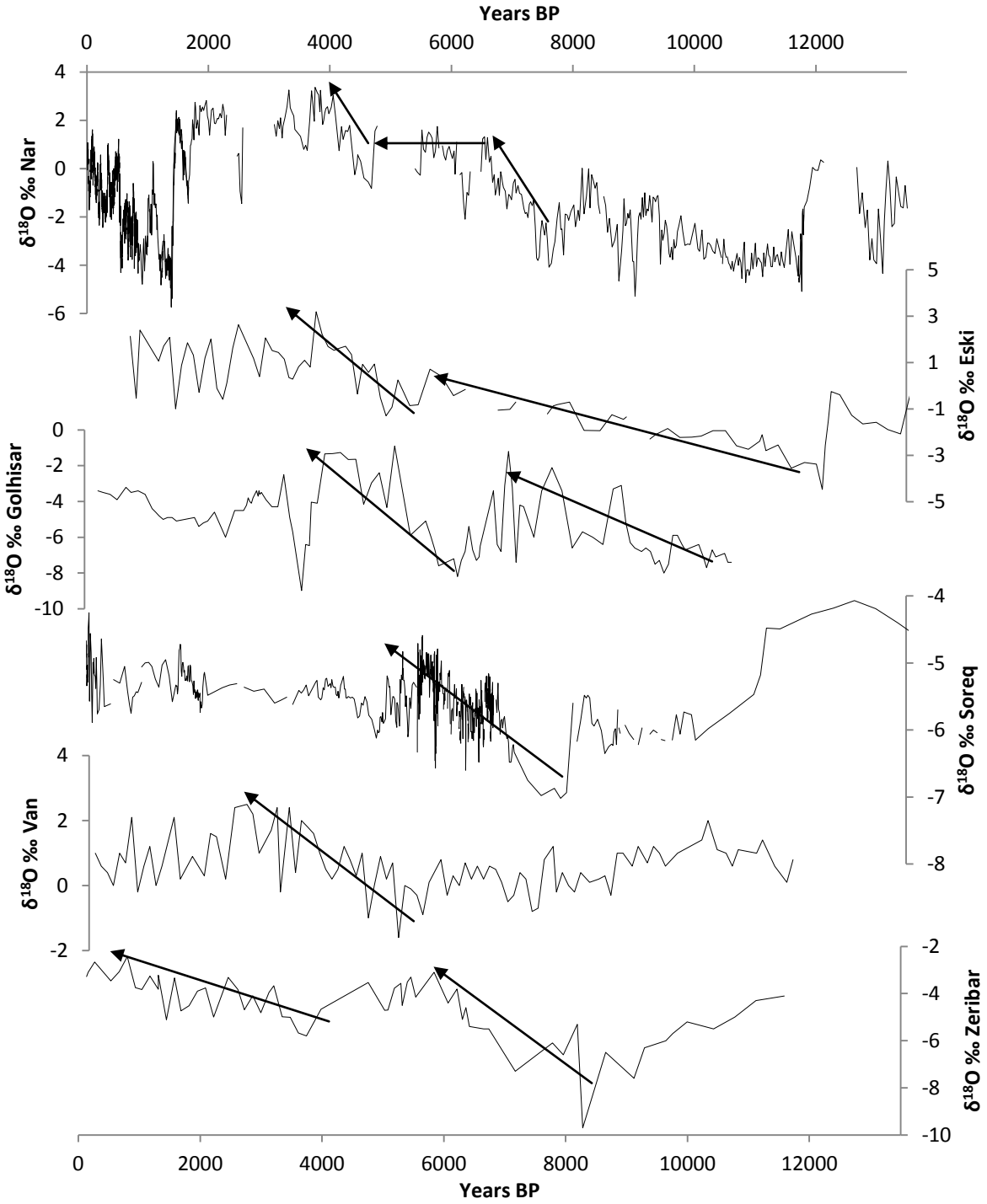

Figure 10.7 *$\delta^{18}O_{carbonate}$ record from Near East lakes arranged in increasing distance from Nar Gölü, with more positive values indicating drier conditions: Eski Acıgöl (Roberts et al., 2001), Gölhisar Gölü (Eastwood et al., 2007), Soreq Cave (Bar-Matthews et al., 1997, Orland et al., 2009, Bar-Matthews and Ayalon, 2011), Lake Van (Wick et al., 2003) and Lake Zeribar (Stevens et al., 2001). See Figure 10.1 for locations.*

10.2.2 The drivers of $\delta^{18}O_{carbonate}$ in the Mid Holocene Transition

As discussed previously, an issue of contention is the interpretation by Stevens et al. (2001, 2006) of the $\delta^{18}O_{carbonate}$ records from Lakes Zeribar and Mirabad in terms of the seasonality of precipitation, with the rise in $\delta^{18}O_{carbonate}$ through the Mid Holocene Transition seen to reflect a shift from winter- to spring-dominated precipitation. They suggested the early Holocene was drier than the late Holocene, based on pollen evidence, despite the fact other $\delta^{18}O_{carbonate}$ records from the Near East are interpreted as showing an increase in aridity. To better constrain the drivers of $\delta^{18}O_{carbonate}$ in the Nar Gölü record, modelling is undertaken.

It has been suggested, based on evidence from pollen (Djamali et al., 2010), microcharcoal (Turner et al., 2008), modelling (Brayshaw et al., 2010) and $\delta^{18}O$ of freshwater mollusc shells from Çatalhöyük (Bar-Yosef Mayer et al., 2012), that the early Holocene Near East saw dry summers and springs, but wetter winters. To investigate the influence that this might have on $\delta^{18}O$, the present seasonal distribution of precipitation at Niğde (Figure 10.8A), used to represent late Holocene conditions, is shifted to a situation where precipitation is winter- not spring-dominated (DJF precipitation twice that in the spring and autumn and no JJA precipitation) (Figure 10.8B). Using the average $\delta^{18}O$ of precipitation from each month from the Ankara GNIP record (1964-2009) (IAEA/WMO, 2013), corrected for 1°C colder temperatures in the early Holocene (Emeis et al., 2000) and assuming the $\delta^{18}O_{precipitation}/T$ was the same as in the present (+0.32‰°C^{-1}), the annual weighted average $\delta^{18}O_{precipitation}$ is calculated. In the present day, the weighted average is –8.2‰. In the early Holocene, with the 1°C lower temperatures and the shift in precipitation distribution, the weighted average is –9.8‰, 1.6‰ lower. Assuming the precipitation distribution was the same in zone 9 as it is now, this suggests only a small proportion of the 5‰ rise from the mean of zone 4 to the mean of zone 9 can be explained by a change in the seasonality of precipitation in central Turkey.

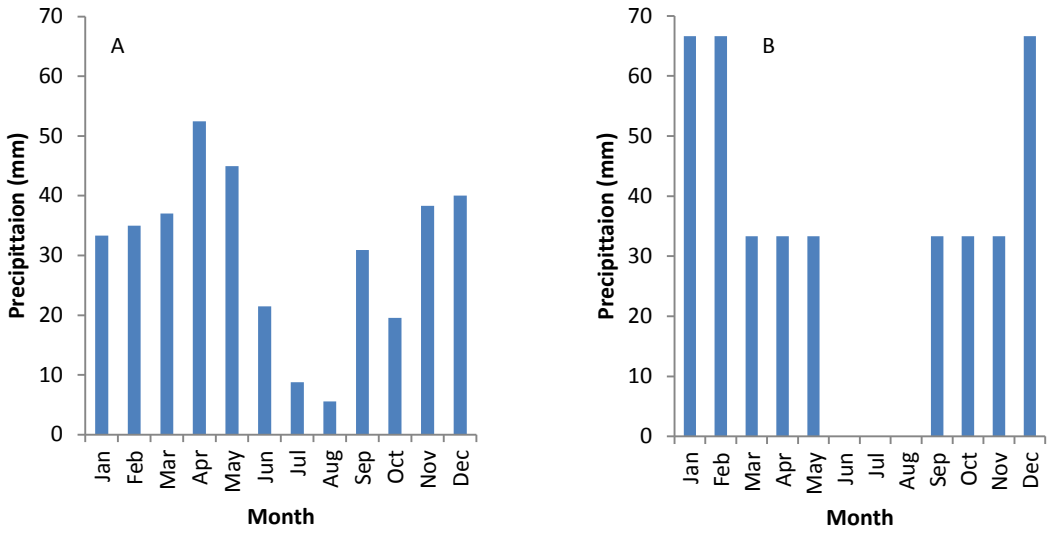

Figure 10.8 *A: Precipitation distribution 1935-2010 from Niğde, B: hypothesised early Holocene precipitation regime assuming an extreme shift to winter-dominated.*

This modelling, however, clearly involves a lot of assumptions, such as the 1°C cooling occurring in every month, a $\delta^{18}O_{precipitation}$/T relationship the same as in the present and a precipitation distribution the same throughout the late Holocene (i.e. the same in zone 9 and in the present). Therefore, more investigation using a proxy for palaeoseasonality is required. In Dean et al. (2013), it was suggested that comparing $\delta^{18}O_{carbonate}$ and $\delta^{18}O_{diatom}$ data from Nar Gölü could provide insights into seasonality because the two hosts form at different times of the year, as was further demonstrated in section 7.2. Here, this work is built upon by extending the diatom isotope record back through the new NAR10 cores. Because $\delta^{18}O_{carbonate}$ and $\delta^{18}O_{diatom}$ data are produced on different scales (VPDB and VSMOW respectively) and because of their different fractionation factors with lakewater, in order to compare them properly they need to be converted to $\delta^{18}O_{lakewater}$ using Eqs. 6.2, 6.5 and 6.11. While the accuracy of the $\delta^{18}O_{lakewater}$ values produced will be limited due to issues with the equations, errors with the mass balancing, etc., it is the only way to compare the data directly. As in Dean et al. (2013), a temperature range of +15-20°C is given for the time of carbonate precipitation and +5-15°C for the time of diatom growth, based on the estimates from the present (Dean et al., 2013). Figure 10.9 shows the estimates of $\delta^{18}O_{lakewater}$, with $\Delta\delta^{18}O_{lakewater}$ (a measure of how much more

positive $\delta^{18}O_{lakewater}$ was at the time of carbonate precipitation compared to the time of diatom growth) also plotted. $\Delta\delta^{18}O_{lakewater}$ could be increased by amplified intra-annual variability in $\delta^{18}O_{lakewater}$ (for example caused by increased winter snowmelt leading to a freshwater lid at the time of diatom growth that had disappeared by the time of carbonate precipitation (Dean et al., 2013)) and/or by a larger difference in the time of year of carbonate precipitation and diatom growth (which may or may not be related to climate). So while it is difficult to interpret, an increase in $\Delta\delta^{18}O_{lakewater}$ may indicate increased seasonality. Due to the errors involved, the $\delta^{18}O_{diatom}$ record is much noisier than the $\delta^{18}O_{carbonate}$ record, so it is best to look at general trends and ignore short term fluctuations in $\Delta\delta^{18}O_{lakewater}$. The very low $\delta^{18}O_{lakewater}$ values at the time of diatom growth and the large $\Delta\delta^{18}O_{lakewater}$ seen ~1,500-1,100 years BP were interpreted as indicating that diatoms grew in a freshwater lid after significant snowmelt (Dean et al., 2013), as will be discussed in more detail in section 10.4. Such low values are not seen in the early Holocene, suggesting there was not enough snow to form a freshwater lid at this time. $\delta^{18}O_{lakewater}$ at the time of carbonate precipitation increases at a greater rate from zones 4 to 9 than $\delta^{18}O_{lakewater}$ at the time of diatom growth: $\Delta\delta^{18}O_{lakewater}$ is smaller in the early Holocene than in zones 8 and 9. This suggests there was less intra-annual variability in $\delta^{18}O_{lakewater}$ (reduced seasonality), and/or a smaller difference in the time of year of carbonate precipitation and diatom growth, in the early Holocene compared to the mid to late Holocene. Even if a freshwater lid did not form in most of the late Holocene, it is possible there was more snow in the late Holocene compared to the early Holocene and this accounted for the increase in $\Delta\delta^{18}O_{lakewater}$.

Since the modelling suggests only +1.6‰ of the change in $\delta^{18}O_{carbonate}$ could be explained by evoking changes in the seasonality of precipitation and $\Delta\delta^{18}O_{lakewater}$ suggests that in fact seasonality was reduced in the early Holocene compared with the late Holocene, changes in the seasonality and type of precipitation are considered unlikely to have been the main cause of the Mid Holocene Transition in Nar Gölü to higher $\delta^{18}O_{lakewater}$. Other factors are also likely to have had only minimal influence on $\delta^{18}O_{carbonate}$ between the early and late Holocene. As discussed, while the shift from the Younger Dryas to the Holocene in $\delta^{18}O_{source}$ is seen to have been

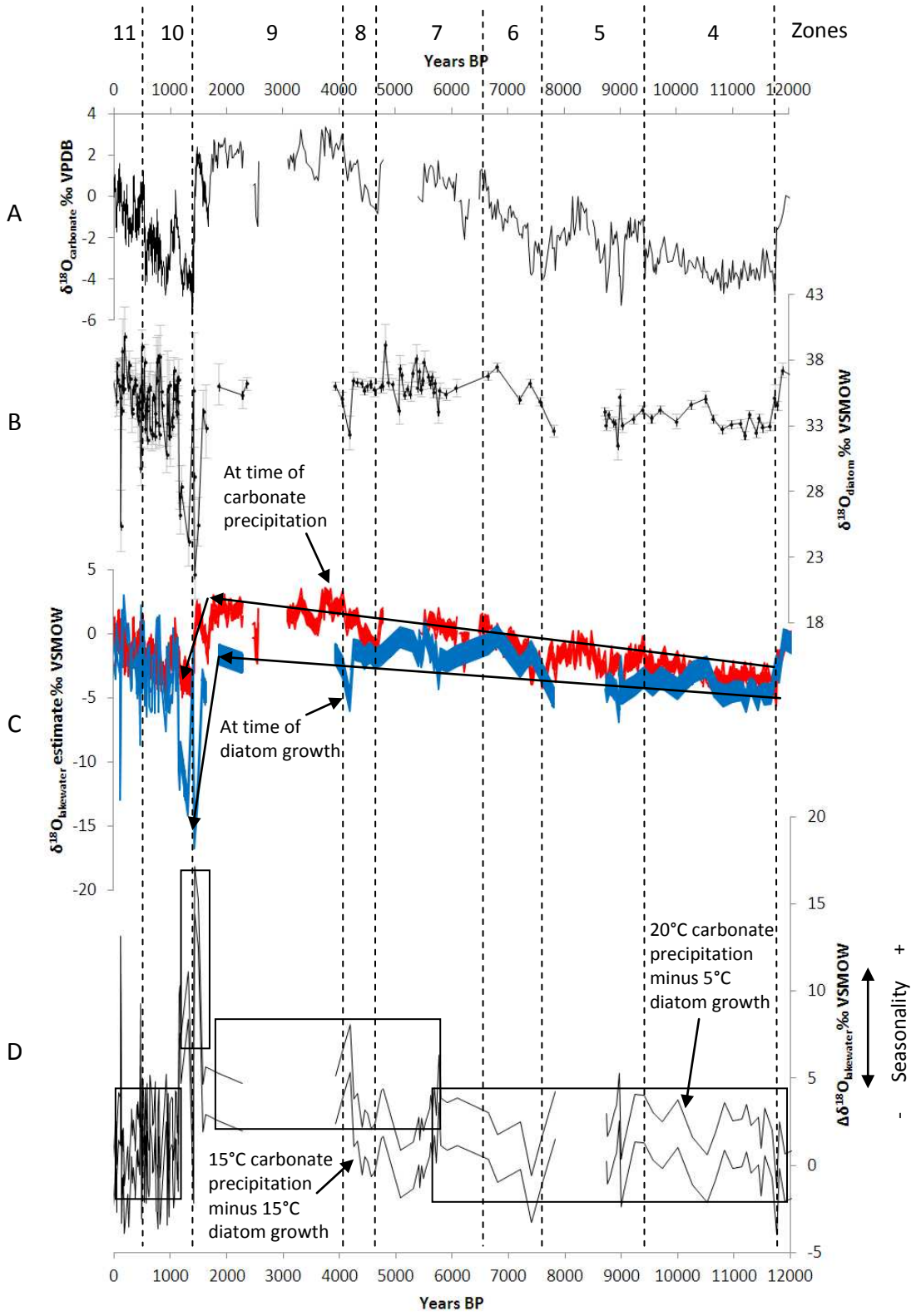

Figure 10.9 *$\delta^{18}O_{carbonate}$ (A) and $\delta^{18}O_{diatom}$ (B) trends, with data converted to $\delta^{18}O_{lakewater}$ assuming a temperature range of +15-20°C for the time of carbonate precipitation and +5-15°C for the time of diatom growth (C) and the measure of how much more positive $\delta^{18}O_{lakewater}$ was at the time of carbonate precipitation than diatom growth (top line +20°C minus +5°C i.e. maximum temperature difference and bottom line +15°C minus +15°C i.e. minimum temperature difference (D).*

substantial, the change between the early and late Holocene was probably far less. Also, if temperature alone was responsible for the 5‰ shift, a 62.5°C rise would be required, suggesting this is not the major cause of the shift: in fact, there is believed to have been a 1°C rise (Emeis et al., 2000). Even if the temperature rise was a few degrees greater, as has been suggested by some studies (e.g. McGarry et al., 2004), it would not be sufficient to explain the increase in $\delta^{18}O_{carbonate}$. While there is a change from calcite in most of zone 4, to aragonite in most of zone 9, the effect this would have had on $\delta^{18}O_{carbonate}$ is again small. Therefore, combining the effects of the seasonality of precipitation plus the temperature effect on $\delta^{18}O_{precipitation}$ (+1.6‰), temperature on carbonate precipitation (–0.24‰) and carbonate mineralogy (~+0.7‰), only 2.1‰ of the shift in $\delta^{18}O_{carbonate}$ from zone 4 to zone 9 can be explained (and less than this if the $\Delta\delta^{18}O_{lakewater}$ data really are showing reduced seasonality in the early Holocene). The rest of the rise in $\delta^{18}O_{carbonate}$ was likely caused by a trend to more negative water balance, and this interpretation is supported by the shift from varved to non-laminated sediments, the change from calcite to aragonite/dolomite, the rise in $\delta^{13}C$ and the increase in benthic relative to planktonic diatom species (chapter 8), proxies that will not have been affected by a change in $\delta^{18}O_{precipitation}$ due to a shift in the seasonality of precipitation.

This all supports the assertion that water balance is the key driver of Near East lake isotope records (Jones and Roberts, 2008) and runs contrary to the interpretations of Stevens et al. (2001, 2006). It also calls into question the interpretation of the Dead Sea pollen record in the Holocene: namely that the period 6,300-3,500 years BP was wetter (with precipitation exceeding 650 mm per year) than the period 9,700-6,500 years BP (less than 350 mm per year) (Litt et al., 2012). As introduced in section 2.2.2, the Soreq Cave record (Bar-Matthews et al., 1997, Bar-Matthews et al., 2003, Bar-Matthews and Ayalon, 2011) was interpreted as showing the opposite: that the early Holocene was drier than the late Holocene, in line with the interpretation of most other records from the region. While the climate of Turkey and Israel do differ, the fact the $\delta^{18}O$ trends of Nar Gölü and Soreq Cave are so similar (Figure 10.7) and that in Nar Gölü it has been shown the early Holocene was very likely wetter than the late Holocene, and the fact other proxy records from the rest of Israel (Neev and

Emery, 1995, Goodfriend, 1999, Frumkin et al., 1999, Frumkin et al., 2000, Gvirtzman and Wieder, 2001, McLaren et al., 2004) also show this, supports the arguments of the Soreq Cave researchers. While $\delta^{18}O_{source}$ will be influencing lake and speleothem $\delta^{18}O$ records, the modelling and multi proxy approach presented here demonstrates that water balance has been the key control on the Nar Gölü record. Similar conclusions were reached based on modelling of the Lake Yammoûneh record from Lebanon (Develle et al., 2010): after accounting for changes in $\delta^{18}O_{source}$, increased rainfall is necessary to explain the low $\delta^{18}O_{carbonate}$ values in the early Holocene.

10.2.3 Examining the drivers of the Holocene aridity trend

The general Holocene trends at Nar Gölü seem to be more similar to those seen in the African (e.g. deMenocal et al., 2000, Adkins et al., 2006, Renssen et al., 2006) and Asian monsoon (e.g. Fleitmann et al., 2003, Dykoski et al., 2005) records, with an increase in aridity through the Holocene of a similar magnitude as the Younger Dryas to the Holocene shift, than to North Atlantic region records where Holocene changes were of a much smaller magnitude (Figure 10.10). This trend has been linked to high summer insolation in the early Holocene and the subsequent decline through the mid Holocene in the Northern Hemisphere (deMenocal et al., 2000, Braconnot et al., 2007, Fleitmann et al., 2007, Renssen et al., 2007, Roberts et al., 2011b) (Figure 10.10). Increased precipitation in Saharan Africa in the early Holocene was caused by a northward movement of the monsoon rains, but the direct influence of the summer monsoon is not thought to have reached the Near East (Arz et al., 2003, Brayshaw et al., 2011b) and as discussed in section 2.2.2 summer drought seems to have persisted for several millennia into the Holocene in the region. Rather, the wet early Holocene in the Near East seems to have been the result of increased precipitation in other seasons, especially the winter (Brayshaw et al., 2011a), made possible because of the increased residual heat left in the oceans as a result of the higher summer insolation (Tzedakis, 2007). Modelling has shown how, through the Holocene, insolation and greenhouse gas concentration changes led to a weakening and poleward shift of the Mediterranean storm track (Black et al., 2011, Brayshaw et al., 2011b), and hence increased aridity in the Near East.

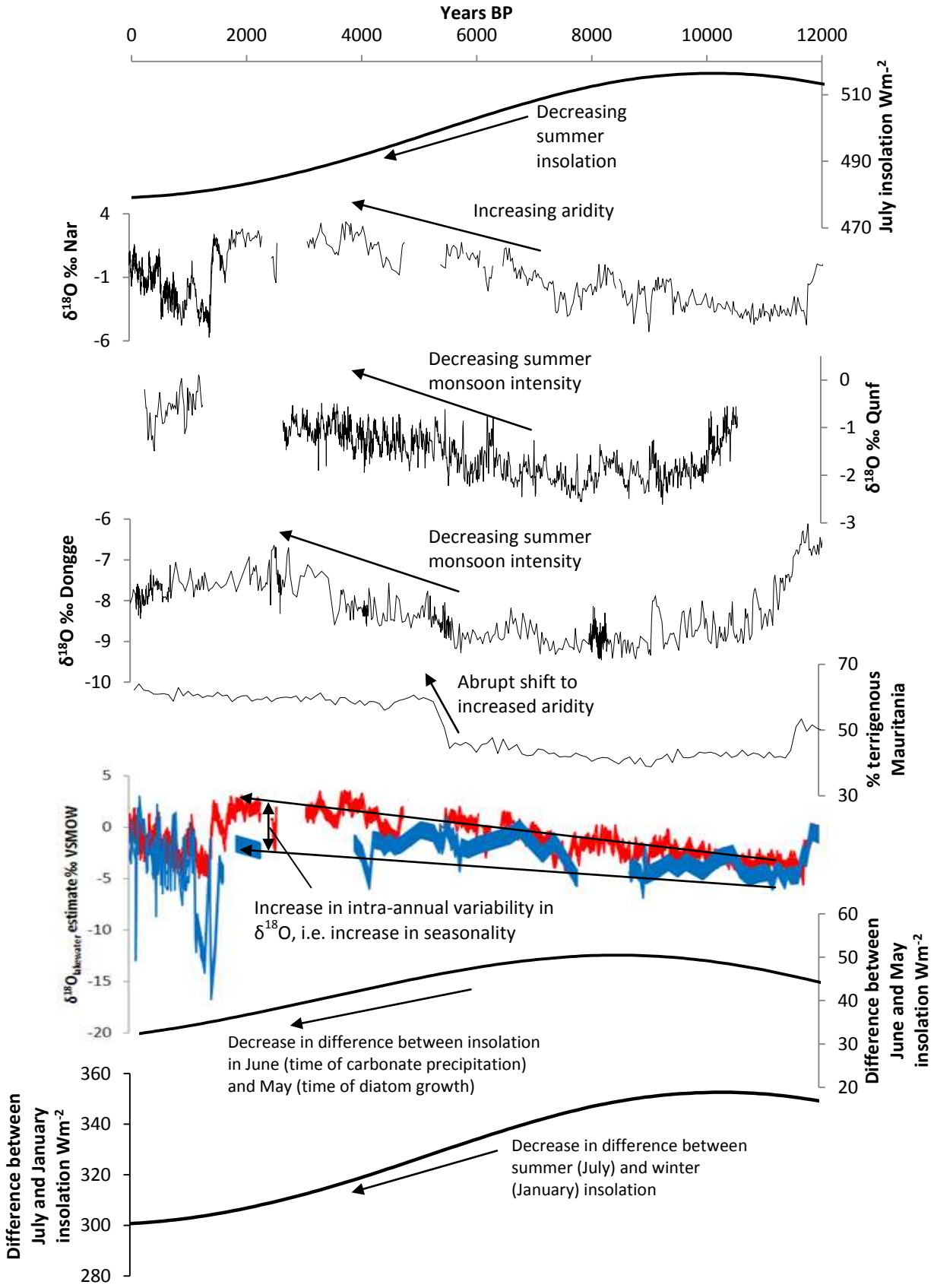

Figure 10.10 *$\delta^{18}O$ from Nar Gölü, Qunf (Fleitmann et al., 2003, 2007) and Dongge (Dykoski et al., 2005) and % terrigenous material from a core off Mauritania (deMenocal et al., 2000) compared to insolation changes for 38°N (the latitude of Nar Gölü, trends similar at latitudes of Qunf and Dongge) calculated from Laskar et al. (2004). $\delta^{18}O_{lakewater}$ calculated for the times of year of carbonate precipitation and diatom growth, and differences between June and May, and July and January, insolation also shown (Laskar et al., 2004).*

Interestingly, while based on the comparison of $\delta^{18}O_{carbonate}$ and $\delta^{18}O_{diatom}$ data there was an increase in intra-annual variability in $\delta^{18}O_{lakewater}$, i.e. increased seasonality, from the early Holocene to the late Holocene, Figure 10.10 shows that the difference in insolation between June (when carbonate precipitation is believed to occur) and May (the time of year diatom growth is estimated to be weighted to), as well as the difference between summer and winter insolation, actually decreases over this time. Modelling has also shown how air temperature seasonality was greater in the Near East in the early Holocene compared to the late Holocene (Brayshaw et al., 2011a). Therefore, it appears that something other than insolation and temperature seasonality caused this increase in intra-annual $\delta^{18}O_{lakewater}$ variability, which as discussed could be due to an increase in snowfall in the late Holocene.

10.2.4 Summary

Modelling suggests the majority of the 5‰ shift from zone 4 in the early Holocene to zone 9 in the late Holocene probably cannot be explained by a change in the seasonality of precipitation, and this is supported by the $\Delta\delta^{18}O_{lakewater}$ comparison, which suggests if anything intra-annual variability was limited in the early Holocene. Even combining potential seasonality changes with changes in temperature, $\delta^{18}O_{source}$ and carbonate mineralogy, it is estimated that less than half of the magnitude of the shift can be explained. Therefore, it appears that the Holocene $\delta^{18}O_{carbonate}$ record is mainly responding to water balance and that the hypothesis of changes in the seasonality of precipitation being a major control on Near East lake isotope records (Stevens et al., 2001, 2006) can be rejected, at least for Nar Gölü. The increase in aridity through the Holocene is likely to be linked to a decline in summer insolation, which led to a weakening and poleward shift in the Mediterranean storm track.

10.3 Holocene centennial scale climate shifts

10.3.1 Early Holocene

In the North Atlantic region records, three main centennial scale climate change events have been identified in the early Holocene: the Pre Boreal Oscillation (PBO), the 9.3 ka event and the 8.2 ka event (Rasmussen et al., 2006). Climate changes at these times have been identified in some Near East records (Bar-Matthews et al., 2003, Landmann and Kempe, 2005, Turner et al., 2008), however a lack of high resolution and well-dated records means investigation of Holocene decadal and centennial scale changes in the region has been limited. Despite the lack of strong chronological control (only one sensible U-Th date) in the Nar Gölü sequence, which means it not possible to investigate whether the three early Holocene events occurred at the same time in Nar Gölü and NGRIP, it is possible to count up through the varved sediments from the start of the Holocene to establish whether or not there were any changes in Nar Gölü that occurred the same amount of time from the start of the Holocene as the three major early Holocene events in NGRIP.

There appear to be increases in aridity in Nar Gölü at around the same number of years from the start of the Holocene as the PBO, 9.3 ka and 8.2 ka cooling events. Drying in Nar Gölü at the time of the PBO is the least well defined, but there are two samples outside of ±1σ from the zone 4 mean (Figure 10.11). There is similarly a trend to increasing aridity in Nar Gölü ~2,336 varve years after the start of the Holocene, very close to the 2,340 years after the start of the Holocene the 9.3 ka event cooing trend starts in NGRIP. However, whereas the cooling in NGRIP and other records from the North Atlantic region such as Ammersee (von Grafenstein et al., 1999) lasts ~100 years, in Nar Gölü there is a dry interval that lasts ~340 years. Aridity at this time also lasts longer in other records away from the North Atlantic, for example Qunf in Oman (Fleitmann et al., 2003, 2007) and Dongge in China (Dykoski et al., 2005).

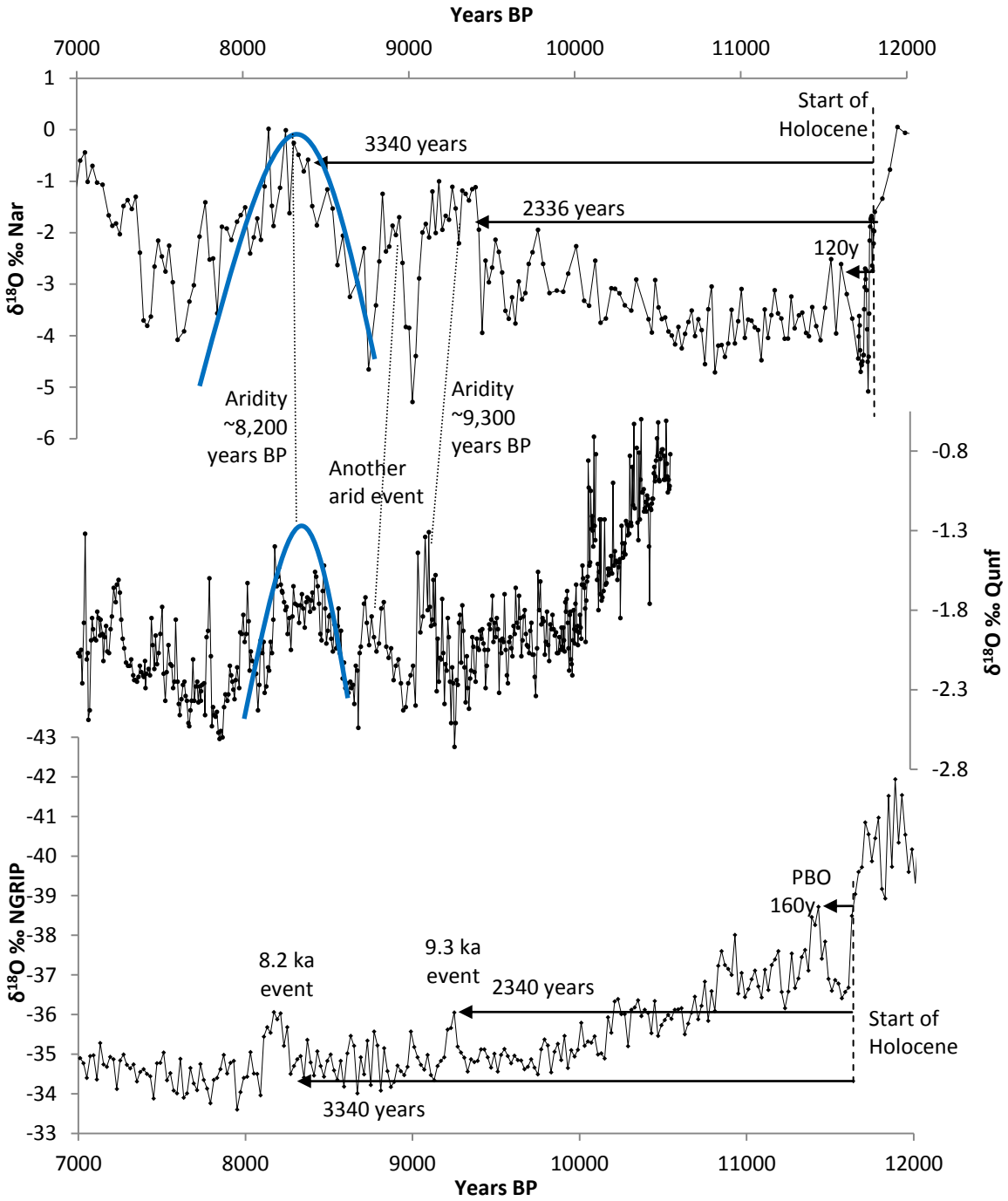

Figure 10.11 *Early Holocene $\delta^{18}O$ records from Nar Gölü, Qunf (Fleitmann et al., 2003, 2007) and NGRIP (Vinther et al., 2006, Rasmussen et al., 2006). The aridity ~9,300 years BP in Nar Gölü (and Qunf) lasts significantly longer than the cooling in NGRIP at this time and the anomaly centred ~8,200 years BP could be the peak of a longer term aridity trend, as highlighted by the blue lines.*

In terms of the 8.2 ka event, while there is a peak in aridity around this time in Nar Gölü (at 8,155 years BP based on the working chronology, or using the U-Th date error, between 8,725 and 7,585 years BP), it actually appears to be the peak of a longer term drying trend lasting ~800 years (Figure 10.11). The 8.2 ka event is seen across the Northern Hemisphere (Alley et al., 1997, Alley and Ágústsdóttir, 2005, Morrill and Jacobsen, 2005) but while in NGRIP it is defined as lasting 160 years (Thomas et al., 2007) and in other isotope records from the North Atlantic region ~150±30 years (Daley et al., 2011), away from the North Atlantic region the effects are often spread over a longer time period (Rohling and Palike, 2005, Wiersma and Renssen, 2006, Thomas et al., 2007). Also, away from the North Atlantic, the magnitude of the change is often lower. For example, the estimated temperature drop in the Balkans from a lake pollen record is 2°C (Bordon et al., 2009), 3°C in the Alboran and Aegean Seas (Dormoy et al., 2009) and 4°C in NE Greece (Pross et al., 2009, Peyron et al., 2011), compared to 6-7°C in Greenland (Alley et al., 1997, Leuenberger et al., 1999). Furthermore, other than the recently published record from Heshang Cave in China showing a drying indistinguishable in duration and evolution from the 8.2 ka event seen in Greenland (Liu et al., 2013) (Figure 10.5), anomalies outside of the North Atlantic region often span 400-600 years forming part of a longer trend since ~8,600 years BP with more sudden changes at 8,200 years BP superimposed on longer term cooling/drying trends (Rohling and Palike, 2005). Specifically, dry events are seen in records from across tropical Africa ~8,500-7,800 years BP (Gasse, 2000), the Black Sea coast of Turkey ~8,400-7,800 years BP (Gokturk et al., 2011), off the Somali coast starting at ~8,500 years BP (Jung et al., 2004, Ivanochko et al., 2005), ~8,400-8,000 years BP in an Aegean pollen record (Kotthoff et al., 2008b), ~8,600-7,900 years BP in Qunf (Fleitmann et al., 2003, 2007) and ~8,500-8,000 years BP in Soreq Cave (Bar-Matthews et al., 1997) (although this record is hampered by a low resolution of analyses at this time) (Figure 10.5). Interestingly, an arid event in between those centred on ~9,300 and 8,200 years BP is seen in both Nar Gölü and Qunf (Figure 10.11); more high resolution records are required to identify whether this is another widespread aridity event.

Slowdowns of North Atlantic thermohaline circulation due to glacial outburst floods have been suggested as the causes of the PBO (Fisher et al., 2002), 9.3 ka (Fleitmann et al., 2008, Yu et al., 2010) and 8.2 ka (Barber et al., 1999, Clarke et al., 2004, Alley and Agustsdottir, 2005, Ellison et al., 2006, Hillaire-Marcel et al., 2007, Thomas et al., 2007, Hoogakker et al., 2011, Hoffman et al., 2012) cooling events. A cooling of the North Atlantic Ocean may lead to increased aridity in the Near East for the reasons discussed in section 10.1.3. The spatial pattern seen at these events, namely a cooling in high latitudes and a drying in parts of the Northern Hemisphere tropics, is consistent with that expected following a slowdown of North Atlantic circulation (Alley and Agustsdottir, 2005, Rohling and Palike, 2005). However, whilst this could account for peak aridity in Nar Gölü at these times, it does not explain why the aridity events ~9,300 and 8,200 years BP last longer in Nar Gölü and other records outside of the North Atlantic region (Rohling and Palike, 2005) than the cooling events in NGRIP. The fact that the Nar Gölü record does not perfectly match NGRIP is not surprising given the geographical distance between the sites. Whilst changes in the North Atlantic are seen as a key driver of Near East hydroclimate in the present and past, it has been demonstrated that other teleconnections are also important, such as Indian monsoon dynamics (Jones et al., 2006, Ziv et al., 2006) and the North Sea-Caspian Pattern Index (Kutiel and Turkes, 2005, Jones et al., 2006), as discussed in section 2.1.1.

For the aridity centred on ~8,200 years BP, solar variability has been proposed as the underlying cause, with $\Delta^{14}C$ production rates showing three broad maxima (indicating solar output minima) 8,400-7,900 years BP (Muscheler et al., 2004, Muscheler et al., 2005). Marshall et al. (2011) have suggested that because the aridity trend is seen in the Northern Hemisphere tropics and sub tropics ~8,600 years BP, this could be seen to be the driver of the 8.2 ka event in the North Atlantic. Potential tropical drivers of change at higher latitudes, linked for example to methane emissions and ENSO changes, are reviewed in Barker et al. (2004). Alternatively, seasonality could be confusing the interpretation of records. For example, while in the Cariaco basin record there is a peak in aridity from a winter proxy (greyscale) 8,250-8,100 years BP (Hughen et al., 1996), proxies for summer

conditions (Fe and Ti concentrations) show a much longer anomaly 8,400-7,750 years BP (Haug et al., 2001). Additionally, the Holzmaar record from Germany is interpreted as showing there were ~75 years of cool, dry winters in the middle of a ~175 year period of summer cooling (Prasad et al., 2009). For this time period, more proxies of winter conditions are therefore required, as are more high resolution and well-dated records from around the world.

10.3.2 Mid to late Holocene

As discussed in section 10.2.1, there was a gradual trend to drier conditions in Nar Gölü that peaked ~3,000-2,000 years BP. Figure 10.12 shows this period was also punctuated by numerous centennial scale climate fluctuations. While the chronology of the Nar Gölü record for this period is not yet good enough to assign dates accurately to these events, based on the current chronology there is an arid period at the end of zone 7 (inferred from >20% dolomite content) that could be synchronous with the arid interval ~5,300-5,000 years BP seen in Soreq Cave (Bar-Matthews and Ayalon, 2011), Lake Van (Lemcke and Stürm, 1997), the Gulf of Oman (Cullen et al., 2000), Syria (Fiorentino et al., 2008), SE Arabia (Parker et al., 2006), Lake Tecer (Kuzucuoglu et al., 2011) and east Africa (Thompson et al., 2006). The period of high $\delta^{18}O_{carbonate}$ at the beginning of zone 9 may be coincident with the arid event seen from ~4,200-3,900 years BP in records from the Gulf of Oman (Cullen et al., 2000), the Indus delta (Staubwasser et al., 2003), the Red Sea (Arz et al., 2006), NW Turkey (Ulgen et al., 2012), the Nile Delta (Bernhardt et al., 2012), Eski Acıgöl (Roberts et al., 2001), Gölhisar Gölü (Eastwood et al., 2007), Lake Tecer (Kuzucuoglu et al., 2011) and the Dead Sea (Migowski et al., 2006, Stein et al., 2010, Litt et al., 2012). It is difficult to compare the magnitude of this arid event to the one centred ~5,200 years BP because the high levels of dolomite meant $\delta^{18}O_{carbonate}$ data could not be produced for the latter. However, the fact that ~5,200 years BP there was >20% dolomite whereas ~4,200 years BP there was <20% dolomite in itself suggests the former may have been more arid, and indeed in Soreq Cave the former drought period was more extreme (Bar-Matthews and Ayalon, 2011). There is also >20% dolomite in Nar Gölü ~3,100 years BP in the middle of zone 9, apparently at the same time as a dry event

at Eski Acıgöl (Roberts et al., 2001), the Sea of Galilee (Langgut et al., 2013), Lake Zeribar (Stevens et al., 2001), the Eastern Mediterranean Sea (Emeis et al., 2000, Schilman et al., 2001), the Dead Sea (Migowski et al., 2006, Stein et al., 2010, Litt et al., 2012), Jeita Cave (Verheyden et al., 2008) and at Lake Tecer (Kuzucuoglu et al., 2011). This may be the driest time of the Holocene at Nar Gölü; as with the drought ~5,200 years BP there is >20% dolomite, but at this time $\delta^{18}O_{carbonate}$ data either side of the gap in the isotope record are higher and sediments are non-laminated.

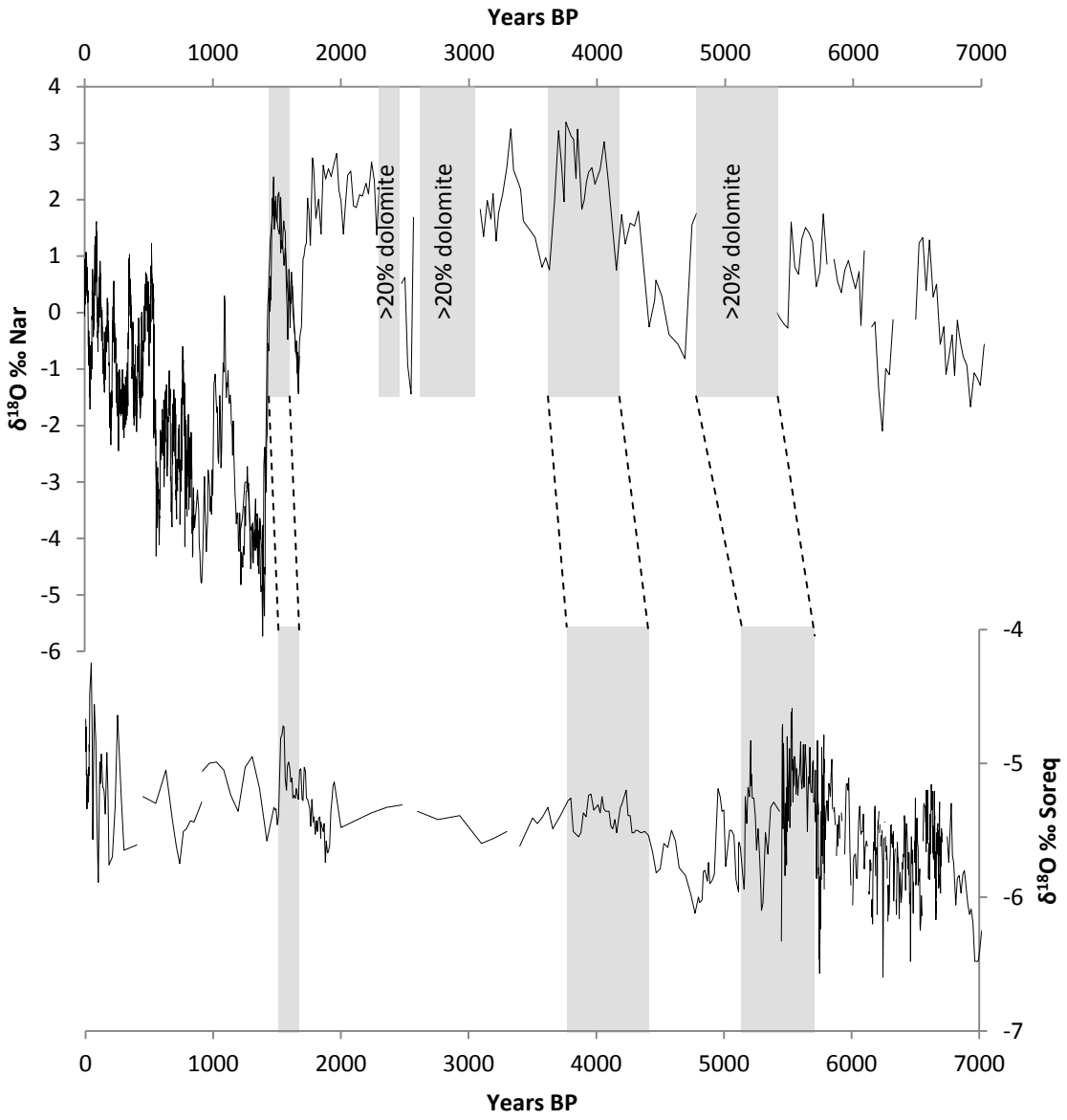

Figure 10.12 *Close up on the mid and late Holocene, compared to the Soreq Cave record (Bar-Matthews et al., 1997, Orland et al., 2009, Bar-Matthews and Ayalon, 2011).*

Again, as with changes in the late glacial (section 10.1.3) and early Holocene (section 10.3.1), it appears that when the North Atlantic is cooler, the Near East is drier. The increases in aridity ~4,200 and 3,100 years BP occur at the same time as cooling events in the North Atlantic: Bond events 3 and 2 (Bond et al., 1997). Unlike in the early Holocene, when large inputs of freshwater from the melting Laurentide ice sheet are hypothesised to have caused North Atlantic coolings known as the PBO, 9.3 ka and 8.2 ka events (Bond events 8, 6 and 5), Bond events 3 and 2 must have been caused by another underlying factor because there were no large freshwater outbursts at this time (Bond et al., 2001). Whilst it is beyond the scope of this thesis to investigate this, the identification of cyclicity in records can assist in the analysis of the drivers of climate, so spectral analysis was performed on the data using the PAST program (Hammer et al., 2001). Only the period from the start of the Holocene to the bottom of the NAR01/02 section was chosen for analysis because the chronology is less secure in the late glacial and the resolution of the record was significantly higher in the NAR01/02 sections. The insolation trend was removed by fitting a third order polynomial through the data before analysis. Ignoring the ~3,000 year cycle because it is over a third of the length of the record being analysed, the two major cycles picked up are at ~1,500 and ~900 years (Figure 10.13). A ~1,500 year periodicity was identified in the flux of ice-rafted debris in North Atlantic ocean cores (Bond et al., 1997) and subsequently in many other records from around the world as reviewed in Wanner et al. (2008), including in the Eski Acıgöl microcharcoal record (Turner et al., 2008) where fire frequency and magnitude increased at times the $\delta^{18}O$ record suggested it was wet and in the Soreq Cave record (Bar-Matthews and Ayalon, 2011). The cycle was hypothesised to be linked to solar variability (Bond et al., 2001), although Debret et al. (2007) argue that the origin of the cycles is yet to be determined. The other most significant cycle is ~900 years, and similar periodicities are seen in Greenland temperatures (Schulz and Paul, 2002), in turbidite records from off west Africa (Zuhlsdorff et al., 2008) and in a forest vegetation record from the western Mediterranean (Fletcher et al., 2013). These too have been linked to solar variability (Debret et al., 2007). Two other cycles, at 1,032 and 1,197 years, are significant at the 0.01 level. Once a firmer chronology is established, it will be possible to draw firmer conclusions.

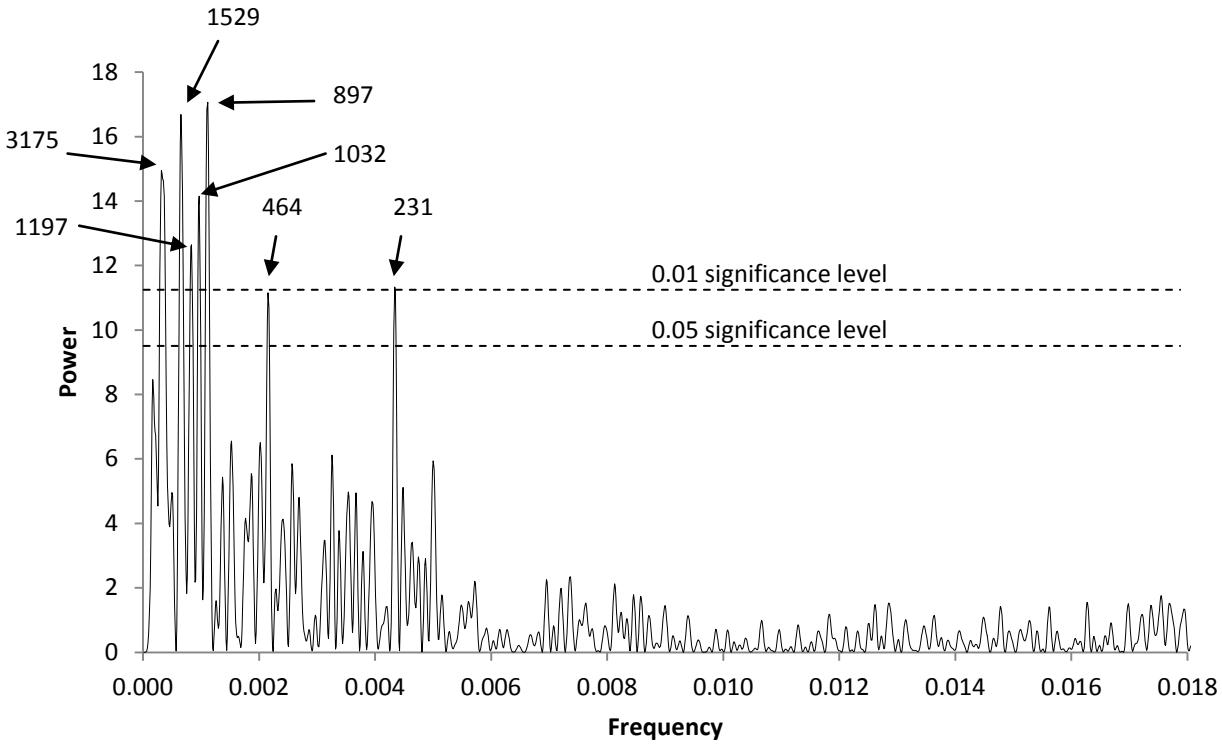

Figure 10.13 *Spectral analysis conducted on $\delta^{18}O_{carbonate}$ data using PAST program, with the 3,175 year peak rejected because the isotope record is too short to pick this up, leaving the two major peaks at 1,529 years and 897 years.*

10.3.3 Summary

Whilst there are aridity peaks in Nar Gölü at the same times as the PBO, 9.3 ka and 8.2 ka event coolings seen in the North Atlantic region, the aridity in Nar Gölü around the time of the latter two events lasted longer, as is also apparent in Qunf (Fleitmann et al., 2003, 2007) and Dongge (Dykoski et al., 2005). In particular, the drying ~8,200 years BP starts several centuries before the cooling in the North Atlantic and it is likely that the aridity trend was initially caused by another factor. However, the fact that the peaks in aridity occurred around the times of the PBO, 9.3 ka and 8.2 ka events perhaps suggests changes in North Atlantic circulation did still have significant impacts on Near East hydroclimate, exacerbating the underlying aridity trend. Furthermore, aridity at Nar Gölü ~4,200 and 3,100 years BP also occurs at around the time of North Atlantic cold periods (Bond events 3 and 2) (Bond et al., 1997). So, as

in the late glacial, it appears that in the Holocene the Near East became drier when the North Atlantic cooled.

10.4 The large shift in the 6th century AD

Figure 10.14, which shows a part of the record which is securely dated by varve counting from the top of the core (section 9.2), shows the large transition in the 6th century AD in detail. The shift to more negative $\delta^{18}O_{carbonate}$ occurs 1,475-1,402 years BP and the period of low values lasts until ~550 years BP at the end of zone 10, interrupted by a temporary rise to higher values peaking ~1,090 years BP. This large shift had already been seen in Jones et al. (2006), but it is only now that the NAR10 record has been produced that this shift can be put into a long term context. Other than the multi-millennial Mid Holocene Transition, it is the largest $\delta^{18}O$ shift seen in the entire record, larger than the Younger Dryas to Holocene transition. Increased wetness is inferred around the 6th century AD in Soreq Cave (Orland et al., 2009) (Figure 10.15), Lake Tecer (Kuzucuoglu et al., 2011), the Eastern Mediterranean Sea (Schilman et al., 2001) and the Dead Sea (Neumann et al., 2007) and Bond Event 1 is dated to ~1,400 years BP (Bond et al., 1997). Moreover, there seems to be a shift in the intensity of the Asian monsoons around the time of the shift in Nar Gölü. While in the mid Holocene there is a gradual drying trend seen in Nar Gölü, Qunf and Dongge (Figure 10.15), after 1,500 years BP there is a gradual wetting trend in Qunf and Dongge and a gradual drying trend in Nar Gölü.

Whilst there are these indications of climate changes from many records at this time, only in Nar Gölü is the shift of such a high magnitude, dwarfing the Younger Dryas to Holocene transition. So whilst it was not one of the original aims of the thesis to investigate this period, it has emerged as one of the most intriguing periods of the record. It could be that there was a climate shift that affected central Turkey more than other parts of the Near East, or that the Nar Gölü system was more sensitive to change than at other times, or a combination of these two factors.

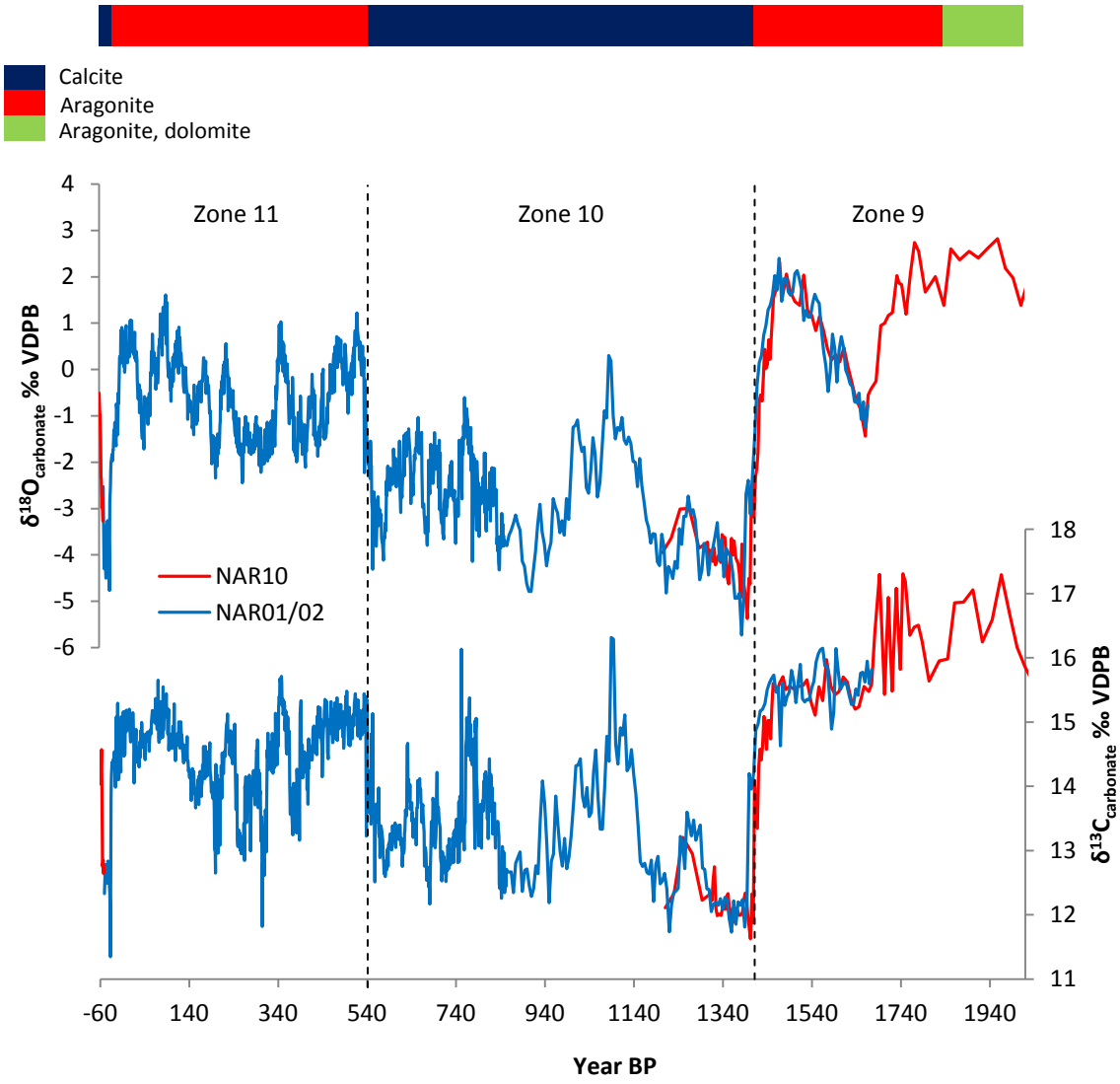

Figure 10.14 *Combination of NAR10 and NAR01/02 (Jones et al., 2006) records, plotted against years BP (where -60 = AD 2010).*

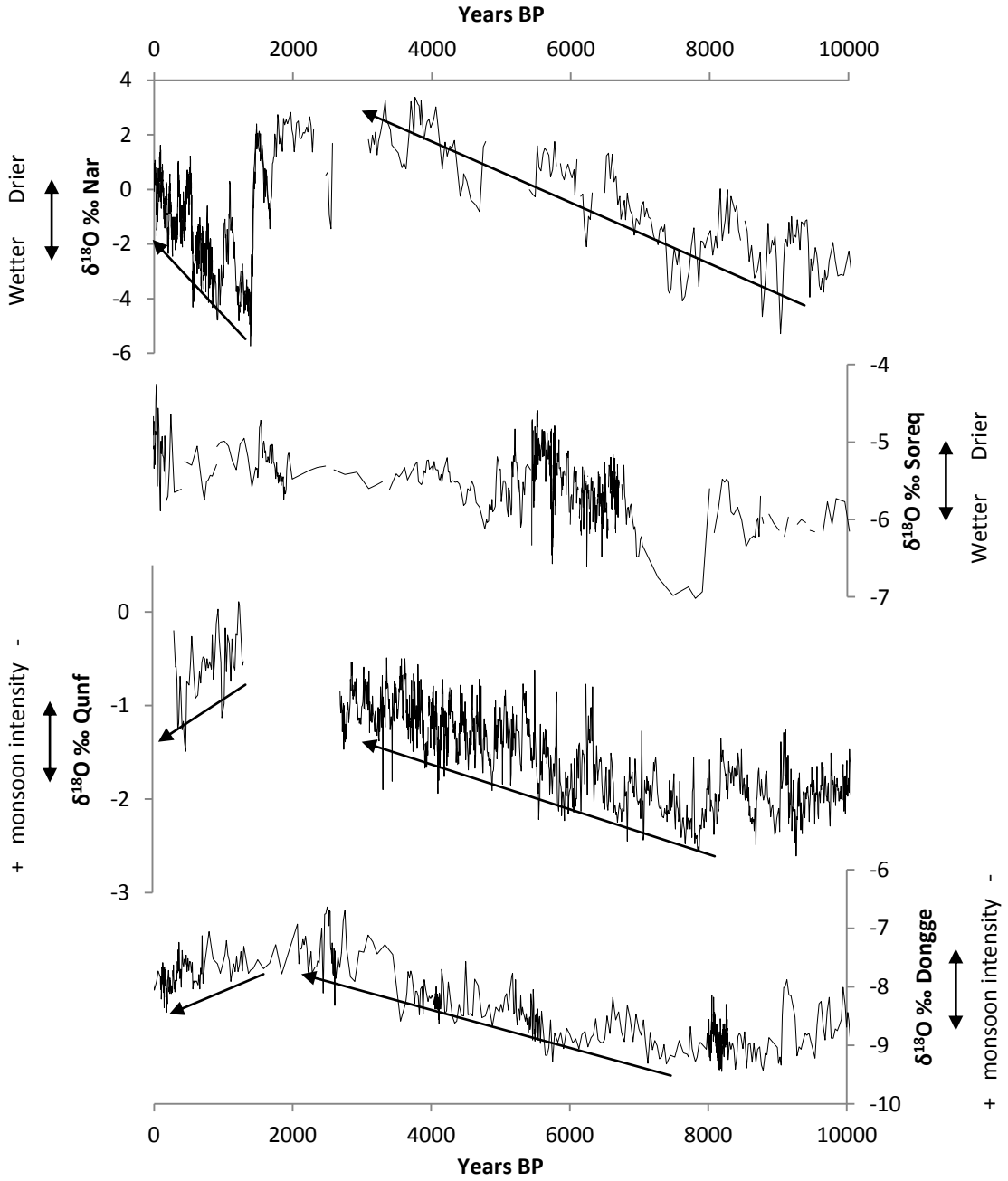

Figure 10.15 *Holocene $\delta^{18}O$ records from Nar Gölü, Soreq Cave (Bar-Matthews et al., 1997, Orland et al., 2009, Bar-Matthews and Ayalon, 2011), Qunf (Fleitmann et al., 2003, 2007) and Dongge (Dykoski et al., 2005).*

On the latter point, increased human disturbance of the catchment over the last ~3,000 years, seen from the Ti record (Allcock, 2013) (Figure 8.7), could have meant catchment deforestation, and with fewer trees there would have been less interception of precipitation. Therefore, whilst there may well have been an increase

in precipitation in central Turkey 1,475-1,402 years BP, its impact may have been enhanced by increased run-off into the lake. Increased sensitivity of the lake is supported by data from the last few decades, with a rise in $\delta^{18}O_{carbonate}$ (with no change in mineralogy) of 4.3‰ over the past 25 years, which is nearly as large as the Younger Dryas to Holocene shift. This suggests that in the present, for a given change in lake depth, there is a larger shift in $\delta^{18}O_{carbonate}$ than at times in the past. If the lake was more sensitive at the time of the 6th century AD transition as well, that could explain why it was of such high magnitude.

Another explanation that could help account for the magnitude of the $\delta^{18}O_{carbonate}$ shift is a change in the seasonality and type of precipitation. A comparison with $\delta^{18}O_{diatom}$ is used to investigate this further. As discussed in section 8.2.4, the low $\delta^{18}O_{diatom}$ values and the large shifts are not considered to be due to temperature, contamination or species assemblage shifts. The other potentially significant variable driving $\delta^{18}O_{diatom}$ is $\delta^{18}O_{lakewater}$, which could be driven by changes in the source of precipitation, $\delta^{18}O_{source}$, the type of precipitation and water balance. There is not thought to have been a shift in the source of precipitation at this time in the region and $\delta^{18}O_{source}$ is not likely to have changed so much, so fast, in this part of the Holocene. Where $\delta^{18}O_{carbonate}$ and $\delta^{18}O_{diatom}$ and estimated $\delta^{18}O_{lakewater}$ from the two hosts follow similar trends, they are likely both responding to water balance, with the small differences in $\Delta\delta^{18}O_{lakewater}$ just the result of intra-annual differences in $\delta^{18}O_{lakewater}$ and differences in the time of year of diatom growth and carbonate precipitation. However, around the 6th century AD transition, $\Delta\delta^{18}O_{lakewater}$ increases to values of ~7-15‰ because $\delta^{18}O_{lakewater}$ at the time of diatom growth decreases to a much greater degree than $\delta^{18}O_{lakewater}$ at the time of carbonate precipitation. $\delta^{18}O_{lakewater}$ values estimated for the time of diatom growth of ~–15‰ are the lowest for the record, suggesting unique conditions in the lake at this time. Changes in the type of precipitation could account for such low values. As discussed in sections 7.2.1 and 10.1.1, snow $\delta^{18}O$ is significantly lower than rain $\delta^{18}O$. Normally in closed lakes, changes in the type of precipitation would be expected to be far outweighed by evaporative effects (Leng and Marshall, 2004). However, large inputs of low $\delta^{18}O$ water may not immediately mix with the rest of the lake water. Large amounts of

spring snowmelt could form a freshwater lid on the lake surface because of the density contrast with the underlying saline waters, and if the majority of diatom growth occurred in this freshwater lid, and if by the time of carbonate precipitation it had mixed with the rest of the lake water, there could have been large differences in the $\delta^{18}O$ of the surface lakewaters in which the two hosts formed.

The freshwater lid hypothesis is complicated and difficult to test, with a threshold required above which there is sufficient snowmelt to form a freshwater lid. However, there is some support for increased snowfall at this time from archival sources, with the people of Cappadocia in the first half of the first millennium AD describing as "reeking of snow" and roads being impassable until Easter (Van Dam, 2002). Significant snowfalls were reported across Anatolia at this time (Stathakopoulos, 2004). From 1935-2010 AD, Niğde (45 km from Nar Gölü) saw on average only 33 snowy days per year, perhaps explaining why a significant freshwater lid does not seem to have formed over the past few decades, with $\Delta\delta^{18}O$ closer to zero. Even if this freshwater lid had disappeared by the time of carbonate precipitation, the lakewater as a whole would have been isotopically more depleted than at times when there was less snowfall, so $\delta^{18}O_{carbonate}$ would have been lowered.

However, even if the sensitivity of the system and increased snowfall exaggerated the magnitude of the $\delta^{18}O_{carbonate}$ transition in relation to, for example, the Younger Dryas to Holocene transition, there must have been a shift to wetter conditions to evoke the response in $\delta^{18}O_{carbonate}$ and the other proxies in the first place. Therefore, in summary, based on multi-proxy analysis, the transition in the 6th century AD seen in Nar Gölü is likely due to a rapid shift to more positive water balance. A shift to wetter conditions is seen in other records from Turkey and the wider Near East at this time, although it is unclear whether the shift was as high magnitude elsewhere as it was at Nar Gölü.

10.5 Examining potential links with the archaeological record

As discussed in sections 1.1 and 2.2.3, since the Near East is arguably the key region in the development of human civilisation and connections between climate and society has previously been postulated, the links between the climate record presented in this thesis and the archaeological record need to be examined.

10.5.1 The origins of agriculture

Present knowledge suggests that whilst there may have been some cultivation of wild grains in the Near East in the Bølling-Allerød and Younger Dryas, it was not until the early Holocene that they became a major means of subsistence (e.g. Willcox et al., 2009, Zeder, 2011). By 10,500-10,000 years BP, there is evidence of domesticated plants at Asikli Höyük (20 km west of Nar Gölü), Tell Aswad near modern day Damascus and 'Ain Ghazal in Jordan (Figure 10.16) (Zohary et al., 2012). A wetting and warming in the early Holocene is seen by some to have supported the development of farming (Gupta, 2004, Bellwood, 2005, Willcox et al., 2009) and a major population expansion (Migowski et al., 2006, Weninger et al., 2009, Maher et al., 2011). The new data from Nar Gölü, with zone 4 (11,700 to 9,400 years BP) showing a sustained period of low $\delta^{18}O$ values, interpreted as indicating wet conditions (Figures 10.3 and 10.18), are particularly important in supporting the findings of these previous studies. Nar Gölü is now the closest climate archive to the important archaeological site of Asikli Höyük and it is vital to have climate records from close to archaeological sites if links between the two are to be made (Jones, 2013). Increased wetness (i.e. more precipitation, less evaporation) would clearly have assisted in the development of agriculture, as it would have meant that there was less water stress. Even in the present day, which seems to be wetter than zone 9 in the late Holocene, central Turkish agriculture is dependent upon irrigation, so in the Younger Dryas, for example, when precipitation was likely to have been lower (section 10.1), rain-fed agriculture by less technologically advanced peoples would have been very difficult.

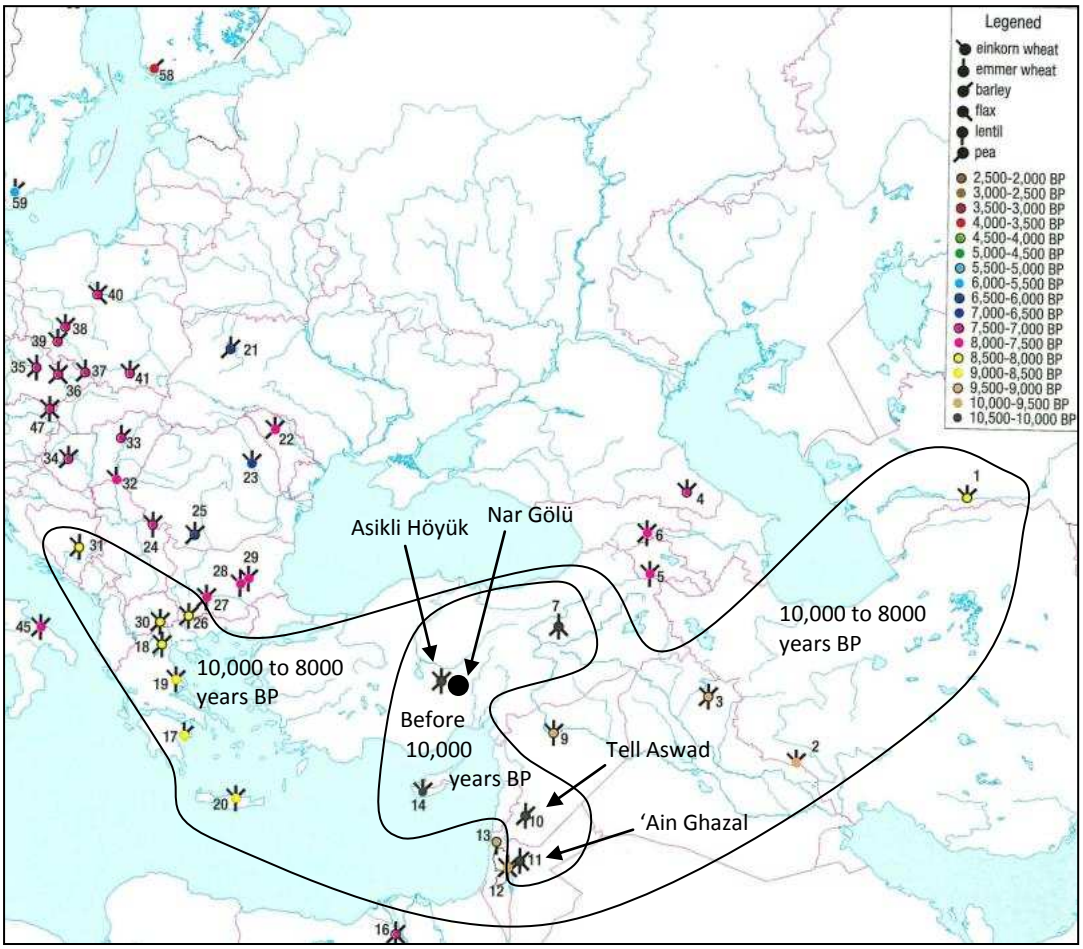

Figure 10.16 *Evidence of cultivation from archaeological sites (Zohary et al., 2012), showing that cereal agriculture first developed in modern day Jordan, Syria and central Turkey at Asikli Höyük close to Nar Gölü.*

It has been hypothesised that the stability of hydroclimate, as well as overall wetness, may have been important (Bellwood, 2005, Willcox et al., 2009), but this could not previously be confirmed as there were no high resolution climate records from the Near East that allowed climate variability to be investigated. The importance of reconstructing the variability of climate is increasingly being recognised, as it is harder for societies to adapt to an increase in variability/extreme conditions than to a change in the average climate state (Hanson et al., 2012, Huntingford et al., 2013). With the Nar Gölü record, it is possible to show for the first time that the earliest Holocene had a more stable hydroclimate than other periods: zone 4 (11,700 to 9,400 years BP) has the lowest standard deviation of $\delta^{18}O_{carbonate}$ of

any zone (Table 8.1), and Ca/Sr ITRAX data (used as a water balance proxy) were also less variable in this part of the core sequence than in the late Holocene (Allcock, 2013). Combined with increased wetness, increased stability of climate is likely to have assisted in the development of agriculture: it would clearly have been easier to domesticate, experiment and grow crops if the hydroclimate did not change from year to year and if early farmers did not have to continuously adapt to variability by changing the time of year they planted crops or the types of crops they grew. Additionally, as discussed in section 10.2.2, it appears there was less of a marked seasonality of precipitation in zone 4 compared to zone 9, and reduced seasonality would also have made it easier for rain-fed agriculture to develop (Feng et al., 2013).

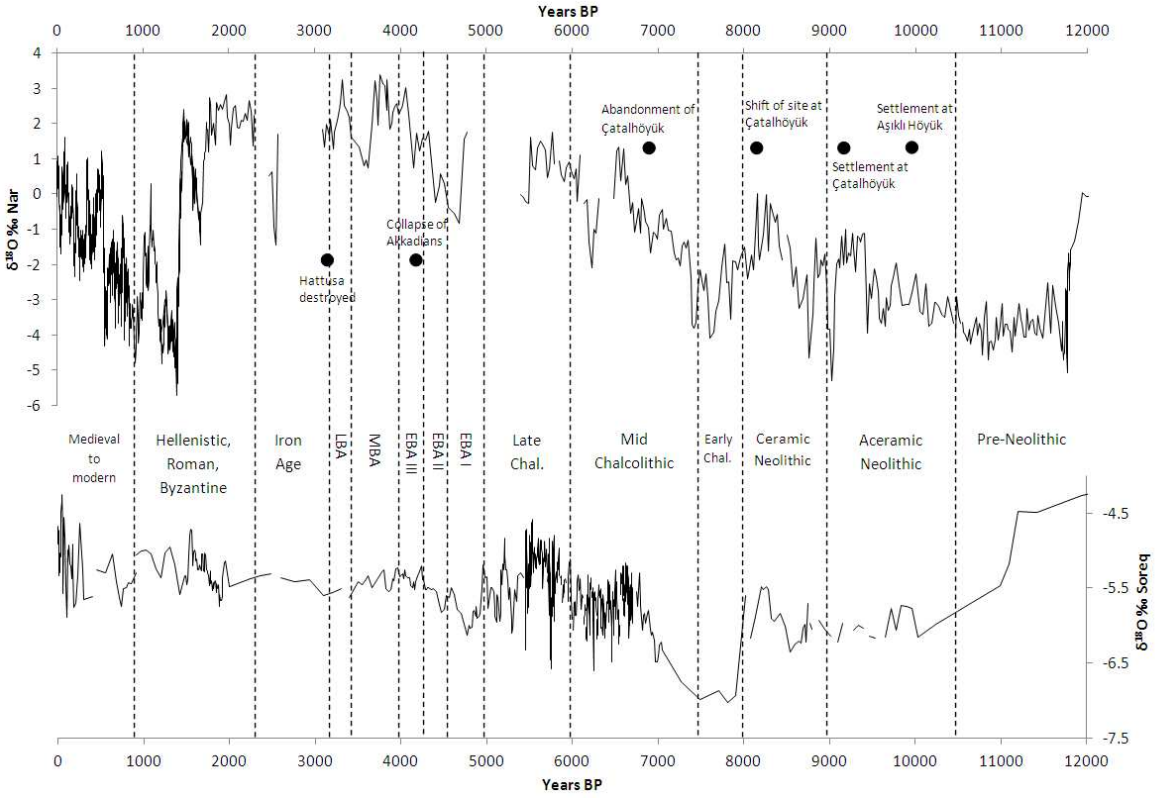

Figure 10.17 *Nar Gölü and Soreq Cave (Bar-Matthews et al., 1997, Orland et al., 2009, Bar-Matthews and Ayalon, 2011) $\delta^{18}O$ data plotted with Turkish archaeological periods separated by the dashed lines (Allcock, 2013 and references therein) (EBA = Early Bronze Age, MBA = Mid Bronze Age and LBA = Late Bronze Age) and major events in Turkish human history (see text for references).*

10.5.2 Societal change ~8,200 years BP

The aridity peak in Nar Gölü centred on ~8,200 years BP (Figure 10.17) and an increase in the variability of climate in zone 5 compared to the earliest Holocene (Table 8.1) coincides with major societal change in the Near East. ~8,200 years BP, the settlement of Çatalhöyük (160 km SW of Nar Gölü) moved, at a time when geoarchaeological investigations suggest river flooding stopped (Roberts and Rosen, 2009). Across the Eastern Mediterranean, from Greece, Sardinia and southern Italy (Berger and Guilaine, 2009), to Cyprus (Weninger et al., 2006), the Sahara (Fagan, 2004, Burroughs, 2005, Gonzalez-Samperiz et al., 2009) and Jericho (Migowski et al., 2006), there was an abandonment of settlements. Based on DNA studies, it has been shown that ~8,200 years BP many early farmers left Anatolia and settled in SE Europe, spreading agriculture to mainland Europe for the first time (Weninger et al., 2006, Berger and Guilaine, 2009, Bramanti et al., 2009, Haak et al., 2010, Zohary et al., 2012) (Figure 10.16). Weninger et al. (2006) suggested that aridity may have forced this migration and it can be seen from Figure 10.17 that there was a peak in aridity ~8,200 years BP in both the Nar Gölü and Soreq Cave records. Combined with an increase in the variability of climate, this would have made agriculture more difficult and could have pushed communities into Europe in search of more hospitable farmland.

10.5.3 Civilisation 'collapses' in the mid and late Holocene

Whilst the chronology of the mid and late Holocene part of the sequence is less secure than the early Holocene, based on the current chronology there do appear to be arid events at Nar Gölü at the times of the three major arid events seen in other records from the region, at ~5,200, 4,200 and 3,100 years BP, which occur at the times of major transitions in the archaeological record (the end of the Late Chalcolithic, of the Early Bronze Age and of the Late Bronze Age) (Figure 10.17). The drought ~5,200 years BP occurred at the same time as the 'collapse' of the late Uruk period society in Mesopotamia (Weiss, 2003). Aridity ~4,200 years BP has been linked with the decline of the Old Kingdom of Egypt (Stanley et al., 2003) and the

Harappan civilisation in the Indus valley (Possehl, 1997, Staubwasser et al., 2003), as well as the Akkadian civilisation ~4,110 years BP (Weiss, 1993). The Akkadians depended on rain-fed agriculture on the northern Mesopotamian plain (Cullen et al., 2000), so a decrease in precipitation could have made farming unsustainable. As discussed in section 10.3.2, the most arid period in the Nar Gölü record in the Holocene is likely to have been ~3,100 years BP, which within dating error coincides with the 'Bronze Age Collapse'. The Hittite civilisation in Anatolia saw significant change at this time, with their capital Hattusa destroyed ~3,180 years BP (Weiss, 1982) (Figure 10.17). Hittite texts referred to drought before their 'collapse' (Akurgal, 2001). At this time there were also crop failures in Syria (Kaniewski et al., 2010) and Egypt suffered its 3rd Intermediate Period (Dodson, 2001). The invasion of the 'sea peoples' (an unidentified group of people) had previously been blamed for societal change at this time, however this population movement could have itself been caused by the climate change (Burroughs, 2005, Gallet et al., 2006).

So whilst the poor chronology of Nar Gölü record at this time precludes robust investigation of the synchronicity of droughts and civilisation 'collapses', in general the period from 4,200 to 1,500 years BP (zone 9) had high $\delta^{18}O_{carbonate}$ values, non-laminated sediments and aragonite/dolomite so is likely to have been substantially drier than central Turkey today and in the early Holocene. Agriculture in central Turkey is presently dependent on irrigation, so if it was drier in zone 9 of the late Holocene and yet people were less technologically advanced, then agriculture would have been even more difficult for that period as a whole. Rapid, short-term fluctuations may have more of a significant impact on societies that are already weakened by longer-term climate change (Parry, 1978), so the rapid increases in aridity seen ~5,200, 4,200 and 3,100 years BP could have pushed civilisations, especially those that failed or refused to adapt (Roberts et al., 2004, Rosen, 2007), over the edge. The more variable climate in the mid to late Holocene compared to zone 4 in the earliest Holocene, seen from the increased standard deviation values of $\delta^{18}O_{carbonate}$ (Table 8.1) and again also in increased Ca/Sr variability (Allcock, 2013), would also have made it more difficult to farm (Sandweiss and Quilter, 2012).

10.5.4 Summary

It is for archaeologists to attempt to establish whether or not climate changes could have been important in the development and decline of civilisations, and it is likely that climate would not have been the sole cause of societal shifts (e.g. Coombes and Barber, 2005). However, in this section it has been shown that there could potentially be climatic explanations for societal change. In the early Holocene when people were first domesticating plants and establishing farming communities, the hydroclimate was substantially wetter and more stable than most of the mid and late Holocene, which would probably have made it easier for people to farm. ~8,200 years BP, arid conditions are inferred at the time of change at the major settlement of Çatalhöyük and a major population movement from Anatolia into Europe. In the late Holocene, the climate was highly variable and arid, with droughts potentially coinciding with major transitions in the archaeological record.

10.6 Overall summary

In this chapter, the working chronology has allowed the interpretations of chapter 8 to be built upon by enabling temperature and $\delta^{18}O_{source}$ data from other records to be used in order to attempt to model the drivers of $\delta^{18}O_{carbonate}$ in Nar Gölü. Water balance was shown to be its key driver, supporting the interpretations made in chapters 7 and 8. It was then possible to compare to other records, initially from the Near East to investigate how widespread changes were across the region, and then from further afield in an attempt to establish the key drivers of Near East hydroclimate through the late glacial and early Holocene. Potential links between climate and societal change were also considered. The major palaeoclimate implications of this thesis are summarised in section 11.2.

Chapter 11 | Conclusions

Using U-Th and varve counting to provide a working chronology and the highest resolution (average <25 years) $\delta^{18}O_{carbonate}$ record from the Near East to date, for the first time it has been possible to investigate in detail the Younger Dryas to Holocene transition in central Turkey as well as centennial scale changes in the early Holocene. Unique insights into palaeoseasonality have been provided by combining $\delta^{18}O_{carbonate}$ and $\delta^{18}O_{diatom}$ data.

11.1 Methodological implications

The isotope record derived from the NAR10 sequence could only be reliably interpreted after a significant amount of limnological monitoring. While Nar Gölü is a closed lake in a semi-arid region and $\delta^{18}O_{carbonate}$ is therefore likely to be a proxy for water balance, monitoring of the lake was still vital (chapter 7). Firstly, comparison of changes in lake depth to $\delta^{18}O_{lakewater}$ to sediment core $\delta^{18}O_{carbonate}$ confirmed this assumption. Secondly, comparison of $\delta^{18}O_{lakewater}$ to sediment trap $\delta^{18}O_{carbonate}$ to sediment core $\delta^{18}O_{carbonate}$ data showed that carbonate was precipitating in equilibrium and that the signal was not altered by diagenesis. Thirdly, it was shown that diatom growth likely occurs earlier in the year than carbonate precipitation so theoretically differences in $\delta^{18}O$ between the two hosts could be used to investigate palaeoseasonality.

In the analysis of core material, there were three main issues that needed to be overcome. Firstly, because its mineral-water fractionation factor is not well constrained and it forms under different conditions to endogenic calcite and aragonite, the presence of dolomite in parts of the sequence had to be dealt with using a quick reaction (section 6.3.4). It is argued that the investigation of carbonate mineralogy is absolutely vital when working with carbonate isotopes and studies that interpret the latter without consideration of the former will be limited in their reliability. Secondly, building on the work of other researchers, the method of mass

balance correcting diatom isotope data was refined, for example showing the importance of determining the $\delta^{18}O$ of contamination and the potential for down-core variability. Thirdly, it has once again been demonstrated that U-Th dating of lacustrine sediments is complicated, but it has been suggested which types of sediments are more likely to be successful than others.

It was confirmed using $\delta^{18}O$-$\delta^{13}C$ co-variance, modelling to account for the influences of factors such as temperature and $\delta^{18}O_{source}$ on $\delta^{18}O_{carbonate}$, and $\delta^{18}O_{diatom}$ data to investigate palaeoseasonality, that the major driver of $\delta^{18}O_{carbonate}$ in the past in Nar Gölü was water balance, as has been the case in the recent past. The combination of $\delta^{18}O_{carbonate}$ and $\delta^{18}O_{diatom}$ data in order to reconstruct seasonality has been done before, but Dean et al. (2013) and the work presented here are the first times that there has been a thorough consideration of the effect of contamination on $\delta^{18}O_{diatom}$ and extensive limnological monitoring to establish the drivers of $\delta^{18}O$ and the times of year of carbonate precipitation and diatom growth.

11.2 Implications for Near East palaeoclimatology

Previously, a lack of high resolution and well-dated records from the Near East has hampered attempts to compare the Younger Dryas to Holocene transition in the Near East to the rapid shifts seen in the North Atlantic. Here, it has been possible to estimate that the transition occurred in central Turkey in <200 years (the majority of it in just 9 years), a rapidity much more similar to North Atlantic region records than to records from further east in the Northern Hemisphere (section 10.1). Likewise, the Bølling-Allerød to Younger Dryas transition in Nar Gölü seems to have been of a similar rapidity to that seen in the North Atlantic. The earliest Holocene in central Turkey saw very stable hydroclimate conditions. There seems to be a drying in central Turkey at the same time as the three key early Holocene coolings seen in Greenland (the PBO, 9.3 ka and 8.2 ka events) (section 10.3). However, the drying events are not short, discrete events as in Greenland. In particular, aridity ~9,300 years BP lasts ~340 varve years in Nar Gölü compared to ~100 years in North Atlantic region records and while there is a peak of aridity ~8,200 years BP in Nar Gölü at the

time of the 8.2 ka event, it appears to be part of much longer term drying trend starting ~8,600 years BP and ending ~7,800 years BP. Other records from outside of the North Atlantic have found similar, multi-centennial scale anomalies.

The Mid Holocene Transition to drier conditions occurred in two phases ~7,400-6,500 and ~4,700-4,000 years BP (although the exact timing is unknown due to the chronological uncertainties in this part of the record). Peak Holocene aridity is reached ~3,000-2,000 years BP (section 10.2). Although gaps in the isotope record ~5,000 and 3,000 years BP due to high dolomite mean that the isotope record is incomplete, the very fact that there were high levels of dolomite forming at this time is taken to indicate aridity. The $\delta^{18}O_{carbonate}$ transition in the 6th century AD, interpreted as a rapid and high magnitude shift to wetter conditions, is larger than the Younger Dryas to Holocene transition in Nar Gölü, but unlike the latter such a large climate shift is not seen elsewhere in the world at this time (section 10.4).

The interpretation of the Younger Dryas as being drier than the early Holocene at Nar Gölü supports the interpretation of most records from the region, for example from Eski Acıgöl (Roberts et al., 2001, Jones et al., 2007), Lake Van (Lemcke and Stürm, 1997), Lake Zeribar (Stevens et al., 2001) and Soreq Cave (Bar-Matthews et al., 1997). It also appears to show an increase in aridity from the early to late Holocene, again supporting the interpretation of many records, for example Eski Acıgöl (Roberts et al., 2001, Jones et al., 2007), Lake Van (Lemcke and Stürm, 1997), Soreq Cave (Bar-Matthews et al., 1997) and Gölhisar Gölü (Eastwood et al., 2007). However, the Dead Sea pollen and sedimentological records are interpreted as showing the Younger Dryas was wetter than the early Holocene and that the early Holocene was drier than the late Holocene (Stein et al., 2010, Litt et al., 2012). Some researchers had suggested that the Soreq Cave $\delta^{18}O$ record was being misinterpreted as a water balance signal whereas actually it was recording changes in $\delta^{18}O_{source}$. The demonstration that water balance is the key influence on $\delta^{18}O_{carbonate}$ in Nar Gölü, the fact the $\delta^{18}O$ trends of Nar Gölü and Soreq Cave are so similar, and the fact other proxy records from Israel also suggest a transition from wet to dry in the Holocene, seems to support the arguments that the Soreq record may be recording water

balance. The interpretation of the $\delta^{18}O$ records from Lakes Zeribar and Mirabad in terms of the seasonality of precipitation (Stevens et al., 2001, Stevens et al., 2006), partly due to the interpretation of the pollen records, is also called into question in this thesis, supporting the assertion of Jones and Roberts (2008) that the key driver of Near East lake isotope records in the Holocene was water balance. This again highlights the discrepancy between the interpretation of the pollen records from the Dead Sea (Litt et al., 2012) and Iran (van Zeist and Bottema, 1977, Bottema, 1986) and the isotope records. It has been shown here, using a multi-proxy approach and a very careful consideration of the drivers of $\delta^{18}O_{carbonate}$, that there was almost certainly a shift from a wet early Holocene to a dry late Holocene, at least at Nar Gölü. The differences between the pollen and isotope records at Nar Gölü were discussed in section 8.2.5: whilst there is an increase in the percentage of arboreal pollen at the beginning of the Holocene, the increase is much slower than the decrease in $\delta^{18}O_{carbonate}$ and does not reach a maximum until ~5,700 years BP. Therefore, palynologists working in the Near East need to take into consideration the limitations of pollen and why it may not be responding to climate (Roberts et al., 2011a, Roberts, in press), as well as considering the limitations of isotope records.

The fact that Nar Gölü is drier when the North Atlantic is colder (during the Younger Dryas, around the times of the PBO, 8.2 ka and 9.3 ka events and ~4,200 and 3,100 years BP) and wetter when the North Atlantic is warmer is taken to suggest changes in the North Atlantic have been a key driver of Near East hydroclimate, as is the case in the present day and discussed in section 10.1.3. The similarity in the rapidity of the Bølling-Allerød to Younger Dryas and Younger Dryas to Holocene transitions between Nar Gölü and North Atlantic region records highlights the strength of the teleconnection. However, particularly during the Holocene, other factors must have been important as well. Unlike in the North Atlantic where the last high magnitude shift was the Younger Dryas to Holocene transition, in the Nar Gölü record, as in records from Africa and of the Asian monsoons, there was a major shift during the mid Holocene: an increase in aridity linked to declining summer insolation. Also, the fact that the aridity trends at Nar Gölü at the times of the 9.3 ka and 8.2 ka events

last longer than in the North Atlantic region suggests additional processes such as the Indian monsoon were having an influence on Near East hydroclimate.

Potential links between climate and societal change have also been considered. In this regard, perhaps the most significant finding from this thesis is what the hydroclimate of central Turkey was like at the time agriculture developed. Whilst other studies had shown that the Near East was wetter in the early Holocene than now, because of the lack of high resolution records it was not possible to investigate the stability of climate. Here, it was possible to show that for over two millennia at the start of the Holocene, when agriculture developed and spread to sites such as Asikli Höyük near to Nar Gölü by 10,000 years BP, the climate was wet and stable. These favourable climate conditions would have made it easier for people to cultivate crops and may explain why agriculture developed at this time. A more variable and arid climate is found from 9,400 years BP until the end of the early Holocene, which could potentially have helped initiate the migration of Near East farmers to Europe. At the moment, the chronology for the mid to late Holocene during peak aridity is not sufficiently constrained to allow for a correlation of decadal and centennial scale climate changes to shifts in the archaeological records. However, three major dry periods, centred on ~5,200, 4,200 and 3,100 years BP, may coincide with major transitions in the archaeological record.

11.3 Future work

Results from this thesis are contributing to work led by other members of the Nar Gölü team including high resolution analysis on the 6th century AD transition period and potential links to the spread of the Justinian Plague, and consideration of the carbon isotope system of Nar Gölü.

In terms of future work on the Nar Gölü record, firstly an improved chronology is required. The U-Th date allows the transition 1989-1957 cm to be identified with a high degree of certainty as the Younger Dryas to Holocene transition and the varve chronology from this point through the early Holocene allows the identification of

centennial and decadal scale droughts. However, whilst this allows it to be shown that the Younger Dryas to Holocene transition was roughly as rapid as in North Atlantic region records and that there were arid events at roughly the same number of years from the start of the Holocene as the PBO, 9.3 ka and 8.2 ka cool events occurred in NGRIP, it is not possible to say whether the changes in Nar Gölü occurred synchronously with those in the North Atlantic, or if there was some sort of lag. Additionally, the lack of varves and U-Th dates in the mid to late Holocene means that it has not been possible to accurately establish whether centennial scale droughts seen in the Nar Gölü record occurred at the same time as previously identified Near East droughts and as the 'collapse' of civilisations. Also, only once the chronology is more secure can spectral analysis be used to reliably identify if there is any cyclicity in the record. The strategy is to run more samples for U-Th that are similar to the one sample that worked: in sections composed of aragonite (which takes up more uranium than calcite) and that are sufficiently heterogeneous that a good spread in detrital contamination between the sub samples can be achieved (to reduce the error when using the isochron approach).

More work could also be undertaken to even better constrain the drivers of $\delta^{18}O_{carbonate}$. Firstly, if an accurate, independent temperature reconstruction was to be produced from the same samples as the $\delta^{18}O_{carbonate}$ record was produced, it would be easier to account for the influence of temperature on $\delta^{18}O_{carbonate}$. It has been proposed that $\delta^{18}O_{cellulose}$ can be used to this end but cellulose extraction from Nar Gölü sediments proved unsuccessful (section 6.5.2). The potential of using a technique such as TEX_{86} analysis (e.g. Powers et al., 2010, Woltering et al., 2011, Blaga et al., 2013) is being explored. Furthermore, whilst a seasonality reconstruction has been attempted, because of the seemingly small difference in the time of year of carbonate precipitation and diatom growth and potential changes in the time of year the two hosts form in the lake, the interpretation of the $\Delta\delta^{18}O$ record has been difficult. An addition to the approach used here would be to use sediment traps that are automated to capture weekly samples to identify diatom species that grow in the lake at set times of the year and then to use micro-manipulation to separate out the diatom species (Snelling et al., 2013) and undertake species-specific diatom isotope

analysis on the palaeo record (e.g. Swann et al., 2013). Finally, the gaps in the carbonate isotope record due to the presence of dolomite mean the record is not continuous and the driest periods in the record cannot be properly investigated. As with the issue of seasonality reconstruction, there is no simple way of dealing with this, although perhaps the same method could be applied whereby calcite and aragonite crystals are separated from dolomite crystals by micro-manipulation.

Some of the outstanding gaps in our knowledge of Near East palaeoclimate over the late glacial and Holocene require more studies on other sites in the region. Perhaps the biggest unanswered question centres around the transition to wetter conditions as seen at Nar Gölü in the 6th century AD. While shifts to wetter conditions at this time are seen in other records, it is unclear whether the shifts were as high magnitude as inferred from the Nar Gölü $\delta^{18}O_{carbonate}$ record. It is possible Nar Gölü was more sensitive to change at this time, which made the transition appear to be higher magnitude than the Younger Dryas to Holocene shift. Continuous, high resolution lake isotope records are required to answer this, and perhaps the best place to start would be the re-coring and analysis of the Eski Acıgöl sequence for this time period. Furthermore, when the political situation allows, Lakes Zeribar and Mirabad should be re-cored and a modern limnological monitoring programme established so that a higher resolution record with a more robust chronology can be produced and so that the drivers of $\delta^{18}O_{lakewater}$ in the present day can be better understood. This would help to further test the hypothesis of Stevens et al. (2001, 2006). More data-model comparisons (e.g. Black et al., 2011) are also required to help disentangle the drivers of Near East climate. Further investigation of the Dead Sea record is required to establish if the differences in reconstructed hydroclimate from Soreq Cave (and Nar Gölü) are real or simply down to misinterpretation of the record. The ongoing ICDP project may assist in this regard. Finally, further high resolution records are also required in order to investigate whether droughts at the times of the PBO and 9.3 ka events are seen elsewhere in the Near East; in the words of Alley and Ágústsdóttir (2005) let the anomaly-hunting continue.

References

ADGER, W. N., AGRAWALA, S., MIRZA, M. M. Q., CONDE, C., O'BRIEN, K., PULHIN, J., PULWARTY, R., SMIT, B. & TAKAHASHI, K. 2007. Assessment of Adaptation Practices, Options, Constraints and Capacity. *In:* PARRY, M. L., CANZIANI, O. F., PALUTIKOF, J. P., VAN DER LINDEN, P. J. & HANSON, C. E. (eds.) *Climate Change 2007: Impacts, Adaptation and Vulnerability. Contribution of Working Group II to the Fourth Assessment Report of the Intergovernmental Panel on Climate Change.* Cambridge: Cambridge University Press.

ADKINS, J., DEMENOCAL, P. & ESHEL, G. 2006. The "African humid period" and the record of marine upwelling from excess Th-230 in Ocean Drilling Program Hole 658C. *Paleoceanography,* 21**,** PA4203.

AGUILERA, M., FERRIO, J. P., PEREZ, G., ARAUS, J. L. & VOLTAS, J. 2012. Holocene changes in precipitation seasonality in the western Mediterranean Basin: a multi-species approach using delta C-13 of archaeobotanical remains. *Journal of Quaternary Science,* 27**,** 192-202.

AKURGAL, E. 2001. *Ancient Civilisations and Ruins of Turkey,* Istanbul, Net T. Yayinlari.

ALAASM, I. S., TAYLOR, B. E. & SOUTH, B. 1990. Stable isotope analysis of multiple carbonate samples using selective acid-extraction. *Chemical Geology,* 80**,** 119-125.

ALGAZE, G. & POURNELLE, J. 2003. Climate Change, Environmental Change, and Social Change at Early Bronze Age Titris Hoyuk. *In:* OZDOGAN, M., HAUPTMANN, H. & BASGELEN, N. (eds.) *From Village to Cities.* Istanbul: Arkeoloji ve Sanat Publications.

ALLCOCK, S. 2013. *Living with a Changing Landscape: Holocene Climate Variability and Socio-Evolutionary Trajectories, Central Turkey.* PhD, Plymouth.

ALLEY, R. B. & AGUSTSDOTTIR, A. M. 2005. The 8k event: cause and consequences of a major Holocene abrupt climate change. *Quaternary Science Reviews,* 24**,** 1123-1149.

ALLEY, R. B. & ÁGÚSTSDÓTTIR, A. M. 2005. The 8k event: cause and consequences of a major Holocene abrupt climate change. *Quaternary Science Reviews,* 24**,** 1123-1149.

ALLEY, R. B., MAROTZKE, J., NORDHAUS, W. D., OVERPECK, J. T., PETEET, D. M., PIELKE, R. A., PIERREHUMBERT, R. T., RHINES, P. B., STOCKER, T. F., TALLEY, L. D. & WALLACE, J. M. 2003. Abrupt climate change. *Science,* 299**,** 2005-2010.

ALLEY, R. B., MAYEWSKI, P. A., SOWERS, T., STUIVER, M., TAYLOR, K. C. & CLARK, P. U. 1997. Holocene climatic instability: a prominent, widespread event 8200 yr ago. *Geology,* 25**,** 483-486.

ALMOGI-LABIN, A., BAR-MATTHEWS, M., SHRIKI, D., KOLOSOVSKY, E., PATERNE, M., SCHILMAN, B., AYALON, A., AIZENSHTAT, Z. & MATTHEWS, A. 2009. Climatic variability during the last ~90 ka of the southern and northern Levantine Basin as evident from marine records and speleothems. *Quaternary Science Reviews,* 28**,** 2882-2896.

ALOISI, G., PIERRE, C., ROUCHY, J. M., FOUCHER, J. P., WOODSIDE, J. & PARTY, M. S. 2000. Methane-related authigenic carbonates of eastern Mediterranean Sea

mud volcanoes and their possible relation to gas hydrate destabilisation. *Earth and Planetary Science Letters,* 184**,** 321-338.

ALPERT, P., KRICHAK, S. O., SHAFIR, H., HAIM, D. & OSETINSKY, I. 2008. Climatic trends to extremes employing regional modeling and statistical interpretation over the E. Mediterranean. *Global and Planetary Change,* 63**,** 163-170.

ANDERSON, L. 2011. Holocene record of precipitation seasonality from lake calcite delta(18)O in the central Rocky Mountains, United States. *Geology,* 39**,** 211-214.

ANDERSON, T. F. & ARTHUR, M. A. 1983. Stable Isotopes of Oxygen and Carbon and their Application to Sedimentologic and Paleoenvironmental Problems. *In:* ARTHUR, M. A., ANDERSON, T. F., KAPLAN, I. R., VEIZER, J. & LAND, L. S. (eds.) *Stable Isotopes in Sedimentary Geology.* Dallas: SEPM short course no. 10.

ARIZTEGUI, D., ASIOLI, A., LOWE, J. J., TRINCARDI, F., VIGLIOTTI, L., TAMBURINI, F., CHONDROGIANNI, C., ACCORSI, C. A., MAZZANTI, M. B., MERCURI, A. M., VAN DER KAARS, S., MCKENZIE, J. A. & OLDFIELD, F. 2000. Palaeoclimate and the formation of sapropel S1: inferences from Late Quaternary lacustrine and marine sequences in the central Mediterranean region. *Palaeogeography Palaeoclimatology Palaeoecology,* 158**,** 215-240.

ARMENTEROS, I. 2010. Diaganesis of Carbonates in Continental Settings. *In:* ALONSO-ZARA, A. M. & TANNER, L. H. (eds.) *Developments in Sedimentology vol. 62. Geochemistry, Diagenesis and Applications.* Amsterdam: Elsevier.

ARNELL, N. W. 2004. Climate change and global water resources: SRES emissions and socio-economic scenarios. *Global Environmental Change - Human and Policy Dimensions,* 14**,** 31-52.

ARZ, H. W., LAMY, F. & PATZOLD, J. 2006. A pronounced dry event recorded around 4.2 ka in brine sediments from the northern Red Sea. *Quaternary Research,* 66**,** 432-441.

ARZ, H. W., LAMY, F., PATZOLD, J., MULLER, P. J. & PRINS, M. 2003. Mediterranean moisture source for an early-Holocene humid period in the northern Red Sea. *Science,* 300**,** 118-121.

AUFGEBAUER, A., PANAGIOTOPOULOS, K., WAGNER, B., SCHAEBITZ, F., VIEHBERG, F. A., VOGEL, H., ZANCHETTA, G., SULPIZIO, R., LENG, M. J. & DAMASCHKE, M. 2012. Climate and environmental change in the Balkans over the last 17 ka recorded in sediments from Lake Prespa (Albania/FYR of Macedonia/Greece). *Quaternary International,* 274**,** 122-135.

AYALON, A., BAR-MATTHEWS, M. & KAUFMAN, A. 1999. Petrography, strontium, barium and uranium concentrations, and strontium and uranium isotope ratios in speleothems as palaeoclimatic proxies: Soreq Cave, Israel. *Holocene,* 9**,** 715-722.

BAHR, A., LAMY, F., ARZ, H. W., MAJOR, C., KWIECIEN, O. & WEFER, G. 2008. Abrupt changes of temperature and water chemistry in the late Pleistocene and early Holocene Black Sea. *Geochemistry Geophysics Geosystems,* 9**,** Q01004.

BAR-MATTHEWS, M. & AYALON, A. 2011. Mid-Holocene climate variations revealed by high-resolution speleothem records from Soreq Cave, Israel and their correlation with cultural changes. *Holocene,* 21**,** 163-171.

BAR-MATTHEWS, M., AYALON, A., GILMOUR, M., MATTHEWS, A. & HAWKESWORTH, C. J. 2003. Sea-land oxygen isotopic relationships from planktonic

foraminifera and speleothems in the Eastern Mediterranean region and their implication for paleorainfall during interglacial intervals. *Geochimica et Cosmochimica Acta,* 67**,** 3181-3199.

BAR-MATTHEWS, M., AYALON, A. & KAUFMAN, A. 1997. Late Quaternary paleoclimate in the eastern Mediterranean region from stable isotope analysis of speleothems at Soreq Cave, Israel. *Quaternary Research,* 47**,** 155-168.

BAR-MATTHEWS, M., AYALON, A., KAUFMAN, A. & WASSERBURG, G. J. 1999. The Eastern Mediterranean paleoclimate as a reflection of regional events: Soreq cave, Israel. *Earth and Planetary Science Letters,* 166**,** 85-95.

BAR-YOSEF MAYER, D. E., LENG, M. J., ALDRIDGE, D. C., ARROWSMITH, C., GUMUS, B. A. & SLOANE, H. J. 2012. Modern and early-middle Holocene shells of the freshwater mollusc Unio, from Catalhoyuk in the Konya Basin, Turkey: preliminary palaeoclimatic implications from molluscan isotope data. *Journal of Archaeological Science,* 39**,** 76-83.

BARBER, D. C., DYKE, A., HILLAIRE-MARCEL, C., JENNINGS, A. E., ANDREWS, J. T., KERWIN, M. W., BILODEAU, G., MCNEELY, R., SOUTHON, J., MOREHEAD, M. D. & GAGNON, J. M. 1999. Forcing of the cold event of 8,200 years ago by catastrophic drainage of Laurentide lakes. *Nature,* 400**,** 344-348.

BARKER, P., FONTES, J. C., GASSE, F. & DRUART, J. C. 1994. Experimental dissolution of diatom silica in concentrated salt-solutions and implications for paleoenvironmental reconstruction. *Limnology and Oceanography,* 39**,** 99-110.

BARKER, P. A., HURRELL, E. R., LENG, M. J., PLESSEN, B., WOLFF, C., CONLEY, D. J., KEPPENS, E., MILNE, I., CUMMING, B. F., LAIRD, K. R., KENDRICK, C. P., WYNN, P. M. & VERSCHUREN, D. 2013. Carbon cycling within an East African lake revealed by the carbon isotope composition of diatom silica: a 25-ka record from Lake Challa, Mt. Kilimanjaro. *Quaternary Science Reviews,* 66**,** 55-63.

BARKER, P. A., HURRELL, E. R., LENG, M. J., WOLFF, C., COCQUYT, C., SLOANE, H. J. & VERSCHUREN, D. 2011. Seasonality in equatorial climate over the past 25 k.y. revealed by oxygen isotope records from Mount Kilimanjaro. *Geology,* 39**,** 1111-1114.

BARKER, P. A., TALBOT, M. R., STREET-PERROTT, F. A., MARRET, F., SCOURSE, J. & ODADA, E. O. 2004. Late Quaternary Climatic Variability in Intertropical Africa. *In:* BATTARBEE, R. W., GASSE, F. & STICKLEY, C. E. (eds.) *Past Climate Variability through Europe and Africa.* Dordrecht: Springer.

BARKER, S., DIZ, P., VAUTRAVERS, M. J., PIKE, J., KNORR, G., HALL, I. R. & BROECKER, W. S. 2009. Interhemispheric Atlantic seesaw response during the last deglaciation. *Nature,* 457**,** 1097-U50.

BARTOV, Y., GOLDSTEIN, S. L., STEIN, M. & ENZEL, Y. 2003. Catastrophic arid episodes in the Eastern Mediterranean linked with the North Atlantic Heinrich events. *Geology,* 31**,** 439-442.

BECK, L., GEHLEN, M., FLANK, A. M., VAN BENNEKOM, A. J. & VAN BEUSEKOM, J. E. E. 2002. The relationship between Al and Si in biogenic silica as determined by PIXE and XAS. *Nuclear Instruments & Methods in Physics Research Section B - Beam Interactions with Materials and Atoms,* 189**,** 180-184.

BELLWOOD, P. 2005. *First Farmers,* Oxford, Blackwell.

BERGER, J. F. & GUILAINE, J. 2009. The 8200 cal BP abrupt environmental change and the Neolithic transition: a Mediterranean perspective. *Quaternary International,* 200**,** 31-49.

BERGLUND, B. E., BIRKS, H. J. B., RALSKA-JASIEWICZOWA, M. & WRIGHT, H. E. 1996. *Palaeoecological Events During the Last 15 000 Years: Regional Synthesis of Palaeoecological Studies of Lakes and Mires in Europe,* New Jersey, John Wiley and Sons.

BERNER, R. A. 1975. The role of magnesium in the crystal growth of calcite and aragonite from sea water. *Geochimica et Cosmochimica Acta,* 39**,** 489-504.

BERNHARDT, C. E., HORTON, B. P. & STANLEY, J. D. 2012. Nile Delta vegetation response to Holocene climate variability. *Geology,* 40**,** 615-618.

BISCHOFF, J. L. & FITZPATRICK, J. A. 1991. U-Series dating of impure carbonates - an isochron technique using total-sample dissolution. *Geochimica et Cosmochimica Acta,* 55**,** 543-554.

BLACK, E., BRAYSHAW, D., BLACK, S. & RAMBEAU, C. 2011. Using Proxy Data, Historical Climate Data and Climate Models to Investigate Aridification During the Holocene. *In:* MITHEN, S. & BLACK, E. (eds.) *Water, Life and Civilisation.* Cambridge: Cambridge University Press.

BLAGA, C. I., REICHART, G., LOTTER, A. F., ANSELMETTI, F. S. & DAMSTE, J. S. S. 2013. A TEX86 lake record suggests simultaneous shifts in temperature in Central Europe and Greenland during the last deglaciation. *Geophysical Research Letters,* 40**,** 50181.

BLANCHET, C. L., TJALLINGII, R., FRANK, M., LORENZEN, J., REITZ, A., BROWN, K., FESEKER, T. & BRUCKMANN, W. 2013. High- and low-latitude forcing of the Nile River regime during the Holocene inferred from laminated sediments of the Nile deep-sea fan. *Earth and Planetary Science Letters,* 364**,** 98-110.

BLARD, P. H., SYLVESTRE, F., TRIPATI, A. K., CLAUDE, C., CAUSSE, C., COUDRAIN, A., CONDOM, T., SEIDEL, J. L., VIMEUX, F., MOREAU, C., DUMOULIN, J. P. & LAVE, J. 2011. Lake highstands on the Altiplano (Tropical Andes) contemporaneous with Heinrich 1 and the Younger Dryas: new insights from C-14, U-Th dating and delta O-18 of carbonates. *Quaternary Science Reviews,* 30**,** 3973-3989.

BOND, G., KROMER, B., BEER, J., MUSCHELER, R., EVANS, M. N., SHOWERS, W., HOFFMANN, S., LOTTI-BOND, R., HAJDAS, I. & BONANI, G. 2001. Persistent solar influence on north Atlantic climate during the Holocene. *Science,* 294**,** 2130-2136.

BOND, G., SHOWERS, W., CHESEBY, M., LOTTI, R., ALMASI, P., DEMENOCAL, P., PRIORE, P., CULLEN, H., HAJDAS, I. & BONANI, G. 1997. A pervasive millennial-scale cycle in North Atlantic Holocene and glacial climates. *Science,* 278**,** 1257-1266.

BORDON, A., PEYRON, O., LEZINE, A. M., BREWER, S. & FOUACHE, E. 2009. Pollen-inferred Late-Glacial and Holocene climate in southern Balkans (Lake Maliq). *Quaternary International,* 200**,** 19-30.

BOTTEMA, S. 1986. A late Quaternary pollen diagram from Lake Urmia (Northwestern Iran). *Review of Palaeobotany and Palynology,* 47**,** 241-247.

BOURDON, B., TURNER, S., HENDERSON, G. M. & LUNDSTROM, C. C. 2003. Introduction to U-series geochemistry. *Reviews in Mineralogy & Geochemistry,* 52**,** 1-21.

BOURKE, S. 2008. *The Middle East,* London, Thames and Hudson.

BRACONNOT, P., OTTO-BLIESNER, B., HARRISON, S., JOUSSAUME, S., PETERCHMITT, J. Y., ABE-OUCHI, A., CRUCIFIX, M., DRIESSCHAERT, E., FICHEFET, T., HEWITT, C. D., KAGEYAMA, M., KITOH, A., LOUTRE, M. F., MARTI, O., MERKEL, U., RAMSTEIN, G., VALDES, P., WEBER, L., YU, Y. & ZHAO, Y. 2007. Results of PMIP2 coupled simulations of the Mid-Holocene and Last Glacial Maximum - Part 2: feedbacks with emphasis on the location of the ITCZ and mid- and high latitudes heat budget. *Climate of the Past,* 3**,** 279-296.

BRAMANTI, B., THOMAS, M. G., HAAK, W., UNTERLAENDER, M., JORES, P., TAMBETS, K., ANTANAITIS-JACOBS, I., HAIDLE, M. N., JANKAUSKAS, R., KIND, C. J., LUETH, F., TERBERGER, T., HILLER, J., MATSUMURA, S., FORSTER, P. & BURGER, J. 2009. Genetic discontinuity between local hunter-gatherers and central Europe's first farmers. *Science,* 326**,** 137-140.

BRANDRISS, M. E., O'NEIL, J. R., EDLUND, M. B. & STOERMER, E. F. 1998. Oxygen isotope fractionation between diatomaceous silica and water. *Geochimica et Cosmochimica Acta,* 62**,** 1119-1125.

BRAYSHAW, D., BLACK, E., HOSKINS, B. & SLINGO, J. 2011b. Past Climates of the Middle East. *In:* MITHEN, S. & BLACK, E. (eds.) *Water, Life and Civilisation.* Cambridge: Cambridge University Press.

BRAYSHAW, D., HOSKINS, B. & BLACK, E. 2010. Some physical drivers of change in the winter storm tracks over the Atlantic and Mediterranean during the Holocene. *Philosophical Transactions of the Royal Society of London,* 368**,** 5185–5223.

BRAYSHAW, D. J., RAMBEAU, C. M. C. & SMITH, S. J. 2011a. Changes in Mediterranean climate during the Holocene: insights from global and regional climate modelling. *Holocene,* 21**,** 15-31.

BREWER, T. S., LENG, M. J., MACKAY, A. W., LAMB, A. L., TYLER, J. J. & MARSH, N. G. 2008. Unravelling contamination signals in biogenic silica oxygen isotope composition: the role of major and trace element geochemistry. *Journal of Quaternary Science,* 23**,** 321-330.

BRISCOE, H. V. A. & ROBINSON, P. L. 1925. A redetermination of the atomic weight of boron. *Journal of the Chemical Society,* 127**,** 696-720.

BRISTOW, T. F., KENNEDY, M. J., MORRISON, K. D. & MROFKA, D. D. 2012. The influence of authigenic clay formation on the mineralogy and stable isotopic record of lacustrine carbonates. *Geochimica et Cosmochimica Acta,* 90**,** 64-82.

BROECKER, W. S. 1963. A preliminary evaluation of Uranium Series inequilibrium as a tool for absolute age measurement on marine carbonates. *Journal of Geophysical Research,* 68**,** 2817-2834.

BROECKER, W. S., KENNETT, J. P., FLOWER, B. P., TELLER, J. T., TRUMBORE, S., BONANI, G. & WOLFLI, W. 1989. Routing of meltwater from the Laurentide ice-sheet during the Younger Dryas cold episode. *Nature,* 341**,** 318-321.

BRONMARK, C. & HANSSON, L. 2005. *The Biology of Lakes and Ponds,* Oxford, Oxford University Press.

BROWN, T. A., JONES, M. K., POWELL, W. & ALLABY, R. G. 2009. The complex origins of domesticated crops in the Fertile Crescent. *Trends in Ecology & Evolution,* 24**,** 103-109.

BURROUGHS, W. J. 2005. *Climate Change in Prehistory,* Cambridge, Cambridge University Press.

CALVERT, S. E. & FONTUGNE, M. R. 2001. On the late Pleistocene-Holocene sapropel record of climatic and oceanographic variability in the eastern Mediterranean. *Paleoceanography,* 16**,** 78-94.

CASTANEDA, I. S., SCHEFUSS, E., PATZOLD, J., DAMSTE, J. S. S., WELDEAB, S. & SCHOUTEN, S. 2010. Millennial-scale sea surface temperature changes in the eastern Mediterranean (Nile River Delta region) over the last 27,000 years. *Paleoceanography,* 25**,** PA1208.

CHAPLIGIN, B., LENG, M. J., WEBB, E., ALEXANDRE, A., DODD, J. P., IJIRI, A., LÜCKE, A., SHEMESH, A., ABELMANN, A., HERZSCHUH, U., LONGSTAFFEC, F. J., MEYER, H., MOSCHEN, R., OKAZAKI, Y., REES, N. H., SHARP, Z. D., SLOANE, H. J., SONZOGNI, C., SWANN, G. E. A., SYLVESTRE, F., TYLER, J. J. & YAM, R. 2011. Inter-laboratory comparison of oxygen isotope compositions from biogenic silica. *Geochimica et Cosmochimica Acta,* 75**,** 7242-7256.

CHAPLIGIN, B., MEYER, H., BRYAN, A., SNYDER, J. & KEMNITZ, H. 2012. Assessment of purification and contamination correction methods for analysing the oxygen isotope composition from biogenic silica. *Chemical Geology,* 300-301**,** 185-199.

CLARKE, G. K. C., LEVERINGTON, D. W., TELLER, J. T. & DYKE, A. S. 2004. Paleohydraulics of the last outburst flood from glacial Lake Agassiz and the 8200 BP cold event. *Quaternary Science Reviews,* 23**,** 389-407.

CLAYTON, R. N. & MAYEDA, T. K. 1963. The use of bromine pentafluoride in the extraction of oxygen from oxides and silicates for isotopic analysis. *Geochimica et Cosmochimica Acta,* 27**,** 43-52.

COHEN, A. S. 2003. *Paleolimnology,* Oxford, Oxford University Press.

COLEMAN, M. L., SHEPHERD, T. J., DURHAM, J. J., ROUSE, J. E. & MOORE, G. R. 1982. Reduction of water with zinc for hydrogen isotope analysis. *Analytical Chemistry,* 54**,** 993-995.

COOMBES, P. & BARBER, K. 2005. Environmental determinism in Holocene research: causality or coincidence? *Area,* 37**,** 303-311.

COPLEN, T. B., KENDALL, C. & HOPPLE, J. 1983. Comparision of stable isotope reference samples. *Nature,* 302**,** 236-238.

CRAIG, H. 1957. Isotopic standards for carbon and oxygen and correction factors for mass-spectrometric analysis of carbon dioxide. *Geochimica et Cosmochimica Acta,* 12**,** 133-149.

CRAIG, H. 1961. Isotopic variations in meteoric waters. *Science,* 133**,** 1833-1834.

CRESPIN, J., SYLVESTRE, F., ALEXANDRE, A., SONZOGNI, C., PAILLES, C. & PERGA, M. E. 2010. Re-examination of the temperature-dependent relationship between delta O-18(diatoms) and delta O-18(lake water) and implications for paleoclimate inferences. *Journal of Paleolimnology,* 44**,** 547-557.

CRUZ, R. V., HARASAWA, H., LAL, M., WU, S., ANOKHIN, Y., PUNSALMAA, B., HONDA, Y., JAFARI, M., LI, C. & HUU NINH, N. 2007. Asia. *In:* PARRY, M. L., CANZIANI, O. F., PALUTIKOF, J. P., VAN DER LINDEN, P. J. & HANSON, C. E. (eds.) *Climate Change 2007: Impacts, Adaptation and Vulnerability. Contribution of Working Group II to the Fourth Assessment Report of the Intergovernmental Panel on Climate Change.* Cambridge: Cambridge University Press.

CULLEN, H. M. & DEMENOCAL, P. B. 2000. North Atlantic influence on Tigris-Euphrates streamflow. *International Journal of Climatology,* 20**,** 853-863.

CULLEN, H. M., DEMENOCAL, P. B., HEMMING, S., HEMMING, G., BROWN, F. H., GUILDERSON, T. & SIROCKO, F. 2000. Climate change and the collapse of the Akkadian empire: evidence from the deep sea. *Geology,* 28**,** 379-382.

DALEY, T. J., THOMAS, E. R., HOLMES, J. A., STREET-PERROTT, F. A., CHAPMAN, M. R., TINDALL, J. C., VALDES, P. J., LOADER, N. J., MARSHALL, J. D., WOLFF, E. W., HOPLEY, P. J., ATKINSON, T., BARBER, K. E., FISHER, E. H., ROBERTSON, I., HUGHES, P. D. M. & ROBERTS, C. N. 2011. The 8200 yr BP cold event in stable isotope records from the North Atlantic region. *Global and Planetary Change,* 79**,** 288-302.

DALFES, H., KUKLA, G. & WEISS, H. (eds.) 1997. *Third Millennium BC Climate Change and Old World Collapse,* Berlin: Springer Verlag.

DANSGAARD, W. 1964. Stable isotopes in precipitation. *Tellus,* 16**,** 436-468.

DARLING, W. G. 2004. Hydrological factors in the interpretation of stable isotopic proxy data present and past: a European perspective. *Quaternary Science Reviews,* 23**,** 743-770.

DARLING, W. G., BATH, A. H., GIBSON, J. J. & ROZANSKI, K. 2006. Isotopes in Water. *In:* LENG, M. J. (ed.) *Isotopes in Palaeoenvironmental Research.* Dordrecht: Springer.

DE CHOUDENS-SANCHEZ, V. & GONZALEZ, L. A. 2009. Calcite and aragonite precipitation under controlled instantaneous supersaturation: elucidating the role of Caco(3) saturation state and Mg/Ca Ratio on calcium carbonate polymorphism. *Journal of Sedimentary Research,* 79**,** 363-376.

DE LANGE, G. J., THOMSON, J., REITZ, A., SLOMP, C. P., PRINCIPATO, M. S., ERBA, E. & CORSELLI, C. 2008. Synchronous basin-wide formation and redox-controlled preservation of a Mediterranean sapropel. *Nature Geoscience,* 1**,** 606-610.

DEAN, J. R., JONES, M. D., LENG, M. J., SLOANE, H. J., ROBERTS, C. N., WOODBRIDGE, J., SWANN, G. E. A., METCALFE, S. E., EASTWOOD, W. J. & YIGITBASIOGLU, H. 2013. Palaeo-seasonality of the last two millennia reconstructed from the oxygen isotope composition of carbonates and diatom silica from Nar Gölü, central Turkey. *Quaternary Science Reviews,* 66**,** 35-44.

DEBRET, M., BOUT-ROUMAZEILLES, V., GROUSSET, F., DESMET, M., MCMANUS, J. F., MASSEI, N., SEBAG, D., PETIT, J. R., COPARD, Y. & TRENTESAUX, A. 2007. The origin of the 1500-year climate cycles in Holocene North-Atlantic records. *Climate of the Past,* 3**,** 569-575.

DEMENOCAL, P., ORTIZ, J., GUILDERSON, T., ADKINS, J., SARNTHEIN, M., BAKER, L. & YARUSINSKY, M. 2000. Abrupt onset and termination of the African Humid Period: rapid climate responses to gradual insolation forcing. *Quaternary Science Reviews,* 19**,** 347-361.

DEMENOCAL, P. B. 2001. Cultural responses to climate change during the Late Holocene. *Science,* 292**,** 667-673.

DEMIR, İ., KILIÇ, G. & COŞKUN, M. 2010. *Technical conference on changing climate and demands for climate services for sustainable development.* Antalya: World Meteorological Organization.

DENG, S. C., DONG, H. L., LV, G., JIANG, H. C., YU, B. S. & BISHOP, M. E. 2010. Microbial dolomite precipitation using sulfate reducing and halophilic

bacteria: results from Qinghai Lake, Tibetan Plateau, NW China. *Chemical Geology,* 278**,** 151-159.

DENTON, G. H., BROECKER, W. S. & ALLEY, R. B. 2006. The mystery interval 17.5 to 14.5 kyrs ago. *PAGES News,* 14**,** 14-16.

DEOCAMPO, D. M. 2010. The Geochemistry of Continental Carbonates. *In:* ALONSO-ZARA, A. M. & TANNER, L. H. (eds.) *Developments in Sedimentology vol. 62. Geochemistry, Diagenesis and Applications.* Amsterdam: Elsevier.

DEVELLE, A. L., HERREROS, J., VIDAL, L., SURSOCK, A. & GASSE, F. 2010. Controlling factors on a paleo-lake oxygen isotope record (Yammouneh, Lebanon) since the Last Glacial Maximum. *Quaternary Science Reviews,* 29**,** 865-886.

DJAMALI, M., AKHANI, H., ANDRIEU-PONEL, V., BRACONNOT, P., BREWER, S., DE BEAULIEU, J. L., FLEITMANN, D., FLEURY, J., GASSE, F., GUIBAL, F., JACKSON, S. T., LEZINE, A. M., MEDAIL, F., PONEL, P., ROBERTS, N. & STEVENS, L. 2010. Indian Summer Monsoon variations could have affected the early-Holocene woodland expansion in the Near East. *Holocene,* 20**,** 813-820.

DODSON, A. M. 2001. Third Intermediate Period. *In:* REDFORD, D. B. (ed.) *The Oxford Encyclopedia of Ancient Egypt.* Oxford: Oxford University Press.

DORMOY, I., PEYRON, O., NEBOUT, N. C., GORING, S., KOTTHOFF, U., MAGNY, M. & PROSS, J. 2009. Terrestrial climate variability and seasonality changes in the Mediterranean region between 15,000 and 4000 years BP deduced from marine pollen records. *Climate of the Past,* 5**,** 615-632.

DYKOSKI, C. A., EDWARDS, R. L., CHENG, H., YUAN, D. X., CAI, Y. J., ZHANG, M. L., LIN, Y. S., QING, J. M., AN, Z. S. & REVENAUGH, J. 2005. A high-resolution, absolute-dated Holocene and deglacial Asian monsoon record from Dongge Cave, China. *Earth and Planetary Science Letters,* 233**,** 71-86.

EASTWOOD, W. J., LENG, M. J., ROBERTS, N. & DAVIS, B. 2007. Holocene climate change in the eastern Mediterranean region: a comparison of stable isotope and pollen data from Lake Golhisar, southwest Turkey. *Journal of Quaternary Science,* 22**,** 327-341.

EDWARDS, R. L., CHEN, J. H. & WASSERBURG, G. J. 1987. U-238-U-234-Th-230-Th-232 systematics and the precise measurement of time over the past 500,000 years. *Earth and Planetary Science Letters,* 81**,** 175-192.

EDWARDS, R. L., GALLUP, C. D. & CHENG, H. 2003. Uranium-series dating of marine and lacustrine carbonates. *Uranium-Series Geochemistry,* 52**,** 363-405.

EDWARDS, T. W. D. & MCANDREWS, J. H. 1989. Paleohydrology of a Canadian Shield lake inferred from O-18 in sediment cellulose. *Canadian Journal of Earth Sciences,* 26**,** 1850-1859.

ELDERFIELD, H. & GANSSEN, G. 2000. Past temperature and delta O-18 of surface ocean waters inferred from foraminiferal Mg/Ca ratios. *Nature,* 405**,** 442-445.

ELLISON, C. R. W., CHAPMAN, M. R. & HALL, I. R. 2006. Surface and deep ocean interactions during the cold climate event 8200 years ago. *Science,* 312**,** 1929-1932.

EMEIS, K. C., STRUCK, U., SCHULZ, H. M., ROSENBERG, R., BERNASCONI, S., ERLENKEUSER, H., SAKAMOTO, T. & MARTINEZ-RUIZ, F. 2000. Temperature and salinity variations of Mediterranean Sea surface waters over the last 16,000 years from records of planktonic stable oxygen isotopes and alkenone

unsaturation ratios. *Palaeogeography Palaeoclimatology Palaeoecology,* 158**,** 259-280.

ENGLAND, A., EASTWOOD, W. J., ROBERTS, C. N., TURNER, R. & HALDON, J. F. 2008. Historical landscape change in Cappadocia (central Turkey): a palaeoecological investigation of annually laminated sediments from Nar lake. *Holocene,* 18**,** 1229-1245.

ENZEL, Y., ARNIT, R., DAYAN, U., CROUVI, O., KAHANA, R., ZIV, B. & SHARON, D. 2008. The climatic and physiographic controls of the eastern Mediterranean over the late Pleistocene climates in the southern Levant and its neighboring deserts. *Global and Planetary Change,* 60**,** 165-192.

EPSTEIN, S. & MAYEDA, T. 1953. Variation in 18O content of waters from natural sources. *Geochimica et Cosmochimica Acta,* 4**,** 231-224.

EREZ, J. & LUZ, B. 1983. Experimental paleotemperature equation for planktonic-foraminifera. *Geochimica et Cosmochimica Acta,* 47**,** 1025-1031.

ESSALLAMI, L., SICRE, M. A., KALLEL, N., LABEYRIE, L. & SIANI, G. 2007. Hydrological changes in the Mediterranean Sea over the last 30,000 years. *Geochemistry Geophysics Geosystems,* 8**,** Q07002.

EVANS, J. P. 2009. 21st century climate change in the Middle East. *Climatic Change,* 92**,** 417-432.

FAGAN, B. 2004. *The Long Summer,* London, Granta.

FENCHEL, T., KING, G. M. & BLACKBURN, T. H. 1998. *Bacterial Biogeochemistry: The Ecophysiology of Mineral Cycling,* San Diego, Academic Press.

FENG, X., PORPORATO, A. & RODRIGUEZ-ITURBE, I. 2013. Changes in rainfall seasonality in the tropics. *Nature Climate Change,* 3**,** 811-815.

FINNÉ, M., HOLMGREN, K., SUNDQVIST, H. S., WEIBERG, E. & LINDBLOM, M. 2011. Climate in the eastern Mediterranean, and adjacent regions, during the past 6000 years - a review. *Journal of Archaeological Science,* 38**,** 3153-3173.

FIORENTINO, G., CARACUTA, V., CALCAGNILE, L., D'ELIA, M., MATTHIAE, P., MAVELLI, F. & QUARTA, G. 2008. Third millennium BC climate change in Syria highlighted by carbon stable isotope analysis of C-14-AMS dated plant remains from Ebla. *Palaeogeography Palaeoclimatology Palaeoecology,* 266**,** 51-58.

FIRESTONE, R. B., WEST, A., KENNETT, J. P., BECKER, L., BUNCH, T. E., REVAY, Z. S., SCHULTZ, P. H., BELGYA, T., KENNETT, D. J., ERLANDSON, J. M., DICKENSON, O. J., GOODYEAR, A. C., HARRIS, R. S., HOWARD, G. A., KLOOSTERMAN, J. B., LECHLER, P., MAYEWSKI, P. A., MONTGOMERY, J., POREDA, R., DARRAH, T., HEE, S. S. Q., SMITHA, A. R., STICH, A., TOPPING, W., WITTKE, J. H. & WOLBACH, W. S. 2007. Evidence for an extraterrestrial impact 12,900 years ago that contributed to the megafaunal extinctions and the Younger Dryas cooling. *PNAS,* 104**,** 16016-16021.

FISHER, T. G., SMITH, D. G. & ANDREWS, J. T. 2002. Preboreal oscillation caused by a glacial Lake Agassiz flood. *Quaternary Science Reviews,* 21**,** 873-878.

FLEITMANN, D., BURNS, S. J., MANGINI, A., MUDELSEE, M., KRAMERS, J., VILLA, I., NEFF, U., AL-SUBBARY, A. A., BUETTNER, A., HIPPLER, D. & MATTER, A. 2007. Holocene ITCZ and Indian monsoon dynamics recorded in stalagmites from Oman and Yemen (Socotra). *Quaternary Science Reviews,* 26**,** 170-188.

FLEITMANN, D., BURNS, S. J., MUDELSEE, M., NEFF, U., KRAMERS, J., MANGINI, A. & MATTER, A. 2003. Holocene forcing of the Indian monsoon recorded in a stalagmite from Southern Oman. *Science,* 300**,** 1737-1739.

FLEITMANN, D., CHENG, H., BADERTSCHER, S., EDWARDS, R. L., MUDELSEE, M., GOKTURK, O. M., FANKHAUSER, A., PICKERING, R., RAIBLE, C. C., MATTER, A., KRAMERS, J. & TUYSUZ, O. 2009. Timing and climatic impact of Greenland interstadials recorded in stalagmites from northern Turkey. *Geophysical Research Letters,* 36**,** L19707.

FLEITMANN, D., MUDELSEE, M., BURNS, S. J., BRADLEY, R. S., KRAMERS, J. & MATTER, A. 2008. Evidence for a widespread climatic anomaly at around 9.2 ka before present. *Paleoceanography,* 23**,** PA1102.

FLETCHER, W. J., DEBRET, M. & GONI, M. F. S. 2013. Mid-Holocene emergence of a low-frequency millennial oscillation in western Mediterranean climate: implications for past dynamics of the North Atlantic atmospheric westerlies. *Holocene,* 23**,** 153-166.

FONTUGNE, M., ARNOLD, M., LABEYRIE, L., PATERNE, M., CALVERT, S. E. & DUPLESSY, J. C. 1994. Palaeoenvironment, Sapropel Chronology and River Nile Discharge During the last 20,000 years as Indicated by Deep Sea Sediment Records in the Eastern Mediterranean. *In:* BAR-YOSEF, O. & KRA, R. (eds.) *Late Quaternary Chronology and Paleoclimates of the Eastern Mediterranean.* Tucson: Radiocarbon.

FRITZ, S. C. 2008. Deciphering climatic history from lake sediments. *Journal of Paleolimnology,* 39**,** 5-16.

FRITZ, S. C., BAKER, P. A., SELTZER, G. O., BALLANTYNE, A., TAPIA, P., CHENG, H. & EDWARDS, R. L. 2007. Quaternary glaciation and hydrologic variation in the South American tropics as reconstructed from the Lake Titicaca drilling project. *Quaternary Research,* 68**,** 410-420.

FROGLEY, M. R., GRIFFITHS, H. I. & HEATON, T. H. E. 2001. Historical biogeography and Late Quaternary environmental change of Lake Pamvotis, Ioannina (north-western Greece): evidence from ostracods. *Journal of Biogeography,* 28**,** 745-756.

FRONVAL, T., JENSEN, N. B. & BUCHARDT, B. 1995. Oxygen-Isotope disequilibrium precipitation of calcite in Lake Arreso, Denmark. *Geology,* 23**,** 463-466.

FRUMKIN, A., FORD, D. C. & SCHWARCZ, H. P. 1999. Continental oxygen isotope record of the last 170,000 years in Jerusalem. *Quaternary Research,* 51**,** 317-327.

FRUMKIN, A., FORD, D. C. & SCHWARCZ, H. P. 2000. Paleoclimate and vegetation of the last glacial cycles in Jerusalem from a speleothem record. *Global Biogeochemical Cycles,* 14**,** 863-870.

GALLET, Y., GENEVEY, A., LE GOFF, M., FLUTEAU, F. & ESHRAGHI, S. A. 2006. Possible impact of the Earth's magnetic field on the history of ancient civilizations. *Earth and Planetary Science Letters,* 246**,** 17-26.

GASSE, F. 2000. Hydrological changes in the African tropics since the Last Glacial Maximum. *Quaternary Science Reviews,* 19**,** 189-211.

GENTY, D., BLAMART, D., GHALEB, B., PLAGNES, V., CAUSSE, C., BAKALOWICZ, M., ZOUARI, K., CHKIR, N., HELLSTROM, J., WAINER, K. & BOURGES, F. 2006. Timing and dynamics of the last deglaciation from European and North

African delta C-13 stalagmite profiles - comparison with Chinese and South Hemisphere stalagmites. *Quaternary Science Reviews,* 25**,** 2118-2142.

GEVREK, A. I. & KAZANCI, N. 2000. A Pleistocene, pyroclastic-poor maar from central Anatolia, Turkey: influence of a local fault on a phreatomagmatic eruption. *Journal of Volcanology and Geothermal Research,* 95**,** 309-317.

GIERLOWSKI-KORDESCH, E. 2010. Lacustrine Carbonates. *In:* ALONSO-ZARA, A. M. & TANNER, L. H. (eds.) *Carbonates in Continental Settings: Facies, Environments and Processes.* Amsterdam: Elsevier.

GIL, I. M., ABRANTES, F. & HEBBELN, D. 2006. The North Atlantic Oscillation forcing through the last 2000 years: spatial variability as revealed by high-resolution marine diatom records from N and SW Europe. *Marine Micropaleontology,* 60**,** 113-129.

GIORGI, F. 2006. Climate change hot-spots. *Geophysical Research Letters,* 33**,** GL025734.

GIORGI, F. & LIONELLO, P. 2008. Climate change projections for the Mediterranean region. *Global and Planetary Change,* 63**,** 90-104.

GLEW, J. R., SMOL, J. P. & LAST, W. M. 2001. Sediment Core Collection and Extrusion. *In:* LAST, W. M. & SMOL, J. P. (eds.) *Tracking Environmental Change Using Lake Sediments. Volume 1: Basin Analysis, Coring and Chronological Techniques.* Dordrecht: Kluwer.

GOKTURK, O. M., FLEITMANN, D., BADERTSCHER, S., CHENG, H., EDWARDS, R. L., LEUENBERGER, M., FANKHAUSER, A., TUYSUZ, O. & KRAMERS, J. 2011. Climate on the southern Black Sea coast during the Holocene: implications from the Sofular Cave record. *Quaternary Science Reviews,* 30**,** 2433-2445.

GOLDSTEIN, S. J. & STIRLING, C. H. 2003. Techniques for measuring uranium-series nuclides: 1992-2002. *Uranium-Series Geochemistry,* 52**,** 23-57.

GONZALEZ-SAMPERIZ, P., UTRILLA, P., MAZO, C., VALERO-GARCES, B., SOPENA, M. C., MORELLON, M., SEBASTIAN, M., MORENO, A. & MARTINEZ-BEA, M. 2009. Patterns of human occupation during the early Holocene in the Central Ebro Basin (NE Spain) in response to the 8.2 ka climatic event. *Quaternary Research,* 71**,** 121-132.

GOODFRIEND, G. A. 1999. Terrestrial stable isotope records of Late Quaternary paleoclimates in the eastern Mediterranean region. *Quaternary Science Reviews,* 18**,** 501-513.

GRIFFITHS, H. I., SCHWALB, A. & STEVENS, L. R. 2001. Environmental change in southwestern Iran: the Holocene ostracod fauna of Lake Mirabad. *Holocene,* 11**,** 757-764.

GROSSMAN, E. 1984. Carbon isotopic fractionation in live benthic foraminifera - comparison with inorganic precipitate studies. *Geochimica et Cosmochimica Acta,* 48**,** 1505-1512.

GROSSMAN, E. L. & KU, T. L. 1986. Oxygen and carbon isotope fractionation in biogenic aragonite - temperature effects. *Chemical Geology,* 59**,** 59-74.

GU, B. H., SCHELSKE, C. L. & HODELL, D. A. 2004. Extreme C-13 enrichments in a shallow hypereutrophic lake: implications for carbon cycling. *Limnology and Oceanography,* 49**,** 1152-1159.

GUPTA, A. K. 2004. Origin of agriculture and domestication of plants and animals linked to early Holocene climate amelioration. *Current Science,* 87**,** 54-59.

GVIRTZMAN, G. & WIEDER, M. 2001. Climate of the last 53,000 years in the eastern Mediterranean, based on soil-sequence stratigraphy in the coastal plain of Israel. *Quaternary Science Reviews,* 20**,** 1827-1849.

HAAK, W., BALANOVSKY, O., SANCHEZ, J. J., KOSHEL, S., ZAPOROZHCHENKO, V., ADLER, C. J., SARKISSIAN, C. S. I. D., BRANDT, G., SCHWARZ, C., NICKLISCH, N., DRESELY, V., FRITSCH, B., BALANOVSKA, E., VILLEMS, R., MELLER, H., ALT, K. W., COOPER, A. & CONSORTIUM, G. 2010. Ancient DNA from European early Neolithic farmers reveals their Near Eastern affinities. *PLOS Biology,* 8**,** e1000536.

HAASE-SCHRAMM, A., GOLDSTEIN, S. L. & STEIN, M. 2004. U-Th dating of Lake Lisan (late Pleistocene Dead Sea) aragonite and implications for glacial East Mediterranean climate change. *Geochimica et Cosmochimica Acta,* 68**,** 985-1005.

HALLIDAY, A. N., LEE, D. C., CHRISTENSEN, J. N., WALDER, A. J., FREEDMAN, P. A., JONES, C. E., HALL, C. M., YI, W. & TEAGLE, D. 1995. Recent developments in inductively-coupled plasma magnetic-sector multiple collector mass-spectrometry. *International Journal of Mass Spectrometry and Ion Processes,* 146**,** 21-33.

HAMMER, O., HARPER, D. A. T. & RYAN, P. D. 2001. *PAST: Paleontological Statistics software package for education and data analysis* [Online]. Available: http://folk.uio.no/ohammer/past [Accessed 1 May 2013].

HANSON, J., SATO, M. M. & RUEDY, R. 2012. Perception of climate change. *PNAS,* 109**,** E2415.

HARDING, A., PALUTIKOF, J. & HOLT, T. 2009. The Climate System. *In:* WOODWARD, J. (ed.) *The Physical Geography of the Mediterranean.* Oxford: Oxford University Press.

HARDY, R. & TUCKER, M. 1988. X-ray Powder Diffraction of Sediments. *In:* TUCKER, M. (ed.) *Techniques in Sedimentology.* Oxford: Blackwell.

HAUG, G. H., HUGHEN, K. A., SIGMAN, D. M., PETERSON, L. C. & ROHL, U. 2001. Southward migration of the intertropical convergence zone through the Holocene. *Science,* 293**,** 1304-1308.

HAYS, P. D. & GROSSMAN, E. L. 1991. Oxygen isotopes in meteoric calcite cements as indicators of continental paleoclimate. *Geology,* 19**,** 441-444.

HEATON, T. H. E. & CHENERY, C. A. 1990. Use of zinc turnings in the reduction of water to hydrogen for isotopic analysis. *NERC Isotope Geosciences Report 24*.

HELLSTROM, J. 2003. Rapid and accurate U/Th dating using parallel ion-counting multi-collector ICP-MS. *Journal of Analytical Atomic Spectrometry,* 18**,** 1346-1351.

HEM, J. D. 1970. *Study and Interpretation of the Chemical Characteristics of Natural Water,* Washington, United States Government Printing Office.

HEMMING, S. R. 2004. Heinrich events: massive late pleistocene detritus layers of the North Atlantic and their global climate imprint. *Reviews of Geophysics,* 42**,** RG1005.

HENDERSON, A. K., NELSON, D. M., HU, F. S., HUANG, Y. S., SHUMAN, B. N. & WILLIAMS, J. W. 2010. Holocene precipitation seasonality captured by a dual hydrogen and oxygen isotope approach at Steel Lake, Minnesota. *Earth and Planetary Science Letters,* 300**,** 205-214.

HILLAIRE-MARCEL, C., DE VERNAL, A. & PIPER, D. J. W. 2007. Lake Agassiz final drainage event in the northwest North Atlantic. *Geophysical Research Letters,* 34**,** L15601.

HILLMAN, G. 1996. Late Pleistocene Changes in Wild Plant-Foods Available to Hunter-Gatherers of the Northern Fertile Crescent: Possible Preludes to Cereal Cultivation. *In:* HARRIS, D. R. (ed.) *The Origins and Spread of Agriculture and Pastoralism in Eurasia.* London: UCL Press.

HOEFS, J. 2009. *Stable Isotope Geochemistry,* Berlin, Springer-Verlag.

HOFFMAN, J. S., CARLSON, A. E., WINSOR, K., KLINKHAMMER, G. P., LEGRANDE, A. N., ANDREWS, J. T. & STRASSER, J. C. 2012. Linking the 8.2 ka event and its freshwater forcing in the Labrador Sea. *Geophysical Research Letters,* 39**,** L18703.

HOLMES, J. A. & CHIVAS, A. 2002. Ostracod Shell Chemistry - Overview. *In:* HOLMES, J. A. & CHIVAS, A. (eds.) *The Ostracoda: Applications in Quaternary Research.* Washington DC: American Geophysical Union.

HOOGAKKER, B. A. A., CHAPMAN, M. R., MCCAVE, I. N., HILLAIRE-MARCEL, C., ELLISON, C. R. W., HALL, I. R. & TELFORD, R. J. 2011. Dynamics of North Atlantic deep water masses during the Holocene. *Paleoceanography,* 26**,** PA4214.

HOWIE, R. A. & BROADHURST, F. M. 1958. X-Ray data for dolomite and ankerite. *American Mineralogist,* 43**,** 1210-1214.

HU, C. Y., HENDERSON, G. M., HUANG, J. H., XIE, S., SUN, Y. & JOHNSON, K. R. 2008. Quantification of Holocene Asian monsoon rainfall from spatially separated cave records. *Earth and Planetary Science Letters,* 266**,** 221-232.

HUGHEN, K. A., OVERPECK, J. T., PETERSON, L. C. & TRUMBORE, S. 1996. Rapid climate changes in the tropical Atlantic region during the last deglaciation. *Nature,* 380**,** 51-54.

HUNTINGFORD, C., JONES, P. D., LIVINA, V. N., LENTON, T. M. & COX, P. M. 2013. No increase in global temperature variability despite changing regional patterns. *Nature,* 500**,** 327-330.

IAEA/WMO. 2013. *Global Network of Isotopes in Precipitation* [Online]. Available: http://www.iaea.org/water [Accessed 4 January 2013].

ILER, R. 1979. *The Chemistry of Silica. Solubility, Polymerization, Colloid and Surface Properties, and Biochemistry,* London, John Wiley and Sons.

ISSAR, A. & ADAR, E. 2010. Progressive development of water resources in the Middle East for sustainable water supply in a period of climate change. *Philosophical Transactions of the Royal Society A - Mathematical Physical and Engineering Sciences,* 368**,** 5339-5350.

ISSAR, A. & ZOHAR, M. 2007. *Climate Change: Environment and History of the Near East,* Berlin, Springer.

ITO, E. 2001. Application of Stable Isotope Techniques to Inorganic and Biogenic Carbonates. *In:* LAST, W. M. & SMOL, J. P. (eds.) *Tracking Environmental Change Using Lake Sediments. Volume 2: Physical and Geochemical Methods.* Dordrecht: Kluwer.

IVANOCHKO, T. S., GANESHRAM, R. S., BRUMMER, G. J. A., GANSSEN, G., JUNG, S. J. A., MORETON, S. G. & KROON, D. 2005. Variations in tropical convection as an

amplifier of global climate change at the millennial scale. *Earth and Planetary Science Letters,* 235**,** 302-314.

JIMENEZ-LOPEZ, C., ROMANEK, C. S., HUERTAS, F. J., OHMOTO, H. & CABALLERO, E. 2004. Oxygen isotope fractionation in synthetic magnesian calcite. *Geochimica et Cosmochimica Acta,* 68**,** 3367-3377.

JONES, M. D. 2004. *High-Resolution Records of Climate Change from Lacustrine Stable Isotopes through the Last Two Millennia in Western Turkey.* PhD, Plymouth.

JONES, M. D. 2013. What do we mean by wet? Geoarchaeology and the reconstruction of water availability. *Quaternary International,* 308-309**,** 76-79.

JONES, M. D., LENG, M. J., ROBERTS, C. N., TURKES, M. & MOYEED, R. 2005. A coupled calibration and modelling approach to the understanding of dry-land lake oxygen isotope records. *Journal of Paleolimnology,* 34**,** 391-411.

JONES, M. D. & ROBERTS, C. N. 2008. Interpreting lake isotope records of Holocene environmental change in the Eastern Mediterranean. *Quaternary International,* 181**,** 32-38.

JONES, M. D., ROBERTS, C. N. & LENG, M. J. 2007. Quantifying climatic change through the last glacial-interglacial transition based on lake isotope palaeohydrology from central Turkey. *Quaternary Research,* 67**,** 463-473.

JONES, M. D., ROBERTS, C. N., LENG, M. J. & TURKES, M. 2006. A high-resolution late Holocene lake isotope record from Turkey and links to North Atlantic and monsoon climate. *Geology,* 34**,** 361-364.

JONES, T. D., LAWSON, I. T., REED, J., WILSON, G. P., LENG, M. J., GIERGA, M., BERNASCONI, S. M., SMITTENBERG, R. H., HAJDAS, I., BRYANT, C. L. & TZEDAKIS, P. C. 2013. Diatom-inferred late Pleistocene and Holocene palaeolimnological changes in the Ioannina basin, northwest Greece. *Journal of Paleolimnology,* 49**,** 185-204.

JUNG, S. J. A., DAVIES, G. R., GANSSEN, G. M. & KROON, D. 2004. Stepwise Holocene aridification in NE Africa deduced from dust-borne radiogenic isotope records. *Earth and Planetary Science Letters,* 221**,** 27-37.

KANIEWSKI, D., PAULISSEN, E., VAN CAMPO, E., WEISS, H., OTTO, T., BRETSCHNEIDER, J. & VAN LERBERGHE, K. 2010. Late second-early first millennium BC abrupt climate changes in coastal Syria and their possible significance for the history of the Eastern Mediterranean. *Quaternary Research,* 74**,** 207-215.

KATZ, A. & NISHRI, A. 2013. Calcium, magnesium and strontium cycling in stratified, hardwater lakes: Lake Kinneret (Sea of Galilee), Israel. *Geochimica et Cosmochimica Acta,* 105**,** 372-394.

KELTS, K. 1988. Environments of Deposition of Lacustrine Petroleum Source Rocks: an Introduction. *In:* FLEET, K., KELTS, K. & TALBOT, M. R. (eds.) *Lacustrine Petroleum Source Rocks.* London: Geological Society of London Special Publication 40.

KELTS, K. & HSU, J. 1978. Freshwater Carbonate Sedimentation. *In:* LERMAN, A. (ed.) *Lakes: Geology, Chemistry and Physics.* New York: Springer-Verlag.

KELTS, K. & MCKENZIE, J. 1982. Diagenetic Dolomite Formation in Quaternary Anoxic Diatomaceous Muds of Deep Sea Drilling Project Leg 64, Gulf of California. *In:*

CURRAY, J. R. & MOORE, D. G. (eds.) *Initial Reports of the Deep Sea Drilling Project 64.* Washington DC: US Government Printing Office.

KELTS, K. & MCKENZIE, J. 1984. A Comparision of Anoxic Dolomite from Deep-Sea Sediments: Quaternary Gulf of California and Messinian Tripoli Formation of Sicily. *In:* GARRISON, R. E. (ed.) *Dolomite of the Monterey Formation and Other Organic-rich Units.* Los Angeles: Society of Economic Paleontologists and Mineralogists.

KELTS, K. & TALBOT, M. 1990. Lacustrine Carbonates as Geochemical Archives of Environmental Change and Biotic/Abiotic Interations. *In:* TILZER, M. & SERRUYA, C. (eds.) *Large Lakes: Ecological Structure and Function.* Berlin: Springer-Verlag.

KIM, S. T., MUCCI, A. & TAYLOR, B. E. 2007b. Phosphoric acid fractionation factors for calcite and aragonite between 25 and 75 degrees C: revisited. *Chemical Geology,* 246**,** 135-146.

KIM, S. T. & O'NEIL, J. R. 1997. Equilibrium and nonequilibrium oxygen isotope effects in synthetic carbonates. *Geochimica et Cosmochimica Acta,* 61**,** 3461-3475.

KIM, S. T., O'NEIL, J. R., HILLAIRE-MARCEL, C. & MUCCI, A. 2007a. Oxygen isotope fractionation between synthetic aragonite and water: influence of temperature and Mg2+ concentration. *Geochimica et Cosmochimica Acta,* 71**,** 4704-4715.

KITOH, A., YATAGAI, A. & ALPERT, P. 2008. First super-high-resolution model projection that the ancient “Fertile Crescent” will disappear in this century. *Hydrological Research Letters,* 2**,** 1-4.

KOLODNY, Y., STEIN, M. & MACHLUS, M. 2005. Sea-Rain-Lake relation in the Last Glacial East Mediterranean revealed by a delta O-18-delta C-13 in Lake Lisan aragonites. *Geochimica et Cosmochimica Acta,* 69**,** 4045-4060.

KOMOR, S. C. 1994. Bottom-Sediment Chemistry in Devils Lake, Northeastern North Dakota. *In:* RENAUT, R. W. & LAST, W. (eds.) *Sedimentology and Geochemistry of Modern and Ancient Saline Lakes.* Tulsa: Society of Economic Paleontologists and Mineralogists Special Publication 50.

KONING, E., GEHLEN, M., FLANK, A. M., CALAS, G. & EPPING, E. 2007. Rapid post-mortem incorporation of aluminum in diatom frustules: evidence from chemical and structural analyses. *Marine Chemistry,* 106**,** 208-222.

KOTTHOFF, U., KOUTSODENDRIS, A., PROSS, J., SCHMIEDL, G., BORNEMANN, A., KAUL, C., MARINO, G., PEYRON, O. & SCHIEBEL, R. 2011. Impact of Lateglacial cold events on the northern Aegean region reconstructed from marine and terrestrial proxy data. *Journal of Quaternary Science,* 26**,** 86-96.

KOTTHOFF, U., MULLER, U. C., PROSS, J., SCHMIEDL, G., LAWSON, I. T., VAN DE SCHOOTBRUGGE, B. & SCHULZ, H. 2008a. Lateglacial and Holocene vegetation dynamics in the Aegean region: an integrated view based on pollen data from marine and terrestrial archives. *Holocene,* 18**,** 1019-1032.

KOTTHOFF, U., PROSS, J., MULLER, U. C., PEYRON, O., SCHMIEDL, G., SCHULZ, H. & BORDON, A. 2008b. Climate dynamics in the borderlands of the Aegean Sea during formation of sapropel S1 deduced from a marine pollen record. *Quaternary Science Reviews,* 27**,** 832-845.

KUPER, R. & KROPELIN, S. 2006. Climate-controlled Holocene occupation in the Sahara: Motor of Africa's evolution. *Science,* 313**,** 803-807.

KUTIEL, H. & BENAROCH, Y. 2002. North Sea-Caspian Pattern (NCP) - an upper level atmospheric teleconnection affecting the Eastern Mediterranean: identification and definition. *Theoretical and Applied Climatology,* 71**,** 17-28.

KUTIEL, H. & TURKES, M. 2005. New evidence for the role of the North Sea-Caspian Pattern on the temperature and precipitation regimes in continental Central Turkey. *Geografiska Annaler Series A - Physical Geography,* 87A**,** 501-513.

KUZUCUOGLU, C. 2009. Climate and Environment in Times of Cultural Changes From the 4th to the 1st Millennium BC in the Near and Middle East. *In:* CARDARELLI, A., CAZZELLA, A., FRANGIPANE, M. & PERONI, R. (eds.) *Reasons for Change. 'Birth', 'Decline', and 'Collapse' of Societies Between the End of the 4th and Beginning of the 1st Millenium BC.* Rome: La Sapienza.

KUZUCUOGLU, C., DORFLER, W., KUNESCH, S. & GOUPILLE, F. 2011. Mid- to late-Holocene climate change in central Turkey: the Tecer Lake record. *Holocene,* 21**,** 173-188.

KUZUCUOGLU, C. & MARRO, C. 2007. *Human Societies and Climate Change at the End of the Third Millennium: Did a Crisis Take Place in Upper Mesopotamia?,* Istanbul, IFEA.

KWIECIEN, O., ARZ, H. W., LAMY, F., PLESSEN, B., BAHR, A. & HAUG, G. H. 2009. North Atlantic control on precipitation pattern in the eastern Mediterranean/Black Sea region during the last glacial. *Quaternary Research,* 71**,** 375-384.

LABEYRIE, L. D. & JUILLET, A. 1982. Oxygen isotopic exchangeability of diatom valve silica - interpretation and consequences for paleoclimatic studies. *Geochimica et Cosmochimica Acta,* 46**,** 967-975.

LAIRD, K. R., KINGSBURY, M. V., LEWIS, C. F. M. & CUMMING, B. F. 2011. Diatom-inferred depth models in 8 Canadian boreal lakes: inferred changes in the benthic:planktonic depth boundary and implications for assessment of past droughts. *Quaternary Science Reviews,* 30**,** 1201-1217.

LAMB, A. L., BREWER, T. S., LENG, M. J., SLOANE, H. J. & LAMB, H. F. 2007. A geochemical method for removing the effect of tephra on lake diatom oxygen isotope records. *Journal of Paleolimnology,* 37**,** 499-516.

LAMB, A. L., LENG, M. J., SLOANE, H. J. & TELFORD, R. J. 2005. A comparison of the palaeoclimate signals from diatom oxygen isotope ratios and carbonate oxygen isotope ratios from a low latitude crater lake. *Palaeogeography Palaeoclimatology Palaeoecology,* 223**,** 290-302.

LAND, L. S. 1980. The Isotopic and Trace Element Geochemistry of Dolomite: the State of the Art. *In:* ZENGER, D. H. (ed.) *Concepts and Models of Dolomitisation.* SEPM Special Publication 28.

LANDMANN, G. & KEMPE, S. 2005. Annual deposition signal versus lake dynamics: microprobe analysis of Lake Van (Turkey) sediments reveals missing varves in the period 11.2-10.2 ka BP. *Facies,* 51**,** 135-145.

LANGGUT, D., FINKELSTEIN, I. & LITT, T. 2013. Climate and the Late Bronze collapse: new evidence from the southern Levant. *Tel Aviv: Journal of the Institute of Archaeology of Tel Aviv University,* 40**,** 149-175.

LAO, Y. & BENSON, L. 1988. Uranium-Series age estimates and paleoclimatic significance of Pleistocene tufas from the Lahontan Basin, California and Nevada. *Quaternary Research,* 30**,** 165-176.

LASKAR, J., ROBUTEL, P., JOUTEL, F., GASTINEAU, M., CORREIA, A. C. M. & LEVRARD, B. 2004. A long-term numerical solution for the insolation quantities of the Earth. *Astronomy & Astrophysics,* 428**,** 261-285.

LAST, W. M. 1990. Lacustrine dolomite - an overview of modern, Holocene, and Pleistocene occurrences. *Earth-Science Reviews,* 27**,** 221-263.

LAWSON, I., FROGLEY, M., BRYANT, C., PREECE, R. & TZEDAKIS, P. 2004. The Lateglacial and Holocene environmental history of the Ioannina basin, north-west Greece. *Quaternary Science Reviews,* 23**,** 1599-1625.

LECOMPTE, M. A., GOODYEAR, A. C., DEMITROFF, M. N., BATCHELOR, D., VOGEL, E. K., MOONEY, C., ROCK, B. N. & SEIDEL, A. W. 2012. Independent evaluation of conflicting microspherule results from different investigations of the Younger Dryas impact hypothesis. *PNAS,* 109**,** E2960-E2969.

LEMCKE, G. & STÜRM, M. 1997. d18O and Trace Element Measurements as Proxy for the Reconstruction of Climate Changes at Lake Van (Turkey): preliminary Results. *In:* DALFEZ, H. N., KUKLA, G. & WEISS, H. (eds.) *Third Millennium BC Climate Change and the Old World Collapse.* Berlin: Springer Verlag.

LENG, M., BARKER, P., GREENWOOD, P., ROBERTS, N. & REED, J. 2001. Oxygen isotope analysis of diatom silica and authigenic calcite from Lake Pinarbasi, Turkey. *Journal of Paleolimnology,* 25**,** 343-349.

LENG, M. J. & BARKER, P. A. 2006. A review of the oxygen isotope composition of lacustrine diatom silica for palaeoclimate reconstruction. *Earth-Science Reviews,* 75**,** 5-27.

LENG, M. J. & HENDERSON, A. C. G. 2013. Recent advances in isotopes as palaeolimnological proxies. *Journal of Paleolimnology,* 49**,** 481-496.

LENG, M. J., JONES, M. D., FROGLEY, M. R., EASTWOOD, W. J., KENDRICK, C. P. & ROBERTS, C. N. 2010. Detrital carbonate influences on bulk oxygen and carbon isotope composition of lacustrine sediments from the Mediterranean. *Global and Planetary Change,* 71**,** 175-182.

LENG, M. J., LAMB, A. L., HEATON, T. H. E., MARSHALL, J. D., WOLFE, B., JONES, M. D., HOLMES, J. A. & ARROWSMITH, C. 2006. Isotopes in Lake Sediments. *In:* LENG, M. J. (ed.) *Isotopes in Palaeoenvironmental Research.* Dordrecht: Springer.

LENG, M. J. & MARSHALL, J. D. 2004. Palaeoclimate interpretation of stable isotope data from lake sediment archives. *Quaternary Science Reviews,* 23**,** 811-831.

LENG, M. J. & SLOANE, H. J. 2008. Combined oxygen and silicon isotope analysis of biogenic silica. *Journal of Quaternary Science,* 23**,** 313-319.

LENG, M. J. & SWANN, G. E. A. 2010. Stable Isotopes from Diatom Silica. *In:* SMOL, J. P. & STOERMER, E. F. (eds.) *The Diatoms: Applications for the Environmental and Earth Sciences.* Cambridge: Cambridge University Press.

LENG, M. J., WAGNER, B., BOEHM, A., PANAGIOTOPOULOS, K., VANE, C. H., SNELLING, A., HAIDON, C., WOODLEY, E., VOGEL, H., ZANCHETTA, G. & BANESCHI, I. 2013. Understanding past climatic and hydrological variability in the Mediterranean from Lake Prespa sediment isotope and geochemical record over the Last Glacial cycle. *Quaternary Science Reviews,* 66**,** 123-136.

LEROY, S. A. G. & ARPE, K. 2007. Glacial refugia for summer-green trees in Europe and south-west Asia as proposed by ECHAM3 time-slice atmospheric model simulations. *Journal of Biogeography,* 34**,** 2115-2128.

LEUENBERGER, M. C., LANG, C. & SCHWANDER, J. 1999. Delta(15)N measurements as a calibration tool for the paleothermometer and gas-ice age differences: a case study for the 8200 BP event on GRIP ice. *Journal of Geophysical Research - Atmospheres,* 104**,** 22163-22170.

LI, H. C. & KU, T. L. 1997. delta C-13-delta O-18 covariance as a paleohydrological indicator for closed-basin lakes. *Palaeogeography Palaeoclimatology Palaeoecology,* 133**,** 69-80.

LIN, J. C., BROECKER, W. S., ANDERSON, R. F., HEMMING, S., RUBENSTONE, J. L. & BONANI, G. 1996. New Th-230/U and C-14 ages from Lake Lahontan carbonates, Nevada, USA, and a discussion of the origin of initial thorium. *Geochimica et Cosmochimica Acta,* 60**,** 2817-2832.

LITT, T., OHLWEIN, C., NEUMANN, F. H., HENSE, A. & STEIN, M. 2012. Holocene climate variability in the Levant from the Dead Sea pollen record. *Quaternary Science Reviews,* 49**,** 95-105.

LIU, Y.-H., HENDERSON, G. M., HU, C.-Y., MASON, A. J., CHARNLEY, N., JOHNSON, K. R. & XIE, S.-C. 2013. Links between the East Asian monsoon and North Atlantic climate during the 8,200 year event. *Nature Geoscience,* 6**,** 117-120.

LIVINGSTONE, D. A. 1955. A lightweight piston sampler for lake deposits. *Ecology,* 36**,** 137-139.

LOWE, J. J. & WALKER, M. J. C. 1997. *Reconstructing Quaternary environments,* Harlow, Pearson.

LUDWIG, K. R. 2012. User's manual for Isoplot 3.75. *Berkeley Geochronological Center Special Publication No. 5*.

LUDWIG, K. R., SIMMONS, K. R., SZABO, B. J., WINOGRAD, I. J., LANDWEHR, J. M., RIGGS, A. C. & HOFFMAN, R. J. 1992. Mass-spectrometric Th-230-U-234-U-238 dating of the Devils-Hole calcite vein. *Science,* 258**,** 284-287.

LUDWIG, K. R. & TITTERINGTON, D. M. 1994. Calculation of (230)Th/U isochrons, ages, and errors. *Geochimica et Cosmochimica Acta,* 58**,** 5031-5042.

LUMSDEN, D. N. 1979. Discrepancy between thin-section and x-ray estimates of dolomite in limestone. *Journal of Sedimentary Petrology,* 49**,** 429-436.

LUO, S. D. & KU, T. L. 1991. U-series isochron dating - a generalized-method employing total-sample dissolution. *Geochimica et Cosmochimica Acta,* 55**,** 555-564.

MACKAY, A. W., KARABANOV, E., LENG, M. J., SLOANE, H. J., MORLEY, D. W., PANIZZO, V. N., KHURSEVICH, G. & WILLIAMS, D. 2008. Reconstructing hydrological variability in Lake Baikal during MIS 11: an application of oxygen isotope analysis of diatom silica. *Journal of Quaternary Science,* 23**,** 365-374.

MACKAY, A. W., SWANN, G. E. A., BREWER, T. S., LENG, M. J., MORLEY, D. W., PIOTROWSKA, N., RIOUAL, P. & WHITE, D. 2011. A reassessment of late glacial-Holocene diatom oxygen isotope record from Lake Baikal using a geochemical mass-balance approach. *Journal of Quaternary Science,* 26**,** 627-634.

MACKERETH, F. J. H. 1958. A portable core sampler for lake deposits. *Limnology and Oceanography,* 3**,** 181-191.

MAGNY, M., DE BEAULIEU, J. L., DRESCHER-SCHNEIDER, R., VANNIERE, B., WALTER-SIMONNET, A. V., MIRAS, Y., MILLETA, L., BOSSUETA, G., PEYRON, O., BRUGLAPAGLIA, E. & LEROUX, A. 2007. Holocene climate changes in the

central Mediterranean as recorded by lake-level fluctuations at Lake Accesa (Tuscany, Italy). *Quaternary Science Reviews,* 26**,** 1736-1758.

MAHER, L. A., BANNING, E. B. & CHAZAN, M. 2011. Oasis or mirage? Assessing the role of abrupt climate change in the prehistory of the southern Levant. *Cambridge Archaeological Journal,* 21**,** 1-29.

MARSHALL, M. H., LAMB, H. F., HUWS, D., DAVIES, S. J., BATES, R., BLOEMENDAL, J., BOYLE, J., LENG, M. J., UMER, M. & BRYANT, C. 2011. Late Pleistocene and Holocene drought events at Lake Tana, the source of the Blue Nile. *Global and Planetary Change,* 78**,** 147-161.

MASI, A., SADORI, L., ZANCHETTA, G., BANESCHI, I. & GIARDINI, M. 2013. Climatic interpretation of carbon isotope content of mid-Holocene archaeological charcoals from eastern Anatolia. *Quaternary International,* 303**,** 64-72.

MAYEWSKI, P. A., ROHLING, E. E., STAGER, J. C., KARLEN, W., MAASCH, K. A., MEEKER, L. D., MEYERSON, E. A., GASSE, F., VAN KREVELD, S., HOLMGREN, K., LEE-THORP, J., ROSQVIST, G., RACK, F., STAUBWASSER, M., SCHNEIDER, R. R. & STEIG, E. J. 2004. Holocene climate variability. *Quaternary Research,* 62**,** 243-255.

MAZZULLO, S. J. 2000. Organogenic dolomitization in peritidal to deep-sea sediments. *Journal of Sedimentary Research,* 70**,** 10-23.

MCCREA, J. 1950. On the isotopic chemistry of carbonates and palaeo-temperature scale. *Journal of Chemical Physics,* 18**,** 849-857.

MCCULLOCH, M. T. & MORTIMER, G. E. 2008. Applications of the U-238-Th-230 decay series to dating of fossil and modern corals using MC-ICPMS. *Australian Journal of Earth Sciences,* 55**,** 955-965.

MCGARRY, S., BAR-MATTHEWS, M., MATTHEWS, A., VAKS, A., SCHILMAN, B. & AYALON, A. 2004. Constraints on hydrological and paleotemperature variations in the Eastern Mediterranean region in the last 140 ka given by the delta D values of speleothem fluid inclusions. *Quaternary Science Reviews,* 23**,** 919-934.

MCGOWAN, S., JUHLER, R. K. & ANDERSON, N. J. 2008. Autotrophic response to lake age, conductivity and temperature in two West Greenland lakes. *Journal of Paleolimnology,* 39**,** 301-317.

MCGOWAN, S., RYVES, D. B. & ANDERSON, N. J. 2003. Holocene records of effective precipitation in West Greenland. *Holocene,* 13**,** 239-249.

MCLAREN, S. J., GILBERTSON, D. D., GRATTAN, J. P., HUNT, C. O., DULLER, G. A. T. & BARKER, G. A. 2004. Quaternary palaeogeomorphologic evolution of the Wadi Faynan area, southern Jordan. *Palaeogeography Palaeoclimatology Palaeoecology,* 205**,** 131-154.

MEEHL, G. A., STOCKER, T. F., COLLINS, P., FRIEDLINGSTEIN, P., GAYE, A. T., GREGORY, J. M., KITOH, A., KNUTTI, R., MURPHY, J. M., NODA, A., RAPER, S. C. B., WATTERSON, I. G., WEAVER, A. J. & ZHAO, Z. C. 2007. Global Climate Projections. *In:* SOLOMON, S., QIN, D., MANNING, M., CHEN, Z., MARQUIS, M., AVERYT, K. B., TIGNOR, M. & MILLER, H. L. (eds.) *Climate Change 2007: The Physical Science Basis. Contribution of Working Group I to the Fourth Assessment Report of the Intergovernmental Panel on Climate Change* Cambridge: Cambridge University Press.

METEOROLOJI-BULTENI 1974. *State Meteorological Services,* Ankara.

MEYERS, P. A. & TERANES, J. L. 2001. Sediment Organic Matter. *In:* LAST, M. & SMOL, J. P. (eds.) *Tracking Environmental Change Using Lake Sediments. Volume 2: Physical and Geochemical Methods.* Dordrecht: Kluwer.

MIGOWSKI, C., STEIN, M., PRASAD, S., NEGENDANK, J. F. W. & AGNON, A. 2006. Holocene climate variability and cultural evolution in the Near East from the Dead Sea sedimentary record. *Quaternary Research,* 66**,** 421-431.

MILNER, A. M., COLLIER, R. E. L., ROUCOUX, K. H., MULLER, U. C., PROSS, J., KALAITZIDIS, S., CHRISTANIS, K. & TZEDAKIS, P. C. 2012. Enhanced seasonality of precipitation in the Mediterranean during the early part of the Last Interglacial. *Geology,* 40**,** 919-922.

MORLEY, D. W., LENG, M. J., MACKAY, A. W. & SLOANE, H. J. 2005. Late glacial and Holocene environmental change in the Lake Baikal region documented by oxygen isotopes from diatom silica. *Global and Planetary Change,* 46**,** 221-233.

MORLEY, D. W., LENG, M. J., MACKAY, A. W., SLOANE, H. J., RIOUAL, P. & BATTARBEE, R. W. 2004. Cleaning of lake sediment samples for diatom oxygen isotope analysis. *Journal of Paleolimnology,* 31**,** 391-401.

MORRILL, C. & JACOBSEN, R. M. 2005. How widespread were climate anomalies 8200 years ago? *Geophysical Research Letters,* 32**,** L19701.

MOSCHEN, R., LUCKE, A., PARPLIES, J., RADTKE, U. & SCHLESER, G. H. 2006. Transfer and early diagenesis of biogenic silica oxygen isotope signals during settling and sedimentation of diatoms in a temperate freshwater lake (Lake Holzmaar, Germany). *Geochimica et Cosmochimica Acta,* 70**,** 4367-4379.

MOSCHEN, R., LUCKE, A. & SCHLESER, G. H. 2005. Sensitivity of biogenic silica oxygen isotopes to changes in surface water temperature and palaeoclimatology. *Geophysical Research Letters,* 32**,** L07708.

MULLER, G., FORSTNER, U. & IRION, G. 1972. Formation and diagenesis of inorganic Ca-Mg carbonates in lacustrine environment. *Naturwissenschaften,* 59**,** 158-164.

MUSCHELER, R., BEER, J. & VONMOOS, M. 2004. Causes and timing of the 8200 yr BP event inferred from the comparison of the GRIP (10)Be and the tree ring Delta(14)C record. *Quaternary Science Reviews,* 23**,** 2101-2111.

MUSCHELER, R., BEER, R., KUBIK, P. W. & SYNAL, H. A. 2005. Geomagnetic field intensity during the last 60,000 years based on Be-10 and Cl-36 from the Summit ice cores and C-14. *Quaternary Science Reviews,* 24**,** 1849-1860.

NEEV, D. & EMERY, K. O. 1995. *The destruction of Sodom, Gomorrah, and Jericho,* Oxford, Oxford University Press.

NEUMANN, F. H., KAGAN, E. J., SCHWAB, M. J. & STEIN, M. 2007. Palynology, sedimentology and palaeoecology of the late Holocene Dead Sea. *Quaternary Science Reviews,* 26**,** 1476-1498.

O'NEIL, J. R., CLAYTON, R. N. & MAYEDA, T. K. 1969. Oxygen isotope fractionation in divalent metal carbonates. *Journal of Chemical Physics,* 51**,** 5547-5559.

O'SULLIVAN, P. E. 1983. Annually-laminated lake sediments and the study of Quaternary environmental changes - a review. *Quaternary Science Reviews,* 1**,** 245-313.

OCAKOGLU, F., KIR, O., YILMAZ, I. O., ACIKALIN, S., ERAYIK, C., TUNOGLU, C. & LEROY, S. A. G. 2013. Early to mid-Holocene lake level and temperature records from

the terraces of Lake Sunnet in NW Turkey. *Palaeogeography Palaeoclimatology Palaeoecology,* 369**,** 175-184.

OJALA, A. E. K., FRANCUS, P., ZOLITSCHKA, B., BESONEN, M. & LAMOUREUX, S. F. 2012. Characteristics of sedimentary varve chronologies - a review. *Quaternary Science Reviews,* 43**,** 45-60.

OJALA, A. E. K., SAARINEN, T. & SALONEN, V.-P. 2000. Preconditions for the formation of annually laminated lake sediments in southern and central Finland. *Boreal Environmental Research,* 5**,** 243-255.

ORLAND, I. J., BAR-MATTHEWS, M., AYALON, A., MATTHEWS, A., KOZDON, R., USHIKUBO, T. & VALLEY, J. W. 2012. Seasonal resolution of Eastern Mediterranean climate change since 34 ka from a Soreq Cave speleothem. *Geochimica et Cosmochimica Acta,* 89**,** 240-255.

ORLAND, I. J., BAR-MATTHEWS, M., KITA, N. T., AYALON, A., MATTHEWS, A. & VALLEY, J. W. 2009. Climate deterioration in the Eastern Mediterranean as revealed by ion microprobe analysis of a speleothem that grew from 2.2 to 0.9 ka in Soreq Cave, Israel. *Quaternary Research,* 71**,** 27-35.

ORTEGA, R., MAIRE, R., DEVES, G. & QUINIF, Y. 2005. High-resolution mapping of uranium and other trace elements in recrystallized aragonite-calcite speleothems from caves in the Pyrenees (France): implication for U-series dating. *Earth and Planetary Science Letters,* 237**,** 911-923.

OSMOND, J. K., MAY, J. P. & TANNER, W. F. 1970. Age of the Cape Kennedy barrier-and-lagoon complex. *Journal of Geophysical Research,* 75**,** 5459-5468.

PANIZZO, V. N., JONES, V. J., BIRKS, H. J. B., BOYLE, J. F., BROOKS, S. J. & LENG, M. J. 2008. A multiproxy palaeolimnological investigation of Holocene environmental change, between c. 10 700 and 7200 years BP, at Holebudalen, southern Norway. *Holocene,* 18**,** 805-817.

PARKER, A. G., GOUDIE, A. S., STOKES, S., WHITE, K., HODSON, M. J., MANNING, M. & KENNET, D. 2006. A record of Holocene climate change from lake geochemical analyses in southeastern Arabia. *Quaternary Research,* 66**,** 465-476.

PARRY, M. L. 1978. *Studies in Historical Geography: Climate Change, Agriculture and Settlement,* Folkestone, Dawson Publishing.

PEYRON, O., GORING, S., DORMOY, I., KOTTHOFF, U., PROSS, J., DE BEAULIEU, J. L., DRESCHER-SCHNEIDER, R., VANNIERE, B. & MAGNY, M. 2011. Holocene seasonality changes in the central Mediterranean region reconstructed from the pollen sequences of Lake Accesa (Italy) and Tenaghi Philippon (Greece). *Holocene,* 21**,** 131-146.

PIETERS, R. & LAWRENCE, G. A. 2009. Effect of salt exclusion from lake ice on seasonal circulation. *Limnology and Oceanography,* 54**,** 401-412.

PLACZEK, C., PATCHETT, P. J., QUADE, J. & WAGNER, J. D. M. 2006. Strategies for successful U-Th dating of paleolake carbonates: an example from the Bolivian Altiplano. *Geochemistry Geophysics Geosystems,* 7**,** Q05024.

POSSEHL, G. L. 1997. The transformation of the Indus civilization (Cultural history, deurbanization, third-millennium-BC). *Journal of World Prehistory,* 11**,** 425-472.

POWERS, L., WERNE, J. P., VANDERWOUDE, A. J., DAMSTE, J. S. S., HOPMANS, E. C. & SCHOUTEN, S. 2010. Applicability and calibration of the TEX86 paleothermometer in lakes. *Organic Geochemistry,* 41**,** 404-413.

PRASAD, S., VOS, H., NEGENDANK, J. F. W., WALDMANN, N., GOLDSTEIN, S. L. & STEIN, M. 2004. Evidence from Lake Lisan of solar influence on decadal- to centennial-scale climate variability during marine oxygen isotope stage 2. *Geology,* 32**,** 581-584.

PRASAD, S., WITT, A., KIENEL, U., DULSKI, P., BAUER, E. & YANCHEVA, G. 2009. The 8.2 ka event: evidence for seasonal differences and the rate of climate change in western Europe. *Global and Planetary Change,* 67**,** 218-226.

PROSS, J., KOTTHOFF, U., MULLER, U. C., PEYRON, O., DORMOY, I., SCHMIEDL, G., KALAITZIDIS, S. & SMITH, A. M. 2009. Massive perturbation in terrestrial ecosystems of the Eastern Mediterranean region associated with the 8.2 kyr BP climatic event. *Geology,* 37**,** 887-890.

RASMUSSEN, S. O., ANDERSEN, K. K., SVENSSON, A. M., STEFFENSEN, J. P., VINTHER, B. M., CLAUSEN, H. B., SIGGAARD-ANDERSEN, M. L., JOHNSEN, S. J., LARSEN, L. B., DAHL-JENSEN, D., BIGLER, M., ROTHLISBERGER, R., FISCHER, H., GOTO-AZUMA, K., HANSSON, M. E. & RUTH, U. 2006. A new Greenland ice core chronology for the last glacial termination. *Journal of Geophysical Research-Atmospheres,* 111**,** 1-16.

REEDER, R. J., NUGENT, M., TAIT, C. D., MORRIS, D. E., HEALD, S. M., BECK, K. M., HESS, W. P. & LANZIROTTI, A. 2001. Coprecipitation of uranium(VI) with calcite: XAFS, micro-XAS, and luminescence characterization. *Geochimica Et Cosmochimica Acta,* 65**,** 3491-3503.

REIMER, A., LANDMANN, G. & KEMPE, S. 2009. Lake Van, eastern Anatolia, hydrochemistry and history. *Aquatic Geochemistry,* 15**,** 195-222.

REN, H., BRUNELLE, B. G., SIGMAN, D. M. & ROBINSON, R. S. 2013. Diagenetic aluminum uptake into diatom frustules and the preservation of diatom-bound organic nitrogen. *Marine Chemistry,* 155**,** 92-101.

RENSSEN, H., BROVKIN, V., FICHEFET, T. & GOOSSE, H. 2006. Simulation of the Holocene climate evolution in Northern Africa: the termination of the African Humid Period. *Quaternary International,* 150**,** 95-102.

RENSSEN, H., GOOSSE, H. & FICHEFET, T. 2007. Simulation of Holocene cooling events in a coupled climate model. *Quaternary Science Reviews,* 26**,** 2019-2029.

ROBERTS, C. N. in press. The Climate of Neolithic Anatolia. *In:* ÖZDOĞAN, M., BAŞGELEM, N. & KUNIHOLM, P. I. (eds.) *The Neolithic in Turkey.* Istanbul: Archaeology and Art Publications.

ROBERTS, C. N., STEVENSON, T., DAVIS, B., CHEDDADI, R., BREWER, S. & ROSEN, A. 2004. Holocene Climate, Environment and Cultural Change in the Circum-Mediterranean Region. *In:* BATTARBEE, R. W., GASSE, F. & STICKLEY, C. E. (eds.) *Past Climate Variability through Europe and Africa.* Dordrecht: Springer.

ROBERTS, C. N., ZANCHETTA, G. & JONES, M. D. 2010. Oxygen isotopes as tracers of Mediterranean climate variability: an introduction. *Global and Planetary Change,* 71**,** 135-140.

ROBERTS, N. 2002. Did prehistoric landscape management retard the post-glacial spread of woodland in Southwest Asia? *Antiquity,* 76**,** 1002-1010.

ROBERTS, N., BRAYSHAW, D., KUZUCUOGLU, C., PEREZ, R. & SADORI, L. 2011b. The mid-Holocene climatic transition in the Mediterranean: causes and consequences. *Holocene,* 21**,** 3-13.

ROBERTS, N., EASTWOOD, W. J., KUZUCUOGLU, C., FIORENTINO, G. & CARACUTA, V. 2011a. Climatic, vegetation and cultural change in the eastern Mediterranean during the mid-Holocene environmental transition. *Holocene,* 21**,** 147-162.

ROBERTS, N., JONES, M. D., BENKADDOUR, A., EASTWOOD, W. J., FILIPPI, M. L., FROGLEY, M. R., LAMB, H. F., LENG, M. J., REED, J. M., STEIN, M., STEVENS, L., VALERO-GARCES, B. & ZANCHETTA, G. 2008. Stable isotope records of Late Quaternary climate and hydrology from Mediterranean lakes: the ISOMED synthesis. *Quaternary Science Reviews,* 27**,** 2426-2441.

ROBERTS, N., REED, J. M., LENG, M. J., KUZUCUOGLU, C., FONTUGNE, M., BERTAUX, J., WOLDRING, H., BOTTEMA, S., BLACK, S., HUNT, E. & KARABIYIKOGLU, M. 2001. The tempo of Holocene climatic change in the eastern Mediterranean region: new high-resolution crater-lake sediment data from central Turkey. *Holocene,* 11**,** 721-736.

ROBERTS, N. & ROSEN, A. 2009. Diversity and complexity in early farming communities of Southwest Asia: new insights into the economic and environmental basis of Neolithic Catalhoyuk. *Current Anthropology,* 50**,** 393-402.

ROBERTS, N. & WRIGHT, H. E. 1993. Vegetational, Lake Level and Climatic History of the Near East and Southwest Asia. *In:* WRIGHT JR, H. E., KUTZBACH, J. E., WEBB III, T., RUDDIMAN, W. F., STREET-PERROTT, F. A. & BARTLEIN, P. J. (eds.) *Global Climates Since the Last Glacial Maximum.* Minneapolis: University of Minnesota Press.

ROBINSON, S. A., BLACK, S., SELLWOOD, B. W. & VALDES, P. J. 2006. A review of palaeoclimates and palaeoenvironments in the Levant and Eastern Mediterranean from 25,000 to 5000 years BP: setting the environmental background for the evolution of human civilisation. *Quaternary Science Reviews,* 25**,** 1517-1541.

ROHLING, E. J., HAYES, A., MAYEWSKI, P. A. & KUCERA, M. 2009. Holocene Climate Variability in the Eastern Mediterranean, and the End of the Bronze Age. *In:* BACHHUBER, C. & ROBERTS, G. (eds.) *Forces of Transformation: The End of the Bronze Age in the Mediterranean.* Oxford: Oxbow Press.

ROHLING, E. J. & PALIKE, H. 2005. Centennial-scale climate cooling with a sudden cold event around 8,200 years ago. *Nature,* 434**,** 975-979.

ROMERO-VIANA, L., JULIA, R., CAMACHO, A., VICENTE, E. & MIRACLE, M. R. 2008. Climate signal in varve thickness: Lake La Cruz (Spain), a case study. *Journal of Paleolimnology,* 40**,** 703-714.

ROSEN, A. 2007. *Civilizing Climate,* Plymouth, AltaMira Press.

ROSENBAUM, J. & SHEPPARD, S. M. F. 1986. An isotopic study of siderites, dolomites and ankerites at high-temperatures. *Geochimica et Cosmochimica Acta,* 50**,** 1147-1150.

ROSSIGNOL-STRICK, M. 1999. The Holocene climatic optimum and pollen records of sapropel 1 in the eastern Mediterranean, 9000-6000 BP. *Quaternary Science Reviews,* 18**,** 515-530.

ROWE, P. J., ATKINSON, T. C. & TURNER, C. 1999. U-series dating of Hoxnian interglacial deposits at Marks Tey, Essex, England. *Journal of Quaternary Science,* 14**,** 693-702.

ROWE, P. J., MASON, J. E., ANDREWS, J. E., MARCA, A. D., THOMAS, L., VAN CALSTEREN, P., JEX, C. N., VONHOF, H. B. & AL-OMARI, S. 2012. Speleothem isotopic evidence of winter rainfall variability in northeast Turkey between 77 and 6 ka. *Quaternary Science Reviews,* 45**,** 60-72.

ROZANSKI, K., ARAGUASARAGUAS, L. & GONFIANTINI, R. 1992. Relation between long-term trends of O-18 isotope composition of precipitation and climate. *Science,* 258**,** 981-985.

ROZANSKI, K., KLISCH, M. A., WACHNIEW, P., GORCZYCA, Z., GOSLAR, T., EDWARDS, T. W. D. & SHEMESH, A. 2010. Oxygen-isotope geothermometers in lacustrine sediments: new insights through combined delta O-18 analyses of aquatic cellulose, authigenic calcite and biogenic silica in Lake Gosciaz, central Poland. *Geochimica et Cosmochimica Acta,* 74**,** 2957-2969.

RUBINSON, M. & CLAYTON, R. N. 1969. Carbon-13 fractionation between aragonite and calcite. *Geochimica et Cosmochimica Acta,* 33**,** 997–1002.

SABINS, F. F. 1962. Grains of detrital, secondary, and primary dolomite from Cretaceous Strata of the western interior. *Geological Society of America Bulletin,* 73**,** 1183-1196.

SAKAGUCHI, A., YAMAMOTO, M., TOMITA, J., MINO, K., SASAKI, K., KASHIWAYA, K. & KAWAI, T. 2009. Uranium-series chronology for sediments of Lake Hovsgol, Mongolia, and the 1-Ma records of uranium and thorium isotopes from the HDP-04 drill core. *Quaternary International,* 205**,** 65-73.

SANDWEISS, D. H. & QUILTER, J. 2012. Collation, Correlation, and Causation in the Prehistory of Coastal Peru. *In:* COOPER, J. & SHEETS, P. (eds.) *Surviving Sudden Environmental Change.* Boulder: University Press of Colorado.

SARıKAYA, M. A., ZREDA, M. & CINER, A. 2009. Glaciations and paleoclimate of Mount Erciyes, central Turkey, since the Last Glacial Maximum, inferred from Cl-36 cosmogenic dating and glacier modeling. *Quaternary Science Reviews,* 28**,** 2326-2341.

SCHIFF, C., KAUFMAN, D., WOLFE, A., DODD, J. & SHARP, Z. 2009. Late Holocene storm-trajectory changes inferred from the oxygen isotope composition of lake diatoms, south Alaska. *Journal of Paleolimnology,* 41**,** 189-208.

SCHILMAN, B., BAR-MATTHEWS, M., ALMOGI-LABIN, A. & LUZ, B. 2001. Global climate instability reflected by Eastern Mediterranean marine records during the late Holocene. *Palaeogeography Palaeoclimatology Palaeoecology,* 176**,** 157-176.

SCHMIDT, M., BOTZ, R., RICKERT, D., BOHRMANN, G., HALL, S. & MANN, S. 2001. Oxygen isotope of marine diatoms and relations to opal-A maturation. *Geochimica et Cosmochimica Acta,* 65.

SCHULZ, M. & PAUL, A. 2002. Holocene Climate Variability on Centennial to Millennial Time Scales: 1. Climate Records from the North Atlantic Realm. *In:* WEFER, G., BERGER, W., BEHRE, K. E. & JANSEN, E. (eds.) *Climate Development and History of the North Atlantic Realm.* Berlin: Springer.

SHAKUN, J. D., BURNS, S. J., FLEITMANN, D., KRAMERS, J., MATTER, A. & AL-SUBARY, A. 2007. A high-resolution, absolute-dated deglacial speleothem record of

Indian Ocean climate from Socotra Island, Yemen. *Earth and Planetary Science Letters,* 259**,** 442-456.

SHANAHAN, T. M., PECK, J. A., MCKAY, N., HEIL, C. W., KING, J., FORMAN, S. L., HOFFMANN, D. L., RICHARDS, D. A., OVERPECK, J. T. & SCHOLZ, C. 2013. Age models for long lacustrine sediment records using multiple dating approaches - an example from Lake Bosumtwi, Ghana. *Quaternary Geochronology,* 15**,** 47-60.

SHAPLEY, M. D., ITO, E. & FORESTER, R. M. 2010. Negative correlations between Mg:Ca and total dissolved solids in lakes: False aridity signals and decoupling mechanism for paleohydrologic proxies. *Geology,* 38**,** 427-430.

SHARMA, T. & CLAYTON, R. N. 1965. Measurement of O18/O16 ratios of total oxygen of carbonates. *Geochimica et Cosmochimica Acta,* 29**,** 1347-1353.

SHARP, Z. 2007. *Stable Isotope Geochemistry,* New Jersey, Pearson.

SHEN, C., WU, C., CHENG, H., EDWARDS, R. L., HSIEH, Y., GALLET, S., CHANG, C., LI, T., LAM, D., KANO, A., HORI, M. & SPOTL, C. 2012. High-precision and high-resolution carbonate 230Th dating by MC-ICP-MS with SEM protocols. *Geochimica et Cosmochimica Acta,* 99**,** 71-76.

SIEGENTHALER, U. & EICHER, U. 1986. Stable Oxygen and Carbon Isotope Analyses. *In:* BERGLUND, B. E. (ed.) *Handbook of Holocene Palaeoecology and Palaeohydrology.* London: John Wiley and Sons Ltd.

SLOANE, H. J. 2004. The preferential reaction of calcite for isotope analysis, from a calcite/dolomite mixture. *NIGL internal report*.

SMITH, R. 2010. *A Geophysical Survey of Nar Golu, Cappadocia, Turkey.* MSc, Plymouth.

SNELLING, A., SWANN, G. E. A., LENG, M. J. & PIKE, J. 2013. A micro-manipulation technique for the purification of diatoms for isotope and geochemical analysis. *Silicon,* 5**,** 13-17.

SNYDER, J. A., WASYLIK, K., FRITZ, S. C. & WRIGHT, H. E. 2001. Diatom-based conductivity reconstruction and palaeoclimatic interpretation of a 40-ka record from Lake Zeribar, Iran. *Holocene,* 11**,** 737-745.

SONDI, I. & JURACIC, M. 2010. Whiting events and the formation of aragonite in Mediterranean Karstic Marine Lakes: new evidence on its biologically induced inorganic origin. *Sedimentology,* 57**,** 85-95.

SONMEZ, F. K., KOMUSCU, A. U., ERKAN, A. & TURGU, E. 2005. An analysis of spatial and temporal dimension of drought vulnerability in Turkey using the standardized precipitation index. *Natural Hazards,* 35**,** 243-264.

STANLEY, J. D., KROM, M. D., CLIFF, R. A. & WOODWARD, J. C. 2003. Short contribution: Nile flow failure at the end of the old kingdom, Egypt: Strontium isotopic and petrologic evidence. *Geoarchaeology,* 18**,** 395-402.

STATHAKOPOULOS, D. 2004. *Famine and Pestilence in the Late Roman and Early Byzantine Empire: A Systematic Survey of Subsistence Crises and Epidemics (Birmingham Byzantine and Ottoman Monographs),* Aldershot, Ashgate.

STAUBWASSER, M., SIROCKO, F., GROOTES, P. M. & SEGL, M. 2003. Climate change at the 4.2 ka BP termination of the Indus valley civilization and Holocene south Asian monsoon variability. *Geophysical Research Letters,* 30**,** 1425.

STEFFENSEN, J. P., ANDERSEN, K. K., BIGLER, M., CLAUSEN, H. B., DAHL-JENSEN, D., FISCHER, H., GOTO-AZUMA, K., HANSSON, M., JOHNSEN, S. J., JOUZEL, J.,

MASSON-DELMOTTE, V., POPP, T., RASMUSSEN, S. O., ROTHLISBERGER, R., RUTH, U., STAUFFER, B., SIGGAARD-ANDERSEN, M. L., SVEINBJORNSDOTTIR, A. E., SVENSSON, A. & WHITE, J. W. C. 2008. High-resolution Greenland Ice Core data show abrupt climate change happens in few years. *Science,* 321**,** 680-684.

STEIN, M., TORFSTEIN, A., GAVRIELI, I. & YECHIELI, Y. 2010. Abrupt aridities and salt deposition in the post-glacial Dead Sea and their North Atlantic connection. *Quaternary Science Reviews,* 29**,** 567-575.

STEVENS, L. R., DJAMALI, M., ANDRIEU-PONEL, V. & DE BEAULIEU, J. L. 2012. Hydroclimatic variations over the last two glacial/interglacial cycles at Lake Urmia, Iran. *Journal of Paleolimnology,* 47**,** 645-660.

STEVENS, L. R., ITO, E., SCHWALB, A. & WRIGHT, H. E. 2006. Timing of atmospheric precipitation in the Zagros Mountains inferred from a multi-proxy record from Lake Mirabad, Iran. *Quaternary Research,* 66**,** 494-500.

STEVENS, L. R., WRIGHT, H. E. & ITO, E. 2001. Proposed changes in seasonality of climate during the Lateglacial and Holocene at Lake Zeribar, Iran. *Holocene,* 11**,** 747-755.

STIRLING, C. H., ESAT, T. M., MCCULLOCH, M. T. & LAMBECK, K. 1995. High-precision U-Series dating of corals from Western-Australia and implications for the timing and duration of the Last Interglacial. *Earth and Planetary Science Letters,* 135**,** 115-130.

STREET-PERROTT, F. A., FICKEN, K. J., HUANG, Y. S. & EGLINTON, G. 2004. Late Quaternary changes in carbon cycling on Mt. Kenya, East Africa: an overview of the delta C-13 record in lacustrine organic matter. *Quaternary Science Reviews,* 23**,** 861-879.

SUPPAN, P., KUNSTMANN, H., HECKEL, A. & RIMMER, A. 2008. Impact of Climate Change on Water Availability in the Near East. *In:* ZEREINI, F. & HOTZL, H. (eds.) *Climate Changes and Water Resources in the Middle East and North Africa.* Berlin: Springer.

SWANN, G. E. A. 2010. A comparison of the Si/Al and Si/time wet-alkaline digestion methods for measurement of biogenic silica in lake sediments. *Journal of Paleolimnology,* 44**,** 375-385.

SWANN, G. E. A. & LENG, M. J. 2009. A review of diatom delta O-18 in palaeoceanography. *Quaternary Science Reviews,* 28**,** 384-398.

SWANN, G. E. A., LENG, M. J., SLOANE, H. J. & MASLIN, M. A. 2008. Isotope offsets in marine diatom delta O-18 over the last 200 ka. *Journal of Quaternary Science,* 23**,** 389-400.

SWANN, G. E. A., LENG, M. J., SLOANE, H. J., MASLIN, M. A. & ONODERA, J. 2007. Diatom oxygen isotopes: evidence of a species effect in the sediment record. *Geochemistry Geophysics Geosystems,* 8**,** Q06012.

SWANN, G. E. A., MASLIN, M. A., LENG, M. J., SLOANE, H. J. & HAUG, G. H. 2006. Diatom delta(18)O evidence for the development of the modern halocline system in the subarctic northwest Pacific at the onset of major Northern Hemisphere glaciation. *Paleoceanography,* 21**,** PA1009.

SWANN, G. E. A. & PATWARDHAN, S. V. 2011. Application of Fourier Transform Infrared Spectroscopy (FTIR) for assessing biogenic silica sample purity in

geochemical analyses and palaeoenvironmental research. *Climate of the Past,* 7**,** 65-74.

SWANN, G. E. A., PIKE, J., SNELLING, A. M., LENG, M. J. & WILLIAMS, M. C. 2013. Seasonally resolved diatom delta O-18 records from the West Antarctic Peninsula over the last deglaciation. *Earth and Planetary Science Letters,* 364**,** 12-23.

TALBOT, M. 1990. A review of the palaeohydrological interpretation of carbon and oxygen isotopic ratios in primary lacustrine carbonates. *Chemical Geology,* 80**,** 261-279.

TALBOT, M. R. & KELTS, K. 1986. Primary and diagenetic carbonates in the anoxic sediments of Lake Bosumtwi, Ghana. *Geology,* 14**,** 912-916.

TAN, E. & UNAL, Y. 2003. Impact of NAO to winter precipitation and temperature variability over Turkey. *Geophysical Research Abstracts,* 5**,** 00626.

TARASOV, L. & PELTIER, W. R. 2005. Arctic freshwater forcing of the Younger Dryas cold reversal. *Nature,* 435**,** 662-665.

TARUTANI, T., CLAYTON, R. N. & MAYEDA, T. K. 1969. The effect of polymorphims and magnesium substitution on oxygen isotope fractionation between calcium carbonate and water. *Geochimica et Cosmochimica Acta,* 33**,** 987-996.

TELLER, J. T. 2012. Importance of freshwater injections into the Arctic Ocean in triggering the Younger Dryas cooling. *PNAS,* 109**,** 19880-19881.

THOMAS, E. R., WOLFF, E. W., MULVANEY, R., STEFFENSEN, J. P., JOHNSEN, S. J., ARROWSMITH, C., WHITE, J. W. C., VAUGHN, B. & POPP, T. 2007. The 8.2 ka event from Greenland ice cores. *Quaternary Science Reviews,* 26**,** 70-81.

THOMPSON, L. G., MOSLEY-THOMPSON, E., BRECHER, H., DAVIS, M., LEON, B., LES, D., LIN, P. N., MASHIOTTA, T. & MOUNTAIN, K. 2006. Abrupt tropical climate change: past and present. *PNAS,* 103**,** 10536-10543.

TIAN, J., NELSON, D. & HU, F. 2011. How well do sediment indicators record past climate? An evaluation using annually laminated sediments. *Journal of Paleolimnology,* 45**,** 73-84.

TORFSTEIN, A., GOLDSTEIN, S. J., KAGAN, E. J. & STEIN, M. 2013. Integrated multi-site U-Th chronology of the last glacial Lake Lisan. *Geochimica et Cosmochimica Acta,* 104.

TORFSTEIN, A., HAASE-SCHRAMM, A., WALDMANN, N., KOLODNY, Y. & STEIN, M. 2009. U-series and oxygen isotope chronology of the mid-Pleistocene Lake Amora (Dead Sea basin). *Geochimica et Cosmochimica Acta,* 73**,** 2603-2630.

TOROS, H. 2012. Spatio-temporal precipitation change assessments over Turkey. *International Journal of Climatology,* 32**,** 1310-1325.

TRIANTAPHYLLOU, M. V., ZIVERI, P., GOGOU, A., MARINO, G., LYKOUSIS, V., BOULOUBASSI, I., EMEIS, K. C., KOULI, K., DIMIZA, M., ROSELL-MELE, A., PAPANIKOLAOU, M., KATSOURAS, G. & NUNEZ, N. 2009. Late Glacial-Holocene climate variability at the south-eastern margin of the Aegean Sea. *Marine Geology,* 266**,** 182-197.

TÜRKEŞ, M. 1996. Spatial and temporal analysis of annual rainfall variations in Turkey. *International Journal of Climatology,* 16**,** 1057-1076.

TÜRKEŞ, M. 1998. Influence of geopotential heights, cyclone frequency and southern oscillation on rainfall variations in Turkey. *International Journal of Climatology,* 18**,** 649-680.

TÜRKEŞ, M. 2003. Cht. 5: Spatial and Temporal Variations in Precipitation and Aridity Index Series of Turkey. *In:* BOLLE, H. J. (ed.) *Mediterranean Climate - Variability and Trends. Regional Climate Studies.* Heidelberg: Springer-Verlag.

TÜRKEŞ, M. & ERLAT, E. 2003. Precipitation changes and variability in turkey linked to the North Atlantic oscillation during the period 1930-2000. *International Journal of Climatology,* 23**,** 1771-1796.

TÜRKEŞ, M. & ERLAT, E. 2005. Climatological responses of winter precipitation in Turkey to variability of the North Atlantic Oscillation during the period 1930-2001. *Theoretical and Applied Climatology,* 81**,** 45-69.

TÜRKEŞ, M., KOC, T. & SARIS, F. 2009. Spatiotemporal variability of precipitation total series over Turkey. *International Journal of Climatology,* 29**,** 1056-1074.

TURNER, R., ROBERTS, N., EASTWOOD, W. J., JENKINS, E. & ROSEN, A. 2010. Fire, climate and the origins of agriculture: micro-charcoal records of biomass burning during the last glacial-interglacial transition in Southwest Asia. *Journal of Quaternary Science,* 25**,** 371-386.

TURNER, R., ROBERTS, N. & JONES, M. D. 2008. Climatic pacing of Mediterranean fire histories from lake sedimentary microcharcoal. *Global and Planetary Change,* 63**,** 317-324.

TYLER, J. J., LENG, M. J. & SLOANE, H. J. 2007. The effects of organic removal treatment on the integrity of delta O-18 measurements from biogenic silica. *Journal of Paleolimnology,* 37**,** 491-497.

TZEDAKIS, P. C. 2007. Seven ambiguities in the Mediterranean palaeoenvironmental narrative. *Quaternary Science Reviews,* 26**,** 2042-2066.

ULGEN, U. B., FRANZ, S. O., BILTEKIN, D., CAGATAY, M. N., ROESER, P. A., DONER, L. & THEIN, J. 2012. Climatic and environmental evolution of Lake Iznik (NW Turkey) over the last similar to 4700 years. *Quaternary International,* 274**,** 88-101.

VAN DAM, R. 2002. *Kingdom of Snow: Roman Rule and Greek Culture in Cappadocia,* Philadelphia, University of Pennsylvania Press.

VAN ZEIST, W. & BOTTEMA, S. 1977. Palynological investigations in Western Iran. *Palaeohistoria,* 19**,** 19-85.

VAN ZEIST, W. & BOTTEMA, S. 1991. *Late Quaternary Vegetation of the Near East,* Wiesbaden, Dr. Ludwig Reichert Verlag.

VANNIERE, B., COLOMBAROLI, D. & ROBERTS, C. N. 2010. A fire paradox in ecosystems around the Mediterranean. *PAGES news,* 18**,** 63-65.

VANNIERE, B., POWER, M. J., ROBERTS, N., TINNER, W., CARRION, J., MAGNY, M., BARTLEIN, P., COLOMBAROLI, D., DANIAU, A. L., FINSINGER, W., GIL-ROMERA, G., KALTENRIEDER, P., PINI, R., SADORI, L., TURNER, R., VALSECCHI, V. & VESCOVI, E. 2011. Circum-Mediterranean fire activity and climate changes during the mid-Holocene environmental transition (8500-2500 cal. BP). *Holocene,* 21**,** 53-73.

VASCONCELOS, C. & MCKENZIE, J. A. 1997. Microbial mediation of modern dolomite precipitation and diagenesis under anoxic conditions (Lagoa Vermelha, Rio de Janeiro, Brazil). *Journal of Sedimentary Research,* 67**,** 378-390.

VASCONCELOS, C., MCKENZIE, J. A., WARTHMANN, R. & BERNASCONI, S. M. 2005. Calibration of the delta O-18 paleothermometer for dolomite precipitated in microbial cultures and natural environments. *Geology,* 33**,** 317-320.

VERHEYDEN, S., NADER, F. H., CHENG, H. J., EDWARDS, L. R. & SWENNEN, R. 2008. Paleoclimate reconstruction in the Levant region from the geochemistry of a Holocene stalagmite from the Jeita cave, Lebanon. *Quaternary Research,* 70**,** 368-381.

VIEHBERG, F. A., ULGEN, U. B., DAMCI, E., FRANZ, S. O., ON, S. A., ROESER, P. A., CAGATAY, M. N., LITT, T. & MELLES, M. 2012. Seasonal hydrochemical changes and spatial sedimentological variations in Lake Iznik (NW Turkey). *Quaternary International,* 274**,** 102-111.

VINTHER, B. M., CLAUSEN, H. B., JOHNSEN, S. J., RASMUSSEN, S. O., ANDERSEN, K. K., BUCHARDT, S. L., DAHL-JENSEN, D., SEIERSTAD, I. K., SIGGAARD-ANDERSEN, M. L., STEFFENSEN, J. P., SVENSSON, A., OLSEN, J. & HEINEMEIER, J. 2006. A synchronized dating of three Greenland ice cores throughout the Holocene. *Journal of Geophysical Research-Atmospheres,* 111**,** D13102.

VON GRAFENSTEIN, U., ERLENKEUSER, H., BRAUER, A., JOUZEL, J. & JOHNSEN, S. J. 1999. A mid-European decadal isotope-climate record from 15,500 to 5000 years BP. *Science,* 284**,** 1654-1657.

WALKER, M. 2005. *Quaternary Dating Methods,* Chichester, Wiley.

WALKER, M. J. C., BERKELHAMMER, M., BJORCK, S., CWYNAR, L. C., FISHER, D. A., LONG, A. J., LOWE, J. J., NEWNHAM, R. M., RASMUSSEN, S. O. & WEISS, H. 2012. Formal subdivision of the Holocene Series/Epoch: a discussion paper by a Working Group of INTIMATE (Integration of ice-core, marine and terrestrial records) and the Subcommission on Quaternary Stratigraphy (International Commission on Stratigraphy). *Journal of Quaternary Science,* 27**,** 649-659.

WANG, Y. J., CHENG, H., EDWARDS, R. L., AN, Z. S., WU, J. Y., SHEN, C. C. & DORALE, J. A. 2001. A high-resolution absolute-dated Late Pleistocene monsoon record from Hulu Cave, China. *Science,* 294**,** 2345-2348.

WANNER, H., BEER, J., BUTIKOFER, J., CROWLEY, T. J., CUBASCH, U., FLUCKIGER, J., GOOSSE, H., GROSJEAN, M., JOOS, F., KAPLAN, J. O., KUTTEL, M., MULLER, S. A., PRENTICE, I. C., SOLOMINA, O., STOCKER, T. F., TARASOV, P., WAGNER, M. & WIDMANN, M. 2008. Mid- to Late Holocene climate change: an overview. *Quaternary Science Reviews,* 27**,** 1791-1828.

WARTHMANN, R., VAN LITH, Y., VASCONCELOS, C., MCKENZIE, J. A. & KARPOFF, A. M. 2000. Bacterially induced dolomite precipitation in anoxic culture experiments. *Geology,* 28**,** 1091-1094.

WASYLIKOWA, K., WITKOWSKI, A., WALANUS, A., HUTOROWICZ, A., ALEXANDROWICZ, S. W. & LANGER, J. J. 2006. Palaeolimnology of Lake Zeribar, Iran, and its climatic implications. *Quaternary Research,* 66**,** 477-493.

WEISS, B. 1982. The decline of Late Bronze-Age civilization as a possible response to climatic-change. *Climatic Change,* 4**,** 173-198.

WEISS, H. 1993. The genesis and collapse of 3rd millennium north Mesopotamian civilization. *Science,* 262**,** 1358-1358.

WEISS, H. 2003. Ninevite Periods and Processes. *In:* ROVA, E. & WEISS, H. (eds.) *The Origins of North Mesopotamian Civilisation.* Turnhout: Brepols.

WENINGER, B., ALRAM-STERN, E., BAUER, E., CLARE, L., DANZEGLOCKE, U., JORIS, O., CLAUDIA, K. E., GARY, R. F., TODOROVA, H. & VAN ANDEL, T. 2006. Climate forcing due to the 8200 cal yr BP event observed at Early Neolithic sites in the eastern Mediterranean. *Quaternary Research,* 66**,** 401-420.

WENINGER, B., CLARE, L., ROHLING, E. J., BAR-YOSEF, O., BOHNER, U., BUDJA, M., BUNDSCHUH, M., FEURDEAN, A., GEBEL, H., JORIS, O., LINSTADTER, J., MAYEWSKI, P. A., MUHLENBRUCH, T., REINGRUBER, A., ROLLEFSON, G., SCHYLE, D., THISSEN, L., TODOROVA, H. & ZEILHOFER, C. 2009. The impact of rapid climate change on prehistoric societies during the Holocene in the Eastern Mediterranean. *Documenta Praehistorica,* 36**,** 7-59.

WICK, L., LEMCKE, G. & STURM, M. 2003. Evidence of Lateglacial and Holocene climatic change and human impact in eastern Anatolia: high-resolution pollen, charcoal, isotopic and geochemical records from the laminated sediments of Lake Van, Turkey. *Holocene,* 13**,** 665-675.

WIERSMA, A. P. & RENSSEN, H. 2006. Model-data comparison for the 8.2 ka BP event: confirmation of a forcing mechanism by catastrophic drainage of Laurentide Lakes. *Quaternary Science Reviews,* 25**,** 63-88.

WILLCOX, G., BUXO, R. & HERVEUX, L. 2009. Late Pleistocene and early Holocene climate and the beginnings of cultivation in northern Syria. *Holocene,* 19**,** 151-158.

WILLEMSE, N. W., VAN DAM, O., VAN HELVOORT, P. J., DANKERS, R., BROMMER, M., SCHOKKER, J., VALSTAR, T. E. & DE WOLF, H. 2004. Physical and chemical limnology of a subsaline athalassic lake in West Greenland. *Hydrobiologia,* 524**,** 167-192.

WILSON, G. P., REED, J. M., LAWSON, I. T., FROGLEY, M. R., PREECE, R. C. & TZEDAKIS, P. C. 2008. Diatom response to the Last Glacial-Interglacial Transition in the Ioannina basin, northwest Greece: implications for Mediterranean palaeoclimate reconstruction. *Quaternary Science Reviews,* 27**,** 428-440.

WISSEL, H., MAYR, C. & LUCKE, A. 2008. A new approach for the isolation of cellulose from aquatic plant tissue and freshwater sediments for stable isotope analysis. *Organic Geochemistry,* 39**,** 1545-1561.

WMO. 2011. *World Weather Information Service* [Online]. Hong Kong: Hong Kong Observatory. Available: http://worldweather.wmo.int/ [Accessed 29/5/2011].

WOLDRING, H. & BOTTEMA, S. 2003. The vegetation history of East-Central Anatolia in relation to Archaeology: the Eski Acigöl pollen evidence compared with the Near Eastern environment. *Palaeohistoria,* 43/44**,** 1–34.

WOLDRING, H. & CAPPERS, R. T. J. 2001. The origin of the 'wild orchards' of Central Anatolia. *Turkish Journal of Botany,* 25**,** 1-9.

WOLFE, B., EDWARDS, T. W. D., ELGOOD, R. & BEUNING, K. 2001. Carbon and Oxygen Isotope Analysis of Lake Sediment Cellulose: Methods and Applications. *In:* LAST, W. M. & SMOL, J. P. (eds.) *Tracking Environmental Change Using Lake Sediments. Volume 2: Physical and Geochemical Methods.* Dordrecht: Kluwer.

WOLFE, B. B., FALCONE, M. D., CLOGG-WRIGHT, K. P., MONGEON, C. L., YI, Y., BROCK, B. E., AMOUR, N. A. S., MARK, W. A. & EDWARDS, T. W. D. 2007. Progress in isotope paleohydrology using lake sediment cellulose. *Journal of Paleolimnology,* 37**,** 221-231.

WOLFE, B. B., KARST-RIDDOCH, T. L., VARDY, S. R., FALCONE, M. D., HALL, R. I. & EDWARDS, T. W. D. 2005. Impacts of climate and river flooding on the hydro-ecology of a floodplain basin, Peace-Athabasca Delta, Canada since AD 1700. *Quaternary Research,* 64**,** 147-162.

WOLTERING, M., JOHNSON, T. C., WERNE, J. P., SCHOUTEN, S. & DAMSTE, J. S. S. 2011. Late Pleistocene temperature history of Southeast Africa: a TEX86 temperature record from Lake Malawi. *Palaeogeography Palaeoclimatology Palaeoecology,* 303**,** 93-102.

WOODBRIDGE, J. & ROBERTS, C. N. 2010. Linking neo- and palaeolimnology: a case study using crater lake diatoms from central Turkey. *Journal of Paleolimnology,* 44**,** 855-871.

WOODBRIDGE, J. & ROBERTS, C. N. 2011. Late Holocene climate of the Eastern Mediterranean inferred from diatom analysis of annually-laminated lake sediments. *Quaternary Science Reviews,* 30**,** 3381-3392.

WOODBRIDGE, J., ROBERTS, C. N. & COX, E. J. 2010. Morphology and ecology of a new centric diatom from Cappadocia (Central Turkey). *Diatom Research,* 25**,** 195-212.

YASUDA, Y., KITAGAWA, H. & NAKAGAWA, T. 2000. The earliest record of major anthropogenic deforestation in the Ghab Valley, northwest Syria: a palynological study. *Quaternary International,* 73-4**,** 127-136.

YU, S. Y., COLMAN, S. M., LOWELL, T. V., MILNE, G. A., FISHER, T. G., BRECKENRIDGE, A., BOYD, M. & TELLER, J. T. 2010. Freshwater outburst from Lake Superior as a trigger for the cold event 9300 years ago. *Science,* 328**,** 1262-1266.

ZEDER, M. A. 2011. The origins of agriculture in the Near East. *Current Anthropology,* 52**,** S221-S235.

ZHAO, J. X., YU, K. F. & FENG, Y. X. 2009. High-precision U-238-U-234-Th-230 disequilibrium dating of the recent past: a review. *Quaternary Geochronology,* 4**,** 423-433.

ZIV, B., DAYAN, U., KUSHNIR, Y., ROTH, C. & ENZEL, Y. 2006. Regional and global atmospheric patterns governing rainfall in the southern Levant. *International Journal of Climatology,* 26**,** 55-73.

ZOHARY, D., HOPF, M. & WEISS, E. 2012. *Domestication of Plants in the Old World,* Oxford, Oxford University Press.

ZOLITSCHKA, B. 2007. Varved Lake Sediments. *In:* ELIAS, S. A. (ed.) *Encyclopedia of Quaternary Science.* Amsterdam: Elsevier.

ZREDA, M., CINER, A., SARIKAYA, M. A., ZWECK, C. & BAYARI, S. 2011. Remarkably extensive glaciation and fast deglaciation and climate change in Turkey near the Pleistocene-Holocene boundary. *Geology,* 39**,** 1051-1054.

ZUHLSDORFF, C., HANEBUTH, T. J. J. & HENRICH, R. 2008. Persistent quasi-periodic turbidite activity off Saharan Africa and its comparability to orbital and climate cyclicities. *Geo-Marine Letters,* 28**,** 87-95.